# Gene Expression Profiling of Cylindrospermopsin Toxicity


## Author

Bain, Peter A



## Published

2007

## Thesis Type

Thesis (PhD Doctorate)

## School

School of Biomolecular and Physical Sciences

## DOI

10.25904/1912/3151

# Gene Expression Profiling of Cylindrospermopsin Toxicity

**Peter A. Bain BSc (Hons)**

*A thesis submitted in fulfillment of the degree of Doctor of Philosophy*

*June 2007*

School of Biomolecular and Physical Sciences

Griffith University, Australia

**Removal Notice**

Some figures from Chapter 3 and Chapter 5 have been removed from the electronic version of this thesis for copyright reasons.

## Statement of Originality

This work has not previously been submitted for a degree or diploma in any university. To the best of my knowledge and belief, the thesis contains no material previously published or written by another person except where due reference is made in the thesis itself.

_____

Peter Bain

*For Robert and Avril Binzer*

## Acknowledgements

The work presented in this thesis was supported by funds from the Cooperative Research Centre for Water Quality and Treatment (CRCWQT).

Firstly I thank my mentor of many years, Bharat Patel, for having faith in my ability and for many and varied interesting discussions on topics academic and otherwise. For gratefully received moral support, endless enthusiasm for the topic and for my contributions to it, Glen Shaw deserves my heartfelt appreciation. Thanks to Jamie Nourse for expert technical advice and for teaching me the finer points of fermented malt product appreciation. Purified cylindrospermopsin was generously provided by Wasa Wickramasinge, Mark Seifert and Dave Ruebhart. For passing on her expertise in microarray analysis and experimental design, I sincerely thank Christine Wells. Emily Dunner and Renee Stirling offered invaluable suggestions on more than one occasion. Phil Pope's comic relief in the lab was highly entertaining, especially when he teamed up with our colleague Li 'Janet' Zhang. Thanks to Denis Mulcahy for generous words of encouragement and advice for myself and my fellow CRCWQT postgrads. My wonderful family helped me through some challenging times over the course of my candidature—with the departure of two wonderful grandparents, it was rough for all of us—I'm lucky to have such a loving family of shoulders to lean on.

Lastly but most importantly, Kylie Cardell—your love is inspiring—I couldn't have done it without you.

## Publications arising from the candidature

Peer-reviewed articles:

**Bain PA, Shaw G and Patel BKC.** Induction of p53-regulated expression in human cell lines exposed to the cyanobacterial toxin cylindrospermopsin. *Journal of Toxicology and Environmental Health Part A*, **70**, 1687-93.

**Neumann C, Bain PA, Shaw G.** Studies of the comparative *in vitro* toxicology of the cyanobacterial metabolite, deoxycylindrospermopsin. *Journal of Toxicology and Environmental Health Part A,* **70**, 1679-86.

**Bain PA, Shaw G and Patel BKC.** Gene expression profiling of cylindrospermopsin toxicity *in vitro*. *In preparation.*

Selected conference papers:

Mechanisms of Cylindrospermopsin Toxicity: A Toxicogenomics Approach. Challenges in Environmental Toxicology in Australasia, Melbourne, July 2006. Oral presentation.

Gene Expression Profiling of Cylindrospermopsin Toxicity. CRCWQT Postgradute Student Conference, Melbourne, July 2006. Oral presentation.

Transcriptional Profiling of Cylindrospermopsin Toxicity. 5th Australian Microarray Conference, Barossa, South Australia, September 2005. Poster presentation.

Activation of the Ribotoxic Stress Response in Human Dermal Fibroblasts and HepG2 Cells Exposed to the Cyanobacterial Toxin Cylindropsermopsin. COMBIO, Adelaide, South Australia, September 2005. Poster presentation.

P53-Regulated Transcription in Human Dermal Fibroblasts and HepG2 Cells in Response to the Cyanobacterial Toxin Cylindrospermopsin. 9th International Conference on Environmental Mutagens, San Francisco, USA, September 2005. Poster presentation.

## Abstract

Cylindrospermopsin (CYN) is a toxic alkaloid produced by several freshwater cyanobacterial species, the most prevalent in Australian waters being *Cylindrospermopsis raciborskii*. The occurrence of CYN-producing cyanobacteria in drinking water sources worldwide poses a potential human health risk, with one well-documented case of human poisoning attributed to the toxin. While extensive characterisation of CYN-induced toxicity has been conducted in rodents both *in vivo* and in primary cell cultures, little is known about mechanisms of toxicity in human cell types. This thesis describes studies undertaken to further define the molecular mechanisms of CYN toxicity in human cells.

Concentration-response relationships were determined in various cultured human cell types using standard toxicity assays. As expected, CYN caused dose-dependent decreases in the growth of three cell lines, HepG2, Caco-2 and HeLa, and one primary cell type, human dermal fibroblasts, according to tetrazolium reduction assays. CYN treatment did not disrupt cellular membranes according to the lactate dehydrogenase release assay in HepG2 or Caco-2 cells after 24, 48 or 72 h exposure, but did cause membrane disruption in fibroblasts after 72 h exposure to relatively high concentrations of the toxin. Apoptosis occurred more readily in HeLa cells than HepG2 cells or fibroblasts, with 72 h exposure to 1 μg/mL required before statistically significant rates of apoptosis occurred in the latter cell types. CYN did not appear to directly affect the structure of actin filaments or microtubules under the conditions used in the present study.

The major portion of the work presented in this thesis comprises a large-scale interrogation of changes in gene expression induced by the toxin in cultured cells. To assess the effects of CYN on global gene expression, relative messenger RNA (mRNA) levels in human dermal fibroblasts and HepG2 cells after 6 h and 24 h exposure to 1 μg/mL CYN were determined using oligonucleotide microarrays representing approximately 19 000 genes. Overall, the number of transcripts significantly altered in abundance was greater in fibroblasts than in HepG2 cells. In both cell types, mRNA levels for genes related to amino acid biosynthesis, carbohydrate metabolism, and

protein folding and transport were reduced after CYN treatment, while transcripts representing genes for apoptosis, RNA biosynthesis and RNA processing increased in abundance. More detailed data analyses revealed the modulation of a number of stress response pathways—genes regulated by NF-κB were induced, DNA damage response pathways were up-regulated, and a large number of genes involved in endoplasmic reticulum stress were strongly down-regulated. Genes for the synthesis and processing of mRNA, tRNA and rRNA were strongly up-regulated, indicating that CYN treatment may increase the turnover of all forms of cellular RNA. A small group of genes were differentially expressed in HepG2 cells and fibroblasts, revealing cell-specific responses to the toxin. Selected changes in transcript level were validated using real-time quantitative reverse transcriptase PCR (qRT-PCR).

The modulation of stress response pathways by CYN, indicated by microarray analysis, was further investigated using other methods. The role of tumour suppressor protein p53 in CYN-mediated gene expression was confirmed by measuring the expression of known p53-regulated genes following CYN treatment of HepG2 cells and human dermal fibroblasts using qRT-PCR. Western blotting of protein extracts from CYN-treated cells showed that p53 protein accumulation occurred in HepG2 cells, providing additional evidence of the activation of the p53 pathway by CYN in this cell line. The immediate-early genes *JUN* and *FOS* were found to be induced by CYN in a concentration-dependent manner, and *MYC* was induced to a lesser extent. The mitogen-activated protein kinase c-Jun $NH_2$-terminal kinase, implicated in the ribotoxic stress response initiated by damage to ribosomal RNA, appeared to become phosphorylated in HeLa cells after CYN exposure, suggesting that ribotoxic stress may occur in response to CYN in at least some cell types. The expression of a reporter gene under the control of a response element specific for NF-κB was induced at the mRNA level but inhibited at the protein level. This shows that while transcription factors such as p53 and NF-κB are apparently activated in response to the toxin, transactivation of target genes may not necessarily manifest a corresponding increase at the protein level.

The current work contributes significantly to the current understanding of cylindrospermopsin toxicity in human-derived cell types, and provides further insight into putative modes of action.

# Contents

**STATEMENT OF ORIGINALITY** ..... **I**

**ACKNOWLEDGEMENTS** ..... **V**

**PUBLICATIONS** ..... **VII**

**ABSTRACT** ..... **IX**

**CONTENTS** ..... **XI**

**LIST OF FIGURES** ..... **XV**

**LIST OF TABLES** ..... **XVII**

**LIST OF ABBREVIATIONS** ..... **XIX**

**CHAPTER 1**

**General Introduction to Cylindrospermopsin Toxicology and Toxicogenomics** .. **1**

1.1 Cylindrospermopsin, a toxic cyanobacterial secondary metabolite ..... 1
1.2 Toxicology of cylindrospermopsin ..... 2
1.2.1 Discovery and properties of cylindrospermopsin ..... 3
1.2.2 CYN toxicity in animals ..... 4
1.2.3 DNA damage ..... 5
1.2.4 Inhibition of protein synthesis ..... 7
1.2.5 Investigating the molecular basis of cylindrospermopsin toxicity ..... 8
1.3 Gene expression profiling in toxicology ..... 9
1.4 Validation of microarray data ..... 14
1.5 Aim of the current study ..... 15
1.6 Experimental approaches ..... 16

**CHAPTER 2**

**Assessment of cylindrospermopsin toxicity in cultured human-derived cells** .... **17**

2.1 Introduction ..... 17
2.1.1 Tetrazolium reduction – MTT and MTS assays ..... 17
2.1.2 ATP assays ..... 18
2.1.3 Membrane integrity assays ..... 19
2.1.4 Altered cytoskeletal morphology as an indicator of cytotoxicity ..... 19
2.1.5 Death by cylindrospermopsin: apoptosis or necrosis? ..... 21
2.1.6 Chapter aims and outcomes ..... 21
2.2 Materials and Methods ..... 22
2.2.1 Cell culture ..... 22
2.2.2 MTS assays ..... 23
2.2.3 LDH release assays ..... 23

2.2.4 ATP assays ..... 24
2.2.5 Apoptosis assays ..... 24
2.2.6 Determination of changes in cell morphology ..... 25
2.3 Results ..... 26
2.3.1 CYN inhibits MTS reduction ..... 26
2.3.2 CYN treatment reduces ATP levels ..... 27
2.3.3 CYN treatment does not induce rapid LDH release ..... 28
2.3.4 CYN induces apoptosis after prolonged exposure ..... 29
2.3.5 Changes in cellular morphology in response to CYN ..... 29
2.4 Discussion ..... 34

**CHAPTER 3**

**Gene expression profiling of cylindrospermopsin toxicity in vitro ..... 39**

3.1 Introduction ..... 39
3.2 Materials and Methods ..... 42
3.2.1 Experimental Design ..... 42
3.2.2 Cylindrospermopsin ..... 43
3.2.3 Cell culture and treatments ..... 44
3.2.4 RNA isolation ..... 44
3.2.5 RNA amplification and labelling ..... 45
3.2.6 Microarray hybridisation ..... 45
3.2.7 Microarray data analysis ..... 46
3.2.8 Validation by qRT-PCR ..... 47
3.3 Results ..... 48
3.3.1 Microarray analysis reveals expression patterns relevant to CYN toxicity . 48
3.3.1.1 Principal components analysis clearly separates samples ..... 48
3.3.1.2 CYN induces a greater degree of variation in HDFs compared to HepG2 cells ..... 49
3.3.1.3. Functional analysis of clusters identifies gene expression associated with well-described biological pathways ..... 50
3.3.1.4 DAVID functional analysis reveals the induction of diverse stress signalling pathways ..... 57
3.3.2 Large changes in expression after 24 h reveal responses common to both cell types ..... 62
3.3.3 CYN induces changes in gene expression associated with specific stress responses ..... 76
3.3.3.1 DNA damage responses ..... 76
3.3.3.2 NF-κB-mediated gene expression ..... 79
3.3.3.3 CYN reduces the expression of endoplasmic reticulum stress genes ..... 82
3.3.4 CYN induces genes for RNA metabolism and processing ..... 85
3.3.5 CYN-mediated expression differs between HDFs and HepG2 cells ..... 87
3.3.6 Validation of expression ratios using qRT-PCR ..... 91
3.4 Discussion ..... 93

**CHAPTER 4**

**Induction of p53-regulated gene expression in response to cylindrospermopsin 99**

4.1 Introduction ..... 99
4.2 Materials And Methods ..... 101

4.2.1 Cell culture ..... 101
4.2.2 CYN treatments and relative gene expression analysis ..... 101
4.2.3 Western immunoblotting ..... 102
4.3 Results ..... 103
4.4 Discussion ..... 106

**CHAPTER 5**

**Preliminary investigations into the roles of AP-1 and NF-κB in cylindrospermopsin-induced gene expression ..... 109**

5.1 Introduction ..... 109
5.2 Materials and Methods ..... 112
5.2.1 Chemicals ..... 112
5.2.2 Cell culture, RNA isolation and qRT-PCR ..... 112
5.2.3 Western blotting ..... 112
5.2.4 Reporter assays ..... 113
5.2.5 qRT-PCR data analysis ..... 116
5.3 Results ..... 116
5.3.1 CYN induces immediate-early gene expression ..... 116
5.3.2 Comparison of JUN induction in response to CYN and other protein synthesis inhibitors ..... 118
5.3.3 CYN treatment activates JNK but does not induce SEAP mRNA expression from pAP1-SEAP in HeLa cells ..... 119
5.3.4 CYN treatment induces transcription from pNF-κB-SEAP ..... 122
5.3.5 Sequence analysis of the $P_{TAL}$ element ..... 123
5.4 Discussion ..... 124

**CHAPTER 6**

**Conclusions and Future Directions ..... 135**

**APPENDIX 1**

**List of oligonucleotide primers used for real-time qRT-PCR ..... 139**

**APPENDIX 2**

**Representative determination of relative mRNA levels by qRT-PCR ..... 143**

**APPENDIX 3**

**Qualitative analysis of RNA samples used for microarray hybridisations ..... 147**

**REFERENCES ..... 154**

# List of Figures

**Figure 1.1 Chemical structure of cylindrospermopsin.** ..... **3**
**Figure 1.2 Overview of DNA microarray technology.** ..... **11**
**Figure 1.3 Flowchart of experimental approaches.** ..... **16**
**Figure 2.1 The effects of CYN on MTS reduction.** ..... **27**
**Figure 2.2 Determination of ATP content in CYN-treated cells.** ..... **28**
**Figure 2.3 LDH leakage from CYN-treated human dermal fibroblasts.** ..... **29**
**Figure 2.4 Rates of apoptosis in CYN-treated cells.** ..... **30**
**Figure 2.5 Structure of the actin cytoskeleton in cells exposed to CYN.** ..... **34**
**Figure 2.6 The effects of CYN on microtubule cytoskeletal structure.** ..... **35**
**Figure 3.1 Experimental design for microarray hybridisations.** ..... **43**
**Figure 3.2 Principal components analysis of variance in the data sets.** ..... **49**
**Figure 3.3. Hierarchical clustering of gene expression profiles.** ..... **57**
**Figure 3.4 CYN induces the expression of genes involved in TNF signalling.** ..... **61**
**Figure 4.1 P53 activation in response to DNA damage.** ..... **100**
**Figure 5.1 Map of the pTAL-SEAP reporter vector.** ..... **114**
**Figure 5.2 Immediate-early gene expression in response to CYN in HDFs and HepG2 cells.** ..... **117**
**Figure 5.3 Relative expression of *FOS*, *JUN* and *MYC* after 24 h exposure to 1 µg/mL CYN.** ..... **118**
**Figure 5.4 Relative JUN mRNA levels in response to translational inhibitors.** ..... **119**
**Figure 5.5 Effects of CYN on JNK activation and AP-1-driven SEAP expression in HeLa cells.** ..... **121**
**Figure 5.6 CYN represses SEAP enzyme activity but induces transcription from pNF-κB-SEAP.** ..... **123**
**Figure 5.7 Putative transcription factor binding sites in the $P_{TAL}$ promoter element.** ..... **124**
**Figure 5.8 Cis-acting elements contributing to transcriptional activation of *FOS* and *JUN*.** ..... **125**
**Figure 5.9 Model of the ribotoxic stress response.** ..... **128**
**Figure 5.10 NF-κB activation pathways.** ..... **130**

# List of Tables

**Table 2.1** Cell types used in the current study.....**22**
**Table 3.1** Overview of large changes in relative mRNA transript levels in response to CYN.....**50**
**Table 3.2** Biological pathways associated with cluster I from figure 3.3A.....**58**
**Table 3.3** Biological pathways associated with cluster II from figure 3.3A.....**60**
**Table 3.4** Genes with large changes in relative transcript level after exposure to 1 μg/ml cylindrospermopsin for 24 h.....**70**
**Table 3.5** Genes associated with stress responses showing altered transcript levels after CYN exposure. .....**78**
**Table 3.6** RNA metabolism genes induced following CYN treatment.....**85**
**Table 3.7** Genes differentially expressed in HDFs and HepG2 cells in response to CYN.....**88**
**Table 3.8** Validation of relative expression levels for selected transcripts using qRT-PCR.....**92**
**Table A1.1** Primer pairs used for qRT-PCR.....**139**

# List of Abbreviations

| | |
|---|---|
| **ANOVA** | Analysis of variance |
| **AP-1** | Activator protein 1 |
| **ATCC** | American Type Culture Collection |
| **ATP** | Adenosine triphosphate |
| **bHLHZ** | Basic helix-loop-helix-leucine zipper transcription factor |
| **bZip** | Basic region leucine zipper |
| **BSA** | Bovine serum albumin |
| **CCD** | Charge-coupled device |
| **cDNA** | Complementary DNA |
| **cRNA** | Complementary RNA |
| **Cy3** | A water-soluble fluorescent dyes of the cyanine dye family |
| **Cy5** | A water-soluble fluorescent dyes of the cyanine dye family |
| **CYN** | Cylindrospermopsin |
| **CYP450** | Cytochrome P450 |
| **DAPI** | 4',6-Diamidino-2-phenylindole |
| **DAVID** | Database for Annotation, Visualisation and Integrated Discovery (Dennis et al., 2003) |
| **DMEM** | Dulbecco's modified Eagle's medium |
| **DNA** | Deoxyribonucleic acid |
| **dNTPs** | Deoxyribonucleoside triphosphates |
| **dsDNA** | Double-stranded DNA |
| **dsRNA** | Double-stranded RNA |
| **$EC_{50}$** | Concentration of a compound giving an assay result equivalent to 50% of the maximum observed response |
| **EDTA** | Ethylenediaminetetraacetic acid |
| **ER** | Endoplasmic reticulum |
| **FBS** | Foetal bovine serum |
| **FITC** | Fluorescein isothiocyanate |
| **GAPDH** | Glyceraldehyde-3-phosphate dehydrogenase |
| **GO** | Gene Ontology (Ashburner et al., 2000) |
| **GSH** | The reduced form of glutathione |
| **HDF** | Human dermal fibroblast |
| **HRP** | Horseradish peroxidase |
| **IP** | Intraperintoneal |
| **$LD_{50}$** | A dose of toxin which is lethal to 50% of test animals |
| **LDH** | Lactate dehydrogenase |

| | |
|---|---|
| **MAPK** | Mitogen-activated protein kinase |
| **MQW** | Milli-Q water |
| **mRNA** | Messenger RNA |
| **MTS** | 3-(4,5-dimethylthiazol-2-yl)-5-(3-carboxymethoxyphenyl)-2-(4-sulfophenyl)-2H-tetrazolium, inner salt |
| **MTT** | 3-(4,5-dimethylthiazol-2-yl)-2,5-diphenyl tetrazolium bromide |
| **$NAD^+$** | Nicotinamide adenine dinucleotide |
| **NADH** | Reduced nicotinamide adenine dinucleotide |
| **$NADP^+$** | Nicotinamide adenine dinucleotide phosphate |
| **NADPH** | Reduced nicotinamide adenine dinucleotide phosphate |
| **NF-κB** | Nuclear factor kappa B |
| **ND** | Not determined |
| **NP** | Not present |
| **PBS** | Phosphate-buffered saline |
| **PCA** | Principle components analysis |
| **PCR** | Polymerase chain reaction |
| **PKR** | dsRNA-activated protein kinase |
| **PMA** | Phorbol 12-myristate 13-acetate |
| **qRT-PCR** | Quantitative RT-PCR (reverse transcription of RNA followed by real-time detection and relative quantification of PCR products from cDNA) |
| **RIN** | RNA Integrity Number |
| **RNA** | Ribonucleic acid |
| **rRNA** | Ribosomal RNA |
| **SDS** | Sodium dodecylsulphate |
| **SEM** | Standard error of the mean |
| **SSC** | Salt / sodium citrate solution (1X SSC contains 150 mM sodium chloride and 15 mM sodium citrate)\ |
| **TAL** | TATA-like element |
| **TPA** | 12-O-tetradecanoylphorbol-13-acetate (see also PMA) |
| **TRE** | TPA responsive element |
| **TRITC** | Texas red isothiocyanate |
| **tRNA** | Transfer RNA |
| **TUNEL** | Terminal transferase 3'-UTP nick end-labelling |
| **UPR** | Unfolded protein response |
| **UV** | Ultraviolet |

# Chapter 1

## *General Introduction to Cylindrospermopsin Toxicology and Toxicogenomics*

### 1.1 Cylindrospermopsin, a toxic cyanobacterial secondary metabolite

Cyanobacteria are prokaryotic micro-organisms that utilise chlorophyll *a* and pigments to perform oxygenic photosynthesis (Castenholz and Waterbury, 1989). While best known for forming blooms in aquatic habitats, cyanobacteria are also ubiquitous in diverse environments exposed to sunlight, including rock, intertidal areas and soil. Considered as one of the most important primary producers in the early stages of life on Earth, they were also probably the first group of organisms to produce atmospheric oxygen (Mur et al., 1999). Cyanobacteria are abundant in marine and freshwater environments, and many species produce dense blooms in appropriate conditions of light, temperature and nutrient levels.

A common feature amongst bloom-forming cyanobacteria is the production of secondary metabolites, some of which are potent toxins. Three main structural groups of cyanobacterial toxins are currently known—cyclic peptides, lipopolysaccharides and alkaloids. Cyclic peptides such as microcystins and nodularin are well characterised hepatotoxins that exhibit protein phoshatase-inhibiting activity and disrupt the cytoskeleton in hepatocytes (Dawson, 1998; Gulledgea et al., 2002; Runnegar et al., 1995a). Cyanobacterial lipopolysaccharides have endotoxic and dermatotoxic properties

but are not well studied (Stewart et al., 2006). Alkaloid cyanotoxins include the neurotoxic anatoxins and saxitoxins, as well as the topic of this report, cylindrospermopsin.

At least 40 different toxigenic cyanobacterial species are known to exist, of about 2000 total species in 150 genera (Haider et al., 2003). Cyanobacterial toxins represent a health risk for humans and animals, particularly during blooms in surface water reservoirs used for domestic supply or in rivers and dams used by livestock. In Queensland, Australia, the warm climate encourages the growth of a toxic filamentous species, *Cylindrospermopsis raciborskii*, which is well known amongst researchers as the probable cause of the most serious case of human cyanotoxin poisoning in Australian recorded history (Byth, 1980). The widespread occurrence of *C.raciborskii* at high cell counts in reservoirs throughout Queensland (McGregor and Fabbro, 2000) indicates that this organism requires close monitoring and will continue to be of concern to the water industry and farmers alike. Since its isolation from *C.raciboskii*, cylindrospermopsin has been the topic of intensive research. The potential risk to humans and the specific mode of action with respect to DNA damage and protein synthesis inhibition are some areas where knowledge is currently incomplete.

## 1.2 Toxicology of cylindrospermopsin

Research into CYN has generally followed one of two paths—the investigation of factors that lead to the presence of the toxin in drinking water (e.g. microbial production of CYN, microbiology and water treatment systems), and the determination of biological effects of the toxin itself (e.g. dose-response relationships in animals and cells, histopathology, modes of toxicity). This report is concerned primarily with the latter issue, consequently microbiology and water treatment will not be discussed in detail. An important point to consider is that while effective methods for the removal of many classes of cyanobacterial toxin have been developed, a single process suitable for all cyanotoxins has yet to be found (Hrudey, 1999). This is due to the diverse chemical properties exhibited by different classes of toxin. CYN is a stable compound under a range of environmental conditions (Chiswell et al., 1999) and there is some evidence of the formation of harmful disinfection by-products as a result of chlorination (Senogles-Derham et al., 2003). Despite the low probability of acutely dangerous quantities of

CYN entering the domestic water supply, a potential risk exists in the form of long-term exposure to low doses of CYN in drinking water. Accidental exposures during recreational activity may also occur.

### *1.2.1 Discovery and properties of cylindrospermopsin*

*C.raciborskii* is assumed to be the causative agent of one of the most severe human poisoning incidents involving a cyanobacterium (Hawkins et al., 1985). The incident occurred on Palm Island in North Queensland, where a cyanobacterial bloom in the local water reservoir resulted in the hospitalisation of 148 people showing symptoms of severe hepatoenteritis (Bourke and Hawes, 1983; Byth, 1980). *C.raciborskii* was later identified as the only potentially toxigenic cyanobacterial species detectable in samples taken from the reservoir (Hawkins et al., 1985).

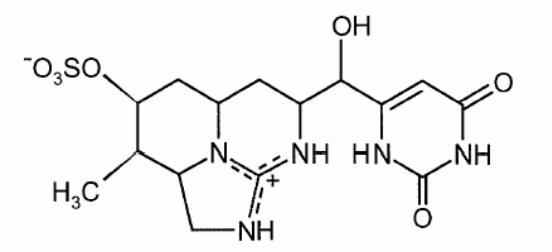


**Figure 1.1 Chemical structure of cylindrospermopsin.**

Ohtani and colleages (1992) subsequently purified CYN from *C.raciborskii* and determined the chemical structure, which consists of a cyclic sulphated guanidinium group linked to hydroxymethyluracil (Figure 1.1). CYN is a highly water-soluble zwitterionic compound with a molecular weight of 415 Daltons (Ohtani et al., 1992). Under a range of adverse conditions such as high temperature (100°C), UV light and sunlight, pure CYN in solution is extremely stable (Chiswell et al., 1999).

In Australia, *C.raciborskii* is the most common CYN-producing organism, but the toxin is also synthesised by other cyanobacteria found worldwide, including *Aphanizomenon ovalisporum* in Australia and Israel (Banker et al., 1997; Shaw et al., 1999), *Umezakia natans* in Japan (Harada et al., 1994), and *Raphidiopsis curvata* in China (Li et al., 2001c). Originally thought to be confined to tropical regions, *C.raciborskii* is now

known to exist in temperate climates (Padisak, 1997), with a numerous phylogenetic groups that can be separated according to geodraphical origin (Neilan et al., 2003). Strains isolated from Brazil produce saxitoxins in addition to CYN (Lagos et al., 1999), while a number of non-toxic strains have been reported to occur in France, Mexico and Hungary (Bernard et al., 2003). CYN-producing strains are found in the USA (Burns et al., 2000), and Thailand (Li et al., 2001b), and a strain has been isolated in Portugal that produces a toxin yet to be characterised (Saker et al., 2003). In addition to the aforementioned human poisoning incident, *C.raciborskii* has been implicated in livestock deaths (Thomas et al., 1998) and is the likely cause of human poisonings in anecdotal reports from the Australian outback (Hayman, 1992).

### *1.2.2 CYN toxicity in animals*

Cylindropsermopsin toxicity was first investigated using a mouse bioassay. This revealed that the major observable effect, severe liver damage, occurred at least 24 hours after relatively low doses of crude *C.raciborskii* extract delivered via intraperitoneal (IP) injection (Hawkins et al., 1985). Higher IP doses of crude extract produced liver damage after six to nine hours, while high doses delivered via the oral route produced lesions in the oesophageal mucosa, kidneys, heart and thymus, indicating a general cytotoxic effect (Seawright et al., 1999). Oral dosing of *C.raciborskii* extract resulted in a lowest lethal dose within the test group of 4.4 mg/kg CYN equivalent after 4 days, with a median lethal dose of between 4.4 and 6.9 mg/kg after 5-6 days (Seawright et al., 1999). Shaw et al., (2000) confirmed the oral $LD_{50}$ for cell-free extract as 6 mg/kg CYN equivalent. In the case of pure CYN, the 24 hour $LD_{50}$ in mice dosed via the intraperitoneal (I.P.) route was 2.1 mg/kg, with the $LD_{50}$ after 5 days approximately ten-fold lower, at 0.2 mg/kg (Terao et al., 1994). These observations suggest a somewhat delayed activity compared to many cyanobacterial toxins. For example, the most potent forms of microcystin can kill mice within 1-2 hours of exposure, and cyanobacterial neurotoxins in the saxitoxin family of compounds exhibit lethal activity within 15 minutes (Falconer, 1999).

In treated mice, CYN consistently induces lipid accumulation in the liver, an effect seen in animals dosed with purified CYN or a cell-free extract of *C.raciborskii* via both intraperitoneal and oral routes (Hawkins et al., 1985; Seawright et al., 1999; Shaw et al.,

2000; Terao et al., 1994). Lipid vacuolation in the cytoplasm of hepatocytes was attributed to a possible disruption of protein synthesis, after ribosome detachment from the endoplasmic reticulum was observed in electron microscopic examinations of liver sections (Terao et al., 1994). Loss of protein synthesis and a subsequent reduction of lipoprotein formation was suggested by Terao and colleages (1994) as a possible cause of the observed lipid accumulation. The authors confirmed this hypothesis using an *in vitro* translation assay. The inhibitory effects of CYN on protein synthesis have since been further characterised *in vitro,* and are discussed in more detail below (Section 1.2.3).

### *1.2.3 DNA damage*

The presence of a uracil moiety in the structure of CYN led to speculation that an interaction with nucleic acids may occur, and that DNA damage may arise due to the potentially reactive guanidinium moiety (Humpage et al., 2000). Indeed, Shaw et al. (2000) showed that CYN could produce an adduct that was detectable in DNA purified from the liver of treated mice. The authors suggested that adduction may possibly be due to a CYN metabolite resulting from the action of liver-specific enzymes. The potential for genotoxicity has also been investigated using the cytokinesis-block micronucleus (CBMN) assay in a lymphoblastoid cell line (Humpage et al., 2000) and by assaying DNA fragmentation *in vivo* (Shen et al., 2002b).

CBMN assays revealed an increase in the number of micronuclei of 8-fold compared to control cultures after treatment with 10 µg/ml CYN for 24 hours. A unique feature observed in CYN-treated cultures was the occurrence of 'multimicronucleated' cells in which nuclei appeared to have degraded into multiple fragments (Humpage et al., 2000). This did not occur with the model clastogen, mitomycin-c. Staining for centromeres revealed the presence of whole chromosomes within micronuclei, suggesting that in addition to inducing double-stranded DNA breaks, CYN produced an aneugenic effect (loss of whole chromosomes; Humpage et al., 2000).

Shen et al., (2002) further investigated the potential for CYN genotoxicity by examining fragmentation of chromosomal DNA isolated from the livers of mice treated dosed intraperitoneally with 0.2 mg/kg CYN. The data revealed that DNA strand breakage occurred *in vivo*, confirming the aforementioned *in vitro* observations (Humpage et al.,

2000), although it is not clear whether the observed DNA fragmentation is directly attributable to CYN, a result of cell death by apoptosis, or simply due to degradation of free DNA following hepatocyte necrosis.

Although no conclusive studies have been undertaken, a preliminary investigaiton revealed limited evidence of tumour formation in mice dosed with *C.raciborskii* extracts (Falconer and Humpage 2001). While findings were not statistically significant, the authors stressed the requirement for further investigation. A subsequent study of the effects of untreated and chlorine-treated cell-free extracts of *C.raciborskii* in p53-deficient mice did not result in tumour growth (Senogles-Derham et al., 2003), but it must be considered that doses were relatively low (CYN daily intake of 0.03 μg/kg), and that the study was not designed as an assessment of the carcinogenic potential of purified CYN. The tumour-promoting potential of CYN was investigated by assaying for protein phosphatase inhibition by CYN (Chong et al., 2002). No inhibition was detected, indicating that CYN would probably not de-regulate cellular proliferation as has been predicted for the microcystins.

In cultured Chinese hamster ovary cells (CHO K1 cells) treated with CYN, DNA damage did not occur, as measured using the comet assay, but cell morphology was significantly altered (Fessard and Bernard, 2003). Rounding up of cells occurred after 24 hours at 0.5 μg/ml and 1 μg/ml CYN, and some blebbing was observed. The comet assay did not reveal significant DNA damage at these dosage levels, although in the aforementioned study by Humpage et al. (2000) this was the lowest concentration used, the highest being ten-fold greater. Fessard and Bernard (2003) also investigated the induction of apoptosis, which only occurred at very low levels above control cultures, and was not considered significant. This is in agreement with observations in human lymphoblastoid cells, where even high CYN concentrations did not appear to induce apoptosis (Humpage et al., 2000). Cell morphology was seen to be altered in the early stages of treatment in CHO K1 cells, prior to membrane disruption (Fessard and Bernard, 2003), suggesting that CYN causes cell death in CHO cells by a mechanism different to that occurring in primary hepatocytes. Like isolated primary hepatocytes, CYN-mediated DNA damage observed in liver extracts (Shen et al., 2002b), may be due to metabolic 'activation' via enzymatic processes. In other cell types, it may be possible that DNA damage only occurs at very high CYN concentrations as a downstream result

of protein synthesis inhibition—possibly via the depletion of DNA repair enzymes or DNA binding proteins such as histones.

### *1.2.4 Inhibition of protein synthesis*

In primary mouse hepatocytes, CYN toxicity was shown be associated with a significant depletion of reduced glutathione (GSH) (Runnegar et al., 1994). Subsequent investigations revealed that CYN inhibited GSH synthesis (Runnegar et al., 1995b). Terao et al. (1994) had also shown that CYN inhibits protein synthesis in cell-free rabbit reticulocyte lysates, indicating that the apparent inhibition of GSH synthesis may be symptomatic of a more generalised effect on protein synthesis at the level of translation, resulting in the depletion of GSH-synthetase levels. In support of this were observations in liver sections from treated mice of a dissociation of ribosomes from the endoplasmic reticulum, an effect also seen following treatment with cycloheximide, a well-described protein synthesis inhibitor (Terao et al., 1994). Humpage et al. (2000) hinted at the involvement of protein synthesis inhibition in CYN-mediated aneugenesis, since a disruption of mitotic processes may arise from a deficiency in cytoskeletal proteins such as tubulin. Further investigations into the concentration-dependent effects on *in vitro* protein synthesis resulted in the development of a sensitive assay for the toxin (Froscio et al., 2001). A similar system has also been used to test the toxicity of various synthetic analogues (Runnegar et al., 2002), and a recent study shows that plant protein synthesis is also inhibited by CYN (Metcalf et al., 2004).

Despite some similarities, a detailed comparison of the *in vivo* effects of CYN with those of cycloheximide revealed differences that suggest a more complex mode of action than simply the inhibition of translation (Terao et al., 1994). Specifically, lipid droplet accumulation in the livers of treated animals was suggested as a possible indication of the involvement of free radicals in CYN toxicity. The fact that the main target organ is the liver indicates a possible involvement of the unique metabolic processes that occur in this organ. Shaw et al. (2000) found that liver damage in mice occurred mainly in the periacinar region, where CYP450 activity is localized. Inhibition of cytochrome-P450 (CYP450) enzymes improves the survival of primary hepatocytes treated with CYN (Runnegar et al., 1995b), and primary hepatocytes are considerably more susceptible to CYN toxicity than continuous cell lines (Chong et al., 2002; Shaw

et al., 2000). This has been attributed to CYP450 activity by a number of researchers (Runnegar et al., 1994; Shaw et al., 2000). The currently accepted hypothesis is that CYP450-mediated metabolism of CYN may result in the formation of a compound with enhanced cytotoxicity and a different mode of action. Froscio et al. (2003) have confirmed that CYN-mediated cytotoxicity and translational inhibition can be considered as distinct—in CYN-treated primary mouse hepatocytes, CYP450 inhibitors significantly reduced cytotoxicity but had little effect on protein synthesis inhibition. The authors suggest that while protein synthesis inhibition is probably responsible for the general effect in all cell types, it may not be the primary cause of acute toxicity in hepatocytes. The need further investigation into the processes involved in bio-activation of CYN is clear.

### *1.2.5 Investigating the molecular basis of cylindrospermopsin toxicity*

The specific molecular interactions that result in CYN-mediated toxicity are currently not known. Shaw et al. (2000) have suggested that the covalent binding of CYN or a metabolite to nucleic acids *in vivo* may be associated with protein synthesis inhibition due to disruption of enzymatic activity (e.g. transcription of DNA or base-pairing between tRNA and mRNA during translation). As previously mentioned, the concept of a non-covalent interaction (hydrogen bonding) between the uracil moiety of CYN and adenine residues in cellular nucleic acids has been postulated The possibility of DNA intercalation has also been shown using molecular modelling (Falconer, 2005), suggesting another possible mode of interaction.

In primary mouse hepatocytes, DNA damage measured using the comet assay was shown to be reduced by CYP450 inhibitors (Humpage et al., 2005). Conversely, the induction of centromere-negative micronuclei in human lymphoblastoid cells occurs without apparent dependence on phase I metabolism, though at significantly higher CYN concentrations (Humpage et al., 2000). As mentioned above CYN was not genotoxic to CHO K1 as measured using the comet assay (Fessard and Bernard, 2003). These data indicate that there may be differing mechanisms of DNA damage, depending on the metabolic capabilities of the target cell.

The possibility of a role for oxidative stress in genotoxicity induced by CYN has also been investigated (Humpage et al., 2005). This avenue of research was stimulated by

findings that CYN causes depletion of glutathione (Runnegar et al., 1994; Runnegar et al., 1995b), and hence alters the redox state of the cell. While genotoxic effects were clearly apparent in primary mouse hepatocytes after CYN exposure, Humpage and colleagues (2005) did not find any evidence for the involvement of oxidative stress. These contradictory findings highlight our lack of understanding of the processes underlying DNA damage in CYN-exposed cells and tissues, a facet of CYN cytotoxicity with important implications for chronic exposure.

The inhibition of protein synthesis by CYN is likely to be the principal mode of action in cells not capable of expressing enzymes capable of the putative metabolic activation of CYN (Froscio et al., 2003). That CYN inhibits mRNA translation has been comprehensively established by two independent groups using *in vitro* translation assays based on rabbit reticulocyte lysates (Froscio et al., 2001; Froscio et al., 2003; Terao et al., 1994). Froscio and colleagues (2003) showed that in primary mouse hepatocytes CYP450 inhibitors do not affect on protein synthesis inhibition by CYN, but reduce cytotoxicity measured using cell membrane integrity assays. Translational inhibition was not affected by CYP450 inhibitors, and as such can probably be attributed to the native compound. The accumulated evidence suggests strongly that metabolism in rodent hepatocytes results in the generation of potent derivative with a different mode of action to that of native CYN, but the nature of the metabolite, and the specific enzymes responsible, are yet to be determined. Similar investigations in human primary hepatocytes and other cell types are clearly needed.

While CYN cytotoxicity is investigated in a number of human-derived cell types in Chapter 2 of this thesis, the focus of the project was to investigate mechanisms underlying CYN toxicity using an approach based around determining changes in gene expression elicited by the toxin at the whole-genome level.

## 1.3 Gene expression profiling in toxicology

Traditional toxicological approaches, such as dose-effect studies in animals, provide important information about potential effects in humans but do not generally offer insight into molecular mechanisms of toxicity. Mechanism-based risk assessment involves evaluating the potential toxicity of a compound by determining the mode of action, which can predict particularly dangerous effects such as genotoxicity and

carcinogenicity (Pennie et al., 2004), and is a concept of great appeal to toxicologists and pharmacologists alike. The varied effects of different classes of toxic compounds result in defined changes in the gene expression profiles of tissues or cells (Huang et al., 2004). These alterations in patterns of mRNA transcripts (i.e. changes in the transcriptome) can be detected using a powerful nucleic acid hybridisation technique known as microarray analysis.

In the last two decades, rapid advances in genomics have helped to identify large numbers of functional genes. The exploitation of this data for the production of DNA probes has facilitated the advent of a method for large-scale gene expression analysis known as DNA microarray technology (Shena, 1995). Microarrays (Figure 1.2) are arrangements of up to hundreds of thousands of probes, consisting of either oligonucleotides or complementary DNA (cDNA), immobilised on glass slides or nylon membranes. For transcriptional studies, each probe is derived from a known messenger mRNA transcript, such that a high-density array can represent a large proportion of the protein-coding transcripts in a cell. In a competitive microarray experiment, mRNA from different sample groups is labelled with different fluorophores during the enzymatic synthesis of complementary DNA or RNA. Hybridisation to spotted probes on the array, followed by scanning and determination of spot intensity ratios indicative of relative mRNA quantity. Data processing and statistical analysis reveals changes in relative transcript level between samples, inferring genes that are induced or repressed in response to a given stimulus. The end result is effectively a snapshot of the gene expression occurring at the time of sampling—performing multiple analyses at different time points or treatment regimes results in the generation of gene expression profiles.

Commonly referred to as ‘toxicogenomics’, the use of microarray-based gene expression analysis to define responses to a toxic compound at a molecular level is gaining popularity. There are a number of proposed applications in toxicology and pharmacology (Afshari et al., 1999):

- Determining safety limits for drug clinical trials
- Identification of toxic substances by comparison of gene expression patterns with those arising from known toxins

- Elucidation of toxic mechanisms by identification of gene expression networks
- Assessing exposure to a toxin by using toxicant-induced gene expression as a biomarker
- Extrapolating the effects of toxins between different species
- Assessing differences between acute and chronic exposure

Microarray formats utilised in toxicogenomics range from focussed arrays of one to two thousand genes involved in xenobiotic metabolism and stress responses, to high-density arrays covering the majority of protein-coding genes for a given animal model or cell line. One of the most promising uses for the technology is the generation of expression profiles characteristic of a given class of chemical compounds. This data could be applied to problems such as predicting the toxicity of novel pharmaceuticals, or identifying classes to which newly identified toxins belong. This concept relies on the fact that in a given model, changes in gene expression in response to chemical exposure are specific to a compound or class of compounds. Numerous reports of class-specific expression profiles can be found in the literature.

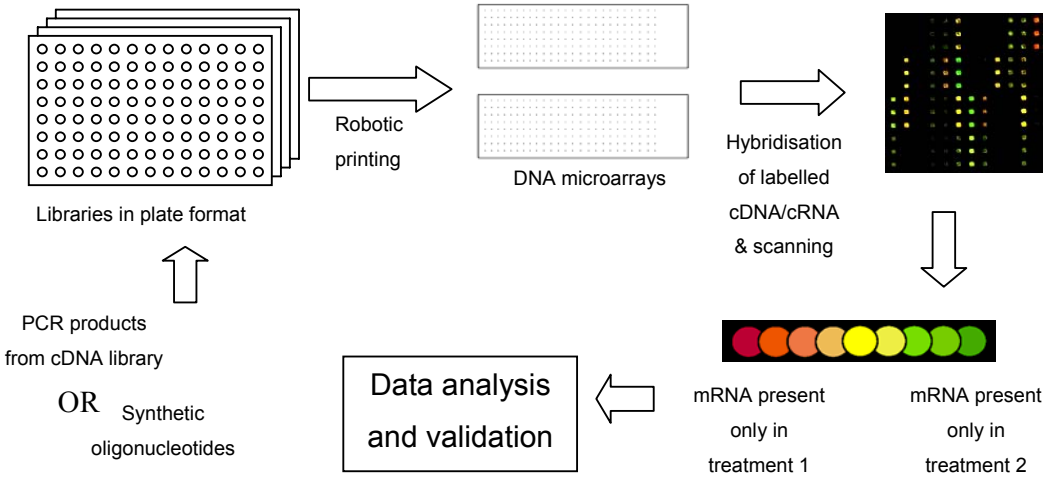


**Figure 1.2 Overview of DNA microarray technology.** Brief flowchart of a typical microarray procedure, from spotting DNA onto solid supports such as a glass slides, to hybridisation, in this case a direct competetive hybridisation, followed by scanning and data analysis.

Microarray-generated gene expression profiles obtained from rat livers following dosing with various hepatotoxicants correlated well with histopathological observations (Waring et al., 2001). Changes in gene expression were also consistent with the modes of action of the various toxins. Another group, also working with rat hepatotoxins, used microarrays to generate expression profiles specific to particular classes of compounds (Hamadeh et al., 2002b). The authors used a ~1,700-gene array and could distinguish changes in gene expression resulting from treatment with two classes of chemicals: peroxisome proliferators and enzyme inducers. Applying this technique in the analysis of liver RNA from rats treated with an unknown compound belonging to one of these classes, the same authors were able to successfully predict the class of compound to which the rats were exposed (Hamadeh et al., 2002a).

While class prediction and toxin identification represent attractive applications for large-scale expression profiling, the amount of data currently available is probably not sufficient to enable accurate identification of toxin classes based purely on gene expression profiling. The situation is further complicated by the sheer number of different array platforms available and the variability in responses displayed by different animal and cell models. Extrapolating animal data to estimate human risk assessment is also an issue of concern. Multifaceted approaches involving the use of human-derived cell cultures in addition to animal models may help to address these issues.

***Inference of toxic mechanism using microarray-based expression profiling.*** Although there is considerable enthusiasm for the potential application of transcriptional profiling in determining mechanisms of toxicity, there are currently relatively few examples in the literature. Reilly et al., (2001) identified new possible modes of action of the well-characterised hepatotoxin acetaminophen (APAP) using microarray analysis of liver injury in mice. An *in vitro* analysis of ochratoxin A using a toxicology-specific array proved useful in determining early changes in cells exposed to the toxin (Gennari et al., 2004). The only human study so far was conducted in China, where global gene expression in liver biopsies from arsenic-exposed and non-exposed individuals were compared (Lu et al., 2001). The mechanisms implicated by transcription profiling correlated closely with the observed effects, which included tumour formation in the liver. Lead toxicity was also investigated *in vitro* using microarray technology, resulting in the identification of proteins involved in disruption of the blood-brain barrier (Bouton

et al., 2001; Hossain et al., 2000). Recently, possible mechanisms of a potential cancer chemotherapy agent were elucidated using microarray analysis (Zhang et al., 2004). As array technology improves, the number of successful investigations based on large-scale expression profiling will undoubtedly increase.

***Microarrays in biomarker discovery.*** Another promising application of toxicogenomics is the development of biological markers of toxin exposure. Biomarkers are useful for assessing exposure of test animals to toxic compounds at low doses that would not normally result in gross histopathological abnormalities. Additionally, biomarkers comprising serum or urine components indicative of toxin exposure are vital for human epidemiological toxicology studies—the discovery of characteristic endpoints that can replace corresponding clinical endpoints of toxicity is possible through the identification of biomarkers (Ilyin et al., 2004).

Amin et al., (2004) have identified biomarkers of kidney damage induced by various nephrotoxins. Damage to specific areas of the kidney could be defined by the distinct expression profiles obtained, and there was a specific response to each toxin tested that allowed the elucidation of gene-based markers (Amin et al., 2004). Similarly, Harris et al., (2004) evaluated hepatic responses to various toxic challenges using microarrays and suggested that identification of biomarkers of exposure may be possible. Putative transcriptional markers of exposure to low-dose gamma radiation have also been identified using microarray analysis (Amundson et al., 2000). Determination of easily detectable markers of adverse responses is often required during the development of pharmaceutical drugs, where microarrays have also proven useful (Suter et al., 2004).

***Caveats and considerations.*** Limitations of transcriptional profiling become apparent when factors associated with biological experiments are considered. For example, gene expression responses may differ considerably between species, and even in the case of housekeeping genes in different strains of the same species of model organism (Lee et al., 2002). The effects observed in cultured cells may differ greatly from that seen in whole organisms (or tissues or organs thereof). This point is well illustrated by a study comparing the transcriptome of primary liver cells to that of whole liver (Harris et al., 2004). After 24 hours, and as time in culture progressed, primary hepatocytes appeared to lose the expression of many genes normally strongly expressed in whole liver.

Common problems encountered during a microarray experiment include variability between printed arrays, and issues associated with RNA quality and labelling efficiency. Array quality is increasing as commercial companies fine-tune production techniques, and inter-array or inter-spot variability is usually only a problem with smaller print runs. Biological replicates should be utilised wherever possible, and technical replicates are often useful in determining non-biological variation in the resulting data. Considering to the relative expense involved in purchasing arrays and the amount of time required for data analysis, cost can become a limiting factor when planning a microarray experiment.

Variation across different platforms and animal or cell models can be considerable, reducing the potential for inter-laboratory comparisons of microarray data. However, despite some degree of variation, a study using the same animal model in different laboratories with different microarray platforms resulted in the identification of gene expression changes associated with the same biological pathways (Ulrich et al., 2004). Further development in this area, particularly with respect to establishing uniform models and array technologies across institutions, may enable the development of a reliable system allowing the identification of novel toxins, and the prediction of toxicity of compounds such as new drugs.

Another point to consider is that gene expression (from gene to protein) is a complex process governed not only by transcription but also by many translational and post-translational events that cannot be measured using DNA arrays. In the context of molecular toxicology, this complexity has been acknowledged (Choudhuri, 2004) and must be taken into account when considering the biological significance of changing mRNA levels. It may be important to concurrently investigate protein quantity (or phosphorylation status) before definite conclusions can be drawn regarding the expression of particular genes.

## 1.4 Validation of microarray data

Ratification of microarray analysis is often achieved using alternative methods for mRNA quantification such as Northern blotting or quantitative reverse-transcription polymerase chain reaction. As a quantitative technique, qRT-PCR is considerably more sensitive than Northern blotting and has been employed in numerous studies as a

reliable means of validating microarray data (Ace and Okulicz, 2004; Rajeevan et al., 2001).

Real-time monitoring of PCR reaction products can be achieved using a wide variety of chemistries. One of the simplest is based on the detection of double-stranded DNA (dsDNA) using SYBR Green I (Schneeberger et al., 1995). SYBR Green I is an intercalating dye that exhibits greatly increased fluorescence when bound to dsDNA, and is therefore useful in detecting amplification products in a PCR reaction. The drawback is that the resulting detection is not sequence-specific. This can be taken into account by generating melt peaks derived from dissociation curves for each amplicon. Because SYBR Green I exhibits little fluorescence when not bound to double-stranded DNA, capturing fluorescence over time while increasing temperature will reveal the melting temperature of the reaction products. Taking the negative first derivative of the dissociation curves results in a graph showing melt peaks centred around the melting temperature of the DNA duplex. A single peak will result if the PCR primers are specific, while multiple peaks, each dependent on amplicon size and G+C content, will result from non-specific amplification. This procedure allows the differentiation of specific amplification products and co-amplified artifacts such as primer dimers (Ririe et al., 1997). Provided primer specificity is high and the reaction is well optimised for each targeted transcript, this is a powerful and economical technique for mRNA quantification.

Further validation of microarray data can be achieved by investigating expression at the level of protein, since post-transcriptional events play a large role in determining whether a gene is truly expressed. Western blotting with specific antibodies can be used to check both quantity and phosphorylation status of signalling proteins involved in altered gene expression (Vrana et al., 2003).

## 1.5 Aim of the current study

The primary aim of the project was to determine the effects of cylindrospermopsin on global gene expression in cultured human cell lines, in order to provide further insight into the molecular processes underlying known mechanisms of CYN toxicity and to discover new putative mechanisms.

## 1.6 Experimental approaches

Presented below is a flow diagram representing the experimental approaches used to address the aim of the project.

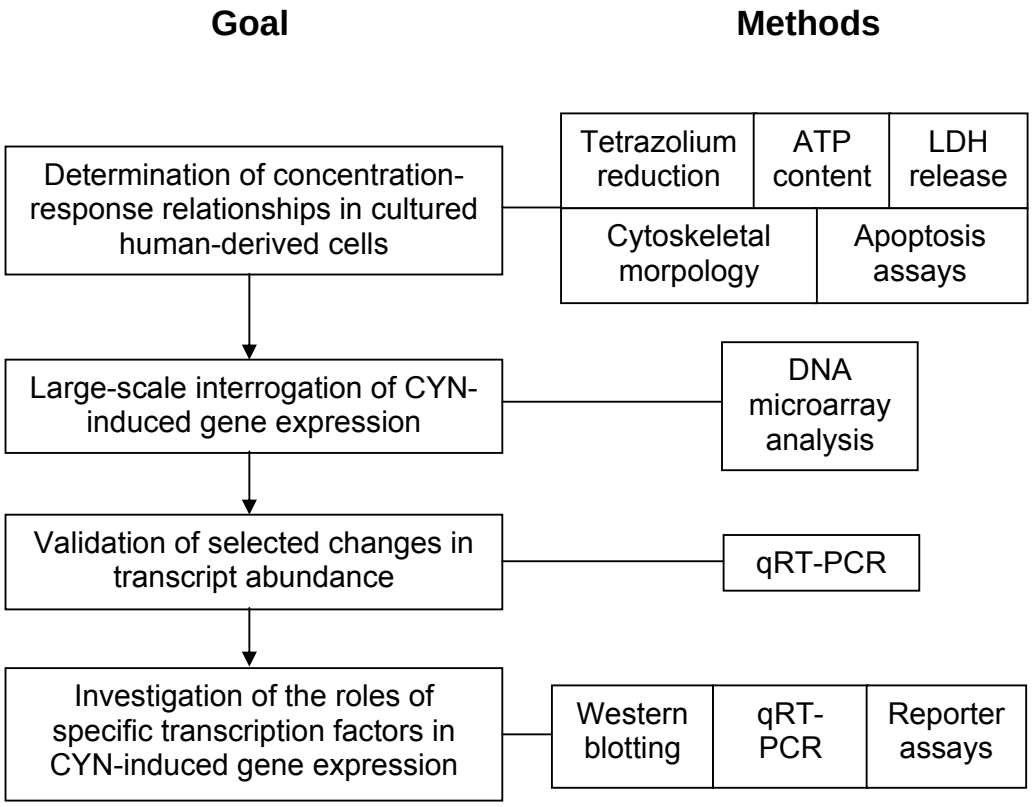


**Figure 1.3 Flowchart of experimental approaches.**

# Chapter 2

## *Assessment of cylindrospermopsin toxicity in cultured human-derived cells*

### 2.1 Introduction

At the commencement of this project, a comprehensive investigation of cylindrospermopsin (CYN) toxicity in human cell lines had not been reported, with existing literature focusing on toxicity in rodents and in primary rodent hepatocytes. It was therefore necessary to determine concentration-response relationships for endpoints relevant to cytotoxicity in a range of cultured human-derived cell types prior to investigating responses at the level of gene expression.

In cultured cells, cytotoxicity is variously defined using assays that measure membrane integrity, metabolic rate, proliferation, apoptosis, or cytoskeletal structure. Measuring different endpoints can result in wide variations in $EC_{50}$ values for a particular compound (Weyermann et al., 2005), suggesting that the best approach when investigating a toxin in a given model to utilise a variety of assays.

#### *2.1.1 Tetrazolium reduction – MTT and MTS assays*

This assay estimates cell number and viability relative to control cultures by measuring metabolic activity. The basis of the assay lies in the ability of cellular reductases to cleave the tetrazolium ring structure, resulting in the generation of formazan products and an associated change in the colour of the compound. The most commonly used tetrazolium compound is (3-(4,5-dimethylthiazol-2-yl)-2,5-diphenyl tetrazolium

bromide (MTT). Reductase activity is related to cellular metabolic rate, such that the rate of reduction of tetrazolium to formazan products is proportional to metabolic activity in a cell population. Tetrazolium compounds can be reduced by complexes of the mitochondrial respiratory chain or cytosolic reductases—using succinate as an electron donor, MTT is reduced in mitochondria by a complex II enzyme, succinate dehydrogenase, and via an additional process involving cytochrome *c* (Slater et al., 1963), but if NADH and NADPH are used as electron donors, most MTT reduction occurs externally of mitochondria in soluble fractions of the cytoplasm (Berridge and Tan, 1993). Thus, MTT reduction can be seen as a general indicator of the amount of reduced electron carriers in the cell and hence provides a measure of metabolic activity in a cell population.

A simple colorimetric assay for MTT reduction facilitates the rapid measurement of cellular proliferation and cytotoxicity (Mosmann, 1983). In brief, the assay involves incubating cells in culture with MTT, which is converted in metabolically active cells from the native yellow compound to the insoluble, vivid blue MTT-formazan. An acidic reagent is added to solubilise the product, and the absorbance of light at the appropriate wavelength is then measured in a spectrophotometer. The assay is suitable for the simultaneous testing of many parameters and is easily performed in a 96-well culture plate. Alternative tetrazolium compounds that omit the need for a solubilisation reagent have been investigated in order to simplify the assay. One compound, 3-(4,5-dimethylthiazol-2-yl)-5-(3-carboxymethoxyphenyl)-2-(4-sulfophenyl)-2H-tetrazolium, inner salt (MTS), is converted to highly soluble formazan products and is more readily reduced than MTT in certain cell types (Cory et al., 1991). The use of MTS, combined with a suitable electron acceptor, simplifies the protocol by omitting the need for solubilisation procedures. A commercially available MTS reduction assay (Promega, 2003b) is employed in the present study as an indicator of the metabolic activity of cells in culture.

### *2.1.2 ATP assays*

ATP assays provide an alternative method of assessing relative cell number or metabolic activity. In living cells, chemical energy is produced, stored and utilised in the form of phosphorylated nucleosides, primarily ATP. Disruption of metabolic

processes resulting in the depletion of ATP levels can result in catastrophic damage to cellular components and membranes, and subsequent cell death by necrosis.

In the present study, cellular ATP content is measured using the luciferase-luciferin bioluminescence assay (Higashi et al., 1985; Stanley, 1986). Firefly luciferase catalyses the ATP-dependent, chemiluminescent oxidation of luciferin (Kauzmann et al., 1949), with the amount of light emitted being linearly proportional to ATP concentration in a cell lysate.

### *2.1.3 Membrane integrity assays*

Disruption of the plasma membrane is a common form of cellular damage resulting from exposure to cytotoxic agents, occurring primarily as a result of necrotic cell death, but also in the late stages of apoptosis. This is commonly measured by one of two methods. Dye exclusion analysis involves suspending cells in a dye-containing solution and counting cells under a microscope—cells that exclude the dye are considered viable, while non-viable cells with disrupted membranes appear with dye visible throughout the cytoplasm. An alternative method relies on the leakage of cytoplasmic enzymes that can be detected using specific assays.

When membrane integrity is compromised, cytoplasmic proteins are released into the surrounding medium. In this report, cylindrospermopsin toxicity is assessed using a commercially available assay that measures lactate dehydrogenase (LDH) activity in culture media (Moravec, 1994). This assay is based on the methods of Decker and Lohmann-Matthes (Decker and Lohmann-Matthes, 1988), and Korzeniewski and Callewaert (Korzeniewski and Callewaert, 1983). In this assay, resazurin is reduced by NADH (in the presence of diaphorin) resulting from LDH-mediated oxidation of lactate to pyruvate, giving the fluorescent compound resorufin. After treatment with the compound of interest, fluorescence due to LDH activity is compared to that resulting from detergent-lysed control cultures.

### *2.1.4 Altered cytoskeletal morphology as an indicator of cytotoxicity*

The cytoskeleton is composed primarily of two types of filamentous protein structures—actin microfilaments, also known as filamentous actin or F-actin, and

microtubules, which are made up of polymerised α- and β-tubulin heterodimers (Alberts et al., 2002). Some cell types also contain filamentous structural proteins known as intermediate filaments, an example of which is the keratin family. The dynamic assembly and disassembly of actin microfilaments and microtubules is essential for their correct function (Mitchison, 1995). Modulation of cytoskeletal dynamics, resulting in the alteration of cell shape, is a direct mechanism of action of many cytotoxic compounds, but also occurs as part of the widespread changes induced during cell death by apoptosis. Naturally-occurring toxins capable of directly interfering with actin cytoskeletal dynamics include phalloidin, which binds and stabilises filamentous actin, and cytochalasin, which prevents filament assembly (Cooper, 1987). Inhibitors of microtubule dynamics include the stabilising compound taxol (Schiff et al., 1979; Schiff and Horwitz, 1980), and various tubulin-binding compounds such as vinblastine and colchicine that prevent polymerisation (Owellen et al., 1972).

Apoptosis also induces cytoskeletal rearrangements. During apoptosis, proteolytic enzymes known as executioner caspases cleave a large number of substrates (reviewed by (Fischer et al., 2003), including cytoskeletal proteins such as β-actin, α-tubulin, filamin, various keratins, and β-spectrin. As a result, caspases directly induce the characteristic morphological changes associated with apoptosis. In culture, the early stages of apoptosis visible as ‘rounding up’, where adherent cells gradually adopt a rounded appearance, displaying reduced contact with the flask surface in the region of the cell periphery. As apoptosis progresses, cells become almost spherical and release membrane blebs prior to the complete fragmentation of the cell and detachment from the growth surface.

CYN has been shown to affect the morphology of CHO cells (Fessard and Bernard, 2003), and is a proposed modulator of microtubule assembly in human lymphoblastoid cells, increasing the frequency of aneuploidy (Humpage et al., 2000). It is not clear whether CYN directly affects the assembly or stability of filamentous actin or microtubules. In this chapter, cytoskeletal structure following CYN exposure was assessed to determine whether CYN is a direct inhibitor of cytoskeletal dynamics.

### 2.1.5 Death by cylindrospermopsin: apoptosis or necrosis?

Cell death occurs by one of two means—apoptosis, a highly regulated process often referred to as 'programmed cell death', or necrosis, an unregulated process resulting in disruption of the plasma membrane and leakage of cellular contents into the surrounding environment. In the body, apoptosis prevents inflammation by breaking cells down into small blebs that are rapidly engulfed by macrophages. Conversely, necrosis results in the release of all endogenous cellular material, including factors that induce extensive inflammation in surrounding tissue. Necrosis is widely regarded as a passive form of cell death resulting from the depletion of cellular adenosine triphosphate (ATP), and is often associated with toxic insult (Edinger and Thompson, 2004). Apoptosis, on the other hand, requires ATP and is tightly regulated, playing an important role in tissue remodelling during development, and cellular 'suicide' in response to exogenous signals such as tumour necrosis factor (TNF), or intracellular signals resulting from excessive damage to essential cellular components (e.g. DNA damage).

Early-stage apoptosis can be differentiated experimentally from necrosis and late-stage apoptosis by analysing membrane integrity—apoptotic cells retain membrane integrity until the late stages of the process, while membrane disruption is a hallmark of necrotic cell death. CYN induces LDH release in primary rodent hepatocytes within 24 h (Froscio et al., 2003; Humpage et al., 2005; Runnegar et al., 1994), suggesting necrotic cell death, while no increase in the number of necrotic cells was observed in human lymphoblastoid cells treated for 24 h with up to 10 μg/ml CYN (Humpage et al., 2000).

### 2.1.6 Chapter aims and outcomes

The primary objective of the project as a whole was to investigate altered gene expression in cultured human cells in response to cylindrospermopsin. To determine the most appropriate conditions for gene expression analyses, concentration-response relationships for various toxicological endpoints were established and are reported in the present chapter. CYN toxicity was determined in a range of human-derived cell types using well-established biochemical cytotoxicity tests, morphological indicators and apoptosis assays. Appropriate exposure conditions for subsequent investigations were defined.

## 2.2 Materials and Methods

### *2.2.1 Cell culture*

Cells used in this investigation (Table 1) were obtained from the American Type Culture Collection (ATCC), except for primary human dermal fibroblasts, which were kindly provided by Emily Dunner of Dianne Watters' laboratory (Griffith University). Late passage number Caco-2 and HepG2 cells were originally provided by Sarah Wilkins (Queensland Institute for Medical Research). HepG2 and Caco2 cells from ATCC were the gift of Ngari Tinkle (National Research Centre for Environmental Toxicology). All cell types were grown at 37ºC under a 5% $CO_2$ humidified atmosphere in Dulbecco's modified Eagle's medium (DMEM, Gibco-Invitrogen), containing 4.5 g/L glucose, 42 µg/mL L-glutamine, 110 µg/mL sodium pyruvate, 4 µg/mL pyridoxine-HCl, and supplemented with 10% foetal bovine serum (Gibco-Invitrogen), 100 units/mL penicillin (Gibco-Invitrogen) and 100 µg/mL streptomycin (Gibco-Invitrogen). Antibiotics were omitted for toxin exposures.

**Table 2.1** Cell types used in the current study.

| Designation | ATCC number | Description |
|---|---|---|
| HDF | — | Human dermal fibroblasts (primary diploid fibroblasts from skin biopsy) |
| HepG2 | HB-8065 | Hepatocellular carcinoma |
| Caco-2 | HTB-37 | Colorectal adenocarcinoma |
| HeLa | CCL2 | Cervical epithelial adenocarcinoma |

Cells were routinely maintained as monolayers in 25 $cm^2$ tissue-culture flasks fitted with 0.22 µm filter caps. Sub-culturing was carried out every 2 to 4 days upon reaching 70-90% confluence. For cell sub-culturing, monolayers were rinsed twice with PBS and incubated at 37°C with 1 mL of pre-warmed trypsin/EDTA solution until cells had detached from the flask surface. Fresh medium (2 to 3 mL) was added and separation of cells was achieved by gentle pipetting up and down. The resulting suspension was

diluted in fresh medium at a ratio of 1:2 to 1:10 depending on the growth rate of the cell line.

### *2.2.2 MTS assays*

For toxin treatments, cells were trypsinised, resuspended in antibiotics-free medium, counted using a haemocytometer and seeded into clear, tissue culture-specific 96-well plates. For HepG2, C3A, HeLa and Caco-2 cells, 5000 cells were seeded in triplicate in a total of 0.1 mL medium. For HDFs, cells were seeded at 2000 cells per well. To allow for background absorbance due to factors present in the growth medium, three wells per treatment group contained media only. After 24 h incubation, media were exchanged with fresh pre-warmed media containing cylindrospermopsin at the indicated concentrations, or with medium containing vehicle only (Milli-Q water [MQW]). All wells contained an equal volume of vehicle in order to allow for dilution of the media.

MTS reduction assays were conducted after 24, 48 or 72 h toxin exposure, essentially according to the manufacturer's instructions (Promega, 2003b). Briefly, 10 µL of assay solution was added to each well and the plates incubated at 37°C, 5 % $CO_2$ for 1 to 3 h. Absorbance readings at 490 nm were measured using a standard plate reader (Molecular Devices). Mean background absorbance of the media-only wells was subtracted from absorbance readings for each well, and readings from toxin-treated wells were expressed as a percentage of those obtained from control wells.

### *2.2.3 LDH release assays*

Cells were seeded into 96-well opaque black tissue culture-specific plates (Corning) and treated as described above (Section 2.2.2), except that an additional vehicle control was included to provide a 'maximum LDH release' control, where cells are artificially lysed with detergent solution. After 24, 48 or 72 h incubation with toxin dilutions, LDH activity in the media was determined using a fluorescent LDH release assay (Promega, 2003c) according to the manufacturer's instructions. Briefly, plates were equilibrated to room temperature before adding 2 µL of lysis solution to one set of vehicle control wells. Following a short incubation (~1 min), 0.1 mL of assay reagent was added to each well and plate was incubated at room temperature (~22°C) for 10 mins on an orbital shaker at low speed. To stop the reaction, 50 µL of stop solution was added to

each well and mixed gently by shaking for 10 seconds by hand. Fluorescence was measured using 560 nm excitation and 590 nm emission filters in a Victor 2 plate reader (Wallac). LDH release was expressed as a percentage of fluorescence readings from detergent-lysed vehicle controls.

### *2.2.4 ATP assays*

Cells were seeded into 96-well plates in a total of 0.1 mL medium as described in Section 2.2.2. Medium-only controls (no cells) and vehicle controls (cells treated with MQW) were included. Treatments were conducted as described in Section 2.2.3). After 24, 48 and 72 h, cellular ATP content was measured using a luminescent ATP assay (Promega, 2003a) essentially as described by the manufacturer, except that following cell lysis, the assay mixture was transferred to white, opaque, 96-well plates to facilitate the reading of luminescence. Plates were equilibrated to room temperature prior to adding a volume of freshly prepared assay reagent to each well equal to the volume of growth medium. After a short incubation (~2 mins) on an orbital shaker at low speed, the solution containing lysed cells and assay reagent was transferred to the wells of white, opaque 96-well plates. Luminescence was read for 1 second per well using a luminescence-capable plate reader (Wallac). ATP content was expressed as a percentage of vehicle controls.

### *2.2.5 Apoptosis assays*

Cells were seeded at a density of $5x10^4$ cells per well into the wells of standard 24-well plates containing 10 mm glass cover slips. After overnight growth, media were replaced with medium containing CYN or an equal volume of vehicle (MQW). Treatments were performed in duplicate, and at least three independent experiments were conducted for each condition. After incubation as indicated, media were removed and the cells fixed by incubating with cold methanol for 5 minutes at -20°C. Cover slips were then immersed in PBS for 10 mins, prior to staining with 1 nM 4',6-Diamidino-2-phenylindole (DAPI) for 5 mins. After two gentle washes with PBS, cover slips were mounted on standard glass slides.

Images were captured using a fluorescence microscope (Nikon) fitted with a CCD camera connected to a computer running V++ software (Digital Optics). At least ten

random fields were captured from each cover slip at 200X magnification, with representative images captured at 400X magnification. Nuclei showing chromatin condensation, pronounced shrinkage or fragmentation were scored as apoptotic, and rates of apoptosis were expressed as a percentage of total cells counted. At least 600 cells were counted for each experimental condition.

### *2.2.6 Determination of changes in cell morphology*

Cells were seeded into the wells of standard 24-well plates (or 4-well miniature plates with equivalent volumes) containing glass cover slips (pre-sterilised by autoclaving), in a total of 0.5 mL growth medium. After 24 h growth, media were exchanged for fresh media containing toxin as indicated. Controls were treated with an equal volume of vehicle. After the indicated incubation times, cells were fixed and stained as follows.

***Filamentous actin staining using fluorescent phalloidin conjugates.*** After treatment, cells on cover slips were rinsed three times with PBS and fixed with 4% paraformaldehyde in PBS for 30 mins. After three rinses with PBS, cover slips were incubated with 50 mM glycine in PBS for 10 mins, followed by 0.25 % Triton-X100 in PBS for 10 mins. After rinsing briefly three times with PBS, cover slips were incubated in the dark for 30 mins with 50 ng/mL FITC-conjugated phalloidin and 4 ng/mL DAPI in PBS. After washing twice with 0.1 % triton X-100 and three times in PBS, cover slips were mounted on standard glass slides. Visualisation and imaging were performed as described in section 2.2.6.

***Immunofluorescence staining of microtubules and actin filaments***. Cells were grown on glass cover slips and treated as described above in section 2.2.6. Following a brief rinse in PBS, cells were fixed and permeabilised in cold methanol at minus 20°C for 6 mins. Methanol was removed and the cover slips immersed in PBS for 10 mins at room temperature. Cover slips were then incubated for 1 h in blocking solution (5 % BSA and 1 % goat serum in PBS), followed incubated overnight at 4°C with polyclonal primary antibody (rabbit anti-tubulin [Sigma-Aldrich] or rabbit anti-actin [Sigma-Aldrich]) diluted 1:60 in blocking solution. Following three washes in PBS for 5 mins each wash, secondary antibody (anti-rabbit IgG conjugated to TRITC [Sigma-Aldrich]) diluted 1:100 in PBS containing 5 % BSA and 1 % goat serum was added and the cover slips incubated at room temperature for 1 h. Specificity was confirmed by omitting the

primary antibody in selected wells. Cover slips were rinsed three times in PBS and mounted on standard glass slides. Visualisation and imaging were performed as described above in section 2.2.6.

## 2.3 Results

### *2.3.1 CYN inhibits MTS reduction*

As expected, cylindrospermopsin treatment inhibited MTS reduction in treated cell populations, indicating a relative decrease in cell number or general metabolic activity compared to controls. MTS reduction was inhibited in a dose-dependent manner in all cell lines tested after 24, 48 or 72 h exposure (Figure 2.1), with longer exposure times resulting in a greater inhibitory effect relative to controls.

In general, CYN concentrations above 1 μg/mL produced obvious inhibitory effects on MTS reduction after 24h, with an increased magnitude of inhibition apparent after longer exposures. The only primary cell type utilised in this study, human dermal fibroblasts (HDFs), showed a more pronounced separation of concentration-response curves for 24, 48 and 72 h than the transformed cell types, with the exception of HeLa cells which were also well-separated. HeLa cells appeared to be particularly susceptible to CYN after long exposure times. C3A cells responded in a similar fashion to HepG2, from which the C3A line is derived (data not shown).

The effect of CYN on MTS reduction in late passage number HepG2 and Caco-2 cells (greater than 50 passages) was compared with early passage number cells (between 3 and 15 passages) obtained from ATCC (Figure 2.1). HepG2 cells showed little difference between early and late passage number cells. Conversely, late passage number Caco-2 cells appeared to be less susceptible to CYN toxicity than early passage number cultures. This suggests that prolonged culturing may select for a subpopulation of Caco-2 cells that responds differently to early passage number cultures. This is consistent with reports of the apparent heterogeneity of the parent ATCC cell line that undergoes selection under various culture conditions (reviewed by Sambuy et al., 2005).

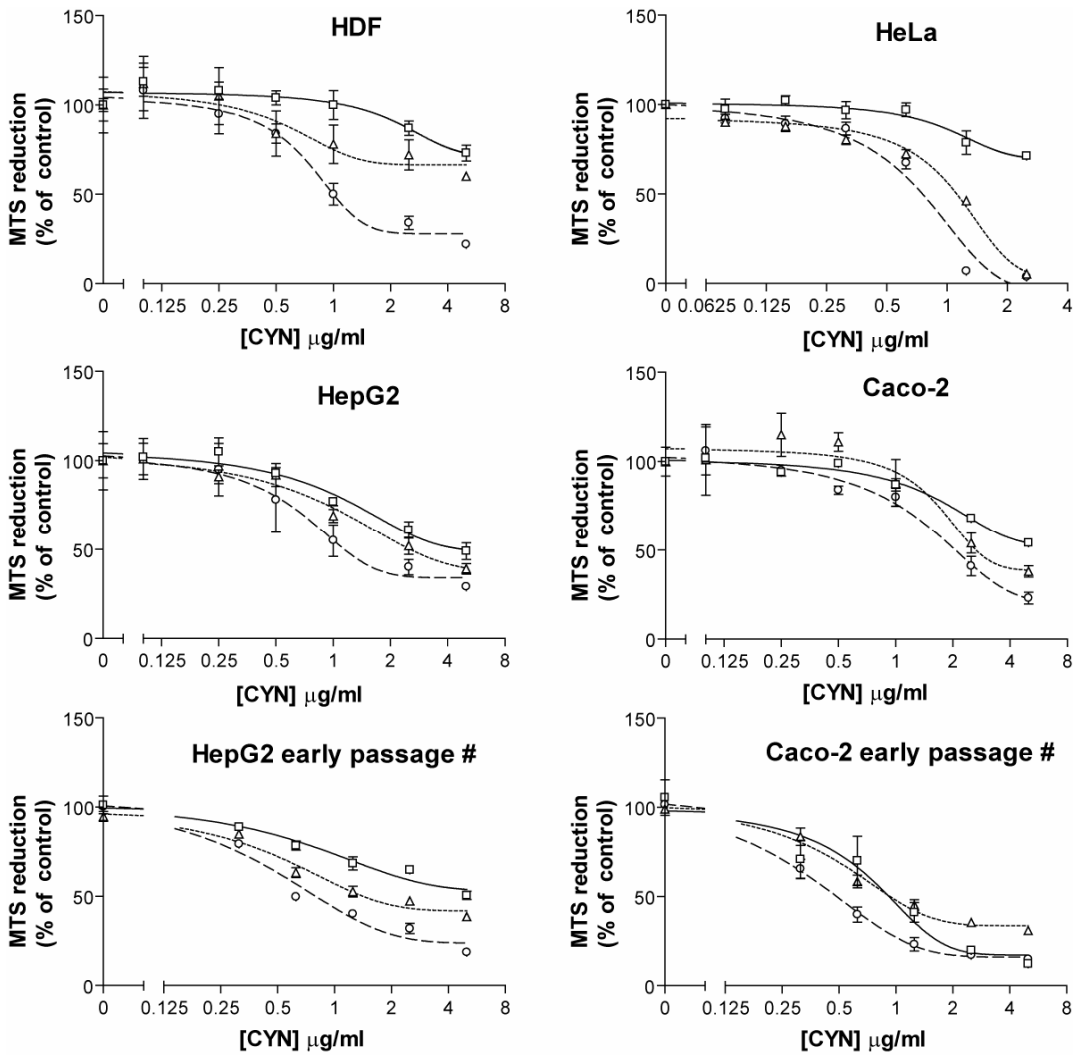


**Figure 2.1 The effects of CYN on MTS reduction.** Cells were treated for 24 h (—□—), 48 h (····△····), or 72 h (---○---), with 0, 0.1, 0.25, 0.5, 1 and 5 µg/mL cylindrospermopsin. Values are expressed as a percentage of MTS reduction in vehicle controls. Data points represent means ± SEM for three replicates, and are representative of at least two indepentent experiments. Non-linear regressions were performed using GraphPad Prism.

### *2.3.2 CYN treatment reduces ATP levels*

Following exposure to CYN for 24, 48 or 72 h, ATP levels were determined for two cell lines, HepG2 and HeLa (Figure 2.2). Dose-response curves for ATP content were similar to those obtained for inhibition of MTS reduction, although relative ATP content after 24 h appeared slightly higher than corresponding measurements for MTS reduction. Similar to the MTS assay results, HeLa cells displayed steep dose-response curves after 48 and 72 h, which is likely to be associated with the induction of apoptosis

in this cell line after these exposure times. Apoptosis is an ATP-dependent process that causes rapid depletion of intracellular ATP stores. In addition, the disruption of general metabolic activity by CYN, as suggested by the inhibitory effect on MTS reduction, is likely to cause a corresponding drop in ATP content. ATP levels were not investigated in the other cell lines used in this chapter.

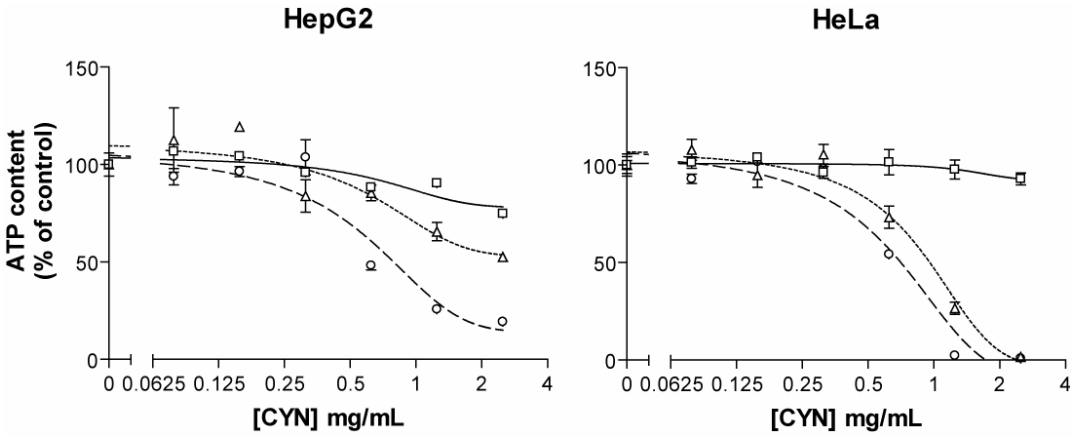


**Figure 2.2 Determination of ATP content in CYN-treated cells.** Cells were treated for 24 h (—□—), 48 h (····△····), or 72 h (---○---), with 0, 0.1, 0.25, 0.5, 1 and 5 µg/mL cylindrospermopsin, and ATP was measured using the luciferase-luciferin bioluminescence assay. Values are expressed as a percentage of control cultures. Data points represent means ± SEM for three replicates. Curves were fitted to the data using GraphPad Prism software (non-linear regression, sigmoidal dose-response curve).

### *2.3.3 CYN treatment does not induce rapid LDH release*

CYN treatment did not induce LDH leakage from HepG2 and Caco-2 cells (late passage number), even after 72 h exposure to concentrations of up to 5 µg/mL (data not shown). In HDFs, some LDH leakage occurred after 72 h exposure to concentrations above 0.5 µg/ml CYN, with no activity detectable after 24 or 48 h (Figure 2.3). The rapid release of LDH reported in CYN-treated primary hepatocytes (Froscio et al., 2003; Humpage et al., 2005; Runnegar et al., 1994) may be indicative of cell death by necrosis, which does not appear to occur in the cell lines used in this study. LDH leakage from HDFs after 48 h or more may be attributable to membrane disruption during the final stages of apoptosis. Alternatively, HDFs in culture may undergo cell death by both necrosis and apoptosis in response to CYN.

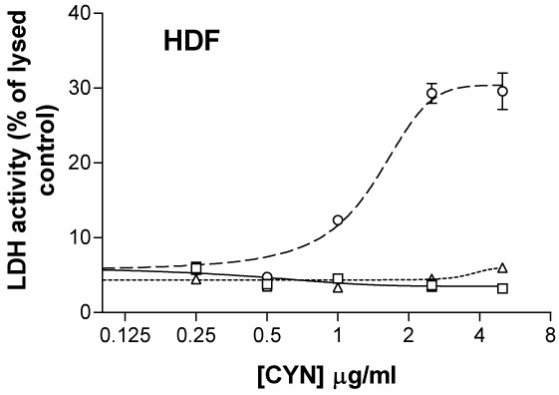


**Figure 2.3 LDH leakage from CYN-treated human dermal fibroblasts.** Lactate dehydrogenase release from human dermal fibroblasts treated with varying concentrations of cylindrospermopsin for 24 h (—□—), 48 h (····△····), or 72 h (---○---). Values are expressed as a percentage of activity in vehicle controls lysed with detergent. Data points represent means ± SEM for three replicates, and are typical of two independent experiments. Sigmoidal dose-response were fitted to data using non-linear regression (GraphPad Prism).

### *2.3.4 CYN induces apoptosis after prolonged exposure*

Apoptosis was assessed by examining DAPI-stained nuclei for chromatin condensation, fragmentation or pronounced shrinkage of the nucleus (Figure 2.4). It is important to note that this method detects only the late stages of apoptosis, and a more complete investigation could be achieved using a combination of more sensitive assays (caspase activity assays or TUNEL assays may be applicable). However, the method used in the present study did detect significant differences between rates of apoptosis in different cell lines used. It was apparent that HeLa cells underwent widespread apoptosis after 48-72 h exposure to 1 μg/mL CYN, with a significantly lesser proportion of apoptotic cells in HepG2 and HDF cultures under the same conditions (Figure 2.4B). There was no significant difference between rates of apoptosis in HDFs and HepG2 cells, which both required 72 h exposure for rates of apoptosis significantly different from controls.

### *2.3.5 Changes in cellular morphology in response to CYN*

***HDFs***. Under high CYN concentrations (10 μg/mL), HDFs stained for actin filaments showed signs of rounding up after 24 h exposure which was more pronounced after 48 h (Figure 2.5C). After 72 h exposure to this concentration, only a few cells remained attached to the cover slips. Interestingly, the morphology of these remaining cells did not appear to be apoptotic, suggesting that apoptotic cells may have been washed from

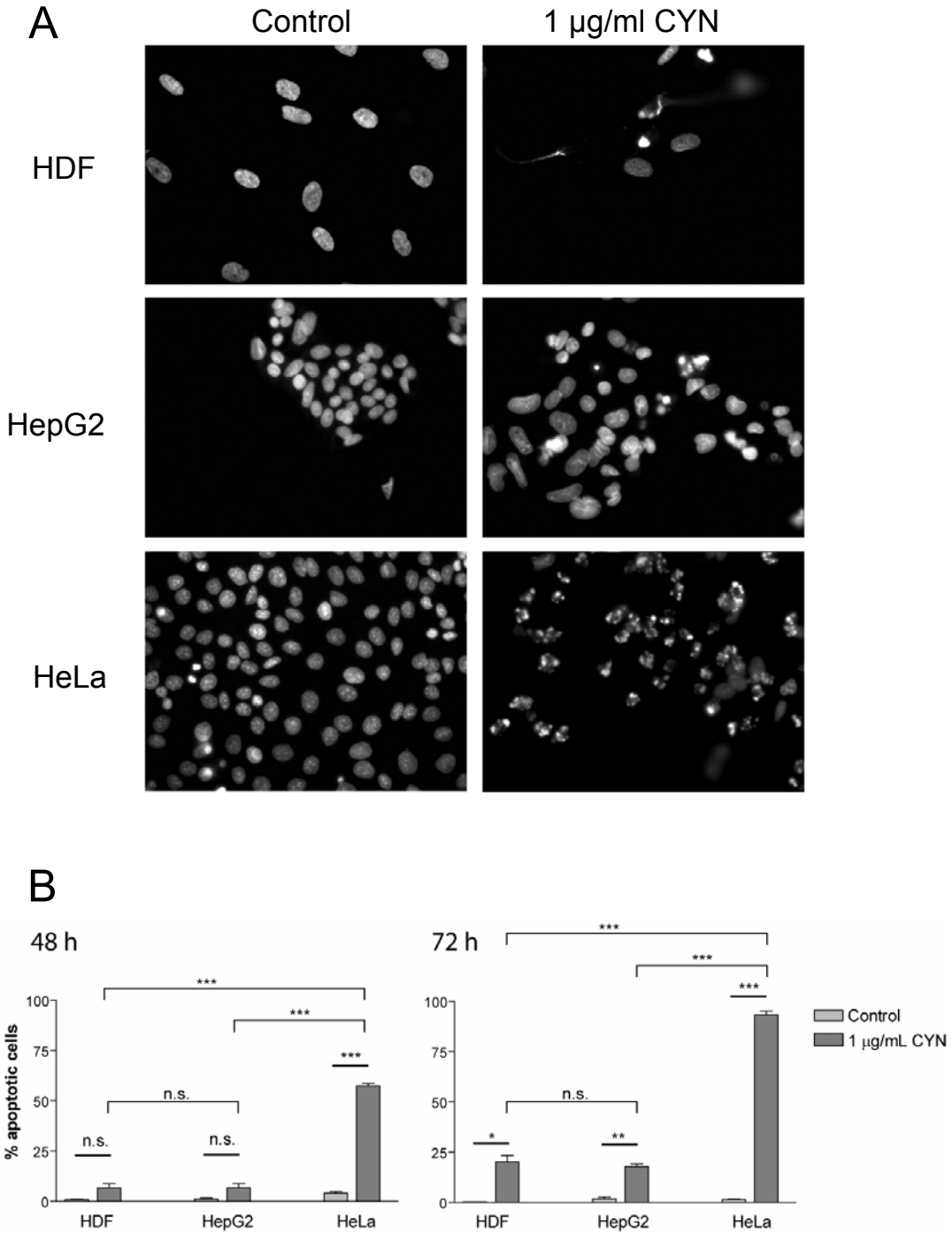


**Figure 2.4 Rates of apoptosis in CYN-treated cells.** (A) Representative images of DAPI-stained nuclei following 72 h exposure to 1 µg/ml CYN. (B) Percentage of apoptotic nuclei following 48 or 72 h exposure to 1 µg/ml CYN. Error bars represent SEM for three independent experiments (n = 3). *$p < 0.05$, ** $p < 0.01$, *** $p < 0.001$, n.s. – not significant, using Student's *t*-test.

the surface of the cover slips during the staining procedure. Under more careful washing conditions and a lower CYN concentration (1 µg/mL), apoptotic morphology was apparent in approximately 25 % of HDFs after 72 h (Figure 2.4).

Similarly, tubulin staining in CYN-treated HDFs did not reveal major changes to the number or appearance of microtubules compared to control cells (Figure 2.6). Cells that did not appear apoptotic after 72 h under 1 µg/mL CYN these conditions showed reduced attachment to the surface of the cover slips and rounding up. Microtubules appeared normal in these cells, indicating that CYN does not affect assembly or stability of actin filaments prior to the induction of apoptosis. This data indicates that CYN does not appear to be a direct inhibitor of microtubule stability or dynamics.

***Caco-2 cells***. Caco-2 cells (late passage number) treated with 5 µg/mL CYN also displayed signs of rounding up that increased with exposure time, although because of the tendency of this cell line to grow in tightly packed monolayers, this was less obvious than in HDFs. After 48 h there was an obvious reduction in cell number, with membrane blebbing apparent in some cells (Figure 2.5A). Cortical actin staining was reduced compared to controls, and intracellular junctions were less visible. After 72 h exposure to 5 µg/mL CYN, actin staining in cells remaining on the coverslips revealed rough, rounded edges and disorganised clumps of cells. Nevertheless, the apparent actin filament rearrangements seemed to associated with rounding up, implying that filamentous actin is not likely to be an early target of CYN toxicity in these cells. Tubulin staining was not conducted in Caco-2 cells.

***HepG2 cells***. HepG2 cells exposed to 5 µg/ml CYN and stained for actin using FITC-phalloidin did not appear to round up, even after 72 h exposure, with the exception of cells with apoptotic morphology (Figure 2.5B). Intense staining at cell cortices was retained in treated cells, but compared to controls the cells were irregularly shaped with rough edges. The nuclei of treated cells (5 µg/ml for 72 h) were either large and unusually shaped, or appeared apoptotic, with condensed chromatin or fragmented nuclei.

With the exception of apoptotic cells, tubulin staining was also similar to controls in cells exposed to 1 µg/ml CYN for 72 h (Figure 2.6), with microtubules radiating

throughout the cytoplasm and increased staining intensity around nuclei. The edges of cells were less defined than controls, indicating a degree of rounding up.

A feature of treated HepG2 cells that was not apparent in other cell types was the highly irregular size and shape of nuclei. After 72 h exposure to 1 µg/mL CYN, many nuclei appeared to be larger than control nuclei, and were misshapen.

***HeLa cells***. Anti-tubulin antibody staining of HeLa cells treated for 72 h with 1 µg/ml CYN showed that most cells were fully rounded up, with membrane blebbing and fragmentation consistent with typical apoptotic morphology (Figure 2.6). Cells that did not appear to be apoptotic retained relatively normal microtubule filaments but showed signs of rounding up. This response was similar to that observed in CYN-treated HDFs, Caco-2 and HepG2 cells, suggesting that micotubule filaments are not a primary target of CYN toxicity.

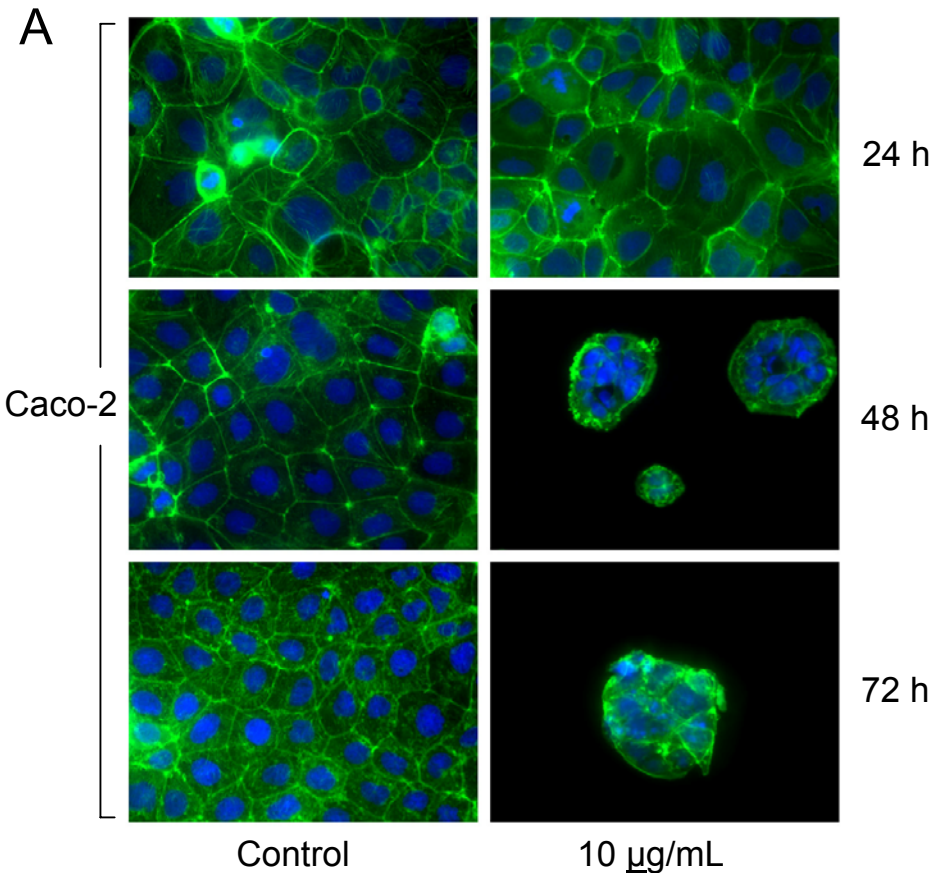

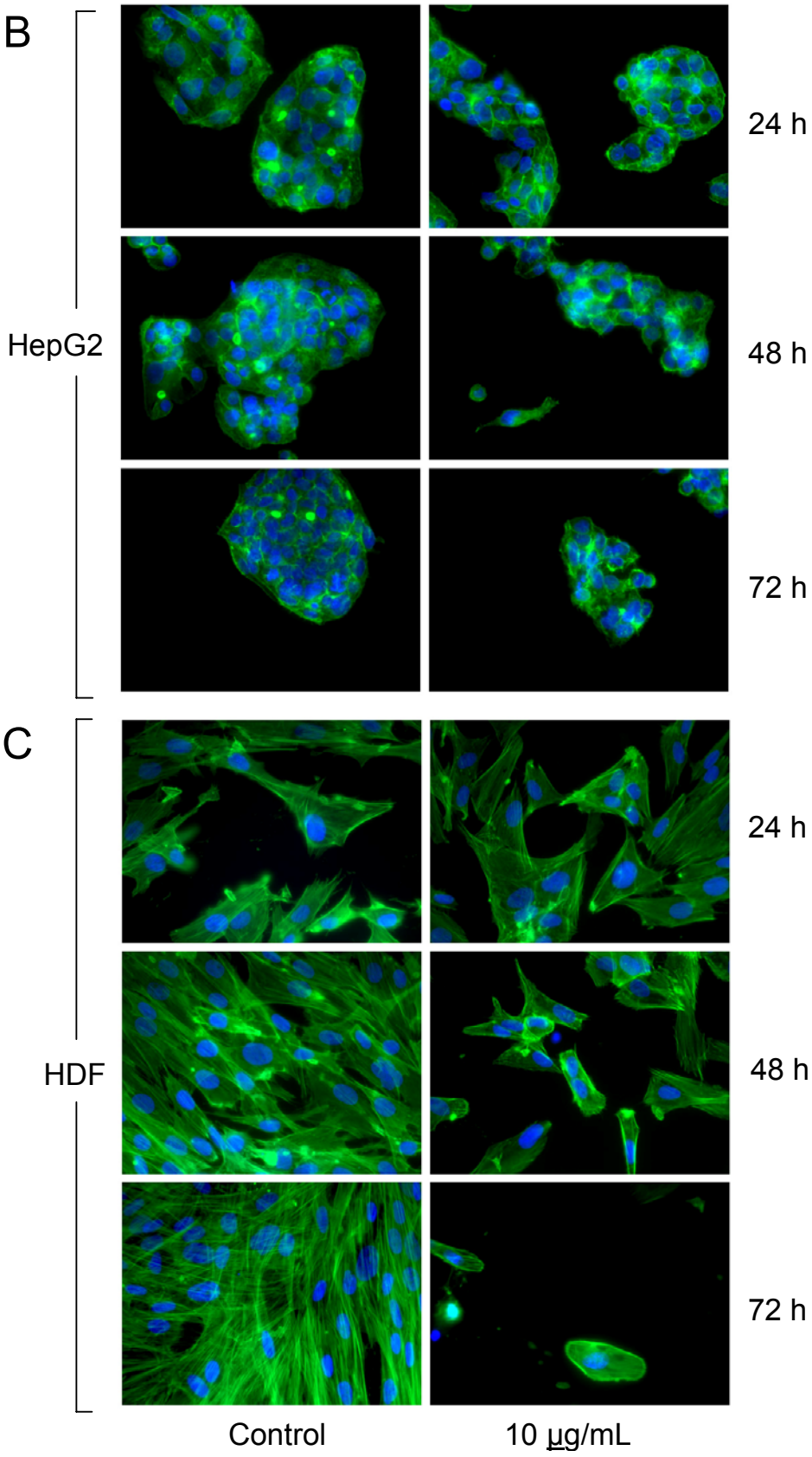
B
HepG2
24 h
48 h
72 h
C
HDF
24 h
48 h
72 h
Control
10 µg/mL

**Figure 2.5 Structure of the actin cytoskeleton in cells exposed to CYN.** Representative images of Caco-2 cells (A), HepG2 cells (B) and HDFs (C) exposed to the indicated CYN concentrations for 24, 48 or 72 h. Actin was stained with FITC-conjugated phalloidin (shown in green), and DNA was stained with DAPI (blue). Controls were included to allow for any detrimental effects due to growth for 72 hours without changing media. Representative images are shown.

## 2.4 Discussion

The results presented in this chapter describe CYN toxicity in a variety of human-derived cell types. The use of multiple approaches reduced the possibility of under- or over-estimating cytotoxicity. For example, if LDH release was the only indicator used, CYN would not appear to be toxic at all in Caco-2 or HepG2 cells.

In terms of MTS reduction, all cell lines used in this study responded to CYN in a similar fashion, with concentrations between 0.5 and 5 μg/ml CYN resulting in strong inhibition of MTS reduction. Longer exposures produced steeper dose-response curves, consistent with reports of delayed cytotoxicity of CYN in animal studies (Hawkins et al., 1997; Metcalf et al., 2002). Due to the relatively low CYN concentration in stock solutions, it was not possible to achieve the high concentrations in media necessary for accurate calculation of $EC_{50}$ values. Nevertheless, it appeared that CYN produced approximately similar concentration-response relationships in most of the cell types investigated, with the possible exception of HeLa cells. Interestingly, HeLa cells readily underwent apoptosis in response to CYN treatment, suggesting that the strong inhibitory effect of CYN on MTS reduction and ATP content after 48 hours or more may be an artefact of apoptotic cell death in this cell line.

In terms of proliferation, cell number was consistently reduced in CYN-treated cultures (data not shown), and it is likely that MTS reduction assays provided a good estimate of the anti-proliferative effects of CYN. However, tetrazolium reduction assays do not correlate well with other assays of cell proliferation under certain conditions (Marionnet et al., 1997). The use of alternative methods, such as measuring rates of DNA synthesis using radioactive nucleotides or bromodeoxyuracil incorporation, may provide more accurate estimates of the inhibition of cellular proliferation in CYN-treated cells.

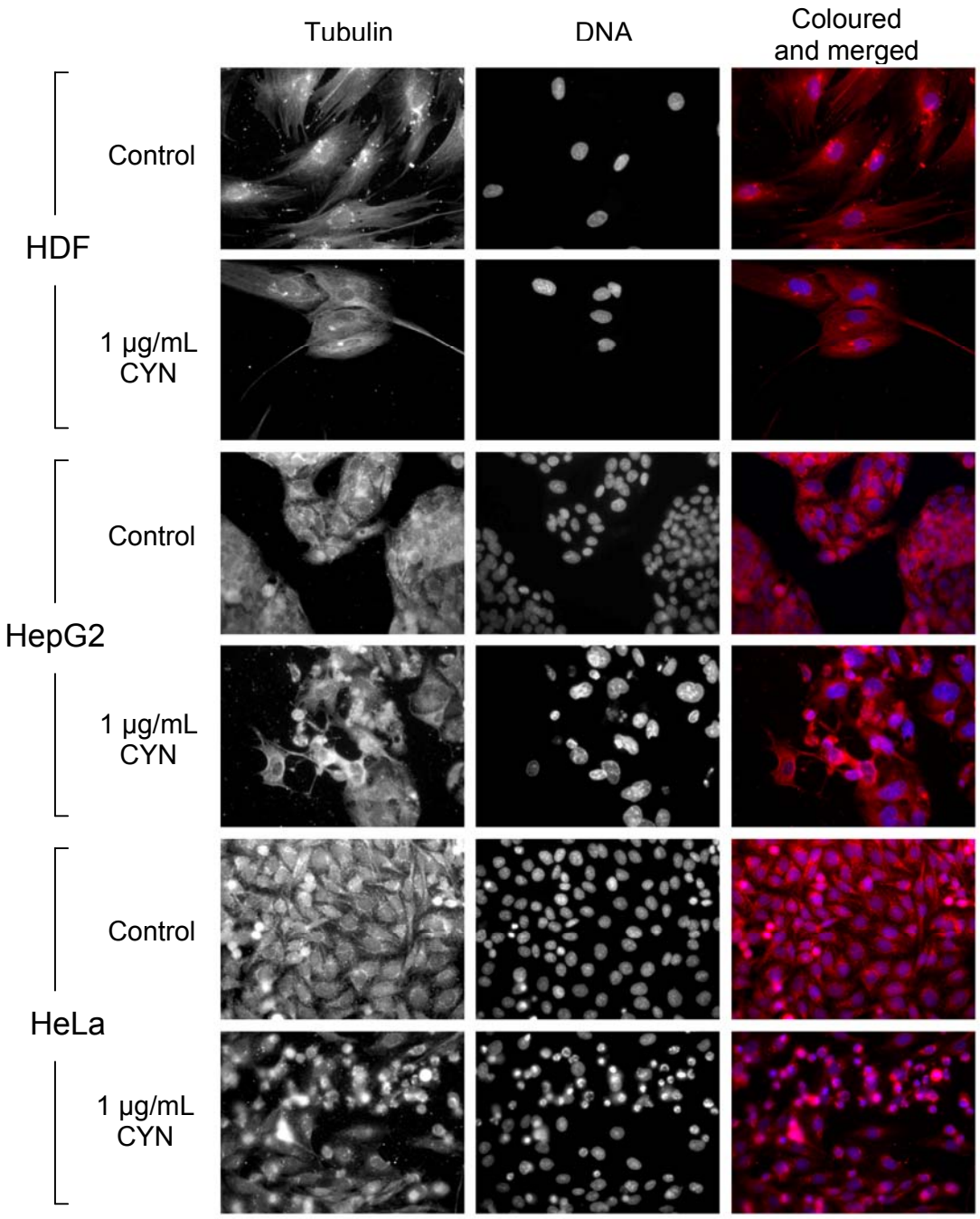


**Figure 2.6 The effects of CYN on microtubule cytoskeletal structure.** Representative images of cells treated for 72 h with 1 µg/mL CYN. Microtubules were visualised using anti-tubulin primary antibody and TRITC-conjugated secondary antibody. DNA was stained with DAPI. CYN appears to affect microtubules only in cells undergoing apoptosis, with relatively normal appearance and distribution in non-apoptotic cells.

Cytoskeletal filaments do not appear to be early targets of CYN toxicity. An investigation of CYN toxicity in CHO-K1 cells reported that CYN treatment altered actin microfilament and microtubule cytoskeletal structure, but the authors acknowledged the possibility that the observed rounding up and blebbing may be associated with apoptosis (Fessard and Bernard, 2003). This is in agreement with the present study, where extended CYN exposures resulted in morphological changes consistent with apoptosis, but did not appear to directly affect the cytoskeleton. Although there were some structural differences between control and treated cells, actin filaments appeared to retain a relatively normal appearance. A common target of bacterial protein toxins is the Rho GTPase family of proteins that regulate the structure of the actin cytoskeleton (Aktories and Barbieri, 2005). For example, *Clostridium difficile* toxin B causes major reduction of cytoplasmic actin filaments after 1h of toxin treatment. An interaction with Rho is probably unlikely in the case of CYN, as actin cytoskeletal structure was relatively normal following long periods of exposure, except in cells displaying indicators of apoptosis. Rearrangement of the cytoskeleton (rounding up) was apparent after long exposures to 1 µg/mL CYN, or shorter exposures (24 h) under high CYN concentrations, but this was probably associated with the early stages of apoptosis.

Cells exposed to direct inhibitors of microtubule dynamics display markedly reduced cytoplasmic microtubule staining after only 2 h (Pisano et al., 2000). Clearly, CYN does not rapidly alter the number or distribution of microtubule filaments in the cell types used in the present study. Aneuploidy in cells exposed to CYN led researchers to suggest that kinetochore function may be inhibited in treated cells undergoing mitosis, and that this may be associated with protein synthesis inhibition by CYN (Humpage et al., 2000). The data presented here supports this hypothesis—any disruption of kinetochore fibres or other microtubule structures associated with the mitotic spindle is not likely to be directly attributable to CYN binding, since microtubule staining in treated cells appeared normal prior to the induction of apoptosis. Direct inhibitors of tubulin polymerisation are known to rapidly produce anomalous microtubule structure, detectable using immunofluorescent staining within 2 h (Pisano et al., 2000). In the case of CYN, downstream effects of protein synthesis inhibition may include reducing the tubulin pool, which may adversely affect the assembly of the mitotic spindle after long

exposures. Alternatively, cell division could be halted in response to CYN prior to mitosis, and indeed, prior to S phase—a recent report shows that depletion of centrosome proteins induces p53-dependent cell cycle arrest at G1 phase (Mikule et al., 2007). Although general protein synthesis inhibition is likely to reduce cell growth and thus affect numerous cell cycle control pathways, inhibition of centrosome protein synthesis may be contribute to growth arrest in response to CYN.

The primary reason for investigating toxicological endpoints in cultured cells was to determine appropriate conditions for the analysis of gene expression in response to CYN. Theoretically, optimal conditions would result in significant alteration of mRNA levels directly related to the mechanism of action of the toxin and would not produce non-specific effects related to processes such as with cell death by apoptosis. With this in mind, the general conditions chosen for subsequent studies consisted of a 24-hour exposure to 1 μg/mL CYN in culture media. This treatment regime does not appear to induce morphological changes associated with apoptosis in either HepG2 cells or HDFs, and does not compromise membrane integrity, but does have an observable effect on MTS reduction, particularly in HepG2 cells. After 48 or 72 hours, a CYN concentration of 1 μg/mL induces obvious apoptotic morphology, suggesting that events leading to apoptosis, such as CYN-mediated damage to macromolecules, may occur at earlier time points. If this is the case, it is reasonable to assume that damage sensing and signalling would result in measurable changes in the expression of genes involved in damage repair or other functions relevant to toxic mechanism. Higher CYN concentrations will be examined at earlier time points, e.g. 6 h exposure, in order to examine concentration-response relationships for various target genes.

# Chapter 3

## *Gene expression profiling of cylindrospermopsin toxicity* in vitro

### 3.1 Introduction

The modulation of inter- and intracellular cell signalling pathways in response to exogenous factors results in altered gene expression, often due to changes in the abundance or activation status of transcription factors. While protein levels are influenced by numerous parameters such as translational regulation and targeted proteolysis, measuring messenger RNA (mRNA) levels provides a widely accepted estimate of gene expression at the level of transcription, but also detects changes in transcript levels due to altered mRNA stability. In the current study, we aimed to gain insight into specific stress responses and damage repair pathways modulated following CYN exposure by determing relative mRNA levels using genome-wide microarray analysis.

While a number of putative mechanisms of CYN toxicity have been established, the underlying molecular interactions have yet to be determined. With respect to the chemical structure, the uracil component has suggested to researchers that an interaction with cellular nucleic acids or nucleic acid binding proteins may underlie CYN toxicity. Speculatively, binding or damage to ribosomal or messenger RNA may be the basis of CYN-mediated translational inhibition, while DNA damage in treated cells and tissues may also arise from an interaction involving the uracil component of CYN. Indeed the uracil moiety is essential for toxicity *in vivo* (Banker et al., 2001), suggesting an

important role in interactions with putative target molecules. Determining cellular responses to CYN at the level of gene expression may provide further insight into the nature of these interactions. Cells in culture have proven to be useful for gene expression studies in the field of toxicology, particularly for the investigation of mechanisms of toxicity.

The use of *in vitro* cell cultures in toxicology has increased steadily since its inception about 20 years ago (Zucco et al., 2004). Transformed cell lines offer a virtually unlimited supply of cells with a homogenous genetic background, giving consistent responses that can be useful for toxicological applications. Cell lines are routinely applied for such purposes as screening drug candidates for cytotoxicitym, and investigating mechanisms of toxicity of known toxic compounds. It must be acknowledged that results of *in vitro* cell-based assays are often not representative of living tissue, particulary when transformed cell lines are used. On the other hand, cultured primary cells are highly differentiated and can mimic closely the metabolic state of their *in vivo* counterparts. Provided a given primary cell type is capable of proliferation in culture, it is inherently useful in toxicological investigations due to the fact that cell cycle control mechanisms are intact, as opposed to transformed cell lines which often lack one or more cell cyle checkpoints. Numerous studies of altered gene expression in toxin-exposed cells in culture have been published (Kim et al., 2006; Ricicki et al., 2006; Su et al., 2006; Zhou et al., 2005c). Cultured primary cells display altered expression compared to those occurring in the tissues of a living tissue, while gene expression patterns in transformed cell lines often bear little resemblance to the cell type from which they originate. Evaluating the *in vitro* toxicological properties of novel compounds therefore requires a comprehensive approach involving the use of multiple cell models and the thorough investigation of a range of toxicological endpoints.

Due to the enhanced toxicity of CYN in hepatocytes (Ohtani et al., 1992), we chose a liver carcinoma cell line, HepG2, as one of the model cell types for microarray experiments. HepG2 cells express a range of CYP450 family enzymes (Sassa et al., 1987), albeit at significantly lower levels than in primary hepatoctyes (Rodriguez-Antona et al., 2002). A comparative study of basal gene expression in cultured human hepatocytes and HepG2 cells showed that 98% of the 867 genes expressed in primary

hepatocytes were also expressed in HepG2 cells, but that HepG2 expressed a further 920 genes that were not expressed in primary hepatocytes (Harris et al., 2004). Interestingly, this study also identified a number of genes that showed markedly reduced expression in primary hepatocytes compared to whole liver, but which were expressed at relatively high levels in HepG2 cells. These data suggest that neither primary hepatocytes nor HepG2 cells can accurately mimic gene expression in whole liver, but that many genes expressed in liver *in vivo* are also expressed by HepG2 cells. The expression of many non-hepatic genes in HepG2 cells could substantially alter responses to toxicants relative to primary hepatocytes, however, due to the wide use of this cell type in toxicology it was deemed suitable for use in the present study. Another concern was that transformed cells may not be capable of undergoing cell cyle arrest in response to CYN-mediated cellular damage. To compare expression profiles in HepG2 to an untransformed cell type, we chose primary human dermal fibroblasts due to their capacity for proliferative growth in culture conditions.

This chapter describes a high density microarray-based analysis of CYN-induced gene expression in cultured human-derived cells. This approach was undertaken with the view to identifying gene expression endpoints associated with specific stress response pathways modulated by CYN. The possible mechanisms underlying the induction or repression of these pathways are discussed.

***A note on gene and protein symbols used in this and subsequent chapters.*** According to widely accepted guidelines published by the Human Gene Nomenclature Committee (Wain et al., 2002), human gene symbols should be represented by upper case italicised latin characters. This format is adhered to in the current thesis. Protein symbols are used according to convention, and in the case of capitalised symbols can be distinguished from the corresponding genes by the use of standard rather than italicised characters. For example, GADD45α protein is encoded by the *GADD45α* gene. Oncogenes are shown without the c- designation present in the corresponding protein, in adherence to published guidelines (Wain et al., 2002). For example, the *JUN* oncogene encodes the c-Jun protein. For messenger RNA transcripts, the term 'mRNA' is used in conjunction with either the gene or protein symbol. For example, '*GADD45α* mRNA' or 'mRNA for GADD45α' are used interchangeably to describe mRNA transcribed from the *GADD45α* gene.

## 3.2 Materials and Methods

### *3.2.1 Experimental Design*

For hybridisation of labelled cDNAs to microarrays, a 'reference RNA' design was used (Figure 3.1), in which all samples (treated and control) were labelled with Cy3 and co-hybridised with a common reference pool labelled with Cy5. Toxin treaments were conducted for 6 h and 24 h, and expression ratios were obtained by dividing the signal intensities at each time point by the corresponding intensities at 'time 0'. Three separate treatments, RNA isolations, labelling reactions and array hybridisations were performed for each time point.

Because CYN toxicity in HepG2 and HDF cells appeared to require a considerable length of time (Section 2.3.1), more importance was placed on the 24 h time point compared with the 6 h time point. Apoptosis did not occur at significant rates until 72 h exposure to the same CYN concentration used here (1 μg/mL; see Section 2.3.4 and Figure 2.4B), so that gene expression changes after 24 h treatment are are not likely to be erratic, as may be expected during apoptosis. With this in mind, the 'time 0' samples used here were actually vehicle controls (1 % MQW) for the 24 h time point. While this may detract from the validity of changes detected after 6 h, it also strengthens the robustness of data for the 24 h time point, since a conventional time course would not use a vehicle control. The analysis is presented as a time course because the effects of 1 % sterile MQW on gene expression are likely to be negligible compared to the effect of 1 μg/mL CYN. This approach was utilised to reduce the total number of arrays required for the experiment, while maintaining the ability to investigate changes in expression at a relatively early time point (6 h treatment). For real-time quantitative RT-PCR validation of relative mRNA levels (see section 3.3.6), vehicle controls for the 6 h treatments were utilised, ensuring that the changes observed at this time were real.

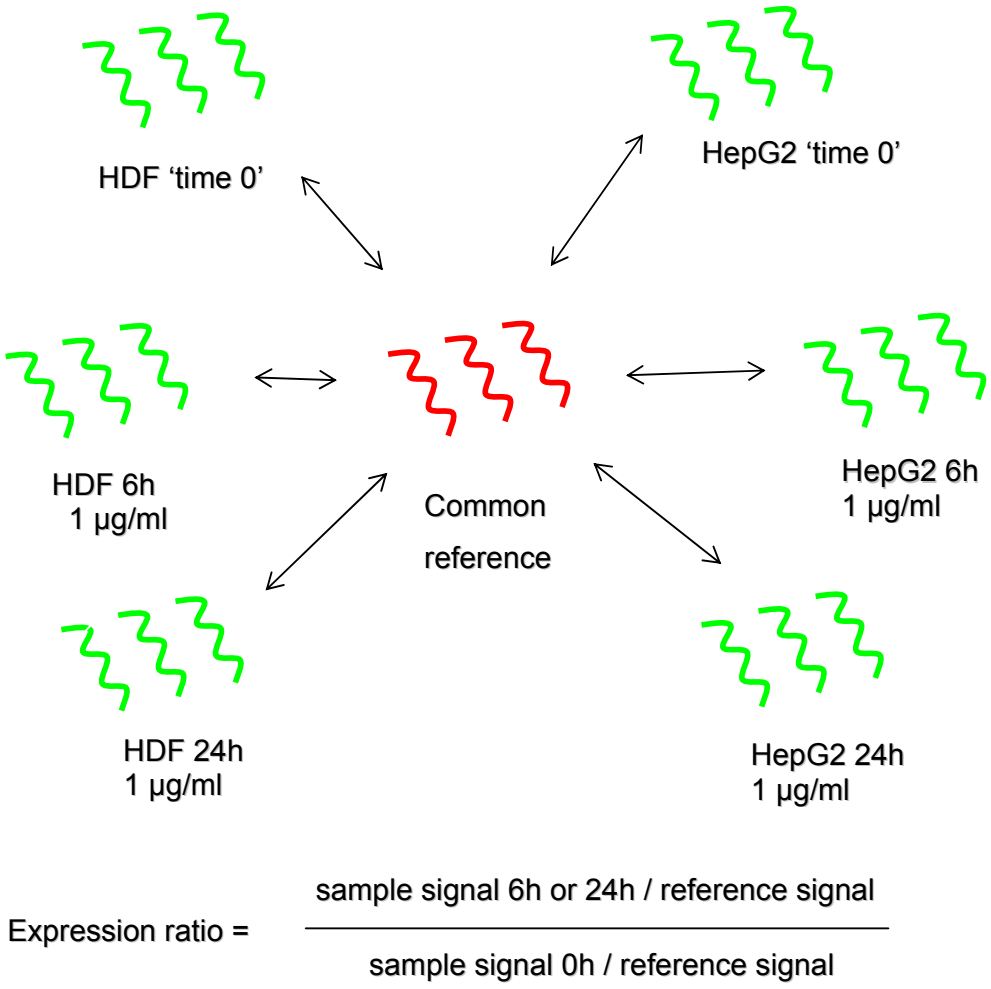


**Figure 3.1 Experimental design for microarray hybridisations.** Three separate treatments were performed for each exposure. Total RNA was isolated from each treatment and labelled with Cy3 during amplification. Amplified and labelled complementary RNA was co-hybridised to the microarrays with Cy5-labelled reference RNA. Expression ratios for samples from 6 h and 24 h exposures were calculated relative to 'time 0' samples.

### *3.2.2 Cylindrospermopsin*

Purified cylindrospermopsin, quantified and qualitatively assessed using methods described previously (Norris et al., 2001), was the kind gift of Dr. Wasa Wickramasinghe (National Research Centre for Environmental Toxicology, Australia). CYN was dissolved in MQW and filtered through 0.22 µm filters (Pall Life Sciences) prior to use.

### 3.2.3 Cell culture and treatments

Human dermal fibroblasts (HDFs), originally sourced from a healthy donor in a clinical setting (Dr Nick Saunders, Centre for Immunology and Cancer Research, University of Queensland, Princess Alexandra Hospital), were the kind gift of Dr. Diane Watters (Griffith University, Australia). HepG2 liver carcinoma cells (ATCC HB-8065) were provided by Dr. Sarah Wilkins (Queensland Institute of Medical Research, Australia). Cells were maintained at 37ºC under a 5% $CO_2$ humidified atmosphere in Dulbecco's modification of Eagle's medium (DMEM, Gibco-Invitrogen) supplemented with 42 µg/ml L-glutamine, 110 µg/ml sodium pyruvate, 4 µg/ml pyridoxine-HCl, 10% foetal bovine serum (Gibco-Invitrogen), 100 units/ml penicillin and 100 µg/ml streptomycin (Gibco-Invitrogen).

Cells were seeded into six-well plates and grown until ~50-60% confluence. Culture media were exchanged with fresh media 24 hours prior to treatment. For toxin exposures, CYN stock solution was added directly to the media to give a final concentration 1 µg/ml (~2.4 µM). Vehicle controls were exposed to a volume of MQW in growth media equal to the volume of CYN stock solution used for toxin treatments. Three separate treatments were performed for each condition.

### 3.2.4 RNA isolation

Following the indicated exposure times, the culture medium was aspirated and cell monolayers were rinsed twice with sterile PBS at room temperature. Cells were lysed *in situ* by scraping into 350 µl of lysis buffer supplied with the RNeasy kit (Qiagen) containing 1% β-mercaptoethanol (Sigma-Aldrich), and the lysates homogenised using Qiagen shredder columns. Total RNA was isolated using RNeasy mini columns (Qiagen) according to the manufacturer's protocol. The optional on-column DNase treatment was included. RNA was eluted with 55 µl of RNase-free water (Qiagen). Eluates were passed through the columns a second time to enhance yield.

Quantitative and qualitative analyses of RNA were achieved by capillary electrophoresis using an Agilent 2100 Bioanalyzer with the RNA 6000 chip as described by the manufacturer (see Appendix 3 for a summary of Bioanalyzer results). Absorbance of UV light at 260 nm and 280 nm was used to estimate protein

contamination. RNA was considered to be of acceptable quality if the $A_{260}/A_{280}$ ratio was above 1.9, the 28S rRNA/18S rRNA ratio was 2.0 and the RNA Integrity Number (RIN; Agilent Bioanalyzer 2100 Expert software release B.02.02) was 9.9 or above.

### *3.2.5 RNA amplification and labelling*

A reference pool of RNA was obtained by mixing equal proportions of all samples used in the array experiments (HepG2 and HDF total RNA from '0 h', 6 h and 24 h). RNA amplifications were carried out using the Superscript Indirect RNA Amplification System (Invitrogen). Briefly, reference total RNA (1 µg), HepG2 total RNA (1 µg), and HDF total RNA (400 ng) were reverse transcribed using an oligo-$dT_{24}$-T7 primer and Superscript III (Invitrogen). Second-strand cDNA synthesis, followed by RNA amplification by *in vitro* transcription, was carried out in the presence of amino-allyl UTP according to the manufacturer's protocol (Invitrogen).

Five micrograms of each cRNA was labelled with amino-allyl reactive Cy5 (reference RNA) or Cy3 (sample RNA) according to the manufacturer's protocol (Amersham). Free amino-allyl groups were blocked with the addition of hydroxylamine as recommended by the manufacturer's protocol (Amersham). Equal amounts of labelled sample RNA and reference RNA were mixed and purified using MEGAclear spin columns (Ambion). After concentrating the purified labelled RNA to < 8 µl in a centrifugal vacuum concentrator (Eppendorf), the volume was restored to 8 µl with MQW. RNA was fragmented prior to hybridisation by adding 2 µl of a buffer containing 0.5 M potassium acetate, 0.15 M magnesium acetate and 0.2 M tris-acetate pH 8.1, and heating to 95ºC for 20 minutes. Fragmentation was stopped by cooling on ice and adding EDTA to a final concentration of 5 mM.

### *3.2.6 Microarray hybridisation*

Compugen Human 19K oligonucleotide arrays (SRC Microarray Facility, University of Queensland) were blocked in a solution containing 2X SSC (Sigma-Aldrich), 0.1 % SDS (Sigma-Aldrich), and 0.1 % molecular biology grade BSA (Sigma-Aldrich). The blocking solution was filtered through a 0.22 µm pore-size syringe filter and heated to 55°C prior to immersing the slides and allowing the solution to cool to room temperature for 30 min. The slides were rinsed briefly in MQW and dried by

centrifugation. Labelled RNAs were heated to 95°C for 5 min in a solution containing 8X SSC (Sigma-Aldrich), 1 % SDS (Sigma-Aldrich), and 50 % deionised formamide (Sigma-Aldrich) in a total volume of 40 µl, and cooled to 42°C in a water bath prior to placing the mixture on the microarrays and positioning coverslips. Hybridisation was performed overnight in sealed, humidified chambers immersed in a water bath at 42°C. Slides were washed for 15 minutes in 0.2X SSC, 0.2% SDS, rinsed twice in 0.2X SSC and dried by centrifugation. Microarray mages were acquired using the GenePix 4000B scanner (Axon), using prescanning to determine optimum photomultiplier settings. Spot detection, grid alignment and spot quality flagging was performed using GenePix Pro 6.0 (Axon).

### *3.2.7 Microarray data analysis*

Data normalisations, statistical analyses and clustering were carried out in GeneSpring versions 7.1 and 7.2 (Agilent). GeneSpring Viewer 5.2 (Agilent) was utilised for Gene Ontology Browser analyses and for manual selection of gene lists for further study.

***Normalisation strategy.*** Data normalisation consisted of a LOWESS adjustment followed by dividing intensity data for each feature in all samples by the corresponding data in the control samples (time zero). These procedures were performed using GeneSpring 7.1 (Agilent – Silicon Genetics). For the LOWESS adjustment, 20% of the data to calculate the fit at each point. Specific samples were then normalised to one another: HDF samples from all time points were normalised against the median of the control HDF samples from ‘time 0’. Similarly, HepG2 samples from all time points were normalised against the median of the HepG2 control samples from ‘time 0’. Each measurement for each gene in all specific samples was divided by the median of that gene's measurements in the corresponding control samples.

***Statistical analyses.*** Principal components analysis (PCA) was carried out using GeneSpring 7.1 (Agilent) on the complete set of all samples from both cell lines and all genes represented on the arrays.

Prior to performing further statistical analyses, data sets were filtered to reduce the list of genes represented on the arrays to a list of genes with signal intensities above mean background levels on the arrays. The filtering strategy omitted genes flagged as absent

in more than six out of the nine samples for each cell type, and accepted genes with signal intensities above background levels in at least three of the nine samples. This procedure was carried out separately for each cell type.

Significant changes in transcript level over the time course were found by analysing filtered data using one-way Welch parametric ANOVA testing (variances not assumed equal) with a *p*-value cut-off of 0.05. Multiple testing corrections, utilising the Benjamini and Hochberg False Discovery Rate, were included in the analysis.

***Hierarchical clustering.*** Hierarchical clustering was carried out in GeneSpring using the Pearson correlation coefficient. Data sets representing genes with significant changes in mRNA levels ($p < 0.05$) over time in both cell lines, HDFs only, or HepG2 cells only, were used to construct three separate dendrograms. Clusters displaying distinct gene expression profiles were selected by hand.

***Functional analysis of selected gene lists.*** Lists of genes of interest were created by various methods such as filtering for significant or large changes, selecting by hand from scatterplots or gene trees, or selecting groups of genes classified through the application of clustering algorithms. These gene lists could then be analysed for overlap with lists of genes involved in biological pathways. The degree of overlap was measured using a variety of techniques. The Gene Ontology (GO) Browser, a component of GeneSpring GX (Agilent) software, was used to search for GO terms with functional associations assigned by the Gene Ontology Consortium (Ashburner et al., 2000) that were over-represented in gene lists. The DAVID 2006 package (Dennis et al., 2003) was used for detecting the occurrence of genes involved in biological pathways and cell signalling. Gene lists were also analysed manually for the presence of genes known to be involved in pathways with potential implications in CYN toxicology, such as DNA damage responses and stess-related signalling pathways.

### *3.2.8 Validation by qRT-PCR*

Relative transcript levels were confirmed for selected genes using SYBR green I quantitative RT-PCR. Total RNA (0.5 μg to 2 μg) was used as a template for DNA synthesis using reverse transcriptase (Fermentas), primed with an anchored oligo-dT primer with the sequence $dT_{29}$-VN (Geneworks). For genes of interest, PCR primers

(Appendix 1) were designed using Primer3 software (Rozen and Skaletsky, 2000) and checked for specificity against the human genome using BLAST (Altschul et al., 1990). Amplicons were designed to be between 80 and 200 base pairs in length to ensure high amplification efficiency and were checked for secondary structure using Mfold (Zuker, 2003). Efficiencies of each primer pair were calculated by plotting cycle takeoff ($C_T$) values resulting from serial ten-fold dilutions of cDNA or specific products against the dilution factor (an automated feature present in the Bio-Rad iQ control software). PCR reactions (25 µl) contained 0.4 µM each primer (Geneworks), 0.5 U HotMaster Taq polymerase (Eppendorf), 1X HotMaster Taq buffer (Eppendorf), 0.25 mM each dNTP (Fermentas), 0.5 mg/ml BSA (Sigma-Aldrich), 5% glycerol (BDH), 10 nM fluorescein (Sigma-Aldrich), 1/40,000 SYBR Green I (Invitrogen - Molecular Probes), 2.5% molecular biology grade DMSO (Sigma-Aldrich) and 5 µl of a 1/50 dilution of cDNA. Reactions were performed in a Bio-Rad iCycler fitted with the iQ real-time detection unit. A two-step thermal cycling protocol was used, with a combined annealing and extension step of 60 seconds at 60°C and denaturation for 15 seconds at 95°C, for 40 to 50 cycles. Fluorescence intensity data were captured at the end of the annealing/extension step. Dissociation curves confirmed the presence of specific PCR products for each primer pair.

Transcript levels in treated samples were calculated relative to vehicle controls for the same exposure times and normalised to relative GAPDH mRNA levels. Data processing and statistical analyses were performed with the aid of the Relative Expression Software Tool (REST) (Pfaffl et al., 2002). This software employs a modified version of the $\Delta\Delta C_T$ method (Livak and Schmittgen, 2001), taking into account differences in PCR efficiency between primer pairs.

## 3.3 Results

### *3.3.1 Microarray analysis reveals expression patterns relevant to CYN toxicity*

#### 3.3.1.1 Principal components analysis clearly separates samples

Principal components analysis clearly separates samples. Principal components analysis (PCA) of all data, performed on all data prior to any processing or filtering, resulted in

the clear separation of each set of triplicate samples (each sample representing the data from single microarray). Visualising the results on a three-dimensional graph, where the axes represent the three principal eigenvectors (Figure 3.2), it appears that the main contributions to variance in the data are associated with time of exposure (component 1, 33.86 % of the variance) and cell type (component 2, 15.99 % variance).

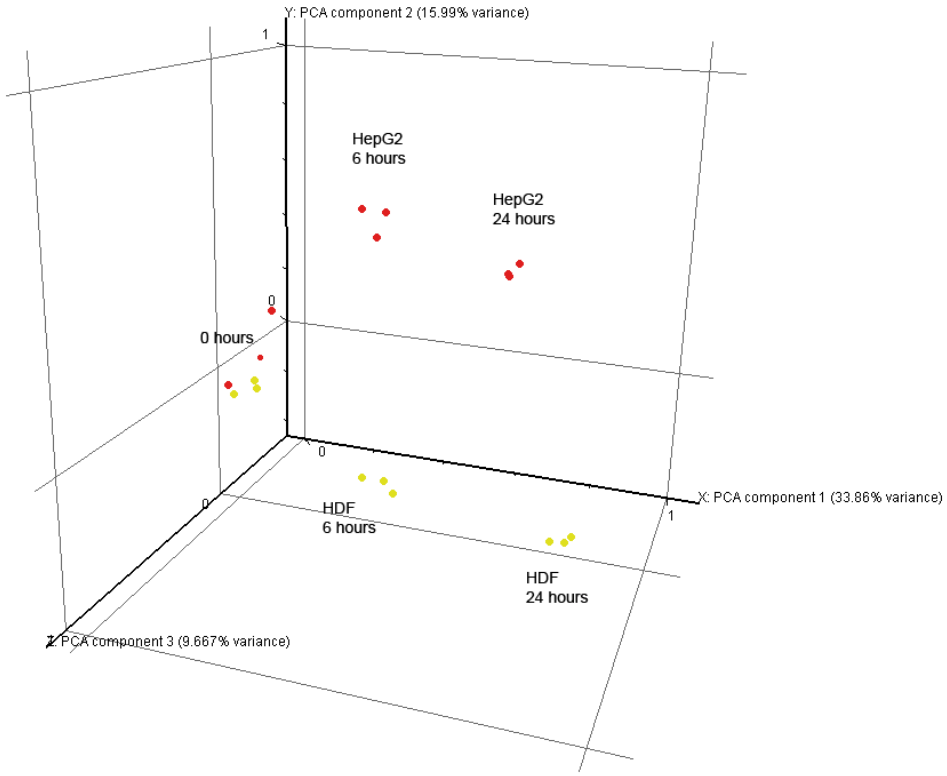


**Figure 3.2 Principal components analysis of variance in the data sets.** Each coloured dot represents data from a single microarray (Yellow dots = HDF; Red dots = HepG2).

### 3.3.1.2 CYN induces a greater degree of variation in HDFs compared to HepG2 cells

Initial data processing consisted of filtering a list of all genes represented on the arrays according to the presence of signal intensities higher than the background in at least three of the nine arrays performed for each cell type. This gives an estimate of the number of transcripts present in samples from each cell type over the time course, which, if factors such as mRNA stability are ignored, equates to the number of genes

expressed in each cell type under the experimental conditions used in this study. Of the 18 692 genes represented on the arrays, HDF cells expressed 4911 genes and HepG2 cells expressed 5126 genes. To facilitate comparison between the two cell types, these lists were combined to give a list of 5909 genes that were expressed in either cell line over the course of the experiment. Analysis of significant changes in expression over time in either cell line by one-way ANOVA ($p < 0.05$; with the Benjamini and Hochberg multiple testing correction) resulted in a list of 1856 genes. Using the same procedure for each cell type separately, relative transcript levels for 1454 genes changed significantly over time in HDFs, compared with 458 in HepG2 cells.

The number of transcripts changing in relative abundance by an arbitrary value of 2-fold or more differed markedly between the two cell types over time (Table 3.1). After 6 hours the apparent variation in HepG2 cells was greater than in HDFs, while after 24 hours a greater number of transcripts changed by more than 2-fold in the HDFs compared to HepG2 cells. This represents only large changes and disregards significant changes below 2-fold, but the general trend of the data suggests a more pronounced overall response by the HDFs over time compared to HepG2 cells.

**Table 3.1** Overview of large changes in relative mRNA transript levels in response to CYN.

| | **6 hours** | | **24 hours** | |
|---|---|---|---|---|
| | Up 2-fold | Down 2-fold | Up 2-fold | Down 2-fold |
| **HDF** | 6 | 13 | 353 | 263 |
| **HepG2** | 12 | 59 | 105 | 83 |

### 3.3.1.3. Functional analysis of clusters identifies gene expression associated with well-described biological pathways

Hierarchical clustering is a convenient method of classifying differentially expressed genes according to their expression profiles. The method consists of two steps: calculation of a similarity matrix using a defined correlation coefficient, followed by the generation of a dendrogram using a clustering algorithm (Eisen et al., 1998). The length of each branch in the dendrogram represents the similarity between genes or clusters.

Hierarchical clustering of expression profiles in both cell types over time, using the Pearson correlation, results in a clear overall separation into two main groups according to a general trend of up- or down-regulation over 24 hours (Figure 3.3A). Lists of genes present in each of these two major groups were generated, and Gene Ontology (GO) functional categories over-represented in each list were determined using the GO Browser tool (in GeneSpring Viewer). This tool enables the statistical comparison of a given gene list with lists of genes present in one of the three GO categories—biological process, cellular component (i.e. location of the product), or molecular function (Ashburner et al., 2000). Genes listed in the tables in figure 3.3A are limited to those present in the biological process category with a *p*-value less than 0.001. Genes present in cluster I (figure 3.3A; negatively regulated over the time course in both cell types) have markedly different functional associations than those found in cluster II (the group of positively regulated genes). Disregarding the broad level categories of 'physiological process', 'cellular physiological process', 'metabolism', 'cellular metabolism' and 'macromolecule metabolism', it appears that cluster I and cluster II are associated with distinct categories of genes. Genes associated with nucleic acid metabolism, RNA processing, and cell death via apoptosis are over-represented in cluster II (generally up-regulated), while cluster I (the down-regulated group) contains numerous categories involving protein transport and amino acid metabolism, as well as a list of 24 genes classified as having a function in protein folding.

Hierarchical clustering of data from each cell type separately provides a more detailed analysis of co-ordinately regulated gene expression following CYN exposure, and reveals some important differences between the two cell types. As with the combined analysis of both cell types described above, clusters of genes changing in HDFs (Figure 3.3B) were analysed for the presence of functional categories using the GO Browser, using a *p*-value limit of 0.001. Cluster I contained no significantly over-represented categories according to this limit. Genes in cluster II, unchanged or slightly downregulated after 6 h, and up-regulated after 24 h, were associated with the positive regulation of cell proliferation and the induction of apoptosis. Cluster III, up-regulated over time, contained genes involved in RNA metabolism and processing, in particular mRNA processing and splicing. Cluster IV, up-regulated after 6 h but generally unchanged after 24 h, did not contain significant associations according to the *p*-value

limit employed. Cluster V, generally up-regulated over time, contained genes associated with RNA metabolism and processing, particularly ribosomal RNA processing. Genes in cluster VI, down-regulated over time, were associated with amino acid metabolism and biosynthesis, as well as transfer RNA aminoacylation. Cluster VII, up-regulated after 6 h and down-regulated after 24 h, contained genes involved with lipid biosynthesis. Genes in cluster VIII, unchanged or slightly down-regulated after 6 h and down-regulated after 24 h, were associated with carbohydrate metabolism. Cluster IX, up-regulated after 6 h and down-regulated after 24 h, were associated with microtubule polymerisation and microtubule-based transport.

In the case of HepG2 cells, the same analysis resulted in few significant functional associations (Figure 3.3C). This was probably due to the fact that relatively few transcripts changed significantly in abundance over time (458 genes, compared to 1,454 in HDFs), such that each cluster chosen for analysis contained fewer genes for the statistical analyses employed in the GO Browser software. To increase the number of functional associations displayed, the *p*-value cutoff for HepG2 cells was raised to 0.005. Genes present in cluster I, up-regulated slightly after 6 h and down-regulated after 24 h, were associated with nitrogen compound metabolism and amine metabolism. Cluster II, down-regulated slightly or unchanged after 6 h, and down-regulated after 24 h, contained genes associated with a diverse range of activities, including alcohol metabolism, lipid biosynthesis, sterol biosynthesis, DNA replication, cholesterol biosynthesis and Golgi vesicle transport. Cluster III, down-regulated over time, did not display any significant associations. Cluster IV, down-regulated after 6 h and up-regulated after 24 h, was associated with metal ion homeostasis. Clusters V and VI did not display significant associations according to the *p*-value limit. Cluster VII, up-regulated over time, was associated with RNA processing and metabolism, and protein biosynthesis.

These findings reveal a number of important differences between the responses of the two cell types used in this study. CYN did not appear to induce apoptosis-related gene expression in HepG2 cells, while in HDFs a number of genes involved in apoptosis were significantly up-regulated after 24 h. HepG2 cells showed a down-regulation after 6 h, and an induction after 24 h, of genes involved with metal ion homeostasis, while HDF cells did not. In HDFs, genes associated with microtubule polymerisation and

movement were induced after 6 h and down-regulated after 24 h, while in HepG2 cells this did not appear to occur. HDFs also showed a reduction in the expression of genes for carbohydrate metabolism which was not apparent in HepG2 cells.

Conversely, a number of responses were similar in both cell types. In particular, the increased expression of genes involved with RNA metabolism occurred over time in both cell types. After 24 h, genes associated with lipid metabolism were down-regulated similarly, as well as some genes involved with amine metabolism. The down-regulation of genes associated with amino acid metabolism in HepG2 cells was not apparent in this analysis, but it is likely that genes for this function are included in the 'amine metabolism' category.

**A**

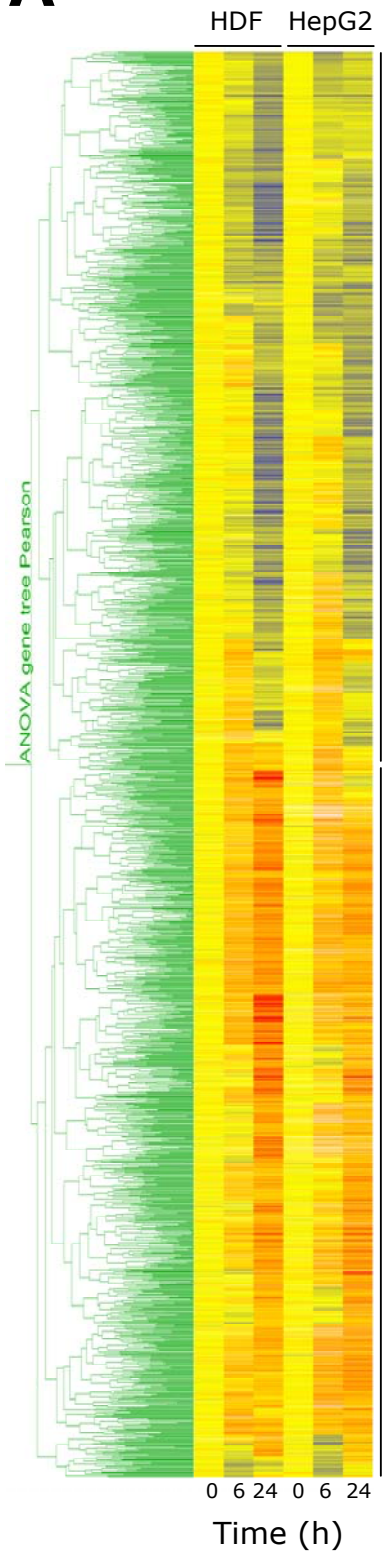


| | Category | Genes in List in Category | % of Genes in List in Category | *p*-Value |
|---|---|---|---|---|
| I | GO:7582: physiological process | 521 | 75.62 | 0.000235 |
| | GO:50875: cellular physiological process | 470 | 68.21 | 0.000484 |
| | GO:8152: metabolism | 369 | 53.56 | 4.34E-05 |
| | GO:44237: cellular metabolism | 346 | 50.22 | 0.000129 |
| | GO:44238: primary metabolism | 327 | 47.46 | 0.000962 |
| | GO:43170: macromolecule metabolism | 227 | 32.95 | 6.20E-06 |
| | GO:9058: biosynthesis | 79 | 11.47 | 0.00024 |
| | GO:6082: organic acid metabolism | 44 | 6.386 | 2.47E-05 |
| | GO:19752: carboxylic acid metabolism | 43 | 6.241 | 4.65E-05 |
| | GO:8104: protein localization | 41 | 5.951 | 0.000849 |
| | GO:45184: establishment of protein localization | 41 | 5.951 | 0.000483 |
| | GO:15031: protein transport | 40 | 5.806 | 0.000441 |
| | GO:6807: nitrogen compound metabolism | 39 | 5.66 | 5.45E-06 |
| | GO:9308: amine metabolism | 38 | 5.515 | 2.96E-06 |
| | GO:6519: amino acid and derivative metabolism | 32 | 4.644 | 1.74E-05 |
| | GO:44262: cellular carbohydrate metabolism | 30 | 4.354 | 5.13E-05 |
| | GO:6520: amino acid metabolism | 29 | 4.209 | 1.25E-05 |
| | GO:6066: alcohol metabolism | 26 | 3.774 | 9.38E-05 |
| | GO:6457: protein folding | 24 | 3.483 | 0.000125 |
| | GO:6006: glucose metabolism | 13 | 1.887 | 0.000631 |
| | GO:9309: amine biosynthesis | 12 | 1.742 | 0.000219 |
| | GO:44271: nitrogen compound biosynthesis | 12 | 1.742 | 0.000219 |
| | GO:8652: amino acid biosynthesis | 11 | 1.597 | 2.71E-05 |
| | GO:9069: serine family amino acid metabolism | 7 | 1.016 | 0.000791 |
| II | GO:50875: cellular physiological process | 484 | 71.7 | 7.36E-08 |
| | GO:8152: metabolism | 389 | 57.63 | 6.37E-10 |
| | GO:44237: cellular metabolism | 380 | 56.3 | 3.03E-12 |
| | GO:44238: primary metabolism | 365 | 54.07 | 1.75E-11 |
| | GO:43170: macromolecule metabolism | 256 | 37.93 | 2.99E-13 |
| | GO:43283: biopolymer metabolism | 186 | 27.56 | 6.18E-10 |
| | GO:19538: protein metabolism | 167 | 24.74 | 1.26E-06 |
| | GO:44260: cellular macromolecule metabolism | 165 | 24.44 | 3.96E-06 |
| | GO:44267: cellular protein metabolism | 164 | 24.3 | 2.07E-06 |
| | GO:6139: nucleobase, nucleoside, nucleotide and nucleic acid metabolism | 201 | 29.78 | 9.59E-11 |
| | GO:9058: biosynthesis | 81 | 12 | 4.26E-05 |
| | GO:44249: cellular biosynthesis | 76 | 11.26 | 8.81E-06 |
| | GO:9059: macromolecule biosynthesis | 57 | 8.444 | 2.81E-07 |
| | GO:6412: protein biosynthesis | 55 | 8.148 | 1.71E-08 |
| | GO:16070: RNA metabolism | 67 | 9.926 | 1.44E-16 |
| | GO:16265: death | 45 | 6.667 | 0.000268 |
| | GO:8219: cell death | 45 | 6.667 | 0.000218 |
| | GO:6915: apoptosis | 45 | 6.667 | 6.02E-05 |
| | GO:43037: translation | 23 | 3.407 | 1.23E-05 |
| | GO:6396: RNA processing | 58 | 8.593 | 1.42E-15 |
| | GO:6397: mRNA processing | 23 | 3.407 | 0.000946 |
| | GO:6399: tRNA metabolism | 16 | 2.37 | 1.40E-06 |
| | GO:8380: RNA splicing | 25 | 3.704 | 1.58E-05 |
| | GO:6413: translational initiation | 11 | 1.63 | 0.000132 |
| | GO:398: nuclear mRNA splicing, via spliceosome | 20 | 2.963 | 0.000218 |
| | GO:7028: cytoplasm organization and biogenesis | 16 | 2.37 | 5.10E-08 |
| | GO:42254: ribosome biogenesis and assembly | 16 | 2.37 | 3.51E-09 |
| | GO:6364: rRNA processing | 13 | 1.926 | 1.01E-08 |
| | GO:16072: rRNA metabolism | 14 | 2.074 | 1.37E-09 |
| | GO:8033: tRNA processing | 10 | 1.481 | 3.06E-06 |
| | GO:6432: phenylalanyl-tRNA aminoacylation | 3 | 0.444 | 0.000223 |

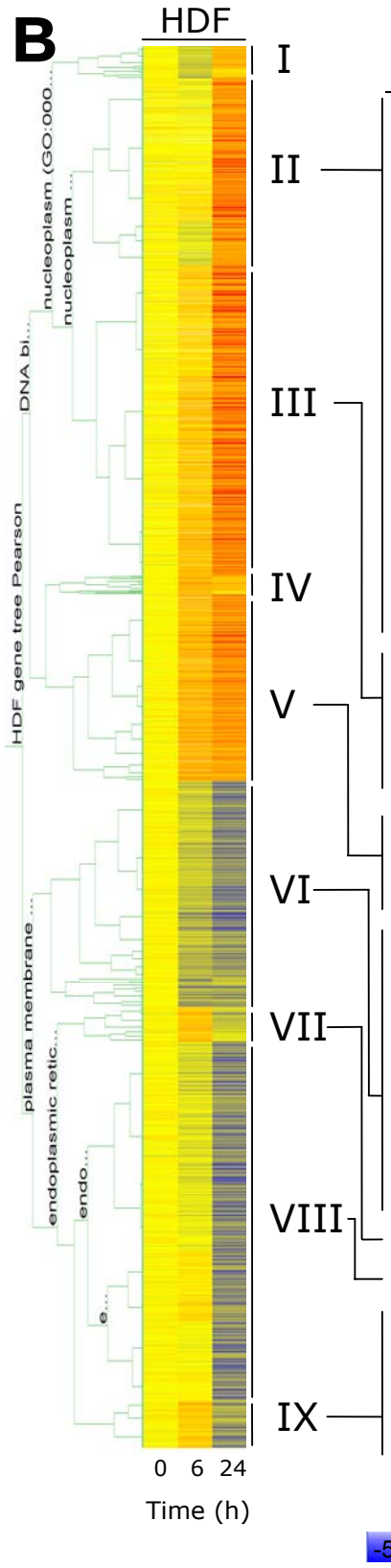


| Category | Genes in List in Category | % of Genes in List in Category | *p*-Value |
|---|---|---|---|
| GO:50875: cellular physiological process | 104 | 77.04 | 0.000173 |
| GO:44238: primary metabolism | 75 | 55.56 | 0.00077 |
| GO:43170: macromolecule metabolism | 52 | 38.52 | 0.000647 |
| GO:50794: regulation of cellular process | 50 | 37.04 | 3.69E-07 |
| GO:50789: regulation of biological process | 50 | 37.04 | 3.67E-06 |
| GO:50791: regulation of physiological process | 47 | 34.81 | 3.28E-06 |
| GO:51244: regulation of cellular physiological process | 47 | 34.81 | 1.06E-06 |
| GO:43283: biopolymer metabolism | 40 | 29.63 | 0.000842 |
| GO:48522: positive regulation of cellular process | 20 | 14.81 | 1.08E-08 |
| GO:48518: positive regulation of biological process | 20 | 14.81 | 8.78E-08 |
| GO:43119: positive regulation of physiological process | 19 | 14.07 | 4.44E-09 |
| GO:51242: positive regulation of cellular physiological process | 19 | 14.07 | 2.28E-09 |
| GO:8283: cell proliferation | 19 | 14.07 | 7.05E-07 |
| GO:16265: death | 18 | 13.33 | 4.70E-06 |
| GO:8219: cell death | 18 | 13.33 | 4.13E-06 |
| GO:12501: programmed cell death | 17 | 12.59 | 8.31E-06 |
| GO:6915: apoptosis | 17 | 12.59 | 8.05E-06 |
| GO:42127: regulation of cell proliferation | 15 | 11.11 | 1.39E-07 |
| GO:8284: positive regulation of cell proliferation | 11 | 8.148 | 3.51E-08 |
| GO:42981: regulation of apoptosis | 10 | 7.407 | 0.000613 |
| GO:43067: regulation of programmed cell death | 10 | 7.407 | 0.000634 |
| GO:6917: induction of apoptosis | 7 | 5.185 | 0.000733 |
| GO:12502: induction of programmed cell death | 7 | 5.185 | 0.000733 |
| GO:16070: RNA metabolism | 22 | 9.205 | 1.29E-05 |
| GO:6396: RNA processing | 19 | 7.95 | 2.51E-05 |
| GO:16071: mRNA metabolism | 14 | 5.858 | 0.000122 |
| GO:6397: mRNA processing | 13 | 5.439 | 0.000197 |
| GO:398: nuclear mRNA splicing, via spliceosome | 11 | 4.603 | 0.000175 |
| GO:377: RNA splicing, via transesterification reactions with bulged adenosine as nucleophile | 11 | 4.603 | 0.000175 |
| GO:43170: macromolecule metabolism | 55 | 38.73 | 0.000391 |
| GO:16070: RNA metabolism | 17 | 11.97 | 4.05E-06 |
| GO:6396: RNA processing | 16 | 11.27 | 1.34E-06 |
| GO:6364: rRNA processing | 4 | 2.817 | 0.000613 |
| GO:16072: rRNA metabolism | 4 | 2.817 | 0.000694 |
| GO:6807: nitrogen compound metabolism | 21 | 12.43 | 3.69E-09 |
| GO:6082: organic acid metabolism | 21 | 12.43 | 2.06E-07 |
| GO:19752: carboxylic acid metabolism | 21 | 12.43 | 1.88E-07 |
| GO:9308: amine metabolism | 19 | 11.24 | 3.92E-08 |
| GO:6519: amino acid and derivative metabolism | 18 | 10.65 | 1.47E-08 |
| GO:6520: amino acid metabolism | 16 | 9.467 | 5.18E-08 |
| GO:8652: amino acid biosynthesis | 6 | 3.55 | 3.26E-05 |
| GO:43038: amino acid activation | 6 | 3.55 | 2.82E-05 |
| GO:43039: tRNA aminoacylation | 6 | 3.55 | 2.82E-05 |
| GO:6418: tRNA aminoacylation for protein translation | 6 | 3.55 | 2.82E-05 |
| GO:6399: tRNA metabolism | 6 | 3.55 | 0.000481 |
| GO:6563: L-serine metabolism | 4 | 2.367 | 1.56E-05 |
| GO:6564: L-serine biosynthesis | 3 | 1.775 | 0.000115 |
| GO:8610: lipid biosynthesis | 4 | 14.81 | 0.00075 |
| GO:5975: carbohydrate metabolism | 19 | 6.786 | 0.000978 |
| GO:46785: microtubule polymerization | 5 | 12.2 | 1.03E-09 |
| GO:30705: cytoskeleton-dependent intracellular transport | 5 | 12.2 | 4.65E-06 |
| GO:7018: microtubule-based movement | 5 | 12.2 | 4.65E-06 |
| GO:226: microtubule cytoskeleton organization and biogenesis | 5 | 12.2 | 7.24E-07 |
| GO:31109: microtubule polymerization or depolymerization | 5 | 12.2 | 7.87E-09 |

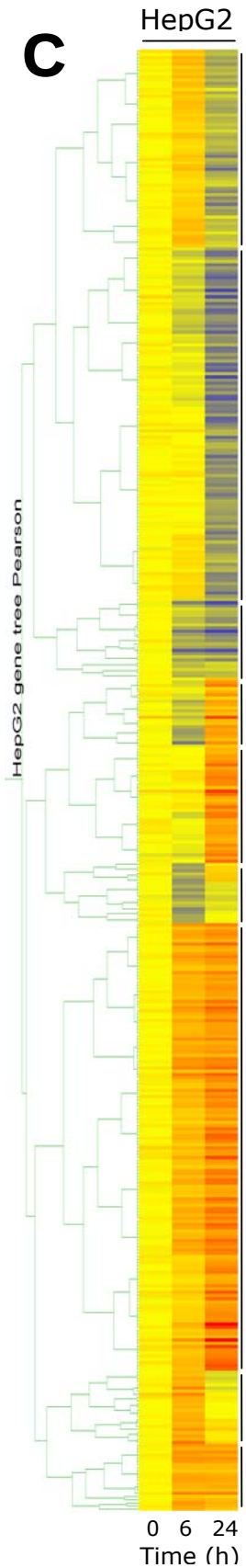


| | Category | Genes in List in Category | % of Genes in List in Category | *p*-Value |
|---|---|---|---|---|
| I | GO:50875: cellular physiological process | 42 | 82.35 | 0.00159 |
| | GO:6807: nitrogen compound metabolism | 6 | 11.76 | 0.00219 |
| | GO:9308: amine metabolism | 6 | 11.76 | 0.00159 |
| II | GO:6066: alcohol metabolism | 7 | 7.692 | 0.000863 |
| | GO:8610: lipid biosynthesis | 6 | 6.593 | 0.00291 |
| | GO:6694: steroid biosynthesis | 6 | 6.593 | 7.30E-06 |
| | GO:16126: sterol biosynthesis | 6 | 6.593 | 5.13E-08 |
| | GO:16125: sterol metabolism | 6 | 6.593 | 5.34E-06 |
| | GO:8202: steroid metabolism | 6 | 6.593 | 0.000275 |
| | GO:6260: DNA replication | 5 | 5.495 | 0.00268 |
| | GO:6261: DNA-dependent DNA replication | 4 | 4.396 | 0.00119 |
| | GO:48193: Golgi vesicle transport | 4 | 4.396 | 0.00194 |
| | GO:6695: cholesterol biosynthesis | 3 | 3.297 | 0.000729 |
| | GO:51052: regulation of DNA metabolism | 3 | 3.297 | 0.000834 |
| | GO:51053: negative regulation of DNA metabolism | 2 | 2.198 | 0.000198 |
| | GO:8156: negative regulation of DNA replication | 2 | 2.198 | 0.000198 |
| | GO:6275: regulation of DNA replication | 2 | 2.198 | 0.0023 |
| III | GO:19725: cell homeostasis | 2 | 11.11 | 0.0047 |
| | GO:6873: cell ion homeostasis | 2 | 11.11 | 0.00337 |
| | GO:30003: cation homeostasis | 2 | 11.11 | 0.00267 |
| IV | GO:6875: metal ion homeostasis | 2 | 11.11 | 0.00215 |
| | GO:46916: transition metal ion homeostasis | 2 | 11.11 | 0.000293 |
| | GO:30005: di-, tri-valent inorganic cation homeostasis | 2 | 11.11 | 0.00177 |
| V | GO:50801: ion homeostasis | 2 | 11.11 | 0.00456 |
| VI | | | | |
| VII | GO:50875: cellular physiological process | 75 | 76.53 | 0.00188 |
| | GO:44238: primary metabolism | 54 | 55.1 | 0.00499 |
| | GO:43170: macromolecule metabolism | 45 | 45.92 | 1.07E-05 |
| | GO:43283: biopolymer metabolism | 32 | 32.65 | 0.000432 |
| | GO:16070: RNA metabolism | 12 | 12.24 | 8.54E-05 |
| | GO:6412: protein biosynthesis | 10 | 10.2 | 0.00317 |
| | GO:6396: RNA processing | 11 | 11.22 | 6.36E-05 |
| | GO:6399: tRNA metabolism | 6 | 6.122 | 2.38E-05 |
| | GO:6364: rRNA processing | 3 | 3.061 | 0.00249 |
| | GO:8033: tRNA processing | 5 | 5.102 | 4.01E-06 |
| | GO:16072: rRNA metabolism | 3 | 3.061 | 0.00273 |
| VIII | GO:9611: response to wounding | 4 | 21.05 | 0.00155 |
| | GO:9966: regulation of signal transduction | 3 | 15.79 | 0.00167 |
| IX | | | | |

**Figure 3.3. Hierarchical clustering of gene expression profiles.** (A) Both HDF and HepG2 cells; (B) HDF cells; (C) HepG2 cells. Gene Ontology categories over-represented in the indicated clusters were derived by limiting lists displayed in the Gene Ontology Browser in GeneSpring GX to a *p*-value cutoff of 0.001 (the cutoff was raised to 0.005 for HepG2 cells). Lists displayed in the tables were further limited to those containing 2 or more genes from any given category. Unlabelled clusters displayed no significant associations according to the *p*-value cutoffs applied.

#### 3.3.1.4 DAVID functional analysis reveals the induction of diverse stress signalling pathways

The Database for Annotation, Visualisation and Integrated Discovery (Dennis et al., 2003) is a comprehensive list of genes from various species linked to information on the biological function of the gene product. The associated Functional Annotation tool performs statistical comparisons of gene lists entered by a user with gene lists in the DAVID database. The software provides a number of visualisation tools to display over-represented genes in tables and biological pathway diagrams derived from projects such as Biocarta (http://www.biocarta.com) and KEGG (Ogata et al., 1999). Biocarta pathways summarise signal transduction associated with various disease states and is compiled from contributions by members of the scientific community. The KEGG pathway database also includes a large number of signalling pathways, but in addition contains an exhaustive list of biosynthetic and metabolic pathways. Using a combination of these two resources provides good coverage of known biological pathways.

The Functional Analysis tool on the DAVID website was used to find biological pathways over-represented in the list of genes occurring in cluster I from figure 3.3A (Table 3.2). This cluster comprises genes that are generally down-regulated after 24 h in both cell types. Only two Biocarta pathways were significantlyassociated with this list ($p < 0.05$), both of which are probably not relevant in the context of cell cultures, applying only to whole organisms ('Stathmin and breast cancer resistance to antmicroubule agents' and 'How progesterone initiates oocyte maturation'). However, a number of KEGG pathways were associated with this cluster at a high level of significance ($p < 0.01$). These include the cell cycle as well as two pathways associated

with energy metabolism ('glycolysis/gluconeogenesis' and 'pyruvate metabolism'), and two involving amino acid metabolism ('glycine, serine and threonine metabolism', and 'tryptophan metabolism'). Three further KEGG pathways were also significantly associated ($p < 0.05$) with the down-regulated cluster ($p < 0.05$): 'propanoate metabolism', 'amino acid-tRNA synthetases', and 'glutamate metabolism'. These findings corroborate the results of Gene Ontology category analysis shown in figure 3.3A, where a large number of genes with functions in amino acid metabolism and glucose metabolism were associated with the group of down-regulated genes represented in cluster I.

**Table 3.2** Biological pathways associated with cluster I from figure 3.3A (generally down-regulated in both cell types after 24 h). Pathways displayed were limited to those with a *p*-value of less than 0.1.

| Pathway | Count | Percentage | *p*-value |
|---|---|---|---|
| *Biocarta pathways* | | | |
| Stathmin and breast cancer resistance to antimicrotubule agents | 5 | 0.60% | 0.013 |
| How progesterone initiates the oocyte maturation | 5 | 0.60% | 0.035 |
| Rab GTPases mark targets in the endocytotic machinery | 4 | 0.50% | 0.067 |
| *KEGG pathways* | | | |
| Glycolysis / gluconeogenesis | 14 | 1.60% | 0.000097 |
| Pyruvate metabolism | 11 | 1.30% | 0.00027 |
| Glycine, serine and threonine metabolism | 11 | 1.30% | 0.00033 |
| Cell cycle | 16 | 1.80% | 0.0039 |
| Tryptophan metabolism | 13 | 1.50% | 0.0083 |
| Propanoate metabolism | 8 | 0.90% | 0.011 |
| Aminoacyl-tRNA synthetases | 7 | 0.80% | 0.013 |
| Glutamate metabolism | 6 | 0.70% | 0.035 |
| Glycerolipid metabolism | 8 | 0.90% | 0.052 |
| Butanoate metabolism | 8 | 0.90% | 0.052 |
| Arginine and proline metabolism | 8 | 0.90% | 0.061 |
| Selenoamino acid metabolism | 6 | 0.70% | 0.063 |
| Caprolactam degradation | 4 | 0.50% | 0.085 |
| Lysine degradation | 8 | 0.90% | 0.094 |
| Parkinson's disease | 4 | 0.50% | 0.097 |

Using the same procedure, cluster II from figure 3.3A (generally up-regulated after 24 h in both cell types) was analysed for the presence of genes involved with biological pathways (Table 3.3). Biocarta pathways significantly associated with this cluster ($p < 0.01$) include two tumour necrosis factor (TNF) receptor signalling pathways and two pathways involving NF-κB signalling, interleukin-1 receptor signalling, and

mitochondrial apoptotic signalling. Additional Biocarta pathways associated with this cluster with moderate significance ($p < 0.05$) were associated with receptor-mediated apoptosis, toll-like receptor signalling and double-stranded RNA-induced gene expression. KEGG pathways associated with cluster II with high significance ($p < 0.01$) include 'pyrimidine metabolism', 'nitrobenzene degradation' and 'folate biosyhthesis'. Interestingly, a number of KEGG pathways involved in amino acid metabolism were also significantly ($p < 0.05$) associated with this cluster: 'tryptophan metabolism', 'histidine metabolism', 'tyrosine metabolism', and 'amino-acyl tRNA synthetases'. These functions did not appear in the Gene Ontology analysis shown in figure 3.3A. Other significant ($p < 0.05$) associations with KEGG pathways include the mitogen-activated protein kinase (MAPK) pathway, 'RNA polymerases', and 'adipocytokine signalling'. The MAPK pathway can be activated by a wide range of cellular stresses, and the possible role of this pathway in CYN toxicity is further discussed in Chapter 5.

This analysis was performed on all clusters shown in figures 3.3B and C, but few clusters showed significant associations with pathways in either the Biocarta or KEGG databases. One exception was cluster III from the HDF gene tree (figure 3.3B), which displayed significant associations with pathways involving TNF-receptor signalling and NF-κB-related signalling. Many of these pathways were similar to those found to be associated with cluster II of figure 3.3A. The TNF receptor 2 pathway was particularly well represented in this cluster (Figure 3.4).

**Table 3.3** Biological pathways associated with cluster II from figure 3.3A (generally up-regulated in both cell types after 24 h), identified using DAVID. Pathways displayed were limited to those with *p*-values < 0.1.

| Pathway | Count | Percentage | *p*-value |
|---|---|---|---|
| *Biocarta pathways* | | | |
| TNFR2 signaling pathway | 7 | 0.80% | 0.00016 |
| NF-kB activation by nontypeable *Hemophilus influenzae* | 7 | 0.80% | 0.0014 |
| TNF/stress related signaling | 7 | 0.80% | 0.0014 |
| Signal transduction through IL1R | 7 | 0.80% | 0.0044 |
| Role of mitochondria in apoptotic signaling | 6 | 0.70% | 0.0048 |
| CD40L signaling pathway | 5 | 0.60% | 0.0054 |
| NF-kB signaling pathway | 6 | 0.70% | 0.0059 |
| Double stranded RNA induced gene expression | 4 | 0.40% | 0.012 |
| HIV-I NEF | 9 | 1.00% | 0.012 |
| Induction of apoptosis through DR3 and DR4/5 death receptors | 6 | 0.70% | 0.018 |
| Keratinocyte differentiation | 7 | 0.80% | 0.019 |
| Toll-like receptor pathway | 6 | 0.70% | 0.04 |
| Chaperones modulate interferon signaling pathway | 4 | 0.40% | 0.068 |
| ATM signaling pathway | 4 | 0.40% | 0.077 |
| MAP kinase signaling pathway | 9 | 1.00% | 0.08 |
| Ceramide signaling pathway | 4 | 0.40% | 0.096 |
| FAS signaling pathway ( CD95 ) | 5 | 0.60% | 0.097 |
| *KEGG pathways* | | | |
| Pyrimidine metabolism | 14 | 1.60% | 0.00017 |
| Nitrobenzene degradation | 5 | 0.60% | 0.0036 |
| Folate biosynthesis | 7 | 0.80% | 0.0039 |
| Aminophosphonate metabolism | 5 | 0.60% | 0.01 |
| Tryptophan metabolism | 10 | 1.10% | 0.011 |
| Pantothenate and CoA biosynthesis | 5 | 0.60% | 0.016 |
| Histidine metabolism | 7 | 0.80% | 0.02 |
| MAPK signaling pathway | 20 | 2.20% | 0.021 |
| RNA polymerase | 5 | 0.60% | 0.028 |
| Adipocytokine signaling pathway | 8 | 0.90% | 0.028 |
| Tyrosine metabolism | 7 | 0.80% | 0.038 |
| Aminoacyl-tRNA synthetases | 5 | 0.60% | 0.043 |
| Tetrachloroethene degradation | 3 | 0.30% | 0.052 |
| Selenoamino acid metabolism | 5 | 0.60% | 0.057 |
| Oxidative phosphorylation | 11 | 1.20% | 0.069 |
| Androgen and estrogen metabolism | 6 | 0.70% | 0.074 |
| Phenylalanine, tyrosine and tryptophan biosynthesis | 3 | 0.30% | 0.075 |
| Apoptosis | 8 | 0.90% | 0.093 |
| Cell cycle | 9 | 1.00% | 0.099 |

**TNF receptor 2 signalling pathway (Biocarta)**

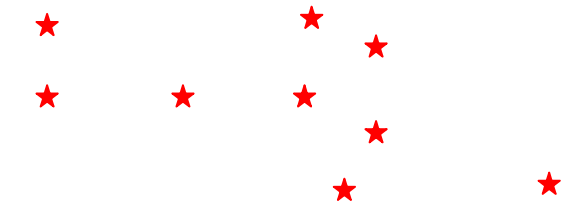

Figure removed, please consult print copy of the thesis held in Griffith University Library

NIK - Mitogen-activated protein kinase kinase kinase 14

Conserved helix-loop-helix ubiquitous kinase

MKP1 - Dual specificity phosphatase 1

IKKβ - Inhibitor of kappa light polypeptide gene enhancer in b-cells, kinase, beta

IKKα -Nuclear factor of kappa light polypeptide gene enhancer in b-cells inhibitor, kinase alpha

IKKAP2 - Immunoglobulin kappa variable 1-27; tumor necrosis factor, alpha-induced protein 3

TRAF2 - TRAF member-associated NF-κB activator, TNF receptor-associated factor 2

TRAF1 - TNF receptor-associated factor 1

TRAF family member-associated NFkB activator

TRAF3 - TNF receptor-associated factor 3

TNF1β - lymphotoxin alpha (TNF superfamily, member 1)

RIP - Receptor (TNFRSF)-interacting serine-threonine kinase 1; RPA interacting protein; hiv-1 rev binding protein; rala binding protein 1

TNFR2 - Tumour necrosis factor receptor superfamily, member 1b

**Figure 3.4 CYN induces the expression of genes involved in TNF signalling.** The TNFR2 signalling pathway is shown (as described by Biocarta, http://www.biocarta.com). Genes present in the DAVID database participating this pathway are listed beside the figure; those present in cluster III of the HDF gene tree (Figure 3.3A) are shown in red and are marked with a red star in the pathway figure.

Despite significant associations between lists of genes in selected clusters and lists of pathway genes, only a small proportion of genes in the clusters are associated with pathways. For example, cluster III from the HDF gene tree contains 323 genes, of which 311 have unique DAVID identifications. Of this list of 311 genes, only 38 can be assigned to Biocarta pathways and 59 to KEGG pathways, using the limits applied in the above analyses ($p < 0.1$). That leaves 298 genes from the original list, after comparison to the Biocarta pathways, which are not assigned any biological function using this method (for KEGG pathways, 284 genes remain unassigned to a pathway). For the large gene lists comprising clusters I and II of the combined gene tree in figure 3.3A, only 2-4% of genes were assigned to pathways. Hence, despite providing an

effective means of detecting highly over-represented functions in selected gene lists, this procedure, like the Gene Ontology browser method, does not provide a comprehensive analysis of possible functions associated with lists of changing genes. These methods do not identify single genes that may be pivotal to a particular pathway or functions, rather they rely on the presence (in the query list) of multiple genes from a given pathway or functional category. Hence, genes with important functions in CYN toxicity may be overlooked by these methods. To address this, genes with large changes in relative gene expression were considered to be worthy of further discussion, as well as groups of co-ordinately regulated genes involved in known stress responses.

### *3.3.2 Large changes in expression after 24 h reveal responses common to both cell types*

The most obvious candidates for a central role in cellular responses to CYN are genes showing large changes in relative transcript level. Genes comprising a list of the ten largest changes in relative transcript level after 24 h treatment (Table 3.4) are chosen for discussion below. Most genes with large changes after 6 h also showed large changes in the same direction after 24 h, and therefore the earlier time point will not be considered in detail.

*GADD45α* was the most highly induced gene in HDFs and the second-most highly induced gene in HepG2 cells in response to CYN. This gene is inducible by DNA damage and other stresses, and encodes a member of the growth arrest and DNA damage-associated, 45 kDa (GADD45), group of proteins (Fornace et al., 1989). This group consists of three distinct proteins with multiple roles in the DNA damage response. The GADD45α protein plays a role in the mediation of cell cycle checkpoints (Wang et al., 1999), coordination of DNA repair (Smith et al., 2000), and apoptosis (Hildesheim et al., 2002). Transcription of the *GADD45α* gene can be controlled by either p53 (Goldwasser et al., 1996) or via BRCA1 (Fan et al., 2002), both of which are associated with DNA damage responses. The role of this gene in a putative DNA damage response induced by CYN is further discussed below (Section 3.3.3.1). CYN also strongly induces expression of the *GADD45B* (8.2-fold in HDFs and 2.6-fold in HepG2 cells), which encodes another member of this group of proteins, GADD45β. GADD45β, originally known as MyD118 due to its discovery in processes associated

with the myeloid differentiation primary response (Abdollahi et al., 1991), bears sequence similarity to GADD45α and has related but distinct functions. In addition to contributing to growth arrest in response to genotoxic stress (Vairapandi et al., 2002), GADD45β can inhibit the activation of c-Jun N-terminal kinase (JNK) an important member of the MAPK signalling pathway (Papa et al., 2004).

The gene for thioredoxin-interacting protein, *TXNIP*, was highly induced in HDFs, and induced in HepG2 cells by more than two-fold, after 24 h exposure to 1 μg/mL CYN. The TXNIP protein is an endogenous inhibitor of thioredoxin, an evolutionarily conserved antioxidant protein (Nishiyama et al., 1999). *TXNIP* expression is induced by stresses such as hypoxia (Le Jan et al., 2006) and hyperglycaemia (Schulze et al., 2004). TXNIP can induce apoptosis in macrophage-like cells, possibly by modulating the redox state (Wang et al., 2006), and is associated with elevated levels of oxidative stress in vascular cells in a mouse diabetes model (Schulze et al., 2004). The possible role of TXNIP in CYN toxicity may be associated with oxidative stress in the cell models used in this study, despite indications that oxidative stress does not play a role in acute hepatocellular toxicity *in vitro* (Humpage et al., 2005).

Interleukin-8 (IL8) mRNA levels were 12-fold higher in treated HDFs and nearly 4-fold higher in treated HepG2 cells after 24 h, relative to the respective controls. IL8 is known to be expressed in cultured dermal fibroblasts (Kristensen et al., 1991; Zhang et al., 1992) and HepG2 cells (Gomez-Quiroz et al., 2003; Holden et al., 2000) in response to a range of stimuli including exposure to interleukin 1 or various cytotoxins. The role of IL8 *in vivo* is associated with inflammation, where it acts as a chemokine, attracting leukocytes to sites of infection or wounding. The promoter of the *IL8* gene contains binding sites for NF-κB, AP-1, C/EBPδ, Oct-1, NFAT-1 and an antioxidant response element (ARE), indicating that numerous signals can culminate in IL8 gene expression (Roebuck, 1999). Of particular interest in the context of CYN toxicity are the response elements for AP-1 (activator protein 1, activated by the MAPK/SAPK stress response pathway) and C/EBPδ (CCAAT element binding protein, delta, the expression of which also strongly induced in response to CYN). Relative mRNA levels for a range of cytokines appear to be elevated following CYN exposure (discussed further below—'NF-κB-mediated gene expression'), which indicates a possible role for inflammatory processes in CYN toxicity.

CYN strongly induced the expression of a gene encoding H4 histone 1, member H (*HIST1H4H*) in both cell types after 24 h exposure (approximately 10-fold in HDFs and 2.5-fold in HepG2). The gene for H4 Histone family 2 (*HIST2H4*) was also strongly induced by CYN (approximately 7.5-fold in HDFs and 3.8-fold in HepG2). Periodic regulation of histone gene expression occurs during the cell cycle and is closely associated with DNA synthesis during S phase (Nelson et al., 2002). The transcription of histone genes is increased three- to five-fold during S phase and depends partially on the activation of cyclin E/cdk2 by phosphorylation (Ma et al., 2000). Interestingly, the down-regulation of genes encoding core histones of the H2, H3 and H4 families can occur after toxin-induced stress in renal tubular epithelial cells (Jeong et al., 1997). In the data presented here, genes for H4 histones are clearly up-regulated strongly and significantly, but the reasons for this are not clear.

Transcript levels for the *TNFRSF12A* gene were elevated in both cell types, and in HepG2 this was the most highly induced gene after 24 h CYN exposure (7.8-fold increase in HDFs and 7.5-fold in HepG2 cells). This gene encodes the receptor for a member of the tumour necrosis factor (TNF) family of cytokines known as TWEAK due to its function as a weak inducer of apoptosis (Chicheportiche et al., 1997). The receptor, known as FN14 (fibroblast growth factor (FGF) -inducible 14 kDa protein) or TWEAKR, is a type 1a transmembrane protein belonging to the TNF receptor superfamily, encoded by the *TNFRSF12A* gene which can be induced by FGF (Meighan-Mantha et al., 1999). TWEAKR and its ligand play a role in the induction of apoptosis. Although, unlike most TNF-family receptors, the TWEAK receptor does not have a death domain, it can induce apoptosis by stimulating the activation of endogenous membrane bound TNF, which results in apoptosis via a TNF receptor 1 (Schneider et al., 1999). TWEAK also induces apoptosis in some types of cancer cells by activating caspases independently of TNF (Nakayama et al., 2002). Interestingly, TWEAKR can also induce anti-apoptotic pathways mediated by NF-κB, through the binding of the TNF-receptor associated factors TRAF1, 2, 3 and 5 (Han et al., 2003). Clearly, the involvement of TWEAK in apoptosis in various cell types is complex, however the strong expression of the gene for TWEAKR after CYN exposure in both cell types used in this report suggests that this TNF-related pathway may be important in cell death processes induced by CYN.

The *TNFAIP3* gene, encoding tumour necrosis factor alpha-inducible protein A20, is strongly induced in HDFs (7.7-fold) and moderately induced in HepG2 cells (2.7-fold) following CYN treatment for 24 h. In response to TNF, A20 reduces TNF-mediated NF-κB-dependent gene expression via multiple mechanisms and is a potent inhibitor of apoptosis (Beyaert et al., 2000; Heyninck and Beyaert, 2005). The modulation of pro- and anti-apoptotic pathways involving NF-κB seems to be a recurrent theme amongst the genes highly expressed in response to CYN.

*NOL5A* encodes nucleolar protein 5A, a protein involved in the assembly of the 60S ribosomal subunit (Hayano et al., 2003). Relative mRNA levels for *NOL5A* were highly elevated in HepG2 cells (3.7-fold) and moderately elevated in HDFs (1.9-fold) after 24 h CYN exposure.

*GDF15* expression was also highly induced in HepG2 cells (3.7-fold) following 24 h CYN exposure, and was significantly induced in HDFs (1.8-fold). This gene encodes growth- and differentiation-factor 15, a member of the transforming growth factor-beta (TGF-β) family of growth and differentiation factors (Hsiao et al., 2000; Paralkar et al., 1998). GDF15 is induced in response to injury in various organs, including the liver (Hsiao et al., 2000; Zimmers et al., 2005). The *GDF15* promoter contains two p53 binding sites and can is activated after p53 overexpression or DNA damage in a p53-null cell line, indicating regulation by both p53-dependent and -independent mechanisms (Li et al., 2000). *GDF15* is often described as a p53-regulated gene and is induced after various stresses including DNA damage (Kim et al., 2007; Kis et al., 2006; Secchiero et al., 2006; Yang et al., 2006). CYN induces the expression of numerous additional p53-regulated genes (see Section 3.3.3.1, also Chapter 4).

*AREG*, induced 4-fold in HepG2 cells and 1.7-fold in HDFs, encodes amphiregulin, a mitogen related to the transforming growth factor alpha (TGF-α) and epidermal growth factor (EGF) families. Amphiregulin expression is induced following exposure to DNA damaging agents in cultured bladder cancer cells (Sorensen et al., 2004), under conditions of oxidative stress in cultured rat gastric epithelial cells (Miyazaki et al., 1996), and after stress induced by fine particulate matter in bronchial epithelial cells (Blanchet et al., 2004).

In HepG2 cells, another highly induced gene was *NT5C* (3.1-fold after 24 h; 1.6-fold in HDFs). This gene encodes a cytosolic pyrimidine 5'-3' nucleotidase that catalyses the removal of phosphate groups from uridine monophosphate (UMP) or deoxycytidine monophosphate (cCMP) (Hoglund and Reichard, 1990; Rampazzo et al., 2000). Nucleotidases such as the one encoded by *NT5C* are responsible for regulation of the cellular nucleotide pool (Bianchi and Spychala, 2003).

The gene for the p62/sequestosome 1 protein, *SQSTM1*, was one of the ten most induced genes in HepG2 cells (3.3-fold after 24 h) and was also significantly induced in HDFs (1.6-fold, $p < 0.05$). Sequestosome 1 recognises and is involved in the transport and sequestration of proteins with polyubiquitin chains, thereby modulating targeted degradation by the 26S proteasome (Seibenhener et al., 2004). This protein also plays a role in regulating NF-κB activity due to its ability to bind TRAF6 and enhance its ubiquitylation (Wooten et al., 2005).

Amongst the most strongly down-regulated genes in HepG2 cells after 24 h exposure was *TARG1* (0.37-fold; 0.66-fold in HDF cells). The product of this gene is a protein with putative functions in differentiation (Piquemal et al., 1999; van Belzen et al., 1997), and endoplasmic reticulum stress responses (Agarwala et al., 2000; Kokame et al., 1996). The promoter of the mouse homologue of human *TARG1, Ngr1,* is repressed by Myc proteins including c-myc (Shimono et al., 1999). Interestingly, c-Myc is induced after CYN exposure (see Chapter 5), which is consistent with the strong down-regulation of *TARG1*. Three other genes encoding endoplasmic reticulum stress-associated proteins are strongly down-regulated in response to CYN – *FKBP14* (0.51-fold in HDFs; 0.37-fold in HepG2 cells), *GRP78* (0.42-fold in HDFs; 0.28-fold in HepG2 cells) and *HERPUD1* (0.39-fold in HDFs; 0.26-fold in HepG2 cells). These genes are discussed further below (Section 3.3.3.3). *RRBP1*, a gene encoding an ER protein that effectively functions as an receptor for the ribosome (Savitz and Meyer, 1990) was also strongly down-regulated in HepG2 cells (0.34-fold) and HDFs (0.35-fold) after 24 h CYN exposure.

The *LIPA* gene, encoding lipase A, was strongly down-regulated in both cell types after 24 h (0.18-fold in HDFs; 0.45-fold in HepG2 cells). Lipase A is a lysosomal enzyme essential for the hydrolysis of cholesterol esters (Ameis et al., 1994). This enzyme is

important for the removal of cholesterol from the body via the synthesis of bile acids (Zhao et al., 2005).

The gene for a member of the ribonuclease A family, *RNASE4*, was down-regulated strongly and significantly in HepG2 cells after 24 h (0.37-fold, $p = 0.0035$) but not significantly down-regulated in HDFs (0.55-fold, $p = 0.245$). RNase 4 cleaves on the 3' side of uridine residues of single-stranded RNA (Rosenberg and Dyer, 1995; Zhou and Strydom, 1993). RNases play an important role in mRNA turnover and the regulation of gene expression.

A number of genes encoding enzymes involved in amino acid metabolism were strongly down-regulated in both cell types. *PHGDH* (0.35-fold in HDFs; 0.39-fold in HepG2) encodes phosphoglycerate dehydrogenase, an enzyme functioning early in the serine biosynthetic pathway (Cho et al., 2000). A gene encoding phosphoserine aminotransferase, a key enzyme of the phosphorlated pathway of serine bioynthesis (Baek et al., 2003) was also strongly down-regulated (0.2-fold in HDFs; 0.51-fold in HepG2 cells). The product of *BCAT1* (0.3-fold in HDFs; 0.33-fold in HepG2) is a branched-chain aminotransferase that catalyses the interconversion of L-amino acids and α-keto acids (Davoodi et al., 1998). Transcription of the *BCAT1* gene is positively regulated by the c-Myc oncoprotein through a conserved promoter element (Ben-Yosef et al., 1996). Despite the strong induction of the *MYC* oncogene following CYN exposure (see Chapter 5 of thesis), *BCAT1* expression is significantly reduced in HepG2 cells and HDFs.

The gene for a glutamine transport enzyme, *SLC38A1*, was strongly down-regulated in both cell types after 24 h exposure (0.25-fold HDFs; 0.45-fold in HepG2). Transcript levels for a related gene, *SLC38A2*, were also reduced (0.2-fold in HDFs; 0.5-fold in HepG2). The products of these genes are members of the sodium-coupled neutral amino acid transporter (SNAT) family of transmembrane solute carriers, which are induced under conditions of amino acid starvation to allow for the rapid restoration of the intracellular amino acid pool once extracellular levels are restored (Mackenzie and Erickson, 2004). SNAT1 (*SLC38A1*) and SNAT2 (*SLC38A2*) both display a preference for glutamine, alanine, asparagine, cysteine, histidine and serine (Mackenzie and Erickson, 2004). SNAT2 expression is more widespread than SNAT1, which is

expressed primarily in the nervous system, retina, placenta and heart (Mackenzie and Erickson, 2004). SNAT2 expression in response to amino acid starvation is controlled partially at the transcriptional level through an amino acid response element present in intron 1 (Palii et al., 2004).

After amino acid deprivation, a stress response conserved from yeast to mammals is induced, involving a marked reduction in global protein synthesis via phosphorylation of eukaryotic initiation factor 2α (eIF2α). Stresses contributing to eIF2α phosphorylation include viral infection, ribotoxic stress, endoplasmic reticulum stress and amino acid starvation. EIF2α phosphorylation results in a reduction in the formation of initiation complexes and prevent cap-dependent translation of most mRNA in the cell (Harding et al., 2000). This enables the selective translation of mRNA for stress-related proteins through alternative initiation processes such as the utilisation of internal ribosome entry sites or alternative initiation codons (Holcik and Sonenberg, 2005; Jackson, 2005). Although this is obviously not detectable by microarray hybridisation, the increased abundance of transcription factors that are under this type of control can induce the transcription of target genes, enhancing their expression during the stress response. Continued translation of SNAT2 is enabled during the amino acid starvation response via an internal ribosome entry site (Gaccioli et al., 2006).

Asparagine synthetase (AS, encoded by the gene *ASNS*) expression is partially controlled through a similar mechanism to SNAT2 expression, although in an indirect fashion: eIF2α phosphorylation results in an increase in the translation of mRNA for the transcription factor known as activating transcription factor 4 (ATF4), which subsequently induces transcription from the *ASNS* gene promoter (Siu et al., 2002; Sun et al., 2004). Interestingly, *ASNS* expression was strongly down-regulated in response to CYN after 24 h exposure (0.17-fold in HDFs; 0.48-fold in HepG2 cells). This adds to the list of genes involved in endoplasmic reticulum stress and general amino acid metabolism that are down-regulated in response to CYN.

*HSPA1B*, encoding a member of the 70 kDa heat shock protein (HSP70) family of chaperonins, is down-regulated in both cell types used in this study after 24 h CYN exposure (0.28-fold in HDFs; 0.28-fold in HepG2). HSP70 proteins assist newly synthesised proteins to adopt the correct conformation, prevent the aggregation of

unfolded or misfolded proteins, translocation of membrane-associated or sectreted proteins to their target membranes, and participate in the regulation of various proteins (reviewed by Mayer and Bukau, 2005). HSP70 proteins also negatively regulate apoptotic cell death through a variety of mechanisms (Gabai et al., 2002; Garrido et al., 2001; Ravagnan et al., 2001; Vayssier and Polla, 1998). *HSPA1B* encodes the major inducible HSP70 family member (Wu et al., 1985), referred to as HSP70-2, heat shock 70 kDa protein 1B, or HSP72. The strong reduction in mRNA for this protein and other chaperonins may be attributable to a reduction in protein synthesis by CYN—a diminished requirement for folding chaperones concievably results in a decrease in the expression of the genes encoding them, although a mechanism for this kind of regulation is not currently known.

**Table 3.4** Genes with large changes in relative transcript level after exposure to 1 μg/ml cylindrospermopsin for 24 h. Expression ratios for up-regulated genes are shown in red type, down-regulated in blue. The genes listed consist of the ten most highly induced or repressed genes in each cell line after 24 hours (there is some overlap for this category in both cell types; genes appearing in the top ten both for both cell types appear once). Summaries of gene function are derived from the NCBI Entrez Gene database (Maglott et al., 2005).

| **Relative mRNA level** HDF (t-test *p* value); HepG2 (t-test *p* value) | **Common name** | **Product** | **Summary function** |
|---|---|---|---|
| 21.11 (0.000647); 6.1 (0.000618) | *GADD45A* | Growth arrest and DNA damage inducible, alpha | This gene is a member of a group of genes whose transcript levels are increased following stressful growth arrest conditions and treatment with DNA-damaging agents. The protein encoded by this gene responds to environmental stresses by mediating activation of the p38/JNK pathway via MTK1/MEKK4 kinase. The DNA damage-induced transcription of this gene is mediated by both p53-dependent and -independent mechanisms. |
| 12.34 (0.000457); 2.37 (0.0011) | *TXNIP* | Thioredoxin interacting protein | No summary function available. Thioredoxin interacting protein is an endogenous inhibitor of thioredoxin, an important antioxidant and signalling protein. |
| 12.0 (0.00198); 3.87 (0.000596) | *IL8* | Interleukin 8 precursor | The protein encoded by this gene is a member of the CXC chemokine family. This chemokine is one of the major mediators of the inflammatory response. This chemokine is secreted by several cell types. It functions as a chemoattractant, and is also a potent angiogenic factor. This gene is believed to play a role in the pathogenesis of bronchiolitis, a common respiratory tract disease caused by viral infection. This gene and other ten members of the CXC chemokine gene family form a chemokine gene cluster in a region mapped to chromosome 4q. |
| 9.97 (0.000462); 2.55 (0.00187) | *HIST1H4H* | H4 histone family, member H | Histones are basic nuclear proteins that are responsible for the nucleosome structure of the chromosomal fiber in eukaryotes. Two molecules of each of the four core histones (H2A, H2B, H3, and H4) form an octamer, around which approximately 146 bp of DNA is wrapped in repeating units, called nucleosomes. The linker histone, H1, interacts with linker DNA between nucleosomes and functions in the compaction of chromatin into higher order structures. This gene is intronless and encodes a member of the histone H4 family. This gene is found in the large histone gene cluster on chromosome 6. |
| 8.79 (0.000773); 2.68 (0.00192) | *CHIC2* | Cysteine-rich hydrophobic domain 2 | This gene encodes a member of the CHIC family of proteins. The encoded protein contains a cysteine-rich hydrophobic (CHIC) motif, and is localized to vesicular structures and the plasma membrane. This gene is associated with some cases of acute myeloid leukemia. |

| | | | |
|---|---|---|---|
| 8.31 (0.00038);<br>2.16 (0.00202) | *FLJ11088* | Hypothetical protein FLJ11088 | No summary function available.Synonyms: p56, HSD8; Homo sapiens GGA binding partner (FLJ11088), mRNA. Gene ontology (Compugen) : cytoskeleton organization and biogenesis [0007010] |
| 8.19 (0.00057);<br>2.56 (0.0065) | *GADD45B* | Growth arrest and DNA damage inducible, beta | This gene is a member of a group of genes whose transcript levels are increased following stressful growth arrest conditions and treatment with DNA-damaging agents. The genes in this group respond to environmental stresses by mediating activation of the p38/JNK pathway. This activation is mediated via their proteins binding and activating MTK1/MEKK4 kinase, which is an upstream activator of both p38 and JNK MAPKs. The function of these genes or their protein products is involved in the regulation of growth and apoptosis. These genes are regulated by different mechanisms, but they are often coordinately expressed and can function cooperatively in inhibiting cell growth. |
| 7.78 (0.000624);<br>7.48 (0.000213) | *TNFRSF12A* | FN14; TWEAKR, type I transmembrane protein Fn14 | No summary function available. Product is a receptor for TWEAK (weak inducer of apoptosis).TIGR annotation: Tumor necrosis factor receptor superfamily member Fn14 precursor (Fibroblast growth factor-inducible immediate-early response protein 14) (FGF-inducible 14) (Tweak-receptor) (TweakR) |
| 7.69 (0.00185);<br>2.74 (0.000235) | *TNFAIP3* | tumor necrosis factor inducible protein A20 | This gene was identified as a gene whose expression is rapidly induced by the tumor necrosis factor (TNF). The protein encoded by this gene is a zinc finger protein, and has been shown to inhibit NF-kappa B activation as well as TNF-mediated apoptosis. Knockout studies of a similar gene in mice suggested that this gene is critical for limiting inflammation by terminating TNF-induced NF-kappa B responses. |
| 7.51 (0.000271);<br>3.76 (0.000146) | *HIST2H4* | Histone 2, H4 | Histones are basic nuclear proteins that are responsible for the nucleosome structure of the chromosomal fiber in eukaryotes. This structure consists of approximately 146 bp of DNA wrapped around a nucleosome, an octamer composed of pairs of each of the four core histones (H2A, H2B, H3, and H4). The chromatin fiber is further compacted through the interaction of a linker histone, H1, with the DNA between the nucleosomes to form higher order chromatin structures. This gene is intronless and encodes a member of the histone H4 family. This gene is found on chromosome 1. |
| 1.96 (0.0049);<br>3.35 (0.0000401) | *LOC90639* | Hypothetical protein LOC90639 | No summary function available. Gene ontology (Compugen) : biological_process unknown [0000004] |
| 1.88 (0.006);<br>3.66 (0.000604) | *NOL5A* | Nucleolar protein 5A | Nop56p is a yeast nucleolar protein that is part of a complex with the nucleolar proteins Nop58p and fibrillarin. Nop56p is required for assembly of the 60S ribosomal subunit and is involved in pre-rRNA processing. The protein encoded by this gene is similar in sequence to Nop56p and is also found in the nucleolus. Multiple transcript variants encoding several different isoforms have been found for this gene, but the full-length nature of most of them have not been determined. |

| | | | |
|---|---|---|---|
| 1.77 (0.0105);<br>3.66 (0.000262) | *GDF15* | Growth differentiation factor 15 | Bone morphogenetic proteins (e.g., BMP5; MIM 112265) are members of the transforming growth factor-beta (see TGFB1; MIM 190180) superfamily and regulate tissue differentiation and maintenance. They are synthesized as precursor molecules that are processed at a dibasic cleavage site to release C-terminal domains containing a characteristic motif of 7 conserved cysteines in the mature protein.[supplied by OMIM] |
| 1.66 (0.00748);<br>4.01 (0.00339) | *AREG* | Amphiregulin preproprotein | The protein encoded by this gene is a member of the epidermal growth factor family. It is an autocrine growth factor as well as a mitogen for astrocytes, Schwann cells, and fibroblasts. It is related to epidermal growth factor (EGF) and transforming growth factor alpha (TGF-alpha). This protein interacts with the EGF/TGF-alpha receptor to promote the growth of normal epithelial cells and inhibits the growth of certain aggressive carcinoma cell lines. This encoded protein is associated with a psoriasis-like skin phenotype. |
| 1.63 (0.000653);<br>3.14 (0.00442) | *NT5C* | 5',3'-nucleotidase, cytosolic | Pyrimidine 5-prime nucleotidase (P5N; EC 3.1.3.5), also called uridine 5-prime monophosphate hydrolase (UMPH), catalyzes the dephosphorylation of the pyrimidine 5-prime monophosphates UMP and CMP to the corresponding nucleosides. There are 2 isozymes of pyrimidine 5-prime nucleotidase in red blood cells, referred to as type I (UMPH1; MIM 606224) and type II (UMPH2).[supplied by OMIM] |
| 1.58 (0.0265);<br>3.32 (0.000171) | *SQSTM1* | Sequestosome 1 | No summary function available. GO biological process : endosome transport; intracellular signaling cascade; positive regulation of transcription from Pol II promoter; protein localization; regulation of I-kappaB kinase/NF-kappaB cascade; response to stress |
| 0.663 (0.0183);<br>0.368 (0.00388) | *TARG1* | N-myc downstream regulated gene 1; Trichosanthin-induced apoptosis-related. | This gene is a member of the N-myc downregulated gene family which belongs to the alpha/beta hydrolase superfamily. The protein encoded by this gene is a cytoplasmic protein involved in stress responses, hormone responses, cell growth, and differentiation. Mutation in this gene has been reported to be causative for hereditary motor and sensory neuropathy-Lom. |
| 0.554 (0.245)<br>0.368 (0.0035) | *RNASE4* | Ribonuclease, RNase A family, 4 precursor | The protein encoded by this gene belongs to the pancreatic ribonuclease family. It plays an important role in mRNA cleavage and has marked specificity towards the 3' side of uridine nucleotides. Alternative splicing occurs at this locus and three transcript variants encoding the same protein have been identified. This gene and ANG share two exons in their 5' UTRs. The downstream exons are unique and contain the coding regions. |
| 0.511 (0.0231);<br>0.372 (0.00167) | *FKBP14* | FK506 binding protein 14, 22 kDa | No summary function available. GO biological process : protein folding. GO cellular component : endoplasmic reticulum. GO molecular function : calcium ion binding; isomerase activity; peptidyl-prolyl cis-trans isomerase activity |

| | | | |
|---|---|---|---|
| 0.422 (0.00556); 0.285 (0.00556) | *HSPA5; BIP; MIF2; GRP78* | Endoplasmic reticulum lumenal Ca2+ binding protein grp78 | When Chinese hamster K12 cells are starved of glucose, the synthesis of several proteins, called glucose-regulated proteins (GRPs), is markedly increased. Hendershot et al. (1994) pointed out that one of these, GRP78 (HSPA5), also referred to as 'immunoglobulin heavy chain-binding protein' (BiP), is a member of the heat-shock protein-70 (HSP70) family and is involved in the folding and assembly of proteins in the endoplasmic reticulum (ER). Because so many ER proteins interact transiently with GRP78, it may play a key role in monitoring protein transport through the cell.[supplied by OMIM] |
| 0.391 (0.0349); 0.267 (0.00285) | *HERPUD1* | Homocysteine-inducible, endoplasmic reticulum stress-inducible, ubiquitin-like domain member 1 isoform 1 | The accumulation of unfolded proteins in the endoplasmic reticulum (ER) triggers the ER stress response. This response includes the inhibition of translation to prevent further accumulation of unfolded proteins, the increased expression of proteins involved in polypeptide folding, known as the unfolded protein response (UPR), and the destruction of misfolded proteins by the ER-associated protein degradation (ERAD) system. This gene may play a role in both UPR and ERAD. Its expression is induced by UPR and it has an ER stress response element in its promoter region while the encoded protein has an N-terminal ubiquitin-like domain which may interact with the ERAD system. This protein has been shown to interact with presenilin proteins and to increase the level of amyloid-beta protein following its overexpression. Alternative splicing of this gene produces multiple transcript variants, some encoding different isoforms. The full-length nature of all transcript variants has not been determined. |
| 0.349 (0.0161); 0.339 (0.00066) | *RRBP1* | Ribosome binding protein 1 | Analysis of cDNA clones indicates that ribosome binding protein 1 may exist in different forms due to removal of tandem repeats, or partial intraexonic splicing of RRBP1. The form presented here is lacking the canine p180 ribosome-binding domain, NQGKKAEGAQ, which is tandemly repeated close to the N-terminus in other forms that haven't been fully characterized. RRBP1 has been excluded as a candidate gene in the cause of Alagille syndrome. SP function : acts as a ribosome receptor and mediates interaction between the ribosome and the endoplasmic reticulum membrane (by similarity). |
| 0.349 (0.0024); 0.386 (0.0178) | *PHGDH* | Phosphoglycerate dehydrogenase | 3-Phosphoglycerate dehydrogenase (PHGDH; EC 1.1.1.95) catalyzes the transition of 3-phosphoglycerate into 3-phosphohydroxypyruvate, which is the first and rate-limiting step in the phosphorylated pathway of serine biosynthesis, using NAD+/NADH as a cofactor.[supplied by OMIM] |
| 0.301 (0.00659); 0.333 (0.000783); | *BCAT1; BCT1; ECA39; MECA39* | Branched chain aminotransferase 1, cytosolic | This gene encodes the cytosolic form of the enzyme branched-chain amino acid transaminase. This enzyme catalyzes the reversible transamination of branched-chain alpha-keto acids to branched-chain L-amino acids essential for cell growth. Two different clinical disorders have been attributed to a defect of branched-chain amino acid transamination: hypervalinemia and hyperleucine-isoleucinemia. As there is also a gene encoding a mitochondrial form of this enzyme, mutations in either gene may contribute to these disorders. |

| | | | |
|---|---|---|---|
| 0.280 (0.00717);<br>0.279 (0.000921) | *HSPA1B* | Heat shock 70kDa protein 1B | This intronless gene encodes a 70kDa heat shock protein which is a member of the heat shock protein 70 family. In conjuction with other heat shock proteins, this protein stabilizes existing proteins against aggregation and mediates the folding of newly translated proteins in the cytosol and in organelles. It is also involved in the ubiquitin-proteasome pathway through interaction with the AU-rich element RNA-binding protein 1. The gene is located in the major histocompatibility complex class III region, in a cluster with two closely related genes which encode similar proteins. |
| 0.248 (0.000203);<br>0.447 (0.00368) | *SLC38A1; ATA1* | Amino acid transporter system A1 | Amino acid transporters play essential roles in the uptake of nutrients, production of energy, chemical metabolism, detoxification, and neurotransmitter cycling. SLC38A1 is an important transporter of glutamine, an intermediate in the detoxification of ammonia and the production of urea. Glutamine serves as a precursor for the synaptic transmitter, glutamate (Gu et al., 2001 [PubMed 11325958]).[supplied by OMIM] |
| 0.246 (0.00242);<br>0.696 (0.00685) | *RPN2* | Ribophorin II precursor | This gene encodes a type I integral membrane protein found only in the rough endoplasmic reticulum. The encoded protein is part of an N-oligosaccharyl transferase complex that links high mannose oligosaccharides to asparagine residues found in the Asn-X-Ser/Thr consensus motif of nascent polypeptide chains. This protein is similar in sequence to the yeast oligosaccharyl transferase subunit SWP1. |
| 0.225 (0.00182);<br>0.490 (0.0159) | *MKNK2* | MAP kinase-interacting serine/threonine kinase 2 | No summary function available. GO biological process : protein amino acid phosphorylation; protein kinase cascade; regulation of translation; response to stress. GO molecular function : ATP binding; protein serine/threonine kinase activity; protein-tyrosine kinase activity; transferase activity |
| 0.219 (0.00109);<br>0.622 (0.0000313) | *GGH* | Gamma-glutamyl hydrolase precursor | This gene catalyzes the hydrolysis of folylpoly-gamma-glutamates and antifolylpoly-gamma-glutamates by the removal of gamma-linked polyglutamates and glutamate. |
| 0.201 (0.000562);<br>0.505 (0.00487) | *SLC38A2* | predicted protein of HQ1068; Homo sapiens PRO1068 mRNA, complete cds. | No summary function available. GO biological process : amino acid transport<br>GO cellular component : integral to membrane<br>GO molecular function : amino acid-polyamine transporter activity |
| 0.198 (0.0191);<br>0.509 (0.00713) | *PSA* | Phosphoserine aminotransferase | The protein encoded by this gene is likely a phosphoserine aminotransferase, based on similarity to proteins in mouse, rabbit, and Drosophila. Alternative splicing of this gene results in two transcript variants encoding different isoforms. GO biological process : L-serine biosynthesis; metabolism; pyridoxine biosynthesis |

| | | | |
|---|---|---|---|
| 0.194 (0.00474);<br>0.378 (0.00754) | *KDELR3* | KDEL receptor 3 isoform a | Retention of resident soluble proteins in the lumen of the endoplasmic reticulum (ER) is achieved in both yeast and animal cells by their continual retrieval from the cis-Golgi, or a pre-Golgi compartment. Sorting of these proteins is dependent on a C-terminal tetrapeptide signal, usually lys-asp-glu-leu (KDEL) in animal cells, and his-asp-glu-leu (HDEL) in S. cerevisiae. This process is mediated by a receptor that recognizes, and binds the tetrapeptide-containing protein, and returns it to the ER. In yeast, the sorting receptor encoded by a single gene, ERD2, is a seven-transmembrane protein. Unlike yeast, several human homologs of the ERD2 gene, constituting the KDEL receptor gene family, have been described. KDELR3 was the third member of the family to be identified, and it encodes a protein highly homologous to KDELR1 and KDELR2 proteins. Two transcript variants of KDELR3 that arise by alternative splicing, and encode different isoforms of KDELR3 receptor, have been described. |
| 0.175 (0.00185);<br>0.454 (0.00802) | *LIPA* | Lipase A precursor | This gene encodes lipase A, the lysosomal acid lipase (also known as cholesterol ester hydrolase). This enzyme functions in the lysosome to catalyze the hydrolysis of cholesteryl esters and triglycerides. Mutations in this gene can result in Wolman disease and cholesteryl ester storage disease. SP function : crucial for the intracellular hydrolysis of cholesteryl esters and triglycerides that have been internalized via receptor- mediated endocytosis of lipoprotein particles. Important in mediating the effect of LDL (low density lipoprotein) uptake on suppression of hydroxymethylglutaryl-CoA reductase and activation of endogenous cellular cholesteryl ester formation. |
| 0.167 (0.000341);<br>0.476 (0.015) | *ASNS* | Asparagine synthetase | The protein encoded by this gene is involved in the synthesis of asparagine. This gene complements a mutation in the temperature-sensitive hamster mutant ts11, which blocks progression through the G1 phase of the cell cycle at nonpermissive temperature. There are three alternatively spliced transcript variants encoding the same protein described for this gene. |

### *3.3.3 CYN induces changes in gene expression associated with specific stress responses*

#### 3.3.3.1 DNA damage responses

As discussed briefly above, one of the most highly induced genes following CYN exposures was *GADD45α* (Fornace et al., 1989), encoding a protein involved in the initiation of stress signalling, growth arrest and repair processes in response to DNA damage (Zhan, 2005). Using qRT-PCR we had previously identified *GADD45α* amongst a group of p53-regulated genes induced by CYN, a finding which is substantiated by the microarray data presented here. P53 is transcription factor that functions as a central coordinator of gene expression in response to DNA damage (Kastan, 1993; Lakin and Jackson, 1999; Levine, 1989; Smith and Seo, 2002). Targets of p53 have various roles in cell cycle control, DNA repair, and the induction of apoptosis.

P53-regulated genes induced in response to CYN, according to microarray analysis described in this chapter, include the *CDKN1A* gene encoding $p21^{WAF1/CIP1}$, a regulator of cyclin-dependent kinases (el-Deiry et al., 1993), the *XPC* gene encoding a nucleotide excision repair protein essential for global genomic DNA repair (Masutani et al., 1994), *P53R2*, encoding a ribonucleotide reductase (Tanaka et al., 2000), *BTG2,* encoding a protein involved in cell cycle control (Rouault et al., 1996), *TP53I3*, a p53-inducible gene encoding a protein thought to be involved in apoptosis (up-regulated in HepG2 cells only), and the *DDB2* gene encoding a damage-specific DNA binding protein (Dualan et al., 1995; Tan and Chu, 2002). Expression ratios for *GADD45α*, *CDKN1A*, *XPC* and *DDB2* were confirmed using qRT-PCR (Table 3.8).

CYN also induced DNA repair-associated genes not reported as being under the transcriptional control of p53—*POLH,* encoding DNA polymerase η, which has a role in translesion DNA synthesis (Masutani et al., 1999), and *ALKBH,* a homologue of the *E.coli* alkylation repair gene alkB (Wei et al., 1996). The induction of *ALKBH* expression was verified using qRT-PCR (Table 3.8). The increased expression of genes encoding specific repair proteins (*XPC, POLH* and *ALKBH*) may be suggestive of the nature of DNA lesions or adducts induced by CYN treatment. For example, XPC and DDB2 proteins are both involved in the recognition and repair of bulky lesions via nucleotide excision repair

(Amundson et al., 2002; Fitch et al., 2003), while AlkB homologues have a role in the direct repair of methylated bases (Aas et al., 2003).

There are three human homologues of *E.coli* AlkB, designated ABH1, ABH2 and ABH3 (Aas et al., 2003; Wei et al., 1996). ABH2 and ABH3 have activities similar to the bacterial AlkB enzyme, namely oxidative demethylation of bases in DNA and RNA, while ABH1 (encoded by *ALKBH*) has not been fully characterised. A recombinant version of ABH1 that was not able to repair damaged DNA or RNA has been described (Aas et al., 2003), the authors suggesting that the bacterial expression system utilised may not have been capable of performing the post-translational modifications required for activity. The high degree of homology of this gene with other members of the family suggests that it may have repair activity *in vivo,* but this is yet to be determined. The fact that *ALKBH1* appears to be inducible also suggests that it may encode an active enzyme.

Addressing the question of whether CYN directly induces DNA damage was a goal of this analysis. The induction of p53-responsive genes, and others involved in DNA repair, indicates that a direct genotoxic effect may be induced by CYN. This is in general agreement with recent findings that low CYN concentrations result in positive comet assays using primary mouse hepatocytes (Humpage et al., 2005).

**Table 3.5** Genes associated with stress responses showing altered transcript levels after CYN exposure (UPR – unfolded protein response; NP – not present, i.e. signal intensities were not above background levels). Asterisks represent significant difference from an expression ratio of 1, according to a one-sample Student's t-test; * $p < 0.05$, ** $p < 0.01$, *** $p < 0.001$.

| | Gene | Product | HDF | | HepG2 | |
|---|---|---|---|---|---|---|
| | | | 6 h | 24 h | 6 h | 24 h |
| DNA damage responses | *GADD45α* | Growth arrest and DNA-damage, 45 kDa | 1.01 | 21.1*** | 1.48 | 6.10*** |
| | *CDKN1A* | Cyclin-dependent kinase inhibitor 1A; p21 | 1.11** | 3.42* | 1.73* | 1.55* |
| | *XPC* | Xeroderma pigmentosum compl. group C | 1.53*** | 3.19** | 2.17* | 2.20*** |
| | *BTG2* | B-cell translocation gene 2 | 1.29 | 2.41** | 1.39 | 1.40* |
| | *TP53I3* | Tumor protein p53 inducible protein 3 | 0.96 | 0.72* | 1.24* | 1.71** |
| | *DDB2* | Damage-specific DNA binding protein 2 | 1.07 | 2.09** | 1.37* | 1.23 |
| | *POLH* | DNA polymerase eta | 1.16 | 2.18* | 1.41 | 0.92 |
| | *ALKBH* | Human homologue of *E.coli* AlkB | 1.65* | 3.06** | 1.74* | 2.28** |
| NF-κB regulated / NF-κB activation | *NFKB1* | NF-κB DNA binding subunit (p50) | 1.41* | 4.02*** | 1.45* | 1.35* |
| | *IL1α* | Interleukin 1, alpha | 1.33 | 5.50*** | 1.44* | 0.98 |
| | *IL6* | Interleukin 6 | 0.97 | 2.88* | NP | NP |
| | *IL8* | Interleukin 8 | 1.61** | 12.0** | 1.57* | 3.87*** |
| | *COX-2* | Cyclooxygenase 2 | 1.28 | 1.83** | NP | NP |
| | *BIRC3* | Baculoviral IAP repeat-containing protein 3 | 1.37 | 2.57** | 1.52 | 1.53** |
| | *SQSTM1* | Sequestosome1 ubiquitin-binding protein | 0.87 | 1.58* | 1.40* | 3.32*** |
| | *MAP3K14* | NF-κB inducing kinase | 1.37** | 2.74** | 1.09 | 2.16** |
| | *IL18* | Interleukin 18 | NP | NP | 0.82* | 2.41** |
| | *NFKBIA* | Cytoplasmic NF-κB inhibitor, alpha | 1.43** | 2.35* | 1.02 | 1.31* |
| | *NFKBIE* | Cytoplasmic NF-κB inhibitor, epsilon | 1.25 | 3.04** | 0.97 | 2.65*** |
| | *TRIB3* | Tribbles 3 homologue | 0.35** | 0.28** | 0.70* | 0.63** |
| | *RNF25* | Ring finger protein 25 | 1.58** | 2.92*** | 1.74 | 2.71*** |
| | *TWEAKR* | Fn14; receptor for TWEAK | 2.53* | 7.78*** | 1.87* | 7.48*** |
| Endplasmic reticulum / UPR | *GRP78* | Glucose-regulated protein, 78 kDa | 0.73 | 0.42** | 0.52* | 0.29** |
| | *GRP94* | Glucose-regulated protein, 94 kDa | 0.74* | 0.57* | 1.04 | 0.72* |
| | *HERPUD1* | Homocysteine-inducible ER stress protein | 0.68 | 0.66* | 0.69** | 0.37** |
| | *TARG1* | Trichosanthin-induced, apoptosis-related | 0.47* | 0.39* | 0.44* | 0.27** |
| | *HYOU1* | Hypoxia up-regulated 1 | 1.04 | 0.95 | 0.72* | 0.58** |
| | *XBP1* | X-box binding protein 1 | 0.63* | 0.18** | 1.45** | 0.77* |
| | *KDELR3* | KDEL receptor 3 | 0.90* | 0.19** | 1.05 | 0.38** |
| | *P4HB; PDI* | Protein disulphide isomerase | 0.93 | 0.69** | 0.50* | 0.50* |
| | *PDIR* | Protein disulphide isomerase-related | 0.92* | 0.41* | 0.88 | 0.54* |
| | *TXNDC5* | Thioredoxin domain containing 5 | 0.92 | 0.43** | 0.84*** | 0.55* |
| | *ERP29* | Endoplasmic reticulum protein 29 precursor | 0.80 | 0.56* | 0.92 | 0.87* |
| | *AHSA1* | Activator of heat shock 90kDa protein | 0.94 | 0.43** | 1.18 | 0.69* |
| | *GADD153* | Growth arrest and DNA-damage, 153 kDa | 0.45* | 0.69* | 1.05 | 1.91** |

#### 3.3.3.2 NF-κB-mediated gene expression

Nuclear factor kappa B (NF-κB) is a heterodimeric transcription factor that mediates gene expression associated with immune responses (Ghosh et al., 1998), cellular stresses (Mercurio and Manning, 1999) and the regulation of apoptosis and survival (Kucharczak et al., 2003). According to a 1999 review, NF-κB is activated by over 150 different stimuli and participates in the regulation of over 150 target genes (Pahl, 1999). Due to the immense interest in NF-κB as a potential target for therapeutics, the current number of known activators and targets undoubtedly exceeds this estimate. Described in this section is a summary of genes regulated by NF-κB, and genes encoding NF-κB regulatory proteins, that displayed altered transcript levels in response to CYN in this study. The possible involvement of this important transcription factor in CYN toxicity is explored in more detail in chapter 5 of this thesis.

Numerous interleukins known to be regulated by NF-κB were up-regulated following CYN exposure (Table 3.5). The *IL1* gene for interleukin 1α (IL-1α), known to be regulated by NF-κB (Mori and Prager, 1996), was induced significantly in HDFs after 24 h CYN treatment, but not in HepG2 cells. IL-1α and IL-1β are important regulators of early responses to infection and injury, participating in priming the innate immune system for increased activity (Fitzgerald and O'Neill, 2000; Martin and Wesche, 2002). IL-6 mRNA levels after 24 h were also increased only in HDFs. IL-6 is an inflammatory cytokine with wide-ranging effects on cellular physiology associated with proliferation, differentiation, survival and apoptosis (Kamimura et al., 2003). Transcription of the *IL6* gene is under the partial control of NF-κB (Libermann and Baltimore, 1990). *IL8* expression, known to be regulated primarily by NF-κB (Kunsch and Rosen, 1993; Roebuck, 1999), was induced by CYN strongly in both HDFs and HepG2 cells over time. IL-8 is the prototypical chemotactic cytokine (chemokine), a family of small, basic proteins that attract specific leukocytes to sites of inflammation (Strieter et al., 1996). IL-8 expression can be induced in HepG2 cells by treatment with lipopolysaccharides, acetaldehyde, or hydrogen peroxide (Gomez-Quiroz et al., 2003). Validation of the expression ratios for *IL1*, *IL6*, and *IL8* was achieved using qRT-PCR (Table 3.8), which resulted in the detection of considerably larger fold-changes, as is often reported for validations of array data using this method.

CYN treatment also induced the expression of genes encoding the inhibitors of NF-κB, IκBα and IκBε (*NFKBIA* and *NFKBIE*, respectively; Table 3.5). NF-κB is regulated by IκB (inhibitor of κB) protein, which binds to NF-κB dimers and prevents their translocation to the nucleus by masking nuclear localisation signals (Baeuerle and Baltimore, 1988; Malek et al., 1998; Whiteside et al., 1997). NF-κB activation occurs through receptor-mediated or stress-induced pathways that result in ubiquitylation and subsequent proteasomal degradation of IκB (discussed in more detail in Chapter 5). In the classical pathway of NF-κB activation, phosphorylation of IκBβ by the IκB kinase complex (IKK) marks it for ubiquitylation and degradation (Hay et al., 1999). The *NFKBIA* and *NFKBIE* genes are transcriptionally up-regulated by NF-κB, therby participating in negative feedback of the pathway following an activation event (Kearns et al., 2006; Nelson et al., 2004). The induction of these genes by CYN is further indication of NF-κB activation in response to the toxin.

*BIRC3*, encoding cellular inhibitor of apoptosis protein 2 (cIAP2), is up-regulated significantly in both cell lines after 24 h (substantially in HDFs; Table 3.5). This gene is induced by TNFα and IL1 through two NF-κB response elements (Hong et al., 2000), and by phorbol-12-mystistate-13-acetate (PMA) via a protein kinase C- (PKC) and NF-κB-dependent pathway (Wang et al., 2003). NF-κB contributes to increased cIAP2 levels during mitotic cell cycle arrest at the G2-M transition, enhancing cell survival (Jin and Lee, 2006). The increased expression of *BIRC3* may contribute to the relatively long CYN exposure times required to induce apoptosis in HDFs and HepG2 cells (Chapter 2).

The gene encoding the ubiquitin binding protein p62/Sequestosome 1, *SQTSM1*, was one of the ten most strongly up-regulated genes in HepG2 (table 3.4), and was significantly up-regulated in HDFs after 24 h (table 3.5). NF-κB participates in the regulation of this gene by binding to an element in the 5' flanking region (Vadlamudi and Shin, 1998).

Relative mRNA levels for genes associated with NF-κB regulation were also seen to be changing after CYN exposure. The gene for IL-18, a member of the interleukin-1 family of cytokines, was induced after 24 h in HepG2 cells but not in HDFs. IL-18 is secreted by sentinel cells of the immune system, regulating immune responses by signalling to cells expressing the IL-18 receptor, including macrophages, natural killer cells, lymphocytes and neutrophils (Reddy, 2004). The binding of IL-18 to its receptor results in the activation

of NF-κB and increased NF-κB-dependent gene expression (Matsumoto et al., 1997; Tsuji-Takayama et al., 1999; Weinstock et al., 2003).

As discussed above, the receptor for TWEAK (TWEAKR) can also induce NF-κB activation via interactions with TRAF1, 2 3 and 5 (Han et al., 2003). The strong induction of *TWEAKR* in both cell types suggests a possible role for this receptor in the activation of NF-κB in reponse to CYN.

*MAP3K14* mRNA levels were significantly higher than controls in both cell lines after 24 h CYN exposure. *MAP3K14* encodes NF-κB-inducing kinase (NIK; also known as MAPK kinase kinase 14), a serine/threonine kinase involved in the activation of NF-κB via the alternative pathway (see section 5.4) through the phosphorylation and activation of IκB kinase alpha (Malinin et al., 1997). The increased expression of *MAP3K14* following CYN treatment indicates an up-regulation of the early regulatory processes of the NF-κB pathway by increasing the pool of NIK available for activation. It is important in this case to acknowledge the limitations of determining mRNA levles in the assessment of signalling pathway activation—increased transcript levels for a given kinase mean that an associated pathway will be activated.

*TRIB3*, encoding a homologue of *Drosophila* tribbles 3, was down-regulated following CYN treatment in both cell types. The TRIB3 protein (also called SINK) is a negative regulator of NF-κB activation and transcription (Wu et al., 2003), suggesting that the observed reduction in *TRIB3* expression may be associated with a corresponding increase in NF-κB activity.

NF-κB is activated in response to many and varied stress-inducing stimuli, including DNA damage, viral infection, UV light, pro-inflammatory cytokines, bacterial lipopolysaccharides and oxidative stress (Mercurio and Manning, 1999). The increased expression of numerous genes known to be regulated by the active NF-κB dimer following exposure to CYN indicates that this toxin also induces NF-κB activation. To confirm this, the activation status of IκBα could be investigated by immunoblotting with antibodies specific for the phosphorylated form. Little is known about the activation mechanism for IκB kinases in response to stress, but it has been suggested that reactive oxygen species (ROS) are involved (Li and Engelhardt, 2006; Li et al., 2001a; Mercurio and Manning, 1999), although this possibility is not wholly supported (Hayakawa et al., 2003). Despite

the apparent lack of involvement of ROS in CYN toxicity in primary mouse hepatocytes (Humpage et al., 2005), it would be interesting to determine whether CYN induces oxidative stress in the cell types used in this study.

#### 3.3.3.3 CYN reduces the expression of endoplasmic reticulum stress genes

Proteins destined for the cell surface, either for secretion or to be embedded in the membrane, are synthesised in the endoplasmic reticulum (ER). Conditions that adversely affect protein folding in the ER can induce the endoplasmic reticulum stress response, involving the expression of chaperonins that assist newly synthesised proteins to adopt the correct conformation. Interestingly, CYN treatment resulted in a marked reduction in the expression of ER stress-responsive genes. Amongst the ten most down-regulated genes listed in Table 3.4 are the well characterised ER stress genes *GRP78*, *TARG1, HERPUD1*, and *FKBP14*. The expression ratios for these and other ER stress genes significantly down-regulated following CYN exposure are listed in Table 3.5.

Most ER stress-responsive genes encode products with functions associated with protein folding. *GRP78* is the major ER HSP70 chaperonin, aiding newly synthesised proteins to fold correctly (Munro and Pelham, 1986; Nigam et al., 1994). The *GRP78* gene is strongly transactivated under conditions detrimental to protein folding in the ER (Li et al., 1993). The highly significant reduction in *GRP78* expression following CYN treatment indicated a reduced need for protein folding chaperones in the ER, consistent with the fact that CYN is a potent inhibitor of protein synthesis.

The *TRA1-GRP94* gene, encoding another ER chaperone known as 'tumour rejection antigen 1' (TRA1; also known as glucose-regulated protein, 94 kDa [GRP94]) was significantly down-regulated in both cell types after 24 h (0.57-fold in HDFs; 0.72-fold in HepG2 cells; $p < 0.05$ for both cell types). *GRP94* and *GRP78* encode well-characterised folding chaperones and are coordinately regulated, with both genes containing similar promoter elements (Liu and Lee, 1991).

*FKBP14* encodes a member of the FKBP family of proteins that bind the immunosuppressive drug FK506 (Patterson et al., 2002). FKBPs have peptidyl-prolyl *cis/trans* isomerase (PPIase) activity, which is a function important for proline-directed protein folding (Fischer and Bang, 1985). FKBP14 is not well studied, however the similar

FKBP13 protein is known to be induced under conditions that promote protein denaturation in the ER (Bush et al., 1994).

Protein folding in the ER is also aided by protein disulphide isomerases (PDIs), a family of thioredoxin-like proteins which direct the formation and isomerisation of disulphide linkages in newly synthesised polypeptide chains. These enzymes can carry out oxidative refolding of proteins, which involves the breaking and rejoining of disulphide bonds (Tu and Weissman, 2004). In humans, PDI is the main protein disulphide isomerase in the ER, encoded by the *P4HB* gene (for prolyl 4-hydroxylase, beta subunit; the PDI protein is multifunctional and is also a subunit of this enzyme which is involved in collagen synthesis (Koivu et al., 1987; Pihlajaniemi et al., 1987)). In addition to PDI, there are numerous homologues with disulphide isomerase activity. One such homologue is known as protein disulphide isomerase-related protein, PDIR (Hayano and Kikuchi, 1995), which has similar activity but differing substrate specificity to that of PDI (Horibe et al., 2004). In CYN-treated HDFs and HepG2s, genes for both PDI and PDIR were significantly down-regulated after 24 h. The 5' proximal promoter region of the *PDI* gene contains six CCAAT boxes (Tasanen et al., 1992), implying the involvement of C/EBP-family transcription factors in the regulation of transcription.

*TARG1* expression was also strongly reduced after CYN treatment (discussed briefly above in 'Large changes in relative transcript level after 24 h CYN exposure'; Table 3.4; Table 3.5). The product of this gene, known variously as Drg1, Cap43, rit42, TDD5, Ndr1 and RTP (reducing agent- and tunicamycin-responsive protein) has a role in ER stress, with *TARG1* expression induced concurrently with *GRP78* expression (Agarwala et al., 2000; Kokame et al., 1996; Zhou et al., 1998). RTP is phosphorylated by protein kinase A, suggesting a possible role in intracellular signalling in response to ER stress (Agarwala et al., 2000).

*HERPUD1* (homocysteine-inducible, endoplasmic reticulum stress-inducible protein, ubiquitin-like domain member 1), encodes a ubiquitin-like ER stress-inducible protein that localises to the ER membrane (Kokame et al., 2000). The strong expression of *HERPUD1* during the unfolded protein response directed by ATF6 through the binding of two ER stress response elements in the promoter region, designated ERSE and ERSE-II (Kokame et al., 2001).

X-box binding protein (XPB-1; encoded by the gene *XBP1*) is a transcription factor involved in the regulation of the unfolded protein response during endoplasmic reticulum stress (Kanemoto et al., 2005; Yoshida et al., 2001). In HDFs, mRNA for XBP was strongly down-regulated by CYN treatment, while in HepG2 cells there was a slight but statistically significant increase in XBP mRNA after 6 h and a significant reduction after 24 h (Table 3.5). Transcriptional activation of *XBP1* is regulated by ATF6 in a similar fashion to *GRP78* expression (Yoshida et al., 2000). Reduced levels of this transcription factor may reinforce the putative role of ATF6 in the observed reduction in ER stress-responsive transcripts.

The expression of a gene encoding a receptor for protein retention in the ER, *KDELR3,* was strongly reduced in both cell types (Tables 3.4 and 3.5). *KDELR2* expression was also significantly reduced after 24 h in both cell types (Table 3.5). The KDEL (lysine, aspartic acid, glutamic acid, leucine) motif is a signal for ER localisation present in the C-termini of proteins involved in essential ER functions, such as the ER stress proteins GRP78 and GRP94 (Kaufman, 1999). Proteins bearing the KDEL motif are able to leave the ER and proceed to the Golgi apparatus, or a pre-Golgi compartment, but are transported rapidly back to the ER by KDEL receptor proteins (Munro and Pelham, 1987; Pelham, 1988). KDEL receptors reside intermittently in the Golgi – when the receptor encounters and binds a protein with the KDEL motif, the recepor-ligand complex is transported to the ER (Lewis and Pelham, 1990; Lewis and Pelham, 1992; Townsley et al., 1993). In this way, the continual retrograde transport of ER-resident proteins maintains the appropriate localisation, despite a degree of cycling between compartments. A strong reduction in the expression of *KDELR3*, and a moderate reduction in *KDELR2* expression (a probe for *KDELR1* was not present on the arrays), may be a result of reduced protein synthesis following CYN treatment, although the mechanism is not clear.

*GADD153*, another gene involved in ER stress responses (Wang et al., 1996), was up-regulated in HepG2 cells after 24 hours but down-regulated in HDFs at both time points, highlighting a cell-type specific response to CYN. GADD153, also known as C/EBP homologous protein (CHOP), is a member of the CCAAT enhancer binding (C/EBP) family of transcription factors. *GADD153* was originally described as one of a set of genes inducible by genotoxic agents (Fornace et al., 1988) but is now known to be most strongly

induced under conditions that exacerbate ER stress (Kaufman, 1999; Wang et al., 1996; Zinszner et al., 1998).

The reduced expression, following CYN exposure, of ER chaperonins and other proteins involved in the unfolded protein response is consistent with a diminished requirement for protein chaperonins as a result of CYN-mediated translational inhibition. This is a clear example of the efficacy of the microarray approach—gene expression patterns consistent with known mechanisms of CYN toxicity are detected by the method, indicating that further mechanisms may be elucidated using this technique.

### *3.3.4 CYN induces genes for RNA metabolism and processing*

In data from both cell types, numerous GO categories involved with RNA processing and metabolism featured in clusters of up-regulated genes (Figure 3.3). These clusters were examined for the presence of genes with specific functions relating to these categories (Table 3.6). Additional genes not present in clusters in Figure 3.3, but also relating to RNA metabolism, are included in the table below. CYN treatment increased the expression of genes encoding proteins with three main roles in RNA metabolism—transfer RNA (tRNA) synthesis and processing, pre-mRNA processing and ribosomal RNA (rRNA) processing.

**Table 3.6** RNA metabolism genes induced following CYN treatment. Asterisks represent significant difference from an expression ratio of 1, according to a one-sample Student's t-test; * $p < 0.05$, ** $p < 0.01$, *** $p < 0.001$.

| | Gene | Product | HDF | | HepG2 | |
|---|---|---|---|---|---|---|
| | | | 6 h | 24 h | 6 h | 24 h |
| tRNA processing | *POL3RD* | RNA polymerase III subunit D | 1.53 | 2.85** | 1.37* | 1.64** |
| | *PUS1* | Pseudouridine synthase 1 | 1.80* | 2.91** | 1.47* | 2.20** |
| | *RPP40* | Ribonuclease P 40kDa subunit | 1.30 | 0.95 | 1.24 | 2.07** |
| | *RPP21* | Ribonuclease P 21kDa subunit | 1.33* | 1.12 | 1.61* | 2.02** |
| | *NUFIP1* | nuclear FMRP interacting protein 1 | 1.47* | 2.03** | 1.63* | 1.68** |
| mRNA processing | *SART3* | SCC antigen recognized by T cells 3 | 1.52* | 2.67** | 1.51 | 1.77** |
| | *CSTF1* | Cleavage stimulation factor, subunit 1 | 1.48* | 1.73* | 1.57* | 1.88** |
| | *CSTF3* | Cleavage stimulation factor, subunit 3 | 1.60** | 1.38** | 1.28* | 0.75* |
| | *KIAA0017* | Splicing factor 3b, subunit 3 | 1.67* | 2.83*** | 1.11 | 1.36* |
| | *HSA9761* | Putative dimethyladenosine transferase | 1.23 | 3.82*** | 1.17 | 1.42** |
| rRNA processing | *NOL5A* | Nucleolar protein 5A | 1.31* | 1.89** | 1.60* | 3.66*** |
| | *DDX47* | DEAD box polypeptide 47 isoform 1 | 1.60** | 2.12*** | 1.0 | 1.31** |
| | *EXOSC4* | Exosome component 4 | 1.42** | 2.21** | 1.27* | 1.36** |
| | *EXOSC9* | Exosome component 9 | 1.44* | 1.57** | 1.16 | 1.36** |

*POL3RD*, encoding subunit D of RNA polymerase III, was induced significantly in both cell types after 24 h. RNA polymerase III transcribes genes for all tRNAs as well as 5S rRNA. Pseudouridine is a modified base present in tRNA and rRNA. *PUS1*, encoding a pseudouridine synthase specific for tRNA (Chen and Patton, 1999; Patton et al., 2005), was significantly up-regulated in both cell types over time. *RPP40*, encoding a 40 kDa subunit of ribonuclease P (Jarrous et al., 1998), was induced significantly over time in HepG2 cells but not in HDFs. The *RPP21* gene, encoding a 21 kDa subunit of RNase P (Jarrous et al., 2001; Jiang et al., 2001), was also induced significantly in HepG2 cells following CYN treatment. Ribonuclease P is required for the maturation of tRNA, cleaving the 5' leader from precursor molecules (Hopper and Phizicky, 2003).

*SART3*, also up-regulated in both HDFs and HepG2 cells, encodes a protein involved in mRNA splicing (Harada et al., 2001). More specifically, SART3 (also known as p110) associates with snRNPs during the recycling of spliceosome components following an mRNA splicing event (Bell et al., 2002; Nottrott et al., 2002). *CSTF1* encodes subunit 1 of a heterotrimeric complex, cleavage stimulation factor (CSTF), involved in the cleavage of 3' ends of mRNA necessary for efficient polyadenylation (Ruegsegger et al., 1996; Takagaki et al., 1992; Takagaki and Manley, 2000). In both HDFs and HepG2 cells, *CSTF1* expression was induced significantly after 6 h and 24 h exposure. Interestingly, *CSTF3* mRNA levels increased in HDFs over time but in HepG2 cells this gene was up-regulated only slightly after 6 h, and down-regulated after 24 h CYN exposure. Signal intensities for array features representing *CSTF2* and *CSTF4* were not greater than background levels.

*NOL5A* was one of the ten most highly induced genes in HepG2 cells (see above), and encodes a protein required for pre-rRNA processing during ribosome biogenesis (Gautier et al., 1997; Hayano et al., 2003). CYN exposure also resulted in the increased expression of *DDX47,* encoding an RNA helicase belonging to the DEAD-box superfamily—a family of highly conserved, ATP-dependent, double-stranded RNA unwinding enzymes containing the motif D-E-A-D (Asp-Glu-Ala-Asp) (Linder, 2006). DEAD-box RNA helicases are required for transcription, pre-mRNA splicing, mRNA export, RNA degradation and ribosome biogenesis (Linder, 2006). The DDX47 protein resides in the nucleolus associated with rRNA precursors, and is therefore thought to be involved in rRNA processing (Sekiguchi et al., 2006). This is supported by the fact that the yeast

homologue of DDX47, Rrp3, is required for proper 18S rRNA processing (O'Day et al., 1996). Also involved in the processing of pre-rRNA is the exosome, a complex of 5'–3' exonucleases important for a variety of RNA degradation processes, including the processing of the 3' ends of 5.8S rRNA precursors (Houseley et al., 2006). CYN treatment resulted in the induction of two genes encoding components of the exosome, *EXOSC4* and *EXOSC9*. Another gene involved in rRNA processing up-regulated in reponse to CYN was *HSA9761*, encoding a protein homologous to a yeast rRNA dimethyladenosine transferase (Stanchi et al., 2001).

Clearly, genes for numerous components of the rRNA processing machinery appear to up-regulated following CYN treatment. This may indicate that rRNA synthesis is increased in response to CYN, which would contradict the negative effects of CYN on cellular proliferation (see Chapter 2), since rRNA synthesis is inextricably linked to cell growth and proliferation. This may suggest a response to rRNA damage, and a subsequent increase in the expression of genes involved in the synthesis and processing of new rRNA.

Increases in relative mRNA levels for transfer RNA (tRNA) processing genes may also be linked to RNA damage. If the inhibition of protein synthesis is due to damage to mRNA or rRNA, then it follows that tRNA is likely to also be damaged by CYN. This could result in the upregulation of genes for tRNA synthesis and processing as can be seen in the present study (Table 3.6). Further work is required to establish whether RNA damage is indeed a mechanism of CYN toxicity.

### *3.3.5 CYN-mediated expression differs between HDFs and HepG2 cells*

The initial motivation for using a liver-derived cell line was that it may express CYP450-family enzymes that have been proposed to potentiate CYN toxicity in rodent hepatocytes. Despite a degree of CYP450-family metabolic capability in HepG2 cells (Rodriguez-Antona et al., 2002; Sassa et al., 1987), activation of CYN to a more potent compound does not appear to occur in these cells. Nevertheless, differing responses at the level of gene expression may be the basis of the observed differences in cytotoxicity after CYN exposure. For example, LDH release occurs in HDFs, but not HepG2 cells, after long CYN exposures (Section 2.3.3). The basis for this may relate to the repertoire of genes differentially expressed in the two cell types in response to CYN, some of which are listed in Table 3.7.

**Table 3.7** Genes differentially expressed in HDFs and HepG2 cells in response to CYN (NP – not present, i.e. signal intensities were not above the average background level). * $p < 0.05$, ** $p < 0.01$, *** $p < 0.001$ according to the one-sample t-test. NP – not present (low expression level).

| Gene | Product | HDF | | HepG2 | |
|---|---|---|---|---|---|
| | | 6 h | 24 h | 6 h | 24 h |
| *TXNRD1* | Thioredoxin reductase 1 (cytosolic) | 0.89 | 0.44*** | 1.46* | 2.24** |
| *DKK1* | Dickkopf-like kinase l | 1.42 | 0.26*** | 1.61** | 1.34* |
| *ENC1* | Ectodermal neural cortex 1 | 1.44* | 6.11*** | 1.09 | 0.65** |
| *GADD153* | Growth arrest and DNA-damage, 153 kDa | 0.45* | 0.69* | 1.05 | 1.91** |
| *CTSC* | Cathepsin C isoform a preproprotein | 1.50* | 5.62*** | 1.28* | 0.72** |
| *SERPINE2* | Serpin, class E, member 2 | 0.77* | 0.57*** | 1.45** | 1.78** |
| *AQP3* | Aquaporin 3 | NP | NP | 1.24 | 4.94*** |

Thioredoxin reductases catalyse the NADPH-dependent reduction of thioredoxins, a family of small proteins important in maintaining the cellular redox state. Thioredoxins are associated with numerous physiological functions in the cell—signalling, DNA replication, regulation of apoptosis, regulation of transcription factors, and oxidant detoxification (Arner and Holmgren, 2000). The two major forms of thioredoxin in higher eukaryotic cells are the cytosolic thioredoxin 1, and the mitochondrial form known as thioredoxin 2. Cytosolic thioredoxin, in its reduced dithiol state, has a protective role against xenobiotic compounds such as oxidants and electrophiles (Watson et al., 2004). Thioredoxin reductase 1 is a cytosolic thioredoxin reductase responsible for reducing the active site of thioredoxin 1 (Nakamura, 2005). The gene encoding this reductase, *TXNRD1*, was strongly up-regulated in HepG2 cells following CYN exposure, but down-regulated in HDFs (Table 3.7). The relative expression ratios were confirmed using qRT-PCR (Table 3.8). Transcriptional regulation of *TXNRD1* is complex, and although constitutive expression of this gene is under the control of a core promoter typical of housekeeping genes (Rundlof et al., 2001), there is some evidence for the existence of alternative promoter regions that may be inducible (Rundlof et al., 2004). Indeed, *TXNRD1* transcription is induced following cadmium exposure via an antioxidant response element (Sakurai et al., 2005). Cadmium is a well-known inducer of cellular oxidative stress (Snow, 1992; Waisberg et al., 2003). In contrast to *TXNRD1*, the expression of the endogenous thioredoxin inhibitor, *TXNIP,* was induced strongly in both cell types in response to CYN (Table 3.4). Transcript levels for thioredoxin itself were unchanged after 6 h but down-regulated after 24 h in HDFs (0.5-fold, $p = 0.011$), and slightly down-regulated in HepG2 cells after 6 h (0.74-fold, $p = 0.016$), but not significantly altered after 24 h. These data suggest a role for oxidative stress in CYN toxicity. The altered expression of *TXNRD1* in the present study

suggests that CYN exposure may modify the cellular redox state, relative to basal conditions during normal cell culture, in a cell-type specific manner.

*DKK1* expression in HDFs and HepG2 cells following CYN exposure also differed. Dickkopf-like kinase 1, encoded by the *DKK1* gene, is an antagonist of the Wnt signalling pathway (Fedi et al., 1999). Wnt genes are involved in the development of the body in multicellular organisms—mutations in these genes result in morphological alterations and developmental abnormalities, or carcinogenesis (Cadigan and Liu, 2006; Cadigan and Nusse, 1997). The canonical Wnt pathway involves the binding of Wnt proteins to a family of receptors known as 'Frizzled', initiating a signalling cascade that results in the stabilisation and nuclear localisation of β-catenin, which subsequently interacts with the T-cell factor/lymphoid enhancer binding (TCF/LEF) group of transcription factors, culminating in the induction of target gene promoters. Wnt signalling can inhibit apoptosis by preventing mitochondrial cytochrome *c* release (Chen et al., 2001). Dickkopf kinases interact with receptors associated with Wnt signalling, and are either agonists or antagonists of the pathway. The human *DKK1* gene (the product of which is an antagonist) is induced in response to DNA damage by various factors, resulting in a sensitisation to ceramide-induced apoptosis (Shou et al., 2002). In HDFs, *DKK1* mRNA levels were strongly reduced after 24 h CYN exposure, while in HepG2 cells, *DKK1* expression was slightly but significantly up-regulated in response to CYN at both 6h and 24 h. The *DKK1* gene is itself a target of β-catenin/TCF transactivation, indicating a negative feedback loop for the Wnt signalling pathway (Niida et al., 2004).

Another target of β-catenin/TCF-mediated transcriptional activation is *ENC1*, a gene originally described as a neural development determinant ('ectodermal neural cortex 1'(Hernandez et al., 1998)). *ENC1* expression in response to CYN is almost the inverse of *DKK1* expression—after 24 h, *ENC1* is strongly induced in HDFs, and in HepG2 cells is slightly but significantly downregulated (Table 3.7). This pattern of expression is consistent with the fact that DKK1 inhibits Wnt signalling. Interestingly, HepG2 cells express a truncated mutant of β-catenin that renders TCF-dependent transcription constitutively active (de La Coste et al., 1998). This mutation inherently prevents the occurrence of transcriptional changes resulting from the modulation of Wnt signalling by DKK1 in HepG2 cells, which could explain the low magnitude of change in *ENC1*

expression relative to control cultures. In HDFs, the strong decrease in relative *DKK1* expression after 24 h may underlie the observed increase in *ENC1* mRNA.

The fact that *GADD153* is down-regulated in HDFs in response to CYN is consistent with the widespread reduction in the expression of ER chaperone genes—*GADD153* expression is known to be co-ordinately regulated with unfolded protein response genes (Oyadomari and Mori, 2004; Wang et al., 1996; Zinszner et al., 1998). Reasons for the up-regulation of *GADD153* in HepG2 cells are less clear. The *GADD153* promoter is activated in response to DNA damage (Luethy and Holbrook, 1992), which may occur differentially in HDFs and HepG2 cells, however, the expression of DNA damage response genes (Table 3.5) seems to be similar in both cell types. In any case, the downstream effects of differential *GADD153* expression may contribute to the differential Wnt/β-catenin/TCF-mediated expression described above. This is apparent from recent findings indicating that GADD153-CHOP is a negative regulator of Wnt signalling (Horndasch et al., 2006). Down-redulation of *GADD153* relative to controls may therefore explain the induction of *ENC1* in HDFs.

*SERPINE2*, encoding a serine protease inhibitor (serpin, clade E, member 2, also known as protease nexin 1, PN1), was also differentially regulated in HDFs and HepG2 cells after CYN exposure. Serpin 2/PN1 inhibits trypsin, thrombin, urokinase and plasmin, but not chymotrypsin (Scott et al., 1985), and is known to be produced by fibroblasts in culture (Baker et al., 1980; Farrell and Cunningham, 1986). Interestingly, the expression profile of a gene encoding the cysteine protease cathepsin C (*CTSC*) was almost the inverse of that of *SERPINE2*. In HDFs, *CSTC* mRNA levels increased significantly over time and *SERPINE2* mRNA levels decreased, while in HepG2 cells the expression of *CTSC* was reduced after 24 h and *SERPINE2* expression increased over time. Cathepsin C is a coordinator of serine protease activation in cytotoxic lymphocytes and mast cells, removing the inhibitory amino-terminal dipeptides (McGuire et al., 1993; Wolters et al., 2001). While serpins do not inhibit the same class of serine proteases, it is interesting to note the apparent inverse regulation of genes for a serine protease inhibitor and a serine protease activator in the two cell types used in the present study.

### *3.3.6 Validation of expression ratios using qRT-PCR*

Relative transcript levels were confirmed using quantitative reverse transcriptase PCR (qRT-PCR) for selected genes of interest (Table 3.8). As commonly reported, the magnitude of gene expression changes measured using arrays sometimes differed to those measured using qRT-PCR, but the direction of change was consistently similar between the two methods. The differences in magnitude can be attributed to the low dynamic range and sensitivity of microarray technology compared with qRT-PCR. Another possible contribution to variation between the two methods is the nature of the experimental design. For the array experiments a time course was conducted whereby subconfluent cultures treated with 1 μg/ml CYN for 6 h and 24 h were compared to cultures treated for "0 h" (actually 24 h vehicle controls; see section 3.2.1). For the qRT-PCR validations, CYN-treated samples were compared against samples treated with an equal volume of sterile Milli-Q water over the same time course. This approach had the advantage of reducing the number of microarrays required for high-throughput gene expresssion anaylses, with the more accurate qRT-PCR method used to validate selected expression ratios in treated cells compared to vehicle controls.

A list of primer pairs used for real-time qRT-PCR appears in Appendix 1.

**Table 3.8** Validation of relative expression levels for selected transcripts using qRT-PCR. NP – not present in microarray data following quality control procedures (Due to higher sensitivity, qRT-PCR was able to detect transcripts with low expression levels). ND – not determined. For array data, asterisks represent significant difference from a theoretical ratio of 1.0 (no change) according to a one-sample Student's t-test; for qRT-PCR data, asterisks represent significant difference between sample cycle threshold values and control cycle threshold values according to the method of Pfaffl et al. (2002); * $p < 0.05$, ** $p < 0.01$, *** $p < 0.001$.

| | HDF | | | | HepG2 | | | |
|---|---|---|---|---|---|---|---|---|
| **Gene** | **6 h** | | **24 h** | | **6 h** | | **24 h** | |
| | *Array* | *qRT-PCR* | *Array* | *qRT-PCR* | *Array* | *qRT-PCR* | *Array* | *qRT-PCR* |
| p53-regulated | | | | | | | | |
| *GADD45α* | 1.01 | 1.89 | ***21.1 | 133.0*** | 1.48 | 1.26 | ***6.1 | 11.40** |
| *CDKN1A* | **1.11 | 0.92 | *3.42 | 3.47** | *1.73 | 1.30 | *1.55 | 1.85 |
| DNA repair | | | | | | | | |
| *XPC* | ***1.53 | 1.66 | **3.19 | 5.07** | *2.17 | ND | ***2.20 | 3.90* |
| *DDB2* | 1.07 | 1.60 | **2.09 | 12.08*** | *1.37 | ND | 1.23 | 2.07 |
| *ALKBH* | *1.65 | 3.03* | **3.06 | 9.96*** | *1.73 | ND | **2.28 | 4.45* |
| NF-κB-regulated | | | | | | | | |
| *IL1α* | 1.33 | 1.32 | ***5.50 | 166.3*** | *1.43 | 1.35 | 0.98 | ND |
| *IL6* | 0.97 | 3.62* | *2.88 | 212.8*** | NP | ND | NP | ND |
| *IL8* | **1.61 | 8.01** | **12.0 | 168.6*** | *1.57 | 2.01** | ***3.87 | 14.21** |
| *TWEAKR* | *2.53 | 1.3 | ***7.78 | 6.36** | **1.87 | 2.51** | ***7.48 | 9.79** |
| ER stress | | | | | | | | |
| *GADD153* | *0.45 | 0.28*** | *0.69 | 0.92 | 1.05 | 0.81 | **1.91 | 8.15* |
| *BiP-GRP78* | 0.73 | 0.70 | **0.42 | 0.53** | *0.52 | 0.68 | **0.29 | 0.21*** |
| *KDELR3* | *0.90 | ND | **0.19 | 0.14*** | 1.05 | 1.00 | **0.38 | 0.36* |
| Miscellaneous | | | | | | | | |
| *TXNRD1* | 0.89 | ND | ***0.44 | 0.61 | *1.46 | 1.55 | **2.24 | 2.21 |
| *AQP3* | NP | ND | NP | 1.97* | 1.26 | ND | ***4.94 | 167.6*** |
| *ENC1* | *1.44 | ND | ***6.10 | 21.08*** | 1.09 | ND | ***0.65 | 0.76 |

## 3.4 Discussion

The present investigation utilised a high-throughput approach to determine changes in gene expression following CYN treatment. This strategy was undertaken with the view to elucidating endpoints of intracellular stress signalling related to specific mechanisms of toxicity.

A general overview of changes in gene expression induced by CYN, in both HDFs and HepG2 cells, was achieved through the examination of a dendrogram derived using hierarchical clustering (figure 3.3A). The dendrogram was divided into just two groups—generally up-regulated and generally down-regulated—consisting of the two major branches of the gene tree. Functional annotation of the genes present in the two groups yielded information consistent with observations of cytotoxicity induced by CYN, even at this broad level of analysis. The reduced expression of genes with products involved in protein transport and folding probably results from a diminished requirement for these functions due to CYN-mediated protein synthesis inhibition. Translational inhibition is a well-described mechanism of CYN cytotoxicity (Froscio et al., 2003; Terao et al., 1994). Similarly, the reduced requirement for amino acids may result in the observed reduction in expression of genes involved with amino acid biosynthesis and metabolism. The increased expression of genes associated with apoptosis is consistent with cellular responses to DNA damage through the activation of the p53 pathway. The induction of genes associated with RNA metabolism is of particular interest, as an interaction between CYN and mRNA may be the underlying mechanism of translational inhibition by CYN.

In both HDFs and HepG2 cells, functional analysis of up-regulated clusters showed a strong involvement of genes associated with RNA metabolism, RNA processing and splicing, and ribosomal RNA synthesis. Increased synthesis and processing of rRNA and tRNA is normally associated with enhanced cell growth and proliferation (White, 2005). Due to the fact that CYN reduces proliferation, one would expect RNA processing components to be down-regulated—in fact the opposite appears to be occurring. One possible explanation is that the cells may be compensating for inactivated ribosomes (or indeed damaged ribosomal RNA) by increasing the synthesis and metabolism of rRNA.

Similarly, increased expression of the processing machinery for tRNA may be associated with a possible detrimental effect on tRNA integrity. Since the present study measured only polyA$^+$ mRNA, further investigation using alternative methods would be required for the investigation of these possibilities.

The concept that cells have specific RNA repair processes is relatively new (Bellacosa and Moss, 2003), but it has been postulated that RNA damage may have a role in neurodegenerative diseases and other disorders (Bregeon and Sarasin, 2005). The induction of a gene (*ALKBH*) encoding a homologue of *E.coli* AlkB (hABH1) is interesting, as a different human homologue of this protein, hABH3, is able to repair methylated RNA (Aas et al., 2003).

CYN treatment resulted in the increased expression of numerous genes involved in DNA damage responses, in particular genes associated with the activation of the p53 transcription factor. The induction of p53-regulated gene expression is a common response to DNA damaging agents (Kastan, 1993; Lakin and Jackson, 1999; Meek, 2004), but it must be noted that a wide variety of other cellular stresses result in p53 activation (Levine et al., 2006). Elucidating the underlying mechanism of p53 activation by CYN is not possible by analysing gene expression at the level of mRNA. Nevertheless, the activation of p53-regulted genes involved in DNA repair may indicate the occurrence of DNA damage in response to CYN—particularly under conditions of low cytotoxicity. Concentrations utilised in the present study are cytotoxic, but only at long exposures—after 24 h, metabolic activity in CYN-treated HDFs, measured by the MTS assay, is not different to controls, and remain above 80% for HepG2 cells, while LDH release (a measure of membrane integrity and cytotoxicity) does not occur under these conditions in either cell type (Section 2.3.3).

The carcinogen benzo(a)pyrene (BaP) induces changes in gene expression associated with DNA adduct formation at levels of exposure that are not cytotoxic (Hockley et al., 2006). Comparing these changes with gene expression induced by CYN reveals a number of similarities. The p53-regulated genes *CDKN1A, DDB2* and *BTG2* are induced by both BaP and CYN in different cell types, while *GDF15* expression is induced in HepG2 cells

by both toxins. These similarities may indicate that CYN treatment results in DNA adduct formation, which would support earlier reports of an adduct in DNA isolated from the livers of CYN-treated mice (Shaw et al., 2000). The induction of nucleotide excision repair genes in the current study (Section 3.3.3.1) is consistent with the repair of bulky adducts, which also results in intermediary single-stranded breaks detectable by the comet assay—this phenmomenon may underlie positive comet assay results reported by Humpage et al. (2005). The characterisation of adducts induced by CYN exposure would be highly informative in terms of deciphering possible mechanisms of genotoxicity attributable to the compound.

DNA damage induces NF-κB activation via pathways that arre either dependent on or independent of IKK (Janssens and Tschopp, 2006). Although the role of NF-κB is often described as anti-apoptotic, some signals can induce NF-κB-dependent expression of pro-apoptotic genes (Kucharczak et al., 2003). The treatment of certain cell types with UV light, or topoisomerase inhibitors that induce DNA strand breakage, results in the down-regulation of the anti-apoptotic NF-κB target genes *BCL2L1* (encoding Bcl-xL) and *XIAP* (x-linked inhibitor of apoptosis) (Campbell et al., 2004). In the present study, *BCL2L1* was up-regulated slightly after 24 h in both cell types (1.47-fold in HDFs, $p < 0.05$; 1.49-fold in HepG2 cells, $p < 0.05$) and *XIAP* was not detectable (signals below background). The gene for the anti-apoptotic protein cIAP2 (*BIRC3*) was also induced by CYN treatment (see above and Table 3.5). While this seems to indicate that NF-κB induces pro-survival genes in response to CYN exposure, the induction of p53-regulated genes suggests that CYN also induces growth arrest and pro-apoptotic gene expression. It has been shown that the tumour suppressor status of a cell can determine the outcome of contrasting NF-κB- and p53-associated gene expression—p53 and NF-κB negatively regulate each other in terms of transcriptional activation (Webster and Perkins, 1999). It seems likely that despite the apparent activation of p53, the concurrent expression of NF-κB-regulated pro-survival genes may extend the survival time of CYN-treated cells. Interestingly, apoptosis induced by CYN was most apparent in HeLa cells (Chapter 2), in which p53 is virally inactivated (Hoppe-Seyler and Butz, 1993; Liang et al., 1993). This suggests that apoptosis induced by CYN after long exposure times is independent of p53.

CYN treatment resulted in the decreased expression of a large number of protein folding chaperones. Reduced chaperonin expression may be a result of protein synthesis inhibition by CYN—lower rates of translation may simply reduce the requirement for folding and transport chaperones, and therefore the activity of transcription factors responsible for the expression of chaperonin genes is similarly reduced. Indeed, the expression of genes associated with protein folding in the ER under adverse conditions is tightly regulated. The unfolded protein response (UPR) is regulated in part by X-box binding protein (*XBP1*) expression, which is a target of the ATF6 transcription factor. The subsequent expression of genes containing X boxes in their promoters is central to the ER stress response (Lee et al., 2003). Reduced mRNA translation during CYN exposure may result in the deactivation of ATF6, down-regulating the expression of *XBP1* and resulting in the subsequent reduction of ER stress-related expression.

ATF6 also directly binds ER stress response elements (ERSE) in the promoters of genes involved in ER stress (Roy and Lee, 1999; Yoshida et al., 1998). Transactivation via ERSEs requires the binding of both ATF6 and the general transcription factor NF-Y/CBF, each to one half of the consensus sequence CCAAT-$N_9$-CCACG (Yoshida et al., 2000). NF-Y/CBF is a member of the C/EBP family of transcription factors that bind CCAAT sequences (Maity and de Crombrugghe, 1998), while activated ATF6 binds to CCACG (Yoshida et al., 2000). ATF6 is constitutively expressed as a 90 kDa protein resident in the ER membrane, referred to as p90ATF6 (Yoshida et al., 1998; Zhu et al., 1997a). Translocation of active ATF6 to the nucleus requires proteolysis of p90ATF6 to a 50 kDa protein capable of binding ERSEs known as p50ATF6 (Haze et al., 1999). This is carried out by proteases known as Site-1 protease (S1P) and Site-2 protease (S2P) (Ye et al., 2000), and relies on the translocation of ATF6 from the ER to the Golgi during ER stress (Chen et al., 2002). GRP78 plays a role in ER stress activation by binding to and masking domains in ATF6 required for Golgi localisation (Shen et al., 2002a). Dissociation of GRP78 during ER stress allows the ATF6 to migrate to the Golgi where proteolysis by S1P and S2P can take place. *HERPUD1* expression is regulated by ATF6—two different ER stress response elements are present in the promoter, ERSE and ERSE-II, both of which are bound by ATF6 in concert with NF-Y (Kokame et al., 2001).

The possible down-regulation of ATF6 activity following CYN treatment may underlie the observed reduction of ER chaperone genes.

There appears to be a coordinated reduction in the expression of ER-resident chaperonins and stress-responsive genes following CYN exposure. Since the induction of ER stress transcripts is tightly and coordinately regulated in response to conditions adverse to protein folding in the ER, it follows that under normal conditions these genes are expressed at a basal level adequate for the proper folding of newly synthesised proteins during the appropriate stages of the cell cycle. It then also follows that under conditions preventing *de novo* protein synthesis, the expression of the genes encoding these chaperonins are down-regulated at the transcriptional level, possibly through a reduction in the abundance or activation state of the pertinent transcription factors. The obvious candidates for this are AFT6 and XBP-1, and it seems likely that CYN treatment may reduce the transactivation activity of ATF6, thereby also reducing the expression of XBP-1 at the level of transcription. This would result in the observed reduction in transcription of genes involved in ER stress. Consistent with this hypothesis are the findings that GRP78 expression is reduced following treatment with the protein synthesis inhibitor deoxynivalenol (Yang et al., 2000), and that GRP78 induction by ER stressors is blocked by the protein synthesis inhibitior cycloheximide (Brostrom et al., 1995; Laitusis et al., 1999). It seems likely that a decrease in the abundance of newly synthesised proteins in the ER results in a reduction in the expression of ER chaperones and UPR-related genes.

The altered expression of genes involved in redox regulation following CYN exposure suggests a role for oxidative stress in the toxicity of this compound. The differential regulation of thioredoxin reductase (*TXNRD1*) expression in HDFs and HepG2 cells suggests that responses to CYN, at least at the level of gene expression, are cell-type specific. It appears that in HepG2 cells, CYN may induce oxidative stress, resulting in the up-regulation of *TXNRD1* to compensate, while in HDFs this gene is down-regulated. This may indicate differing survival signals in the two cell types—in HDFs, a lack of *TXNRD1* induction could be associated with the induction of apoptosis, whereas in transformed cells such as HepG2, pro-survival signal may prevent apoptosis in response to oxidative stress induced by CYN. Previous studies have noted the reduction of cellular

glutathione (GSH) levels in primary rodent hepatocytes after CYN treatment (Humpage et al., 2005; Runnegar et al., 1994; Runnegar et al., 1995b). There is evidence that GSH depletion can be attributed to the inhibition of GSH synthesis by CYN, rather than to the increased utilisation of GSH under conditions of oxidative stress (Runnegar et al., 1995b). This has implications for the maintenace of the cellular redox state, as glutathione is the major non-protein redox regulatory molecule in the cell responsible for scavenging ROS and other oxidants (reviewed by Kwon et al., 2003). A decreased capacity to cope with oxidants may result in the inappropriate oxidation of proteins, or damage to cellular components due to increased levels of ROS.

Increased expression of genes encoding components of intracellular signalling pathways, such as the TNFR2 pathway presented in figure 3.4, represents an up-regulation of the members of the pathway rather than an activation of the pathway itself. This could act as a priming mechanism that confers to the cell an increased potential for signalling, resulting in increased signal strength compared to normal conditions. The logical follow-up to evidence of this kind is to investigate the phosphorylation status, and hence the activation status, of the components of the signalling pathway. Indeed, the measurement of altered mRNA levels described in this study can only reveal the end-points of intracellular signalling in response to the damage initiated by CYN. Investigation of possible upstream mediators of the changes observed is the next step in investigating possible mechanisms of toxicity. The possible role of the tumour suppressor p53 in CYN-induced gene expression is investigated further in Chapter 4, while Chapter 5 describes the results of experiments investigating role of MAPK signalling and NF-κB in gene expression following CYN exposure.

# Chapter 4

## *Induction of p53-regulated gene expression in response to cylindrospermopsin*

### 4.1 Introduction

The 'tumor suppressor' protein p53 is a transcription factor that regulates the expression of a large number of genes associated with growth arrest, apoptosis and DNA repair (Meek, 1998; Sengupta and Harris, 2005). P53 is mutated or inactivated in a large proportion of cancers (Hainaut and Hollstein, 2000), highlighting its role as in the regulation of the cell cycle.

DNA damage is perhaps the most well studied inducer of p53 activation. The specific mechanisms of DNA damage sensing have not been well described but are known to involve the protein kinases ataxia-telangiectasia mutated (ATM), ATM- and Rad3-related kinase (ATR), and DNA-dependent protein kinase (DNA-PK) (reviewed by (Abraham, 2001; Khanna et al., 2001; Yang et al., 2003). Following damage sensing, signals are transduced to effectors of cell cycle arrest and DNA repair such as p53. An overview of the processes leading to p53 activation, and outcomes such as cell cycle arrest and apoptosis, is presented in Figure 4.1. Under normal conditions, p53 turnover is continual, with nuclear export and proteasomal degradation being mediated by a ubiquitin ligase known as Mdm2 (mouse double minute 2 (Honda et al., 1997), which is sometimes referred to in human cells as Hdm2. Stabilization of the p53 protein occurs primarily via

the inhibition of the Mdm2-p53 interaction, which is achieved through various modifications to either protein. Phosphorylation of p53 at a number of specific serine residues inhibits Mdm2 binding (reviewed by (Shieh et al., 1997). Auto-ubiquitylation of Mdm2 may occur after DNA damage induced by gamma radiation (Stommel and Wahl, 2004), resulting in proteolytic degradation of Mdm2 and increased p53 stability. The *MDM2* gene is itself a target of p53 transactivation, providing a negative feedback loop which restores low levels of p53 following activation of the pathway. The ARF tumor suppressor protein also inhibits p53-Mdm2 interaction by binding to Mdm2, resulting in the stabilization of p53 levels (Honda and Yasuda, 1999).

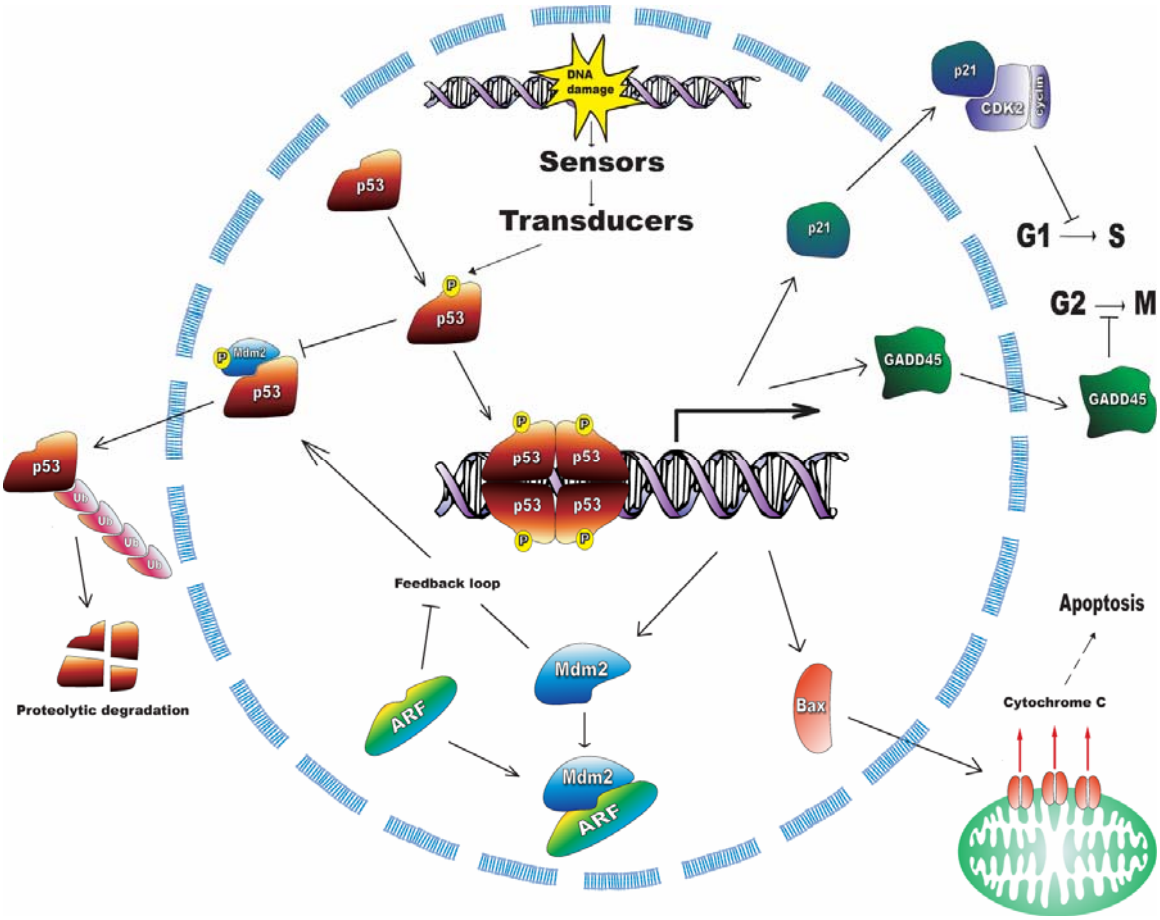


**Figure 4.1 P53 activation in response to DNA damage.** A schematic representation of p53 stabilisation and two possible responses regulated by p53 target genes—cell cycle arrest and apoptosis.

Phosphorylation of p53 at specific residues also modulates its capacity for transcriptional activation. P53 target genes have various functions in growth arrest, apoptosis and DNA

repair. A major target of p53 transactivation is *CDKN1A,* encoding $p21^{WAF1/CIP1}$, a protein that interacts with cyclin-dependent kinases to arrest the cell cycle (Yin et al., 1997). As discussed in Chapter 3, P53 also regulates the expression of growth arrest and DNA damage-related gene *GADD45α* (Hollander et al., 1993). GADD45α protein is known to contribute to cell cycle arrest at the transition from G2 phase to mitosis (Wang et al., 1999), and is also required for some DNA repair pathways following exposure to genotoxic agents (Smith et al., 2000). Apoptosis can be triggered by p53 through the increased expression of genes encoding the Bcl2-family proteins Bax and PUMA (Green, 2000). These proteins induce apoptosis by increasing mitochondrial outer membrane permeability (Harris and Thompson, 2000; Schuler and Green, 2001), resulting in cytochrome *c* release and initiation of the caspase cascade.

Microarray data presented in Chapter 3 revealed that p53-regulated genes were induced by 1 μg/mL CYN, particularly after 24 h exposure. In this chapter, I confirm that CYN induces p53-regulated gene expression after 24 h in dermal fibroblasts and HepG2 cells, and show that the same genes are also induced in a dose-dependent manner after 6 h.

## 4.2 Materials And Methods

### *4.2.1 Cell culture*

Human dermal fibroblasts (HDFs), Caco-2 (HTB-37, ATCC), HepG2 (HB-8065, ATCC) and C3A cells (CRL-10741, ATCC) were grown at 37ºC under a 5% $CO_2$ humidified atmosphere in Dulbecco's modification of Eagle's medium (DMEM, Gibco-Invitrogen), high-glucose, supplemented with 42 μg/mL L-glutamine, 110 μg/mL sodium pyruvate, and 4 μg/mL pyridoxine-HCl. For routine maintenance, media were further supplemented with 10% fetal bovine serum (Gibco-Invitrogen), 100 units/mL penicillin (Gibco-Invitrogen) and 100 μg/mL streptomycin (Gibco-Invitrogen). For toxin exposures, antibiotics were omitted.

### *4.2.2 CYN treatments and relative gene expression analysis*

Cells were seeded into six-well plates and grown for 24-48 h until monolayers reached 60-70% confluence. Culture media were exchanged with fresh medium containing

cylindrospermopsin or an equal volume of vehicle (sterile MQW). Three separate treatments were performed for each condition. Following incubation for the indicated times, total RNA was isolated using silica spin-column purification (RNeasy kit, Qiagen) according to the manufacturer's instructions. Briefly, cells were washed 3 times with sterile phosphate-buffered saline (PBS), scraped into lysis buffer directly in cell culture dishes and transferred to 1.5 mL microcentrifuge tubes. The optional on-column deoxyribonuclease treatment was included to prevent contamination by genomic DNA. RNA was eluted with 50 μL of RNase-free water (Qiagen) and eluates were passed through the columns a second time to improve yields. Total RNA was quantified by measuring absorbance at 260 nm. The presence of contaminating protein was checked by measuring the $A_{260}/A_{280}$ ratio, and RNA integrity was confirmed by agarose gel electrophoresis using standard methods (Ausubel et al. 1999), and denaturing RNA prior to electrophoresis by heating to 70°C in a loading buffer containing 50% formamide.

Relative quantification of mRNA by real-time reverse transcriptase PCR was performed as described in Section 3.2.4.

### *4.2.3 Western immunoblotting*

Cells were seeded into wells of a 24-well plate ($10^4$ per well) and grown for 24 h. Media were exchanged for fresh media containing toxins or vehicle controls and incubated for the indicated times. Monolayers were washed three times with PBS and harvested by scraping into 0.5 mL PBS. Cells were pelleted and lysed on ice. Proteins were separated on 12% polyacrylamide gels using standard procedures (Ausubel et al., 1999) and blotted onto nitrocellulose membranes (Millipore). Membranes were blocked for 1 h with blocking buffer (2% bovine serum albumin and 0.1% Tween-20) in PBS. Immunodetection of total p53 protein was achieved using monoclonal anti-p53 antibody (Sigma-Aldrich). Anti-GAPDH monoclonal antibody (Ambion) was used as a loading control. Bound antibodies were detected with a 1:1 mixture of goat $F_{ab}$- and $F_c$- specific anti-mouse IgG antibodies conjugated to alkaline phosphatase (Sigma-Aldrich). Bands were detected with a chemiluminescent alkaline phosphatase substrate (Pierce) and visualized using a cooled CCD camera (Fujifilm LAS3000).

### *4.3 Results*

In experiments described in the current chapter, I investigated the effects of CYN on the expression of genes known to be regulated by p53.

Changes in p53-regulated gene expression were investigated after 6 h and 24 h exposure to CYN. For the 24 h exposures, a CYN concentration of 1 μg/mL (2.4 μM) was used, which corresponded to MTS reduction measurements of between 80 and 100% of control cultures (see Section 2.3.1). At this concentration, *GAPDH* mRNA levels remained constant when equal total RNA input amounts were used in qRT-PCR analyses. *GAPDH* mRNA levels were also stable after 6 h exposure to CYN concentrations of up to 5 μg/mL. *GAPDH* was therefore used as the reference gene for all gene expression analyses. For the 6 h treatments, concentration-response experiments were conducted using 1, 2.5 and 5 μg/mL CYN.

After 6 h, CYN treatment resulted in significant increases in relative mRNA levels for p53 target genes in HDFs and HepG2 cells according to the statistical analyses employed in the REST software package (Pfaffl et al., 2002), with relative mRNA levels for *CDKN1A, GADD45α, BAX* and *MDM2* generally increasing as CYN concentration increases (Figure 4.2A). *GADD45α* was induced in response to 5 μg/mL CYN by a factor of greater than 10 in both cell lines. This agrees well with the microarray data presented in Chapter 3, where this gene was amongst the most strongly induced in both HDFs and HeG2 cells. *CDKN1A*, another gene shown to be induced using microarray analysis, was found seen to be induced greater than 2-fold using qRT-PCR, but only increases by a statistically significant margin in response to 5 μg/mL CYN in both cell types (Figure 4.2). Likewise, *BAX* mRNA levels were induced significantly in response to 5 μg/mL in both HDFs and HepG2 cells, but not in response to 1 μg/mL or 2.5 μg/mL.

I investigated the accumulation of total p53 protein, rather than phosphorylation of specific residues (for which antibodies are commercially available), as stabilisation and increased transactivation activity is not wholly dependent on phosphorylation but can also be affected by modifications such as ubiquitylation, acetylation or neddylation (Brooks and Gu, 2003; Xu, 2003). P53 protein could not be detected in HDFs using the antibodies

and procedures employed in the present study, but could be detected in HepG2 cell lysates. A small degree of p53 accumulation occurred after 6 h exposure to 5 µg/mL CYN, which was not apparent after 3 h (Figure 4.2B).

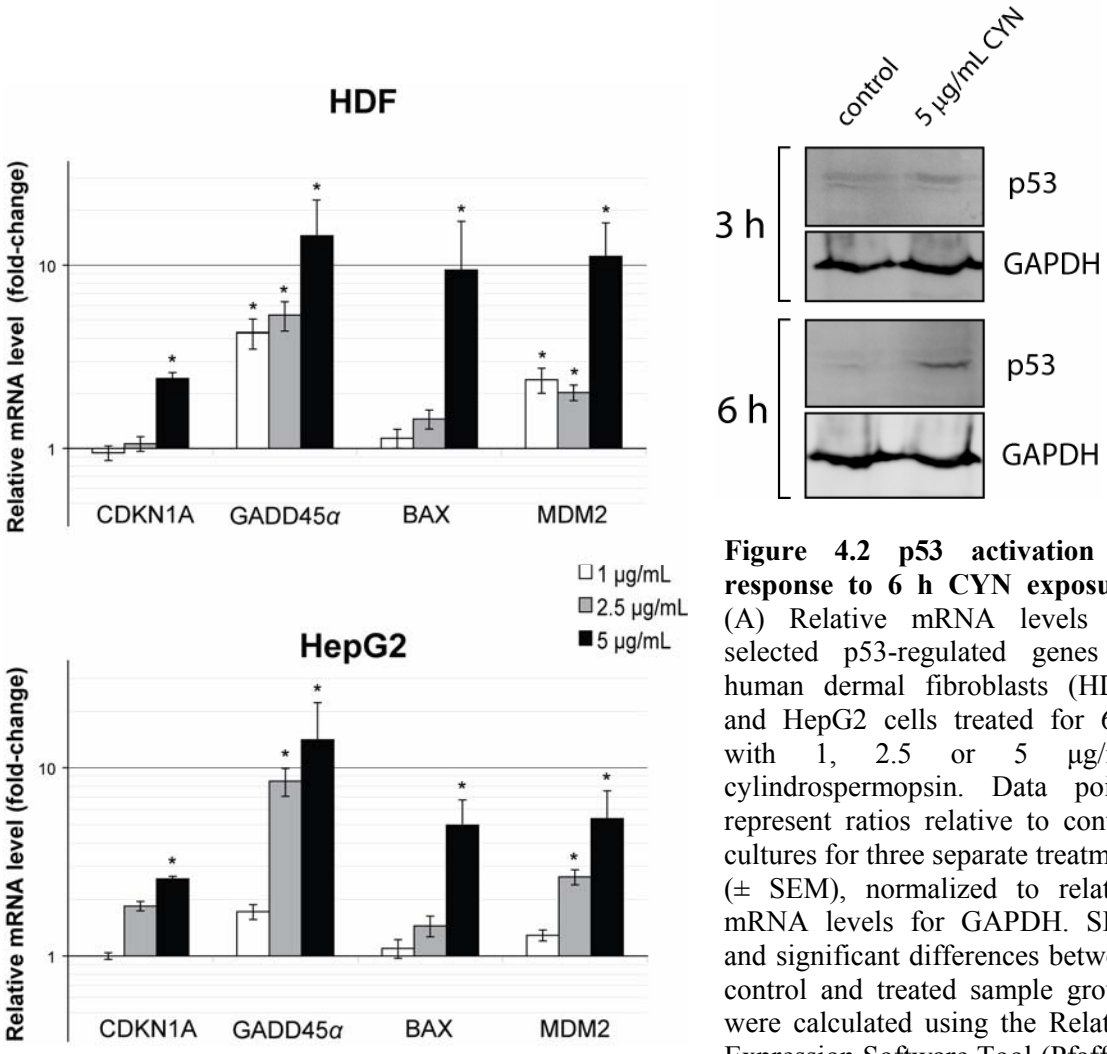


**Figure 4.2 p53 activation in response to 6 h CYN exposure.** (A) Relative mRNA levels for selected p53-regulated genes in human dermal fibroblasts (HDF) and HepG2 cells treated for 6 h with 1, 2.5 or 5 µg/mL cylindrospermopsin. Data points represent ratios relative to control cultures for three separate treatment (± SEM), normalized to relative mRNA levels for GAPDH. SEM and significant differences between control and treated sample groups were calculated using the Relative Expression Software Tool (Pfaffl et al., 2002) *$p < 0.01$.
(B) Immunoblots of HepG2 cell lysates showing p53 accumulation after 6 h.

After 24 h exposure to a concentration of 1 µg/mL CYN, relative mRNA levels for the same set of p53-regulated genes were significantly elevated compared to control cultures in HDFs (Figure 4.3). The degree of induction appeared to be markedly higher in HDFs than in HepG2 cells, which is in general agreement with the differences in magnitude of

gene expression changes observed using microarray analysis (see Chapter 3). It was interesting to note that while the magnitude of changes in expression for this group of genes was different between the two cell lines, the pattern of expression was similar, with *GADD45α* being induced strongly and a similarly moderate induction of *CDKN1A*, *BAX* and *MDM2*.

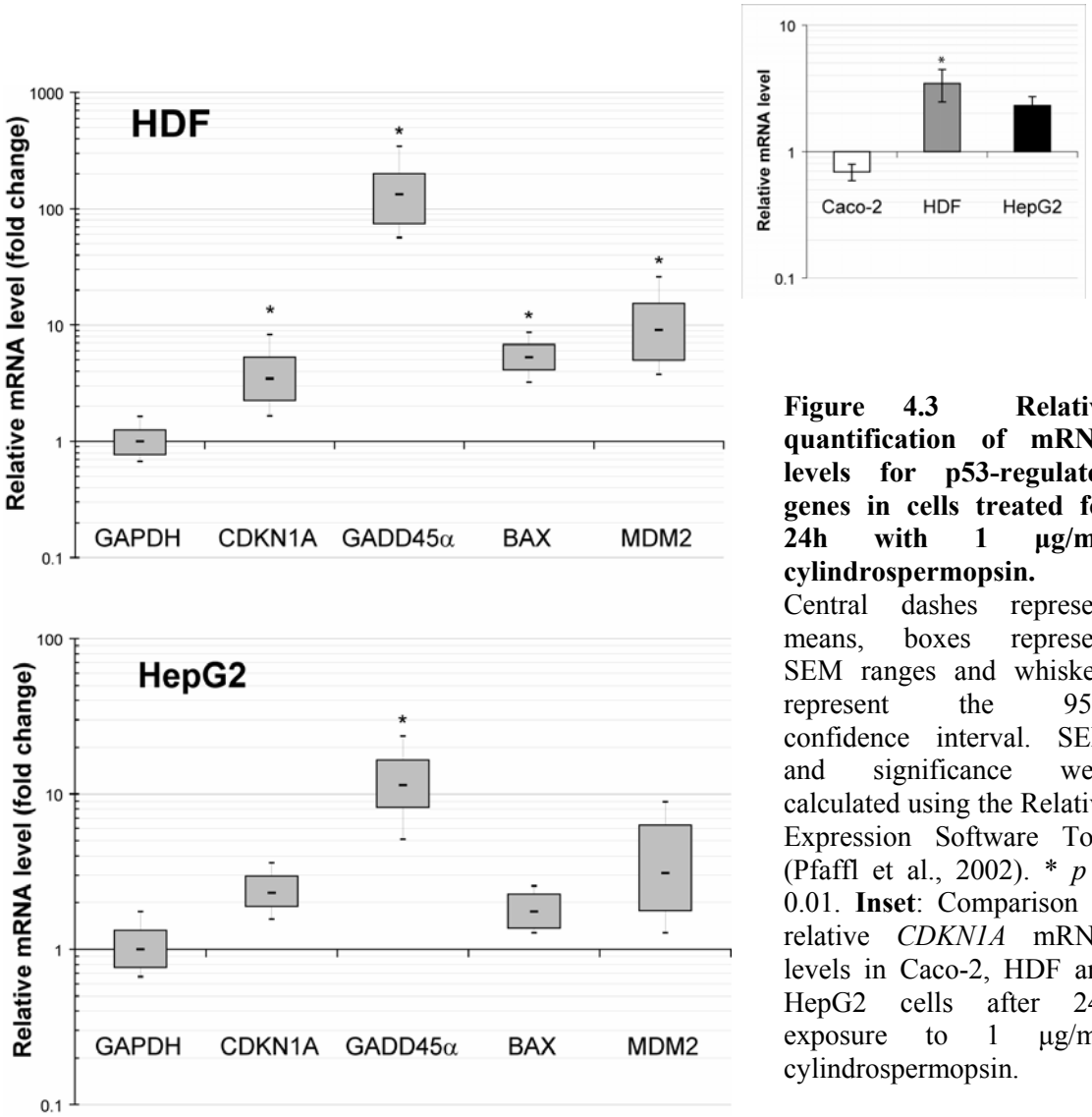


**Figure 4.3 Relative quantification of mRNA levels for p53-regulated genes in cells treated for 24h with 1 µg/mL cylindrospermopsin.** Central dashes represent means, boxes represent SEM ranges and whiskers represent the 95% confidence interval. SEM and significance were calculated using the Relative Expression Software Tool (Pfaffl et al., 2002). * $p < 0.01$. **Inset**: Comparison of relative *CDKN1A* mRNA levels in Caco-2, HDF and HepG2 cells after 24h exposure to 1 µg/mL cylindrospermopsin.

Relative *CDKN1A* mRNA levels were seen to increase in both HDFs and HepG2 cells after 24 h exposure to 1 µg/mL CYN, but not in Caco-2 cells (Figure 4.3 inset), which express a mutant, inactive form of p53 (Gartel et al., 1996). This suggests that p53 may indeed be required for *CDKN1A* induction in response to cylindrospermopsin, but further

experiments are needed before this can be conclusively determined. In p53-proficient cell lines, this could be confirmed by knock-down of p53 expression using interfering RNA, followed by CYN treatment and comparison of *CDKN1A* mRNA levels with control cells.

## 4.4 Discussion

Despite having transactivation-independent functions associated with apoptosis (Chipuk et al., 2004) and DNA repair (Sengupta and Harris, 2005), p53 functions predominantly by altering the transcription of target genes. Consequently, it is widely accepted that the increased expression of genes known to be regulated by p53 provides an indication of p53 activation. HepG2 are capable of expressing wild-type p53 protein (Bressac et al., 1990), and the HDFs used in this study were originally isolated from a healthy patient in a clinical setting, implying normal p53 function. In HDFs and HepG2 cells, elevated mRNA levels for p53-regulated genes were apparent after only 6 h of exposure, suggesting an early activation of the pathway. The upstream stress signals contributing to this phenomenon are presumably the result of damage to cellular components, but from the data presented here it is not possible to speculate on the nature of the damage. The finding that broad-spectrum CYP450 inhibitors inhibit genotoxicity in primary mouse hepatocytes (Humpage et al., 2005) suggests that it is unlikely that DNA damage in the cell types used in this study would be due to a CYN metabolite. However, a DNA damage-related p53 response can not be ruled out, since native CYN has been shown to induce cytogenetic effects in CYP450-deficient human lymphoblastoid cells at relatively low concentrations (Humpage et al., 2000).

An alternative possibility is that native CYN induces p53 activation through processes unrelated to DNA damage. This may be associated with the molecular interactions underlying translational inhibition, since toxins known to inhibit protein synthesis by damaging ribosomal RNA rapidly activate p53 via the mitogen-activated protein kinase (MAPK) pathway (Zhou et al., 2005a). Numerous signalling pathways culminate in the phosphorylation of p53 through MAPK pathway via c-Jun $NH_2$-terminal kinase (JNK)

and p38 MAPK (Bulavin et al., 1999; Buschmann et al., 2001; Milne et al., 1995), although the specificity of these kinases for p53 has not been completely investigated.

While the gene expression data presented in this chapter suggest a possible role for p53 in CYN-induced growth arrest, the antiproliferative effects of CYN described in Chapter 2 were comparable in treated Caco-2 cells (mutant p53) and HepG2 cells (wild-type p53), indicating that alternative inhibitory pathways are also induced by the toxin. Diminished cell growth in all three cell types used in this study might simply result from a reduction in overall protein synthesis, with little impact from putative p53-dependent pathways occurring in HepG2 and HDF cells. Furthermore, translational inhibition by CYN may conceivably reduce the magnitude of p53-dependent responses by preventing, at least in part, protein synthesis from mRNA transcribed after exposure to the toxin.

To identify upstream signalling events occurring after CYN exposure, it may be useful to examine the phosphorylation status of various key serine and threonine residues in the p53 protein. For example, phosphorylation of Ser15 by the ATM (ataxia-telangiectasia mutated) protein kinase is a well-characterised response to DNA damage caused by ionising radiation (Banin et al., 1998; Canman et al., 1998). ATM also activates Chk2 kinase (Matsuoka et al., 1998), which phosphorylates Ser20 of p53 (Shieh et al., 2000). UV light, which induces thymine dimers in DNA as well as causing less specific macromolecular damage, induces the activation of a number of protein kinases capable of phosphorylating p53. P38 MAPK phosphorylates Ser33 and Ser46 following UV exposure (Bulavin et al., 1999), while another MAPK-family protein, JNK, phosphorylates Thr81 (Buschmann et al., 2001; Milne et al., 1995). Ser315 is phosphorylated by cyclin-dependent kinases during different stages of the cell cycle and in response to DNA damage (Bischoff et al., 1990; Blaydes et al., 2001). UV exposure also activates homeodomain-interacting protein kinase 2 (HIPK2), which phosphoylates p53 at Ser46 (D'Orazi et al., 2002), inducing apoptosis in response to severe DNA damage such as ionising radiation-induced double-stranded breaks (Oda et al., 2000). Less severe DNA damage does not induce apoptosis but causes p53-dependent cell-cycle arrest by preventing HIPK2-mediated Ser46 phosphorylation through a mechanism involving Mdm2-regulated HIPK2 degradation (Rinaldo et al., 2007). DNA damage by

ionising radiation also results in the phosphorylation of Ser376 (Offer et al., 2002; Waterman et al., 1998). Finally, Ser392 is phosphorylated after UV exposure but not gamma radiation (Kapoor and Lozano, 1998; Keller et al., 2001).

Acetylation of p53 also occurs in response to DNA damage , indicating that determining post-translational modifications to the p53 protein other than phosphorylation may also aid in the determination of CYN mechanisms. While the upstream transducers of DNA damage signalling remain under investigation, there is currently sufficient knowledge to elucidate pathways contributing to p53 modification in response to CYN by examining the specific nature of the modifications to the protein. In this way, it should be possible to determine whether DNA damage or other stresses induce CYN-mediated p53 activation observed in the current chapter.

The involvement of p53 in CYN toxicity needs to be a priority for future research, particularly because of the important role the protein has in coordinating DNA repair processes. The work presented in this chapter has established that a number of well described p53-regulated genes are induced in cultured cells after CYN exposure, and that there is some evidence for the concurrent accumulation of p53 protein. Follow-up investigations that may be useful in determining CYN-induced damage upstream of p53 activation have been outlined.

# Chapter 5

## *Preliminary investigations into the roles of AP-1 and NF-κB in cylindrospermopsin-induced gene expression*

### 5.1 Introduction

Changes in gene expression associated with cellular stress are typically governed by three major transcription factors—activator protein 1 (AP-1), which targets numerous genes involved in proliferation and apoptosis, nuclear factor κB (NF-κB), an inducer of pro-survival gene expression, and the 'tumour suppressor protein' p53 (discussed in Chapter 4), which mediates gene expression associated with cell cycle arrest, DNA repair, and apoptosis. One or more of these transcription factors are often involved in the expression of immediate-early genes in response to stress-inducing agents such as metal ions (Durham and Snow, 2005), ionizing radiation (Mitchel et al., 1997), and UV light (Zhang et al., 2002). The pattern and magnitude of immediate-early gene expression can determine the fate of a stressed cell, be it growth arrest, proliferation or apoptosis, since many immediate-early gene products are themselves transcription factors (Welch and Chrylogelos, 2002).

By definition, immediate-early genes are expressed rapidly in response to exogenous stimuli and independently of *de novo* protein synthesis—this is an important consideration when investigating gene expression in response to a compound capable of inhibiting translation. Signalling pathways that require new protein synthesis may not result in downstream changes in transcription, while those that can activate transcription

factors directly will continue to operate under conditions of impaired ribosomal activity. The pathways investigated in the current chapter belong to the former category.

Genes represented on the microarrays used in this project did not include the immediate-early genes *JUN*, *FOS* or *MYC,* which encode the proteins c-Jun, c-Fos and c-Myc. These are the cellular counterparts (hence the 'c' designation) of virally-encoded proteins capable of transforming cells to a proliferative phenotype. As such, *JUN*, *FOS* and *MYC* are commonly known as oncogenes. As *JUN* and *FOS* are known to be induced rapidly in response to a variety of stresses, and *MYC* is a well described immediate-early gene, I investigated the expression of these genes in response to CYN using real-time qRT-PCR.

Although the induction of immediate-early genes is intrinsically of interest in the case of CYN toxicity, it may also be reveal mechanistic information. A subset of the mitogen-activated protein kinase (MAPK) pathway, involving the stress-activated protein kinases (SAPKs) Jun $NH_2$-terminal kinase (JNK) and p38 SAPK, is implicated in immediate-early gene expression in response to protein synthesis inhibitors (Iordanov et al., 1997; Zinck et al., 1995). MAPK signalling induced by the disruption of ribosomal function has been found to occur in a manner specific to the mechanism of translational inhibition. Compounds that interfere with ribosomal translocation, such as cycloheximide and emetine, do not appear to induce JNK and p38 MAPK activation, while factors that damage 28S rRNA proximal to the peptidyltrasferase site are strong agonists of these kinases. Peptidyltransferase inhibitors include the enzyme toxins ricin, sarcin, and Shiga toxin, which depurinate 28S rRNA at a specific position in the ricin/sarcin loop, and the small molecule toxins anisomycin and blasticidin, which bind the same region (Iordanov et al., 1997; Smith et al., 2003). This apparent specificity for JNK and p38 activation by damage to the peptidyltransferase loop, termed the 'ribotoxic stress response' (Iordanov et al., 1997), was an attractive starting point for deciphering possible interactions between CYN and ribosomal components—strong activation of JNK and associated downstream gene expression may indicate an interaction between CYN and rRNA.

JNK is a well-characterised contributor to the activation of the dimeric basic region-leucine zipper (bZIP) transcription factor, AP-1. The term 'AP-1' encompasses a large

repertoire of dimers composed of various combinations of Jun, Fos, ATF and Maf proteins (Shaulian and Karin, 2002). The most abundant form of AP-1 is generally considered to be the c-Jun/c-Fos heterodimer, but myriad combinations of related proteins, as well as c-Jun homodimers, also form active AP-1 moieties. Phosphorylation of Ser 63 and Ser73 of c-Jun by JNK increases its transactivation function and enhances interaction with various binding partners (Bogoyevitch and Kobe, 2006). Depending on dimer composition, AP-1 directs the transcription of diverse genes involved in proliferation, oncogenic transformation and apoptosis (Hess et al., 2004).

The approach described in the current chapter was intended to provide initial data with respect to the possible activation of MAPK signalling by CYN, with a focus on the JNK pathway and AP-1 activation. As a preliminary indicator of AP-1 activation, I measured *JUN* mRNA levels in CYN-treated cells relative to controls. I then attempted to confirm the involvement of JNK in cellular responses to CYN by detecting phosphorylated forms of JNK in protein extracts using Western immunoblotting. I also examined the effects of CYN on the expression of a reporter gene under the control of AP-1 sites in transient transfection experiments.

NF-κB plays a central role in the regulation of gene expression in response to cellular stress (Mercurio and Manning, 1999; Pahl, 1999), and contributes strongly to genotoxic stress responses (Bartek and Lukas, 2006; Habraken and Piette, 2006). There is mounting evidence suggesting that NF-κB functions as an inhibitor of apoptosis induced by JNK (Nakano et al., 2006), and hence may play a role in cell survival following CYN exposure. In experiments described in this chapter, the possible involvement of NF-κB in CYN-induced gene expression was investigated using a reporter gene under the control of NF-κB elements.

In summary, the aim of experiments described in the present chapter was to investigate immediate-early gene expression elicited by CYN in cultured human-derived cells, and to determine the involvement of JNK and NF-κB in CYN-induced gene expression.

## 5.2 Materials and Methods

### *5.2.1 Chemicals*

Anisomycin, cycloheximide, emetine, phorbol 12-myristate-13-acetate (PMA; also known as 12-O-tetradecanoylphorbol-13-acetate [TPA]), molecular biology-grade DMSO, and Bovine serum albumin (BSA; Fraction V) were purchased from Sigma-Aldrich.

### *5.2.2 Cell culture, RNA isolation and qRT-PCR*

Cell culture conditions, cylindrospermopsin treatments, purification of total RNA and relative quantification of mRNA levels in treated cells were carried out as described in Sections 3.2.3, 3.2.4 and 3.2.8.

For treatment with cycloheximide, anisomycin and PMA, the toxins were diluted in DMSO to the same molar concentrations before adding equal volumes to cell culture media, and control cultures were treated with an equal volume of DMSO to determine any contributing effects of the solvent. For emetine treatments, the toxin was dissolved in MWQ to the same concentration as CYN stocks, such that the CYN vehicle controls also functioned as vehicle controls for emetine.

### *5.2.3 Western blotting*

Cells were grown to 70-90% confluence in wells of standard 24-well plates, and treated with toxins or vehicle controls for the times indicated. Following treatments, cells were lysed by scraping directly into 100 µl 1X SDS-PAGE sample buffer containing 1/100 Phosphatase Inhibitor Cocktail 1 (Sigma-Aldrich), Protease Inhibitor Cocktail (Roche; 1 tablet per 10 mL buffer), and 100 mM DTT, and incubated on ice for 15 mins. Lysates were homogenised using QIAshredder columns as recommended by the manufacturer (QIAGEN). The resulting homogenised lysates were heated to 95°C for 5 mins and spun for 10 mins at maximum speed in a microcentrifuge. Supernatants (10 to 30 µl) were subjected to SDS-PAGE in 12% acrylamide gels using standard methods (Ausubel et al., 1999) until the dye front reached the bottom of the gel. Proteins were transferred to

nitrocellulose membranes (Millipore) using a semi-dry transfer apparatus (Bio-Rad) according to published methods (Ausubel et al., 1999). Transfer was carried out at 0.8 $mA/cm^2$ for 1 hour.

Membranes were air-dried and stained with Ponceau S solution for 5 mins to check transfer efficiency and equal protein loading. After destaining for 10 mins in MQW, membranes were incubated in blocking solution with gentle agitation for 30 mins to 1 hour. Membranes were incubated overnight with gentle agitation at 4°C with primary antibodies diluted in blocking solution: anti-phospho JNK1/2 monoclonal antibody (Cell Signalling Technology) was used at dilution of 1:1000; anti-GAPDH monoclonal antibody (Ambion) was diluted 1:4000. After washing three times with gentle agitation in PBST for 5 mins each wash, membranes were incubated with secondary antibody (horseradish peroxidase (HRP)-conjugated anti-mouse IgG (Sigma-Aldrich) or HRP-conjugated anti-rabbit IgG (Sigma-Aldrich)) diluted 1:10 000 in PBST containing 2% BSA) for 1 hour with gentle agitation. Bands were developed using a chemiluminescent HRP substrate as recommended by the manufacturer (Pierce), and images were captured using the LAS3000 CCD camera system (Fujifilm).

### *5.2.4 Reporter assays*

Reporter assays were based on commercially available vectors (Mercury™ Pathway Profiling SEAP System, CLONTECH), which encode a secreted alkaline phosphatase (Berger et al., 1988; Cullen and Malim, 1992) under the control of a minimal promoter designated TAL (TATA-like element). Response elements for specific transcription factors are inserted in the region immediately upstream of the TAL element. Plasmids pTAL-SEAP (Figure 5.1), the control vector containing only the minimal TAL promoter, and pAP1-SEAP, containing four copies of a consensus TRE (TPA response element/AP-1 binding site), were the kind gift of Prof Gillian Bushell. Using complementary oligonucleotides, I constructed an NF-κB reporter identical to the commercially available plasmid pNF-κB-SEAP (CLONTECH, 1998).

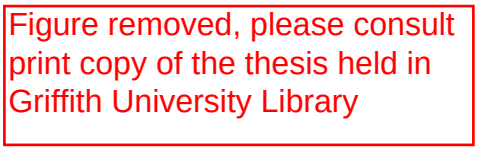


**Figure 5.1 Map of the pTAL-SEAP reporter vector.** Response elements are inserted into the multiple cloning site (MCS; depicted below plasmid map) immediately 3' of the $P_{TAL}$ minimal promoter. Figure from CLONTECH Laboratories, Inc. Protocol PT3271-5 'pTAL-SEAP Vector Information'.

***Construction of the pNF-κB-SEAP reporter vector.*** Oligonucleotides containing the four NF-κB response elements were designed such that restriction sites for *Nhe*I and *Bgl*II were incorporated at the 3' and 5' ends, respectively, relative to the direction of the response elements. The oligonucleotides (sense strand 5'-ATGCTAG CGGGAATTTCCGGGAATTTCCGGGAATTTCCGGGAATTTCCAGATCTAT-3', antisense strand 5'-ATAGATCTGGAAATTCCCGGAAATTCCCGGAAATTCCCG GAAATTCCCGCTAGCAT-3') were purchased from GeneWorks and dissolved in MQW upon receipt. The composition of annealing mixtures was 2 µM each oligo, 10 mM tris-Cl pH 8, 1 mM EDTA pH 8, and 100 mM NaCl. To facilitate efficient annealing, 1.5 mL microcentrifuge tubes containing the oligo mixture were placed in a

heat block at 95°C, and the heat block was then switched off and allowed to cool to ambient temperature. The vector (pTAL-SEAP) and insert (annealed oligos) were prepared by digesting with *Nhe*I (Fermentas) at 37°C for 1 hour in 1X Y-Tango™ buffer (Fermentas), followed by heat inactivation at 65°C for 20 mins, and digestion with *Bgl*II in 2X Y-Tango™ buffer (Fermentas) at 37°C for 2 h followed by heat inactivation for 1 h at 70°C. The digested fragments were isolated by excision of the appropriate bands following agarose gel electrophoresis, and purification using a QIAquick Gel Extraction kit (QIAGEN) according to the manufacturer's protocol. Insert and vector were ligated overnight in a 10 µL reaction volume at 4°C using T4 DNA ligase (Promega) according to the manufacturer's protocol. Ligation products were transformed into competent *E.coli* JM109 by heat shock (Sambrook and Russell, 2003). Positive clones were selected by plating onto LB agar containing 100 µg/mL ampicillin. After growing clones overnight in 5 mL LB broth, plasmids were isolated using a QIAGEN Plasmid Miniprep kit and the insert confirmed by sequencing using standard M13 primers and BigBye 3.1 (Applied Biosytems).

***Transient transfection of cell lines and reporter assays.*** Cells were grown to approximately 90 % confluence in the wells of standard 24-well plates before transient transfection of reporter vectors. For HeLa cells, this was achieved by seeding 6.5 x $10^4$ cells into each well and growing overnight in DMEM containing 10% FBS (composition was as described in Section 2.2.1). Transfection of 0.5 µg plasmid per well was carried out using 1 µl per well of Lipofectamine 2000 as recommended by the manufacturer (Invitrogen), using serum-free Opti-MEM (Gibco-Invitrogen). After overnight growth, cells were treated with toxins or vehicle controls as indicated in the results section.

Following toxin exposures, SEAP in the growth media was quantified using the chemiluminescent alkaline phosphatase substrate Lumiphos (Pierce). Aliquots (20 µl) of growth media were transferred to wells of a 96-well plate designed for luminescence (with white opaque wells). After incubating at 60°C for 20 mins to reduce endogenous phosphatase activity, plates were cooled to room temperature. Immediately prior to reading luminescence, 10 µl of Lumiphos reagent was added to each well and the plate

agitated briefly by hand to mix contents. Luminescence was measured using a Victor 2 plate reader (Wallac), with a capture time of 1 sec per well.

### *5.2.5 qRT-PCR data analysis*

In this chapter, pRT-PCR data analysis was performed RNA from three separate treatments, such that three data points were determined using the Relative Expression Software Tool (Pfaffl et al., 2002). These were then analysed using a one-sample t-test (GraphPad Prism), where the mean normalised relative transcript levels from three separate experiments are compared to a theoretical mean of 1 (i.e. no change in mRNA levels). As in previous chapters, target transcript ratios were normalised to glyceraldehyde-3-phosphate dehydrogenase (GAPDH) mRNA levels.

## 5.3 Results

### *5.3.1 CYN induces immediate-early gene expression*

Treatment of HepG2 cells and HDFs for 6 h with 1, 2.5 and 5 μg/mL CYN resulted in concentration-dependent increases in mRNA for *FOS*, *JUN* and to a lesser extent, *MYC* (Figure 5.2). Data shown are ratios of mRNA levels in treated cultures relative to control cultures, normalised to GAPDH mRNA ratios. Relative mRNA levels for *FOS* were particularly high after 6 h exposure to 5 μg/mL CYN, with over 100-fold expression in both cell types. Preliminary experiments showed that *JUN* and *FOS* mRNA levels in CYN-treated cells were not induced after 30 mins, 1 h or 2 h exposure to 1 μg/ml CYN (data not shown), which indicates that immediate-early gene induction by CYN is slower than that observed in the case of depurination of 28S rRNA by ricin (Iordanov et al., 1997). This may be suggestive of a delayed response as would be typical of a compound that crosses the cell membrane slowly, but the reason for the delay in the case of CYN may not be due to membrane transport.

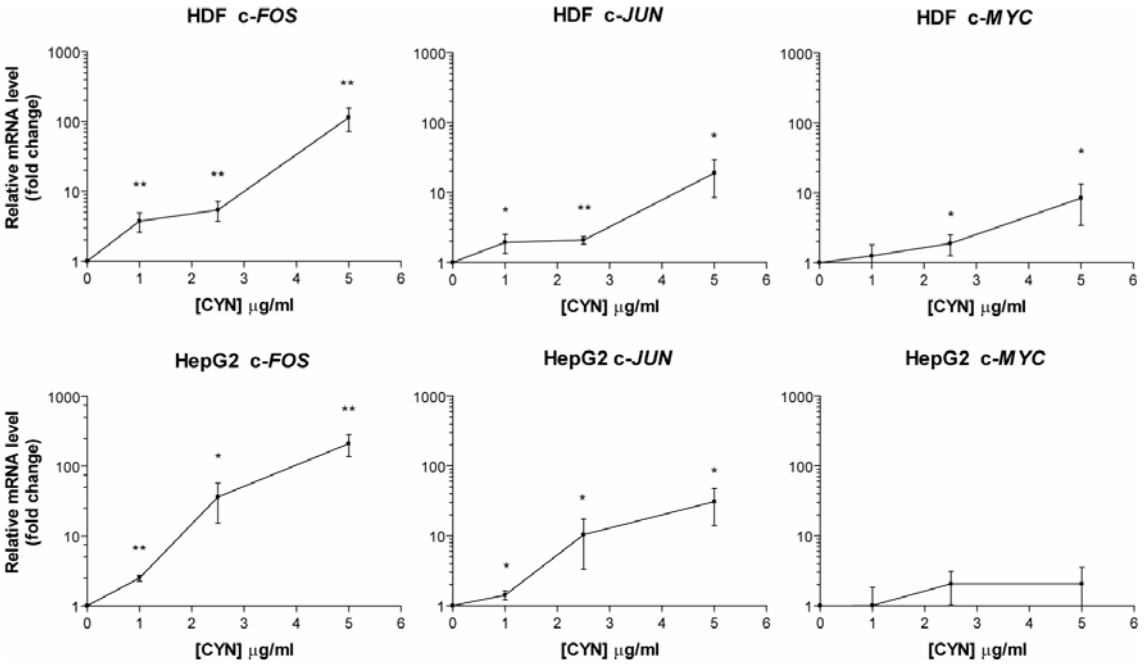


**Figure 5.2 Immediate-early gene expression in response to CYN in HDFs and HepG2 cells.** Messenger RNA levels for *FOS*, *JUN* and *MYC* after 6 h exposure to 1, 2.5 and 5 µg/mL CYN. Fold-change relative to controls were determined using real-time RT-PCR and normalised to GAPDH mRNA levels. Values represent means of three separate experiments, and error bars represent the 95% confidence interval. Significant difference from a theoretical mean of 1 was determined using a one-sample *t*-test (*$p < 0.05$, **$p < 0.01$).

After 24 h exposure to 1 µg/mL, relative transcript levels for *JUN* and *FOS* were not significantly different to controls in either cell line (Figure 5.3), but appeared to be elevated in HepG2 cells. The kinetics of immediate-early gene induction normally follow a pattern of strong initial expression and a rapid a return to relatively normal levels. Sustained and *FOS* expression in HepG2 cells, although not statistically significant, may indicate prolonged activation of JNK as has been observed in response to the microtubule poison taxol (Okano and Rustgi, 2001), and in DNA repair-deficient cells treated with cis-platin (Bulmer et al., 2005). In HDFs, the magnitude of induction was around 2-fold after both 6 h and 24 h treatment with 1 µg/mL CYN, suggesting that *JUN* expression is also sustained in this cell type. On the other hand, *FOS* expression in HDFs appeared to be induced by greater than 3-fold after 6 h under the same concentration, returning to slightly lower than controls after 24 h exposure to 1 µg/mL CYN, which more closely resembles immediate-early gene expression. Clearly, concentration plays a large role in

the magnitude of induction after 6 h treatment, suggesting that higher concentrations over 24 h may result in higher levels of immediate-early gene expression. Prolonged exposure to high CYN concentrations, however, would likely affect the expression of 'housekeeping' genes such as *GAPDH*, adversely affecting normalisation, hence this concentration was not utilised in the present study.

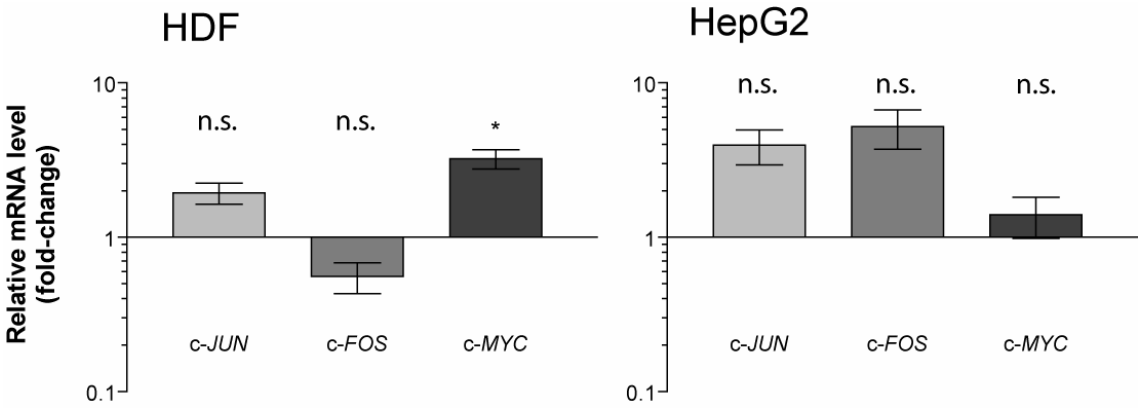


**Figure 5.3 Relative expression of *FOS*, *JUN* and *MYC* after 24 h exposure to 1 µg/mL CYN.** Fold-changes relative to controls were determined using real-time RT-PCR and normalised to GAPDH mRNA levels. Values represent means ±SEM of separate experiments. Significant difference from a theoretical mean of 1 was determined using a one-sample *t*-test (*$p < 0.05$, n.s. – not significant).

### *5.3.2 Comparison of* JUN *induction in response to CYN and other protein synthesis inhibitors*

As a preliminary investigation of the capacity of CYN to induce JNK activation, relative *JUN* mRNA levels were determined in HepG2 cells treated with the protein synthesis inhibitors CYN, anisomycin, emetine and cycloheximide. Although the ideal treatment conditions would result in equivalent inhibition of protein synthesis by the different compounds in HepG2, we did not have the facilities or expertise required to measure protein synthesis inhibition. As such, cells were treated with 10 µM of each inhibitor, despite probable differences in the degree of protein synthesis inhibition by each compound. Statistically significant increases in *JUN* mRNA levels occurred in response to emetine, CYN and anisomysin. Cycloheximide also induced *JUN* expression, and

although t-tests showed that the induction was not statistically significant, it is likely that an almost ten-fold induction would be biologically significant. In any case, the current experiment did not allow differentiation between responses to emetine and anisomycin in HepG2 cells, and thus cannot be reliably used as an indicator of activation of the ribotoxic stress response.

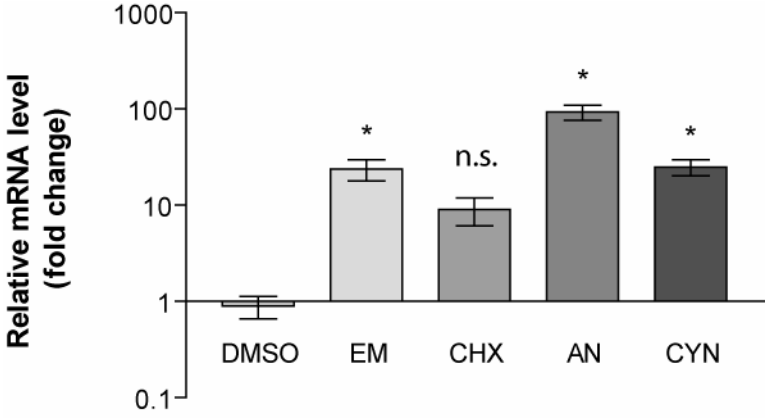


**Figure 5.4 Relative JUN mRNA levels in response to translational inhibitors.** HepG2 cells were exposed to 10 μM of each inhibitor for 6 h, and *JUN* mRNA levels were determined relative to control cultures. Values represent means ±SEM for three replicates. Significant difference from a theoretical mean of 1 was determined using a one-sample *t*-test (*$p < 0.05$, n.s. – not significant). Abbreviations: DMSO – dimethylsulphoxide; EM – emetine; CHX – cycloheximide; AN – anisomycin; CYN – cylindrospermopsin.

Induction of *JUN* expression, while a useful preliminary indicator of AP-1 activation, does not reliably indicate JNK activity because of the heterogeneity of AP-1 dimers. More direct methods such as immunocomplex kinase assays for c-Jun phosphorylation (Pulverer et al., 1991), and Western blotting using antibodies specific for phosphorylated forms of JNK, are likely to be more useful in this regard.

### *5.3.3 CYN treatment activates JNK but does not induce SEAP mRNA expression from pAP1-SEAP in HeLa cells*

To further assess the possible involvement of JNK activation in CYN toxicity, phosphorylated forms of the kinase were detected in treated cells using Western immunoblotting. Despite many attempts to detect activated JNK proteins in HepG2 and HDFs cell lysates, this approach was only marginally successful and could not be reliably

repeated despite the extensive use of positive controls. In HeLa cells, JNK appeared to be phosphorylated after treatment with 0.1 and 1 μM CYN for 4 h (Figure 5.5 A), but not in cells treated with 10 μM CYN (equivalent to 4.15 μg/mL). Treatment with 10 μM anisomycin induced JNK phosphorylation, but 32 μM PMA did not. In the case of PMA this may have been due to the excessively high concentration used, as 100 nM PMA has been shown to strongly induce JNK phosphorylation in HeLa cells (Werlen et al., 1998).

SEAP reporter assays were also conducted to determine whether the AP-1 sites in pAP1-SEAP were CYN-responsive. Initial experiments were performed in HepG2 cells, but low signal intensities suggested that low transfection efficiency may cause problems for this cell line in the context of the SEAP assay. As such, subsequent investigations were carried out in HeLa cells, which produced SEAP activity in the culture media resulting in adequate signal strength.

HeLa cells transiently transfected with pAP1-SEAP were exposed to varying concentrations of phorbol 12-myristate 13-acetate (PMA) or CYN for 6 h, and SEAP activity in the culture media was determined. Control groups transfected with pTAL-SEAP were treated identically in order to determine contributing effects of the pTAL minimal promoter. Neither PMA nor CYN treatment resulted in any change in SEAP activity from cells transfected with pAP1-SEAP or pTAL-SEAP (Figure 5.5 B). This could be due the length of exposure—6 h may not be suffient time to allow the accumulation of sufficient amounts of SEAP in culture media.

To determine whether transcription from SEAP vectors changed after CYN treatment, HeLa cells were transiently transfected with pAP1-SEAP and pTAL-SEAP, treated for 6 h with 0.2 and 2 μg/mL CYN, and total RNA was extracted. Relative SEAP expression was determined using SYBR green real-time qRT-PCR. No significant changes in SEAP mRNA levels from either plasmid were detectable (Figure 5.5 C). While this suggests a lack of AP-1 activity in HeLa cells treated with CYN, the apparent activation of JNK would suggest that at least some AP-1-family dimers should be activated. Alternatively, TREs present in the pAP1-SEAP promoter may not respond to specific the forms of AP-1 putatively activated in response to CYN. The specificity of AP-1 dimers can differ

depending on the composition of the dimer (Bakiri et al., 2002), and this may explain the apparent contradiction between JNK phosphorylation status and AP-1-mediated gene expression seen here. Another possibility is that the experimental conditions may not have allowed sufficient time for SEAP concentrations in the culture media to accumulate to levels above control. It may be useful to repeat these experiments using the more sensitive luciferase reporter system.

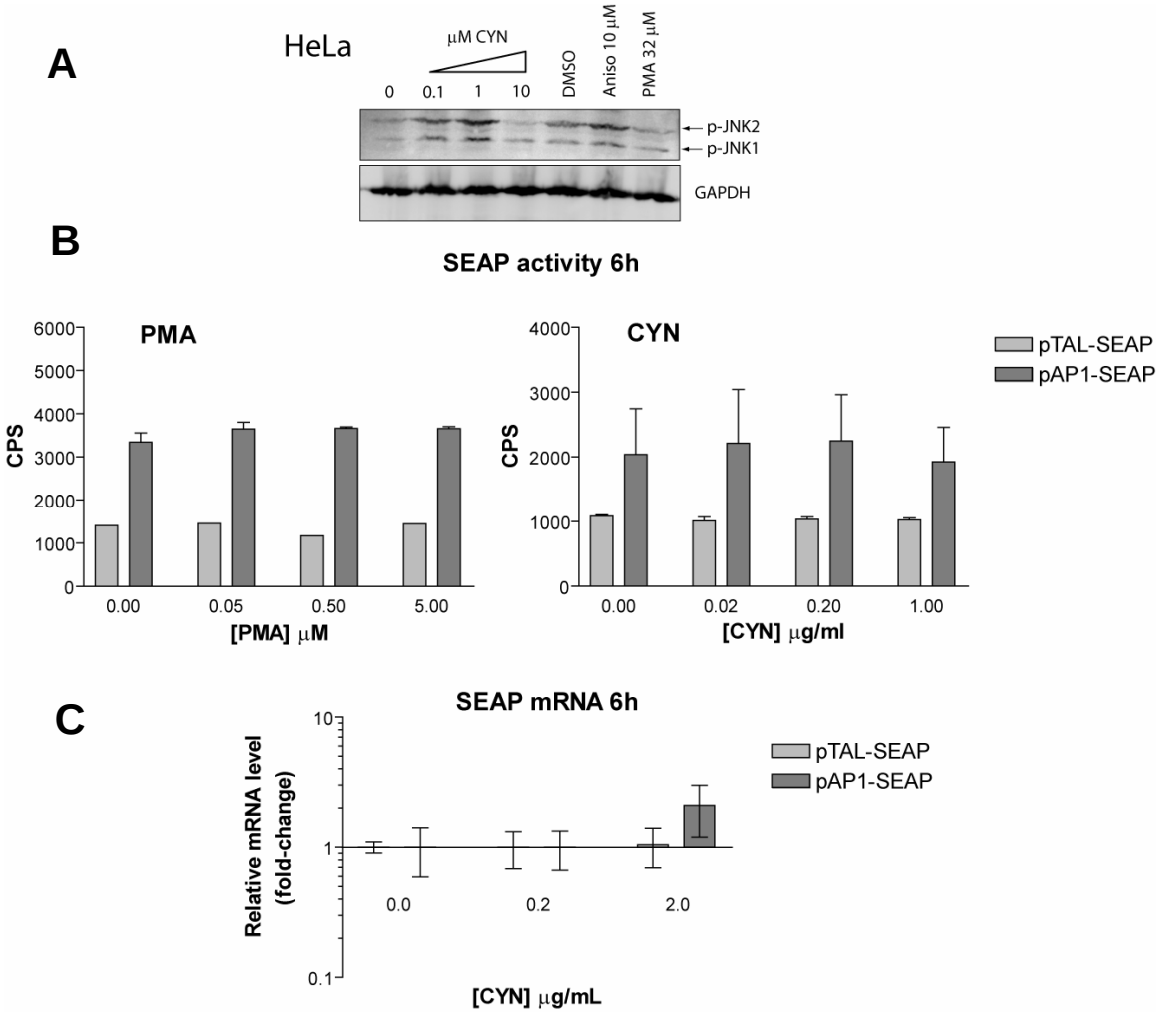


**Figure 5.5 Effects of CYN on JNK activation and AP-1-driven SEAP expression in HeLa cells.** (A) Detection of phosphorylated forms of JNK1/2 (p-JNK1 & p-JNK2) in HeLa cells treated with CYN as indicated for 4 h. Anisomycin treatment was used as a positive control, with DMSO as its vehicle control. PMA treatment was also intended as a positive control but did not induce JNK phosphorylation. (B) SEAP activity in culture media was determined as described in Section 5.2.4. Data shown are means ±SEM of three replicates from a typical experiment. CPS – counts per second (raw luminometer data). (C) Relative SEAP mRNA levels were determined using qRT-PCR and normalised to GAPDH mRNA.

### *5.3.4 CYN treatment induces transcription from pNF-κB-SEAP*

As reported in Chapter 3, CYN exposure resulted in elevated mRNA levels in HepG2 cells and HDFs for a large number of genes known to be under at least partial control of NF-κB (Section 3.3.3.2). To confirm the role of NF-κB in these responses, I examined the effects of CYN on the expression of a reporter gene under the control of four copies of a consensus NF-κB binding site.

As PMA is a known inducer of NF-κB DNA binding activity (Sen and Baltimore, 1986), this compound was used a as a positive control to detect increased expression and secretion of SEAP from HeLa cells transiently transfected with pNF-κB-SEAP (Figure 5.6 A). This induction was statistically significant after 24 h exposure to 0.5 μM PMA (Figure 5.6 A). In CYN-treated cells, SEAP enzyme activity in the culture media increased slightly at low CYN concentration but diminished to less than negative controls under 1 μg/mL CYN. This is likely to be due to translational inhibition associated with increasing CYN concentration. To check whether transcription from NF-κB sites increased in response to CYN, I isolated RNA from CYN-treated cells transfected with pNF-κB-SEAP, and performed quantitative RT-PCR analysis of SEAP mRNA levels relative to control cells. Relative SEAP mRNA levels were unchanged in response to 0.1 μg/mL CYN, but were induced 5-fold by 1 μg/mL CYN after 24 h exposure (Figure 5.6 B). Although not quite statistically significant, this suggests that transcription from NF-κB sites is indeed induced in HeLa cells in response to CYN. The reduction in SEAP activity in the culture media after 24 h exposure to 1 μg/mL CYN is therefore likely to result from translational inhibition.

It was intriguing to note that transcription from the control vector, containing $P_{TAL}$ only, decreased significantly in response to CYN after 24 h treatment (Figure 5.6 B) but not after 6 h (Figure 5.5 C). The down-regulation of the pTAL element may have contributed negatively to SEAP mRNA levels in the case of pNF-κB-SEAP, suggesting that transcription from this plasmid may have been considerably higher if a more minimal TATA box was employed in place of $P_{TAL}$. The presence of *cis*-acting elements in $P_{TAL}$

putatively contributing to this phenomenon was investigated, and is described in the following section.

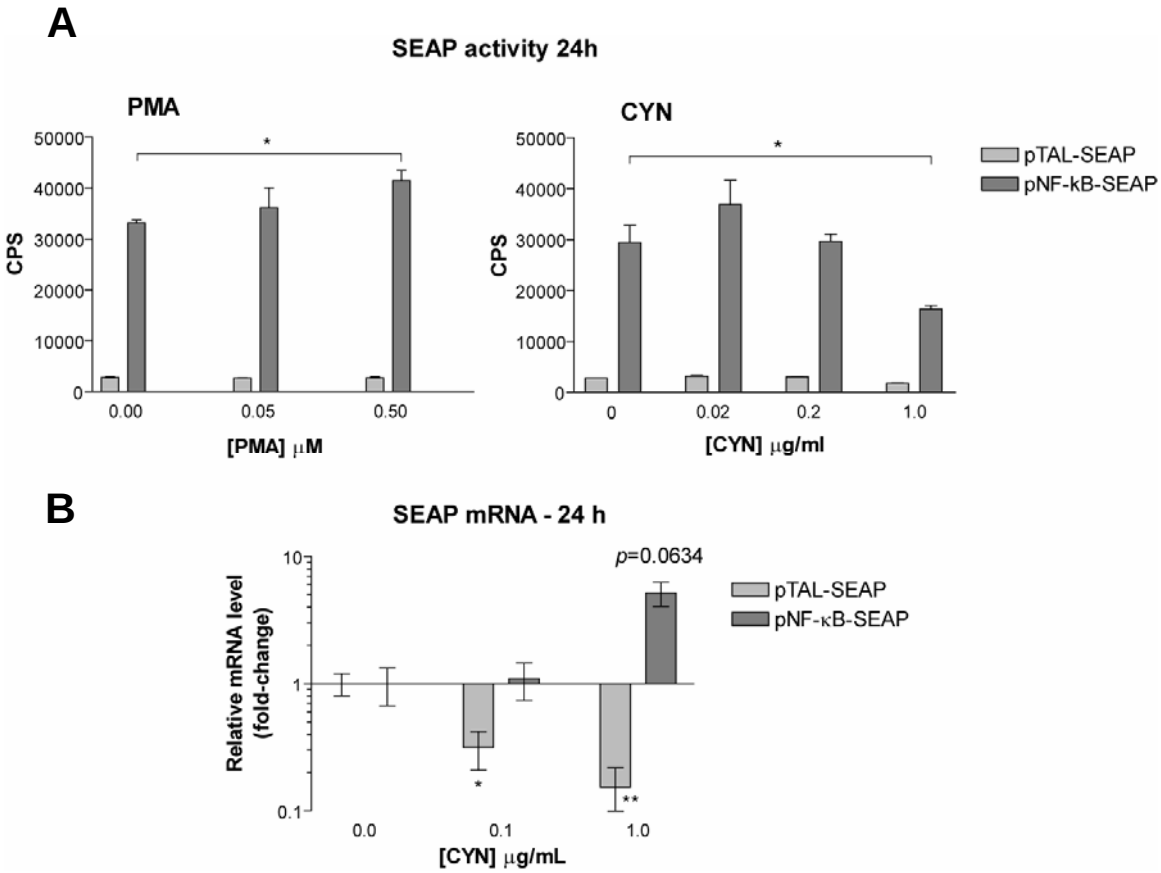


**Figure 5.6 CYN represses SEAP enzyme activity but induces transcription from pNF-κB-SEAP.** HeLa cells were transiently transfected with pNF-κB-SEAP and treated with PMA or CYN as indicated for 24 h. (A) SEAP activity in culture media was determined as described in Section 5.2.4. Data shown are means ±SEM of three replicates from a typical experiment (repeated at least three times) CPS – counts per second (raw luminometer data); *$p < 0.05$, significant difference between SEAP secretion from cells transfected with pNF-κB-SEAP and treated with vehicle control or highest concentration of toxin, using Student's t-test. (B) Relative SEAP mRNA levels were determined using qRT-PCR and normalised to GAPDH mRNA. *$p < 0.05$, **$p < 0.01$, significant difference from 1 (no change in relative mRNA levels) using the one-sample t-test.

### *5.3.5 Sequence analysis of the $P_{TAL}$ element*

Putative transcription factor binding sites in the $P_{TAL}$ minimal promoter were identified using the software tools Alibaba 2.1 (Niels Grabe, http://www.gene-regulation.com/pub/programs/alibaba2/intro.html) and TESS (Schug and Overton, 1997),

which both utilise the TRANSFAC database (Heinemeyer et al., 1998). In addition to the expected TATA-binding protein (TBP) site, correctly oriented elements include two Sp1 sites, a non-canonical AP-1 binding site, a C/EBPα site, and an octamer-binding factor (OBF) site proximal to the TATA element (Figure 5.7).

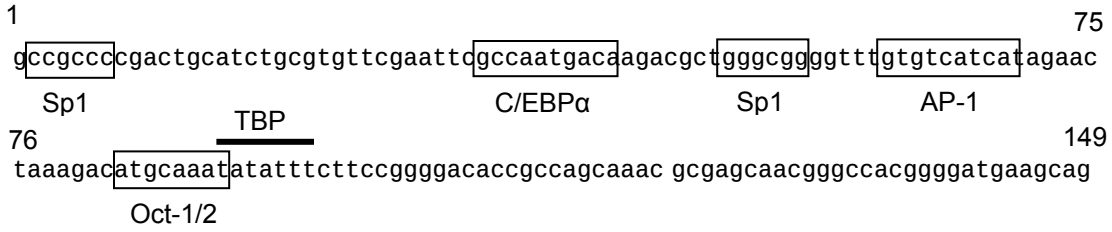


**Figure 5.7 Putative transcription factor binding sites in the $P_{TAL}$ promoter element.**

Octamer-binding protein 1 (Oct-1) and Sp1 are ubiquitously expressed and are responsible for mediating basal-level transcription by RNA polymerase II in the absence of stimuli (Novina and Roy, 1996). Accordingly, the two Sp1 sites and the Oct1/2 site are probably responsible for basal expression levels and are not likely to be involved in down-regulation of the promoter in respnse to CYN. On the other hand, *JUN* overexpression results in the inhibition of DNA binding by C/EBPα, through a protein-protein interaction between leucine zippers of c-Jun and C/EBPα (Rangatia et al., 2003). This may explain the reduced pTAL-SEAP mRNA levels cells treated with CYN for 24 h, but since the assays were performed in HeLa cells in which the expression of *JUN* in response to CYN has not been investigated, further work is required before this can be confirmed.

## 5.4 Discussion

Immediate-early gene expression is clearly induced by CYN in HDFs and HepG2 cells. While this was not surprising—a multitude of chemical and physical stressors are known to induce immediate-early gene expression—this information will contribute significantly to the overall picture of CYN toxicology.

The magnitude of *FOS* induction in response to CYN was considerably higher than that of *JUN* in both HDFs and HepG2 cells. Transcriptional activation of *FOS*, the

prototypical immediate-early gene (Herschman, 1991), occurs in response to numerous signals including growth factors, cytokines and stress. Several *cis*-acting elements in the proximal 5' flanking region (Figure 5.8) contribute to strong *FOS* transcription in response to stimuli. Activation of the *FOS* promoter by growth factors depends on the binding of serum response factor (SRF) to the serum response element (SRE) approximately 300 b.p. upstream of the transcriptional start site (Treisman, 1992). To effectively enhance transcription, SRF forms a ternary complex with accessory proteins of the Ets/ternary complex factor (TCF) family such as Elk-1, $p62^{TCF}$ and SAP-1, which bind a response element immediately 5' of the SRE (reviewed by Edwards, 1994). MAPKs phosphorylate Elk-1 in response to extracellular signals, positively regulating SRF-Elk-1-SRE ternary complex formation and enhancing transcription of *FOS*. Growth hormone (GH) positively regulates *FOS* transcription via another *cis*-acting element bound by CCAAT/enhancer binding proteins (C/EBPs), located immediately downstream of the SRE (Liao et al., 1999). AP-1 also contributes to *FOS* induction through a TRE located in the downstream region proximal to the SRE (Morgan and Birnie, 1992). Perhaps the most pertinent elements in the case of CYN are those involved in *FOS* induction in response to stress.

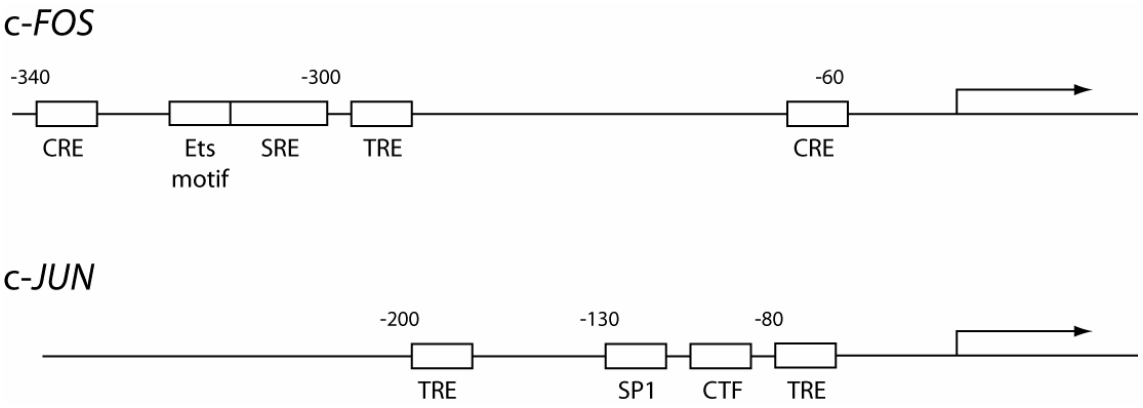


**Figure 5.8 Cis-acting elements contributing to transcriptional activation of *FOS* and *JUN*.** Numbers represent approximate distances in base-pairs from the transcriptional start site. Figure adapted from mulitple sources (Angel et al., 1988; Deschamps et al., 1985; Gilman et al., 1986; Ramirez et al., 1997; van Dam et al., 1993; van Delft et al., 1993).

Inducible transactivation of *FOS* in response to stress occurs mainly through a cAMP response element (CRE) about 60 b.p. upstream of the transcription start (Ahn et al.,

1998). Signalling through at least three separate pathways can activate cAMP response-element binding protein (CREB) and facilitate binding to CREs. Firstly, G-protein coupled (specifically GαS-coupled) cell surface receptors activate adenylate cyclase, raising cAMP levels and resulting in the activation of CREB by protein kinase A (Hagiwara et al., 1993). $Ca^{2+}$-dependent pathways are a second means of CREB activation (Sheng et al., 1991). Thirdly, signalling via the Ras/Raf pathway results in the activation of the MAPK-family kinases ERK1 and ERK2 (extracellular signal regulated kinase 1 and 2; (Barrie et al., 1997), which phosphorylate mitogen- and stress-activated kinase 1 (MSK1)(McCoy et al., 2005), which in turn phosphorylates and activates CREB (Deak et al., 1998). Due to the ambiguity of AP-1 involvement in CYN-induced gene expression shown in the current chapter, the stong induction of *FOS* expression in response to CYN may occur through other elements such as the CREs. MSK1, also activated by p38 MAPK (Deak et al., 1998), has been shown to be important for *FOS* transactivation in response to UV and anisomycin (Wiggin et al., 2002). It would be interesting to determine the activation status of p38 in HDFs and HepG2 cells treated with CYN to establish whether the high *FOS* transactivation observed in the present study occurs as a result of MAPK signalling.

As introduced above, we were particularly interested in *JUN* expression, which is largely under the control of 'activator protein 1' (AP-1), a basic-region leucine zipper (bZIP) transcription factor composed of c-Jun homodimers, heterodimers of c-Jun and c-Fos, or dimers made up of a number of related variants (JunB, JunD, FosB and ATF2 among others). Mitogen-activated protein kinase (MAPK) signalling culminates in the activation of AP-1 dimers, resulting in increased transcription from promoters containing TPA responsive elements (TRE). Two TREs in the *JUN* proximal 5' flanking region are essential for strong expression, with a downstream distal TRE also contributing weakly (Figure 5.8) (Angel et al., 1988; van Dam et al., 1993). Because of the significant induction of *JUN* mRNA in HepG2 and HDF cells following CYN exposure, I expected to observe similar increases in SEAP mRNA levels in HeLa cells transfected with pAP1-SEAP. Despite a small non-significant increase in response to 2 μg/mL CYN, this did not occur.

Activation of MAPKs, particularly JNK, after damage to the peptidyltransferase centre of 28S rRNA (Iordanov et al., 1997), formed the basis of experiments described in the current chapter. Certain inhibitors of translation are known to initiate an intracellular signalling cascade termed the ribotoxic stress response (RSR) (Iordanov et al., 1997). The RSR appears to be induced after damage (or binding) to particular regions of the 28S ribosomal RNA (rRNA; Iordanov et al., 1997). Examples of initiators of the RSR are the peptidyltransferase inhibitor anisomycin (Iordanov et al., 1997; Pestka, 1976), the trichothecene mycotoxins that also bind the peptidyltransferase site in 28S rRNA (Shifrin and Anderson, 1999), and the enzyme toxins ricin, α-sarcin and Shiga toxin that depurinate 28S rRNA at a specific region involved in the peptidyltransferase reaction (Munishkin and Wool, 1995; Smith et al., 2003). After binding or damage to the peptidyltransferase centre, JNK and p38 MAPK become phosphorylated and active (Iordanov et al., 1997). Protein synthesis inhibitors with alternative modes of action—e.g. the inhibitors of ribosomal translocation, cycloheximide and emetine (Pestka, 1976)—block ribosome translocation without inducing strong MAPK activation (Iordanov et al., 1997). In the RSR model proposed by (Zhou et al., 2003) (Figure 5.9), specific damage or binding within the peptidyltransferase site in ribosomal RNA results in the activation of double-stranded RNA (dsRNA)-activated protein kinase (PKR). PKR is a known activator of MKK3/6 and MKK4/7, which in turn can activate p38 and JNK, respectively (Williams, 2001). There are two major forms of JNK expressed in all cell types, JNK1 and JNK2, and a minor form, JNK3, expressed mainly in the brain, heart and testes (Barr and Bogoyevitch, 2001). In order to become active, JNKs are phosphorylated by MAPK kinases 4 or 7 (MKK4 or MKK7), which are activated primarily by environmental stress and cytokines, respectively (reviewed by(Davis, 2000). JNK then phosphorylates numerous substrates with roles in transcriptional activation—c-Jun, JunD, ATF2, Elk-1, c-Myc and p53 amongst others, with highest affinity for c-Jun (Bogoyevitch and Kobe, 2006). c-Jun phosphorylation by JNK on Ser 63 and Ser 73 increases its transactivation activity (Derijard et al., 1994; Karin, 1995), resulting in increased transcription from promoters containing TREs, including that of the *JUN* gene itself (Angel et al., 1988). The induction of *JUN* following CYN exposure in HepG2 cells is consistent with JNK activation, but the observation that emetine could also significantly induce *JUN* in this

cell line suggests that a ribotoxic stress response may not be involved. In HeLa cells, the contradictory findings of apparent JNK phosphorylation and a lack of transcriptional activation from pAP-1-SEAP indicate that further work is required before the involvement of JNK in stress responses to CYN can be confirmed. The possible involvement p38 MAPK should also be investigated, since in addition to the role of p38 in ribotoxic stress (see above), this kinase is also known to phosphorylate p53 (Sanchez-Prieto et al., 2000), which may explain the induction of p53-regulated genes shown in Chapter 4.

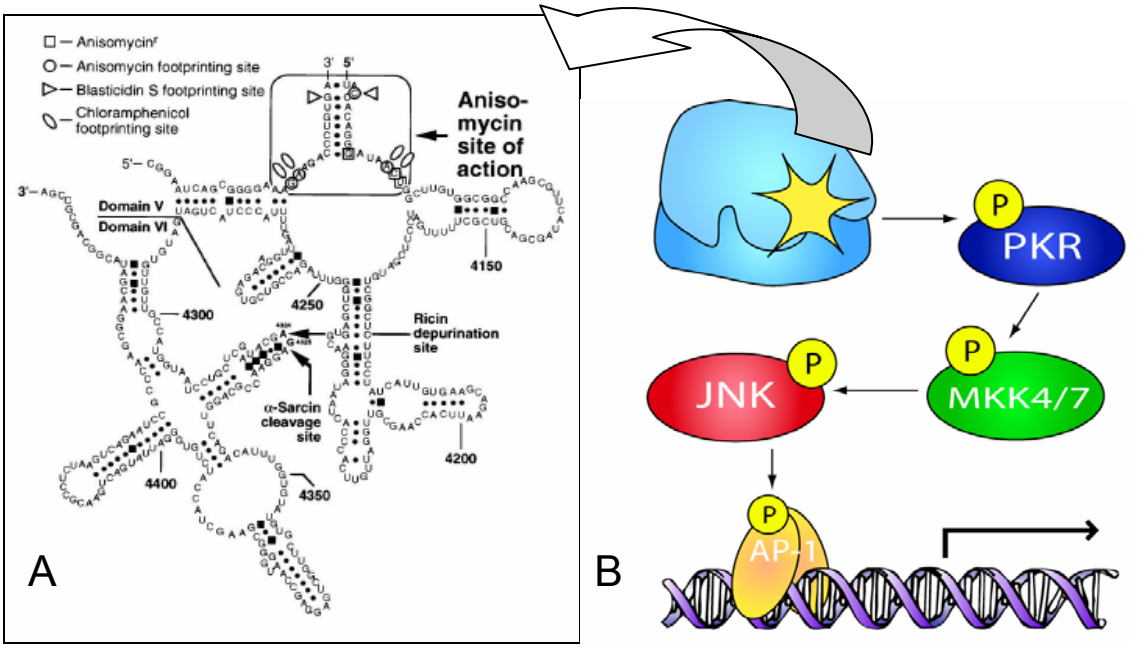


**Figure 5.9 Model of the ribotoxic stress response.** A cartoon representation of the model of the ribotoxic stress response proposed by Zhou et al (2003). **(A)** Site of action of 28S rRNA-damaging inhibitors of translation (figure from Iordanov et al., 1997), that induce the ribotoxic stress response depicted in **(B),** involving PKR-mediated activation of JNK, with downstream events including the phosphorylation of c-Jun, and increased expression of *JUN* and other targets of the AP-1 transcription factor (Cartoon adapted from Zhou et al., 2003).

The term 'nuclear factor κB' (NF-κB) refers to a group of dimeric transcription factors whose subunits contain Rel homology domains (RHDs; in reference to the *Drosophila* protein Relish). RHDs contain regions essential for DNA binding, dimerisation, and interaction with the NF-κB inhibitor IκB, as well as a nuclear localisation signal (NLS). Receptor-mediated regulation of NF-κB dimers occurs by one of two major pathways

(Figure 5.10), both of which occur rapidly following ligand binding. NF-κB can also be activated by additional means associated with oxidative stress (Li and Karin, 1999), DNA damage (Janssens and Tschopp, 2006), and other adverse factors (Mercurio and Manning, 1999). Apart from the steps leading to IKK complex activation, stress-induced NF-κB activation follows the classical pathway, with degradation of IκB leading to nuclear localisation of RelA/p50 dimers (Mercurio and Manning, 1999). Stress-inducing stimuli result in slow and weak activation of RelA/p50 NF-κB dimers compared to that resulting from receptor-mediated activation (Janssens and Tschopp, 2006). In the current study, the apparent increase in transcription from the pNF-κB-SEAP reporter vector after 24 h exposure to 1 μg/mL CYN suggests that NF-κB activation by CYN probably occurs through stress-induced rather than receptor-mediated pathways. However, it cannot be ruled out that cytokine production and signalling induces NF-κB activation in the case of CYN, since the extent of protein synthesis inhibition was not measured in these cells. It would be interesting to determine whether NF-κB activation in response to CYN occurs independently of cytokine signalling, or if there are two phases of activation—a cytokine-dependent phase under low CYN concentrations that do not totally inhibit protein synthesis, and a cytokine-independent phase occurring in response to stress induced by higher CYN concentrations.

Determining the nature of signals upstream of putative IKK complex activation in response to CYN may help to indicate mechanisms of DNA damage by CYN. A well-described outcome of double-stranded DNA breakage is the activation of ATM, which has recently been shown to phosphorylate a component of the IKK complex, NEMO (NF-κB essential modifier also known as IKKγ) (Wu et al., 2006). Modification of NEMO with SUMO (small ubiquitin-like modifier), mediated by a protein called PIDD (p53-inducible death domain protein), prevents nuclear export of NEMO, which normally travels freely between the nucleus and the cytoplasm (Bartek and Lukas, 2006). Phosphorylation of NEMO by ATM in response to double-stranded DNA breakage induces the exchange of SUMO for ubiquitin, allowing nuclear export of NEMO and the formation of active IKK complexes (Figure 5.10).

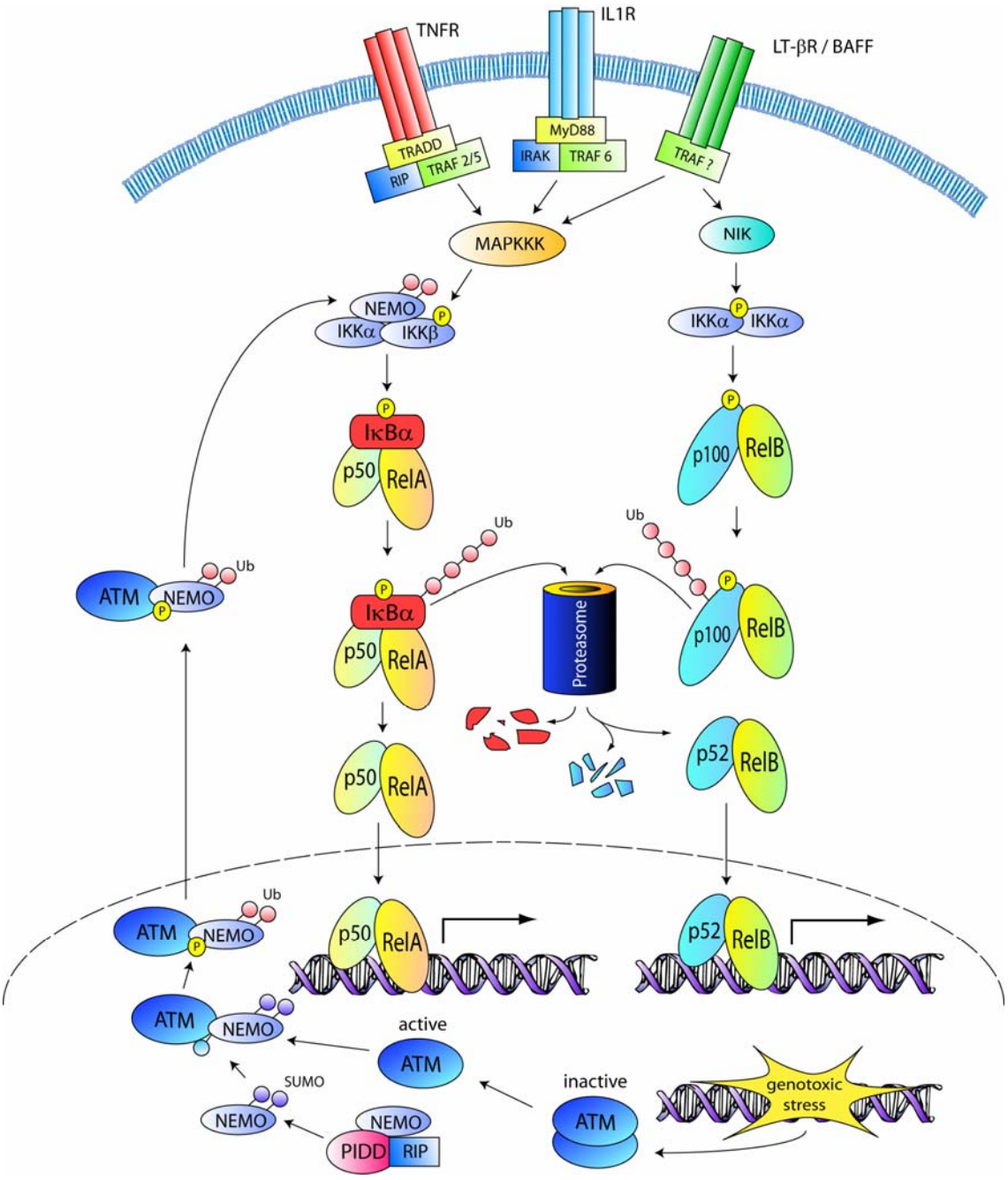


**Figure 5.10 NF-κB activation pathways.** NF-κB target genes are induced by one of two main pathways. The classical NF-κB activation pathway, associated with inflammation and stress responses, involves cytokine receptor signalling through MAPK kinase kinases (MAPKKKs) such as TAK1 or MEKK3. This results in the activation of the IκB kinase complex consisting of IKKα, IKKβ and IKKγ (also known as NEMO). Phosphorylation of IκB (inhibitor of κB) targets it for polyubiquitylation and proteosomal degradation, exposing nuclear localisation signals on p50/RelA. The alternative pathway, controlling gene expression associated with lymphoid organ development, depends on the partial proteasomal degradation of the p52 precursor, p100. This occurs through lymphotoxin β receptor (LT-βR) or B-cell activating factor (BAFF) receptor signalling, which activates NF-κB-inducing kinase (NIK). NIK activates IKKα dimers, resulting

in p100 phosphorylation and enhancing polyubiquitylation. Partial degradation to p52 exposes nuclear localisation signals on p52/RelB, allowing translocation to the nucleus. Genotoxic stress induces NF-κB activation via the classical pathway by enhancing cytoplasmic localisation of NEMO (IKKγ), which under normal conditions translocates freely between the cytoplasm and the nucleus. A number of genotoxic stressors induce NEMO modification by the addition of the small ubiquitin-like modifier, SUMO. SUMOylation by p53-inducible death domain protein (PIDD) prevents the export of NEMO from the nucleus. Double-stranded DNA breaks activate ATM, which phosphorylates NEMO, resulting in the exchange of SUMO with ubiquitin and subsequent nuclear export of NEMO, which can then form an active IKK complex. Figure adapted from a number of relevant reviews and articles (Chen, 2005; Janssens and Tschopp, 2006; Nakano et al., 2006; Wu et al., 2006).

Like MKK3/6 and MKK4/7, NF-κB can also be activated by PKR (Zamanian-Daryoush et al., 2000), suggesting that PKR may constitute a common link between MAPK and NF-κB activation by protein synthesis inhibitors such as CYN. PKR responds to numerous extracellular inputs such as cellular stresses, cytokines, bacterial lipopolysaccharides (LPS) and dsRNA (Williams, 1999). However, regarding protein synthesis inhibitors, there are conflicting reports of PKR-mediated MAPK activation. Zhou and colleagues (2003) observed rapid activation of PKR within 1-5 mins in response to anisomycin and deoxynivalenol, and showed that subsequent JNK activation could be inhibited by reducing PKR expression using antisense RNA constructs. Furthermore, the authors showed a reduction in p38 and ERK phosphorylation after antisense RNA-mediated PKR knockdown, although the magnitude of reduction was less than that observed for JNK. PKR is known to be associated with ribosomes (Samuel, 1993), and contains dsRNA binding domains required for ribosomal association (Wu et al., 1998; Zhu et al., 1997b). These characteristics are consistent with a putative role for PKR in RSR sensing and signalling, however the model proposed by Zhou et al. (2003) is not supported by the finding that phosphorylation of JNK and p38 in anisomycin-treated PKR-null mouse fibroblasts was shown to be identical to treated cells expressing PKR (Goh et al., 2000). In fact, Goh and colleagues (2000) showed that other cellular stresses also induced the activation of both JNK and p38 regardless of the PKR status of the cells—these included UV, osmotic shock, arsenite exposure and heat shock. Conversely, activation of both kinases was reduced in PKR-null cells exposed to external stimuli consisting of TNFα, synthetic dsRNA, and bacterial LPS. These observations raise the question of PKR is indeed critical for RSR signalling, as claimed by Zhou and colleagues (2003). Interestingly, Zhou and colleagues later published an alternative model for the

RSR in a mouse macrophage-like cell line, involving signal transduction by the hematopoietic cell kinase, Hck, or other Src kinases (Zhou et al., 2005b). The authors stressed the need for further investigation of the RSR with respect to damage sensing and signalling to MAPKs, and it seems that cell type may be important in determining the nature of stress signalling in response to ribosomal inactivation.

Shifrin and Anderson (1999) speculated that a conformational change in the ribosome may initiate signalling associated with the early stages of ribotoxic stress. They also observed that pre-treatment with emetine did not completely inhibit subsequent JNK/p38 activation in response to anisomycin, provided the treatment concentrations were relatively high. This contradicts previous findings by Iordanov et al. (1997), who observed that emetine pre-treatment could abrogate the ribotoxic stress response—this group concluded that only actively translating ribosomes could induce the RSR, a hypothesis which is not supported by Shifrin and Anderson's results.

Trichothecene mycotoxins inhibit translation and induce signalling consistent with the ribotoxic stress response (Shifrin and Anderson, 1999). DNA binding by AP-1, NF-κB and C/EBPβ has been shown to increase after treatment with the trichothecene deoxynivalenol (Wong et al., 2002). The induction of gene expression involving AP-1 and NF-κB shown in the present study, and the probable involvement of C/EBPs in *FOS* promoter induction, indicate that there may be similarities between the mode of action of CYN and that of certain trichothecenes. In support of this possibility, deoxynivalenol induces interleukin 6 expression (Moon and Pestka, 2003) and down-regulation of *GRP78* (Yang et al., 2000), as does CYN (see Sections 3.3.3.2 and 3.3.3.3). Comparative toxicological studies of trichothecenes and CYN may help to define the mode of translational inhibition by CYN.

*MYC* expression was observed to be induced significantly in HDF cells after CYN treatment. Myc is a basic helix-loop-helix-leucine zipper (bHLHZ) transcription factor that dimerises with Max to alter the transcription of target genes involved in virtually all cellular processes . With a short mRNA half life, modulation of mRNA stability plays a significant role the regulation of Myc protein synthesis (Dani et al., 1984; Dani et al.,

1985; Rabbitts et al., 1985). *MYC* mRNA levels are as low as a single copy per cell in resting cells, with mitogenic stimulation inducing higher levels. Transformed cells often display deregulated expression of *MYC* at the transcriptional level (Pelengaris and Khan, 2003). *MYC* expression is regulated by a large number of transcription factors, which are controlled by a myriad of signalling pathways including MAPK, JAK/STAT, Ras, IFN-γ, PI3-kinase, Fas, Wnt, TGF-β, interleukins, cytokines, lymphokines, steroid and peptide hormones, pharmacologic agents, NF-κB-activating pathways and E2F-activating pathways (Liu and Levens, 2006). Such an extensive list of pathways makes speculation about possible contributors to CYN-induced *MYC* expression difficult, but the apparent involvement of Myc in cell growth regulation suggests that the protein may be important in cellular responses to CYN-induced stress.

That MAPK and NF-κB pathways can influence *MYC* expression indicates a role for Myc in transcriptional responses to exogenous stressors. Recent work indicates that Myc is involved in the expression of genes required for the synthesis of reduced glutathione (GSH), suggesting a role for Myc in cellular responses to oxidative stress. Benassi and colleages (Benassi et al., 2006) found that Myc appears to mediate the transcriptional induction of genes encoding both subunits of an important enzyme involved in GSH synthesis, γ-glutamyl-cysteine synthetase (γ-GCS). Reduced rates of GSH synthesis following CYN exposure reported by Runnegar and colleages (1994, 1995) may be a result of reduced γ-GCS levels—most likely as a result of protein synthesis inhibition by CYN. The induction of *MYC* observed in the present study may underlie a pro-survival response involving the increased production of antioxidants such as GSH. Translational inhibition by CYN may negatively regulate consecutive steps in γ-GCS expression—in addition to reducing translation of γ-GCS mRNA, CYN may cause Myc protein levels to remain low so that Myc target genes, such as those encoding subunity of γ-GCS, are not induced.

At odds with a role for Myc in pro-survival gene expression are reports that stability of the protein is reduced following exposure to a variety of stressors. Hyperosmolarity and DNA damaging agents activate a kinase known as Pak2 that phosphorylates Myc, promoting its degradation (Huang, 2004). JNK1 phosphorylates a different region of the

Myc protein, reducing stability by promoting ubiquitylation and degradation (Alarcon-Vargas and Ronai, 2004), suggesting that stress-induced JNK1 activation can also reduce Myc protein levels. As such, while *MYC* mRNA levels appear to increase following CYN treatment, protein levels are likely to diminish through reduced stability via JNK1, as well as through reduced translation attributable to CYN. Even if CYN treatment does result in elevated Myc protein levels, a pro-survival outcome is not assured. While capable of promoting cellular proliferation, increased Myc protein levels can also sensitise cells to apoptosis (reviewed by (Meyer et al., 2006). Specifically, when high Myc activity is combined with an anti-proliferative signal, increased rates of apoptosis are observed. This occurs largely through the stabilisation of p53 via Myc-mediated ARF expression (Zindy et al., 1998), which reduces Mdm2-p53 interaction, allowing p53 accumulation and the subsequent induction of pro-apoptotic gene expression.

The upstream signalling pathways contributing to immediate-early gene induction by CYN are likely to be numerous and highly complex. The investigations described in the current chapter are only preliminary, but appear to confirm the involvement of NF-κB in CYN-induced gene expression. Regarding the mechanism of translational inhibition, further work is required before the involvement of ribotoxic stress can be confirmed, but the apparent activation of JNK and the strong induction of *FOS* and *JUN* expression comprise important initial data in support of this possibility.

# Chapter 6

## *Conclusions and Future Directions*

Despite extensive research, the molecular mechanisms underlying cylindrospermopsin toxicity are yet to be determined. It is not known whether CYN has a single molecular target or if there may be a more general mode of action. The aim of the current work was to investigate changes in gene expression induced by CYN in an attempt to reveal more about the nature of stress signalling and repair pathways initiated in treated human-derived cells, with the view to identifying putative modes of action of the compound.

This is the first large-scale study of altered gene expression in response to CYN, excluding an investigation of gene expression in the livers of CYN-exposed mice using low-density membrane cDNA arrays (S.Shen, unpublished observations). While S.Shen's study examined the expression of selected genes known to be involved in responses to toxins *in vivo*, the current study utilised high-density arrays in an effort to discover pathways involved in CYN toxicity in human cells *in vitro*. The use of homogenous cell populations is recommended for high-throughput analyses of gene expression so that the complexity of the experimental system is sufficiently low to enable the detection of statistically significant changes in mRNA level (Firestein and Pisetsky, 2002). In this thesis, treatment of cultured cells ensured that CYN-induced changes in gene expression occurred against a uniform background—a single cell type was exposed to the toxin, rather than a population of different cell types as would occur in living tissue. The efficacy of the current approach was substantiated by the detection of differentially

regulated genes with functions related to putative modes of action of the compound, particularly with respect to protein synthesis inhibition and DNA damage—protein folding pathways appeared to be down-regulated, while genes for DNA repair and apoptosis were up-regulated. Accordingly, the collective function of other groups of differentially regulated genes may be indicative of additional modes of action or the underlying mechanisms thereof.

While a definitive mechanism was not indicated by the results of the current study, the data provide numerous starting points for further work. Genes for RNA synthesis and processing were shown to be induced by CYN in both HDFs and HepG2 cells. While this requires confirmation using alternative techinques, the upregulation of numerous genes involved in RNA biogenesis suggests that CYN may deplete or damage various forms of RNA. It is tempting to speculate that damage to mRNA may underlie translational inhibition by CYN. Research into RNA damage is an emerging field which is seeing increasing interest (Begley and Samson, 2003). That damaged RNA can easily be replaced through transcription does not mean that the potential adverse effects of accumulated damaged RNA would be trivial. Given the many and varied roles of RNA, including not only protein synthesis (mRNA, tRNA and rRNA) but also non-coding functions that derive from a large proportion of the human genome previously considered to be 'junk DNA' (Mattick and Makunin, 2006), the probablility that RNA damage produces observable detrimental effects is high.

The increased expression of numerous genes known to be regulated by p53 is an important finding, given that this transcription factor is essential for the maintenance of genome integrity. The putative activation of p53 in response to CYN supports published reports of CYN-induced DNA damage, although both p53 activation and the mode of DNA damage by CYN need to be confirmed in a range of human cell lines and primary cells. The comet assay is perhaps most commonly used assay for genotoxicity, but unfortunately this assay cannot distinguish between direct DNA damage, single stranded breaks arising from nucleotide excision repair, and DNA fragmentation due to apoptosis or necrotic cell death. The induction of nucleotide excision repair genes (Section 3.3.3.1) supports the hypothesis that CYN induces bulky adducts. A priority for future work

should to characterise the adduct repoted to occur in DNA isolated the livers of CYN-exposed mice Shaw et al. (2000), and to establish whether this adduct appears in treated human cells.

Studies outlined in Chapters 4 and 5 confirmed the involvement of p53 and NF-κB in stress responses elicited by the CYN, but showed that the participation of the MAPK pathway was clear. Microarray analysis showed that genes in the pathway were transcriptionally up-reguated in response to CYN (Section 3.3.1.4). While JNK phosphorylation could be seen in HeLa cells, the reporter system utilised to check for AP-1 regulated expression was probably not suitable for the intended exposure time frame of 6 h. While the 'ribotoxic stress response' has not been fully defined, further work on MAPK signalling using a comparative approach—numerous inhibitors of translation with known mechanisms are commercially available—may help to identify the mode of ribosomal inactivation by CYN.

The results of NF-κB reporter assays appear to confirm the involvement of this transcription factor in CYN-induced stress responses, which was initially indicated by the induction of a large number of NF-κB-regulated genes (Section 3.3.3.2). According to current knowledge, NF-κB and JNK are linked through reactive oxygen species (ROS) NF-κB inhibits JNK by preventing the accumulation of ROS, which would normally result in JNK activation (Nakano et al., 2006). This mechanism contributes to the fate of the cell—NF-κB induces pro-survival gene expression, while JNK activation can result in apoptosis. That both NF-κB and JNK were identified in the current study to be involved with CYN-induced cellular stress suggests a role for free radicals at some point in the process of CYN toxicity. Humpage and colleagues (2005) showed that a common indicator of oxidative stress, lipid peroxidation, did not increase in CYN-treated primary mouse hepatocytes, but it may be of interest to look for this and other markers in other cell types. The differential regulation of thioredoxin reductase expression in HepG2 cells and HDFs (Section 3.3.5) suggests that the putative role of oxidative stress in CYN toxicity may be cell-type specific.

The large-scale gene expression analysis presented here appears to correlate well with observable phenotypes in CYN-treated cells. The results of toxicity studies in human cells, and preliminary investigations of stress response pathways, have further defined putative modes of action of the compound. Taken together, the data will contribute strongly to the co-operative effort currently underway to better characterise this important natural toxin.

# Appendix 1

## *List of oligonucleotide primers used for real-time qRT-PCR*

**Table A1.1** Primer pairs used for qRT-PCR.

| Gene symbol | Product | GenBank accession (mRNA) | Primer pair (5' - 3') |
|---|---|---|---|
| *ACTB* | Actin, beta | NM_001101 | GTGGATCAGCAAGCAGGAGTAT |
| | | | GCCATGCCAATCTCATCTT |
| *ALKBH* | AlkB, alkylation repair homolog (*E. coli*) | NM_006020 | TTGTGTATTGCCGTGGACTT |
| | | | AGAGGCTGAGAAGGCTGTTG |
| *AQP3* | Aquaporin 3 | NM_004925 | GCATGTGTGTGCATGTGTGT |
| | | | TCCCTTGCCCTGAATATCTG |
| *BAX* | Bcl-2-associated X protein; apoptosis regulator | NM_138761 | GGGGACGAACTGGACAGTAA |
| | | | CAGTTGAAGTTGCCGTCAGA |
| *BCL2* | B-cell CLL/lymphoma 2 | NM_000657 | ATGTGTGTGGAGAGCGTCAA |
| | | | ACCTACCCAGCCTCCGTTAT |
| *CDKN1A* | p21; cyclin-dependent kinase inhibitor 1A | NM_000389 | GAAGACCATGTGGACCTGTC |
| | | | CGGATTAGGGCTTCCTCTTG |
| *CDKN2A; ARF* | $p14^{ARF}$; Cyclin-dependent kinase inhibitor 2A; Encoded by transcript variant 4 | NM_058195 | AGTTAAGGGGGCAGGAGTG |
| | | | GGATGTGAACCACGAAAACC |
| *CEBPD* | CCAAT/enhancer binding protein delta | NM_005195 | ATCGACTTCAGCGCCTACAT |
| | | | CGCCTTGTGATTGCTGTTG |
| *COX2* | Prostaglandin-endoperoxide synthase 2 | NM_000963 | TGGGAAGAGGGAGAAAATGA |
| | | | GGCACTGAAACATTCGCATA |
| *CYP1A2* | Cytochrome P450, family 1, subfamily A, polypeptide 2 | NM_000761 | ACCTTCCGACACTCCTCCTT |
| | | | ACCTGCCACTGGTTTACGAA |
| *DDB2* | Damage-specific DNA binding protein 2 (48kD) | NM_000107 | GGGAACAACTAGGCTGCAAG |
| | | | GTGACCACCATTCGGCTACT |
| *E2F1* | Transcription factor E2F-1 | AF516106 | TACCCCAACTCCCTCTACCC |
| | | | GTCTCCCTCCCTCACTTTCC |
| *ELK1* | Member of ETS oncogene family; member of the ETS family of transcription factors | NM_005229 | ATTCCACCTTCACCATCCAG |
| | | | CCTCTTCAGCCTCCAGACAG |

| | | | |
|---|---|---|---|
| *ENC1* | Ectodermal-neural cortex (with BTB-like domain); tumor protein p53 inducible protein 10 | NM_003633 | GTGTGGAACAGCATCACCAC<br>TGGCCTCTCCGAAGTAGAAA |
| *FOS* | c-Fos; homolog of v-fos (FBJ murine osteosarcoma viral oncogene) | NM_005252 | GACTTCCTGTTCCCAGCATCAT<br>TGGCCACAGAGCTGGAGC |
| *GADD45α* | Growth arrest and DNA-damage-inducible, alpha | NM_001924 | GGCCCGGAGATAGATGACTT<br>TTTTCCTTCCTGCATGGTTC |
| *GAPDH* | Glyceraldehyde-3-phosphate dehydrogenase | NM_002046 | CTCCTCTGACTTCAACAGCGA<br>GTCTTACTCCTTGGAGGCC |
| *IL1* | Interleukin 1 alpha | M28983 | CCATAGCCAGGAAACTCTGC<br>TTGCAGGTGGAATTGAATGA |
| *IL18* | Interleukin 18 proprotein | NM_001562 | GGAATTGTCTCCCAGTGCAT<br>GAAGCGATCTGGAAGGTCTG |
| *IL2* | Interleukin 2 | NM_000586 | AACATTTTGACACCCCCATAA<br>ATTGTGGCAGGAGTTGAGGT |
| *JUN* | c-Jun oncogene; cellular homologue of the putative transforming gene of avian sarcoma virus 17 | NM_002228 | AGAGGAAGCGCATGAGGAA<br>GTTTAAGCTGTGCCACCTGTT |
| *KDELR3* | KDEL receptor 3 isoform a | NM_016657 | TGCTGGAGATCCTCTGGACT<br>CCGGTACAGACCCAGAAAGA |
| *MDM2* | Mouse double minute 2 homolog isoform MDM2 | NM_002392 | GTATCAGGCAGGGGAGAGTG<br>GAAGCCAATTCTCACGAAGG |
| *MT1R* | Metallothionein 1R | X97261 | GCAAGTGCAAAGAGTGCAAA<br>ACATCTGGGAGCAGGTCTGT |
| *MT2A* | Metallothionein 2A | NM_005953 | GCAAATGCAAAGAGTGCAAA<br>ATCCAGGTTTGTGGAAGTCG |
| *MYC* | c-Myc; v-myc myelocytomatosis viral oncogene homolog | NM_002467 | CTCCTGGCAAAAGGTCAG<br>TCGGTTGTTGCTGATCTGTC |
| *NOS2A* | iNOS; Inducible nitric oxide synthase 2a, hepatocytes | NM_000625 | CTCTATGTTTGCGGGGATGT<br>TTCTTCGCCTCGTAAGGAAA |
| *PUMA* | Bcl-2 binding component 3; | NM_014417 | CCACCACCATCTCAGGAAAG<br>ACGTTTGGCTCATTTGCTCT |
| *RELA* | NF-kappa-B transcription factor subunit p65/RelA | NM_021975 | CATCCCATCTTTGACAATCG<br>TGGTCCCGTGAAATACACCT |
| *TNFRSF12A* | Tweak-receptor; TWEAKR; Tumour necrosis factor receptor superfamily member 12A; Fn14 | NM_016639 | TTTCTGGCTTTTTGGTCTGG<br>GGCACATTGTCACTGGATCA |
| *TP53* | Tumour suppressor protein 53 kDa; p53 | NM_000546 | ACCATGGCCAGCCAACTTT |

| | | | |
|---|---|---|---|
| | | | TTCTGCAAGCACATCTGCAT |
| *TXNRD1* | Thioredoxin reductase 1 | NM_003330 | CTTGTGGCCTTTCTGAGGAG |
| | | | CTCTTGACGGAATCGTCCAT |
| *XPC* | Xeroderma pigmentosum, complementation group C | NM_004628 | CTGCCATCCTTGGGTATTGT |
| | | | GCCTCACCACTCTTGCTTTC |

# Appendix 2

### *Representative determination of relative mRNA levels by qRT-PCR*

The following example shows a representative example of relative mRNA determination by SYBR Green I quantitative reverse-transcription PCR, performed as described in Section 3.2.8. This example is useful because the normalising gene, *GAPDH*, appears to be slightly induced by the treatment. This may be due to inaccuracies of quantitation of total RNA inputs and highlights the importance of using internal controls for qRT-PCR. Melt peaks derived from dissociation curves show a single clean peak for each amplicon which can be clearly differentiated from the lower peak resulting from non-specific amplification in the no-template controls, presumably due to primer-dimer artefacts.

**Cell type:** HepG2
**Toxin treatment:** 1 µg/mL cylindrospermopsin, 24 h
**Control treatment:** 1% MQW in growth medium, 24 h

*GAPDH* amplification curves, exported directly from Bio-Rad iCycler software:

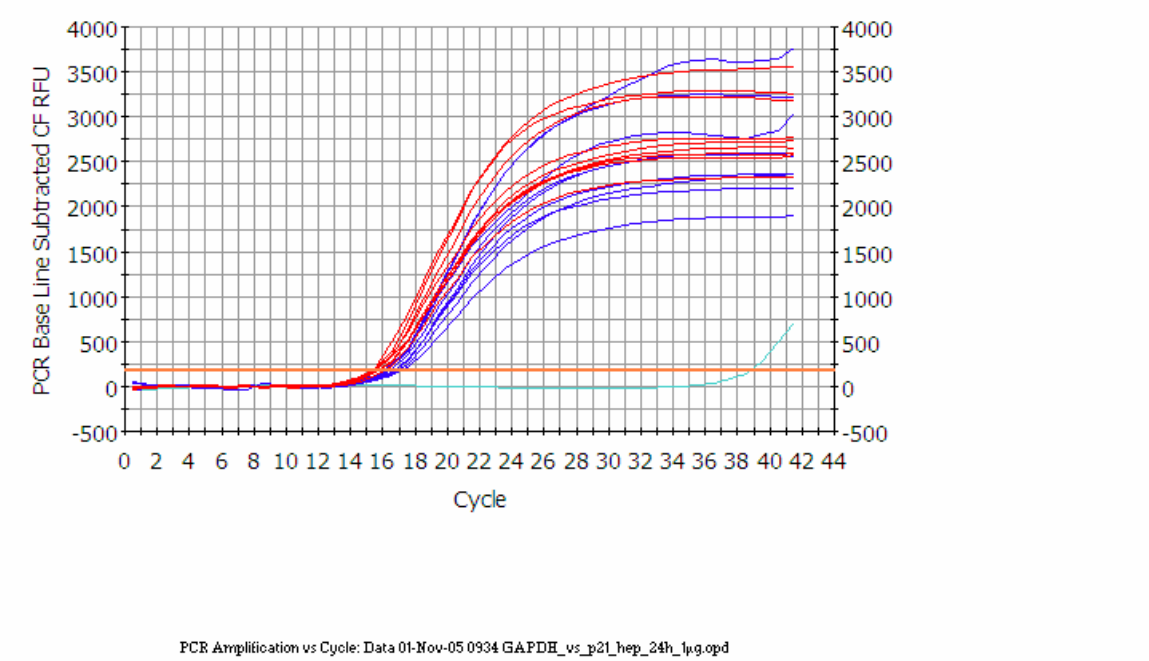

*CDKN1A* amplification curves:

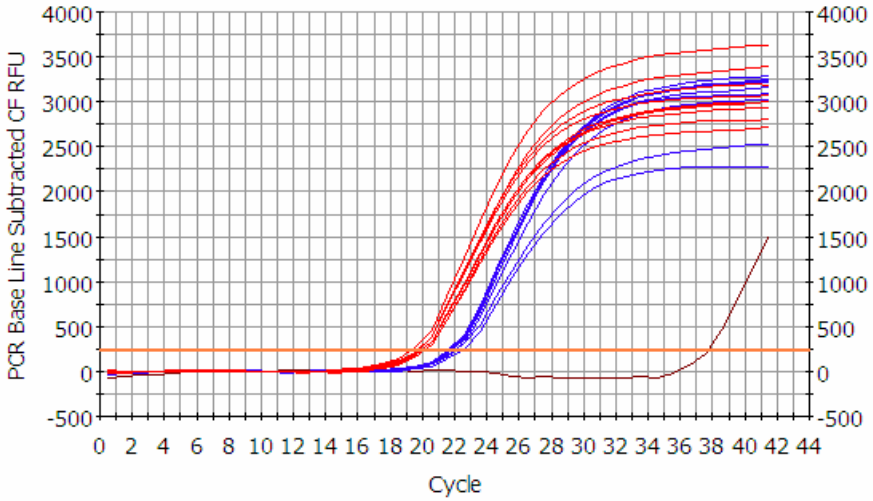


PCR Amplification vs Cycle: Data 01-Nov-05 0934 GAPDH_vs_p21_hep_24h_1µg.opd

*GAPDH* raw data:

| **Sample** | **$C_T$*** |
|---|---|
| 24h control 1a | 16.0 |
| 24h control 1b | 16.3 |
| 24h control 1c | 16.6 |
| 24h control 2a | 16.1 |
| 24h control 2b | 16.7 |
| 24h control 2c | 16.7 |
| 24h control 3a | 16.4 |
| 24h control 3b | 17.1 |
| 24h control 3c | 16.9 |
| 24h 1ug/ml 1a | 15.2 |
| 24h 1ug/ml 1b | 15.4 |
| 24h 1ug/ml 1c | 15.8 |
| 24h 1ug/ml 2a | 15.7 |
| 24h 1ug/ml 2b | 15.4 |
| 24h 1ug/ml 2c | 15.7 |
| 24h 1ug/ml 3a | 15.3 |
| 24h 1ug/ml 3b | 15.5 |
| 24h 1ug/ml 3c | 16.0 |
| no template | 38.8 |

*CDKN1A* raw data:

| **Sample** | **$C_T$*** |
|---|---|
| 24h control 1a | 22.4 |
| 24h control 1b | 21.8 |
| 24h control 1c | 21.9 |
| 24h control 2a | 21.7 |
| 24h control 2b | 21.8 |
| 24h control 2c | 21.6 |
| 24h control 3a | 21.7 |
| 24h control 3b | 21.6 |
| 24h control 3c | 22 |
| 24h 1ug/ml 1a | 19.7 |
| 24h 1ug/ml 1b | 19.7 |
| 24h 1ug/ml 1c | 19.3 |
| 24h 1ug/ml 2a | 20.1 |
| 24h 1ug/ml 2b | 19.9 |
| 24h 1ug/ml 2c | 19.9 |
| 24h 1ug/ml 3a | 20.1 |
| 24h 1ug/ml 3b | 19.8 |
| 24h 1ug/ml 3c | 19.9 |
| no template | 37.7 |

*$C_T$ – threshold cycle

*GAPDH* melt peaks derived from dissociation curves:

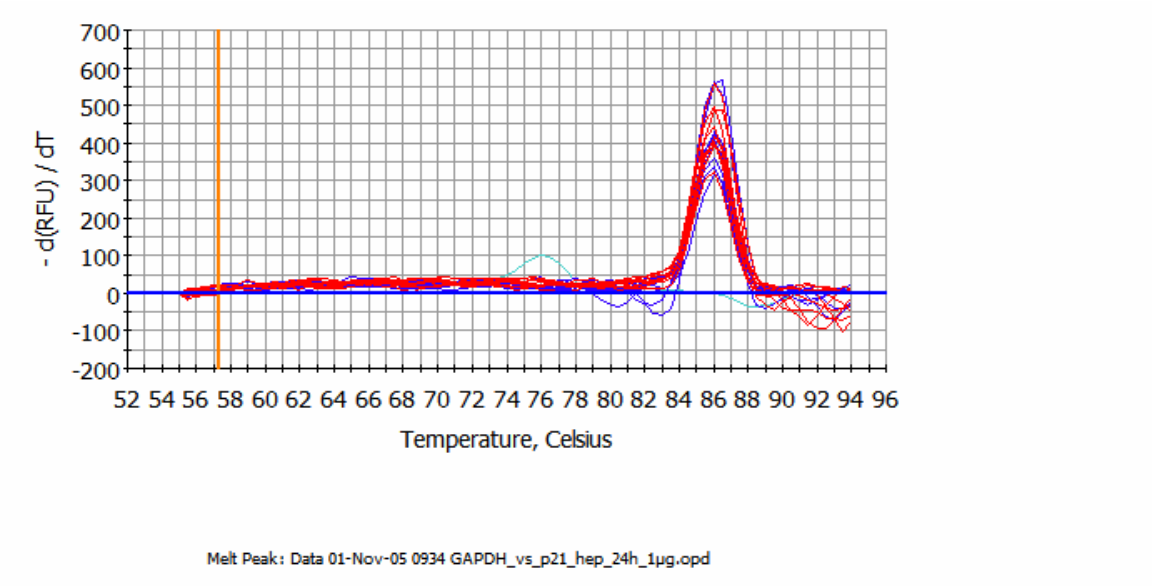


*CDKN1A* melt peaks derived from dissociation curves:

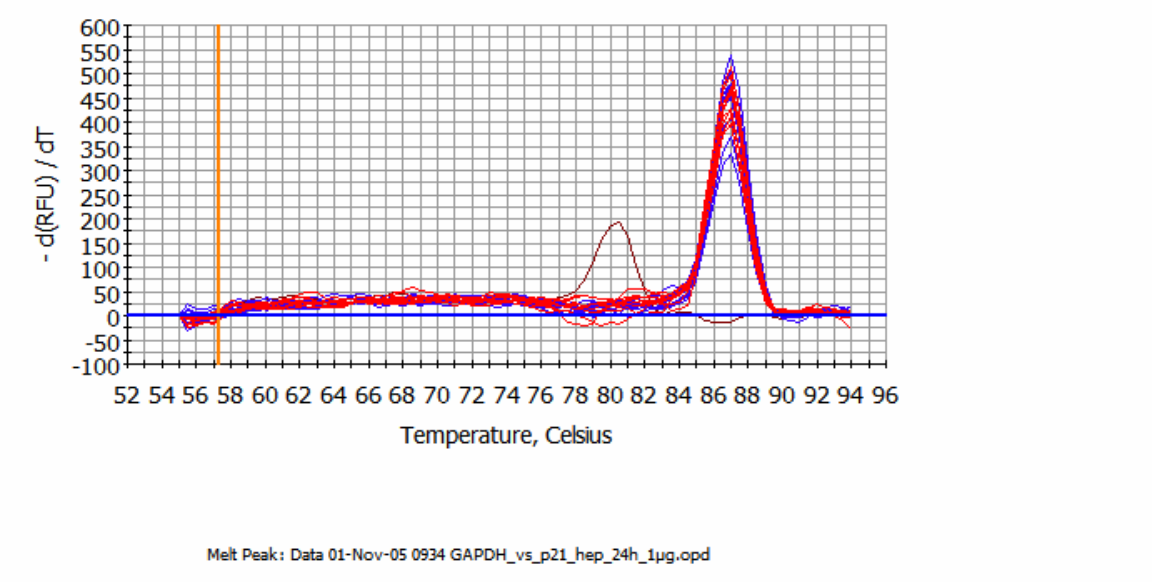


Relative transcript levels were determined by the method of Pfaffl et al. (2002), using REST 2005 beta v.1.9.12: The normalised expression ratio is 1.846 ($p$ = 0.579, using 50,000 iterations for the fixed reallocation randomisation test). Without normalisation, the expression ratio would be 3.636 ($p < 0.001$).

# Appendix 3

## *Qualitative analysis of RNA samples used for microarray hybridisations*

Qualitative analyses of total RNA used in microarray experiments was achieved using the Bioanalyzer 2100 (Agilent). This instrument uses disposable capillary electrophresis units for the quantitative separation of fluorescently stained nucleic acids according to size. Comparison of peak area with a control ladder also allows the accurate determination of quantity. The RNA 6000 chip was used for the current analysis. The data shown in the following pages corresponds to the samples according to the folowing legend:

Chip 1: HepG2 samples

**File i.d.: 2100 expert_EukaryoteTotal RNA Nano_DE34903905_2005-07-21_10-30-00.xad**

| | |
|---|---|
| Sample 1 | 6 h vehicle control (MQW), treatment 1 |
| Sample 2 | 6 h vehicle control (MQW), treatment 2 |
| Sample 3 | 6 h vehicle control (MQW), treatment 3 |
| Sample 4 | 24 h vehicle control (MQW), treatment 1 |
| Sample 5 | 24 h vehicle control (MQW), treatment 2 |
| Sample 6 | 24 h vehicle control (MQW), treatment 3 |
| Sample 7 | 6 h 1 µg/mL CYN, treatment 1 |
| Sample 8 | 6 h 1 µg/mL CYN, treatment 2 |
| Sample 9 | 6 h 1 µg/mL CYN, treatment 3 |
| Sample 10 | 24 h 1 µg/mL CYN, treatment 1 |
| Sample 11 | 24 h 1 µg/mL CYN, treatment 2 |
| Sample 12 | 24 h 1 µg/mL CYN, treatment 3 |

Chip 2: HDF samples

**File i.d.: 2100 expert_EukaryoteTotal RNA Nano_DE34903905_2005-07-21_11-34-40.xad**

| | |
|---|---|
| Sample 1 | 6 h vehicle control (MQW), treatment 1 |
| Sample 2 | 6 h vehicle control (MQW), treatment 2 |
| Sample 3 | 6 h vehicle control (MQW), treatment 3 |
| Sample 4 | 24 h vehicle control (MQW), treatment 1 |
| Sample 5 | 24 h vehicle control (MQW), treatment 2 |
| Sample 6 | 24 h vehicle control (MQW), treatment 3 |
| Sample 7 | 6 h 1 µg/mL CYN, treatment 1 |
| Sample 8 | 6 h 1 µg/mL CYN, treatment 2 |
| Sample 9 | 6 h 1 µg/mL CYN, treatment 3 |
| Sample 10 | 24 h 1 µg/mL CYN, treatment 1 |
| Sample 11 | 24 h 1 µg/mL CYN, treatment 2 |
| Sample 12 | 24 h 1 µg/mL CYN, treatment 3 |

**2100 expert_EukaryoteTotal RNA Nano_DE34903905_2005-07-21_10-30-00.xad** Page 1 of 3

Assay Class: EukaryoteTotal RNA Nano
Data Path: C:\... EukaryoteTotal RNA Nano DE34903905 2005-07-21 10-30-00.xad

Created: 21/07/2005 10:30:00 AM
Modified: 21/07/2005 10:57:13 AM

## Electropherogram Summary

Sample 1

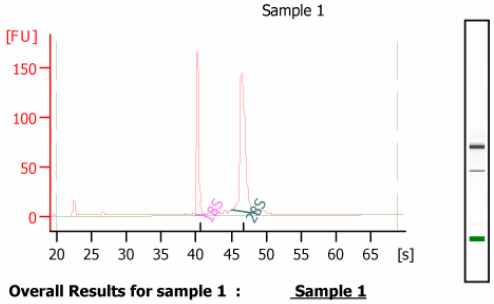


**Overall Results for sample 1 : Sample 1**

| | |
|---|---|
| RNA Area: | 525.4 |
| RNA Concentration: | 245 ng/µl |
| rRNA Ratio [28s / 18s]: | 2.0 |
| RNA Integrity Number (RIN): | 10.0 (B.02.03) |

**Fragment table for sample 1 : Sample 1**

| Name | Start Time [s] | End Time [s] | Area | % of total Area |
|---|---|---|---|---|
| 18S | 39.86 | 41.31 | 133.4 | 25.4 |
| 28S | 45.00 | 48.34 | 269.2 | 51.2 |

Sample 2

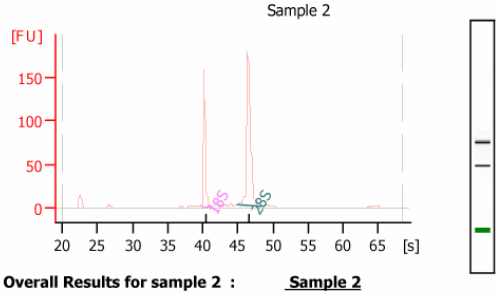


**Overall Results for sample 2 : Sample 2**

| | |
|---|---|
| RNA Area: | 465.6 |
| RNA Concentration: | 217 ng/µl |
| rRNA Ratio [28s / 18s]: | 2.0 |
| RNA Integrity Number (RIN): | 10.0 (B.02.03) |

**Fragment table for sample 2 : Sample 2**

| Name | Start Time [s] | End Time [s] | Area | % of total Area |
|---|---|---|---|---|
| 18S | 39.88 | 41.23 | 123.4 | 26.5 |
| 28S | 45.00 | 48.13 | 245.7 | 52.8 |

Sample 3

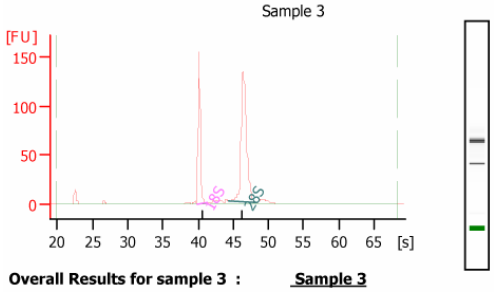


**Overall Results for sample 3 : Sample 3**

| | |
|---|---|
| RNA Area: | 489.5 |
| RNA Concentration: | 228 ng/µl |
| rRNA Ratio [28s / 18s]: | 2.1 |
| RNA Integrity Number (RIN): | 10.0 (B.02.03) |

**Fragment table for sample 3 : Sample 3**

| Name | Start Time [s] | End Time [s] | Area | % of total Area |
|---|---|---|---|---|
| 18S | 39.80 | 41.23 | 125.4 | 25.6 |
| 28S | 44.41 | 48.27 | 261.6 | 53.4 |

Sample 4

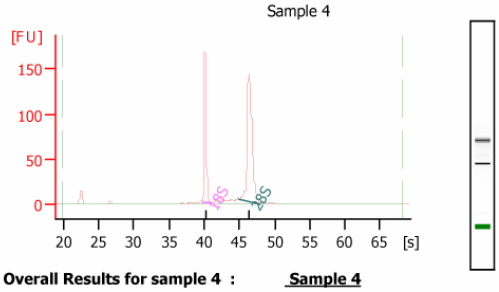


**Overall Results for sample 4 : Sample 4**

| | |
|---|---|
| RNA Area: | 498.1 |
| RNA Concentration: | 232 ng/µl |
| rRNA Ratio [28s / 18s]: | 1.9 |
| RNA Integrity Number (RIN): | 9.9 (B.02.03) |

**Fragment table for sample 4 : Sample 4**

| Name | Start Time [s] | End Time [s] | Area | % of total Area |
|---|---|---|---|---|
| 18S | 39.81 | 40.99 | 129.7 | 26.0 |
| 28S | 45.05 | 48.02 | 244.2 | 49.0 |

  

Assay Class: EukaryoteTotal RNA Nano
Data Path: C:\... EukaryoteTotal RNA Nano DE34903905 2005-07-21 10-30-00.xad

Created: 21/07/2005 10:30:00 AM
Modified: 21/07/2005 10:57:13 AM

**Electropherogram Summary Continued ...**

Sample 5

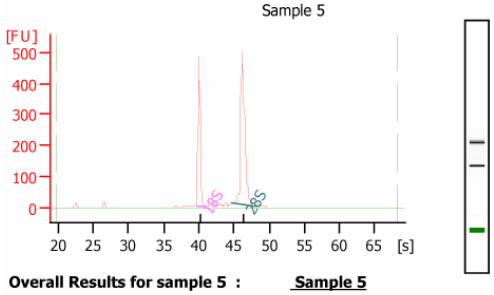


**Overall Results for sample 5 : Sample 5**

| | |
|---|---|
| RNA Area: | 1,424.7 |
| RNA Concentration: | 665 ng/µl |
| rRNA Ratio [28s / 18s]: | 1.8 |
| RNA Integrity Number (RIN): | 10.0 (B.02.03) |

**Fragment table for sample 5 : Sample 5**

| Name | Start Time [s] | End Time [s] | Area | % of total Area |
|---|---|---|---|---|
| 18S | 39.71 | 40.99 | 406.2 | 28.5 |
| 28S | 44.80 | 47.92 | 732.5 | 51.4 |

Sample 6

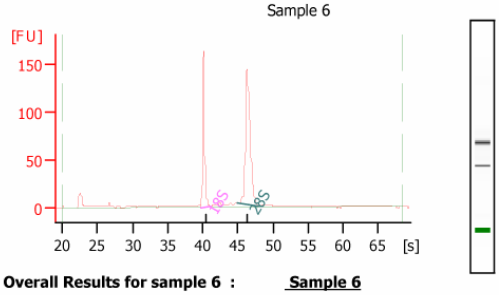


**Overall Results for sample 6 : Sample 6**

| | |
|---|---|
| RNA Area: | 461.4 |
| RNA Concentration: | 215 ng/µl |
| rRNA Ratio [28s / 18s]: | 2.0 |
| RNA Integrity Number (RIN): | 10.0 (B.02.03) |

**Fragment table for sample 6 : Sample 6**

| Name | Start Time [s] | End Time [s] | Area | % of total Area |
|---|---|---|---|---|
| 18S | 39.78 | 41.18 | 127.8 | 27.7 |
| 28S | 44.90 | 48.08 | 250.3 | 54.2 |

Sample 7

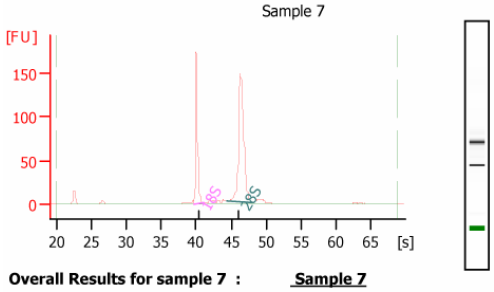


**Overall Results for sample 7 : Sample 7**

| | |
|---|---|
| RNA Area: | 542.2 |
| RNA Concentration: | 253 ng/µl |
| rRNA Ratio [28s / 18s]: | 2.0 |
| RNA Integrity Number (RIN): | 10.0 (B.02.03) |

**Fragment table for sample 7 : Sample 7**

| Name | Start Time [s] | End Time [s] | Area | % of total Area |
|---|---|---|---|---|
| 18S | 39.71 | 41.11 | 141.1 | 26.0 |
| 28S | 44.30 | 48.04 | 285.7 | 52.7 |

Sample 8

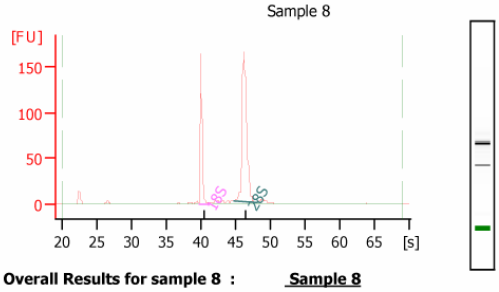


**Overall Results for sample 8 : Sample 8**

| | |
|---|---|
| RNA Area: | 488.2 |
| RNA Concentration: | 228 ng/µl |
| rRNA Ratio [28s / 18s]: | 2.0 |
| RNA Integrity Number (RIN): | 10.0 (B.02.03) |

**Fragment table for sample 8 : Sample 8**

| Name | Start Time [s] | End Time [s] | Area | % of total Area |
|---|---|---|---|---|
| 18S | 39.70 | 41.10 | 127.1 | 26.0 |
| 28S | 44.85 | 47.95 | 257.6 | 52.8 |

  

Assay Class: EukaryoteTotal RNA Nano
Data Path: C:\... EukaryoteTotal RNA Nano DE34903905 2005-07-21 10-30-00.xad

Created: 21/07/2005 10:30:00 AM
Modified: 21/07/2005 10:57:13 AM

**Electropherogram Summary Continued ...**

Sample 9

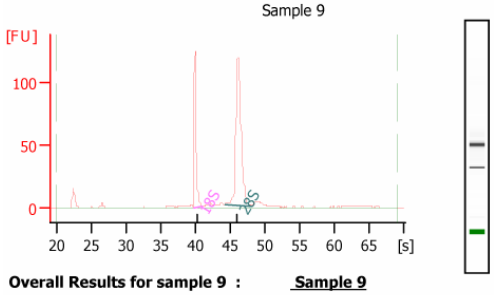


**Overall Results for sample 9 : Sample 9**

| | |
|---|---|
| RNA Area: | 400.8 |
| RNA Concentration: | 187 ng/µl |
| rRNA Ratio [28s / 18s]: | 2.1 |
| RNA Integrity Number (RIN): | 10.0 (B.02.03) |

**Fragment table for sample 9 : Sample 9**

| Name | Start Time [s] | End Time [s] | Area | % of total Area |
|---|---|---|---|---|
| 18S | 39.74 | 41.14 | 103.3 | 25.8 |
| 28S | 44.25 | 47.96 | 214.4 | 53.5 |

Sample 10

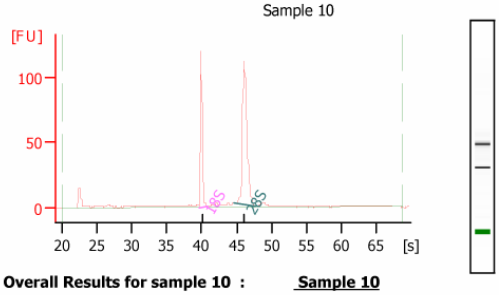


**Overall Results for sample 10 : Sample 10**

| | |
|---|---|
| RNA Area: | 335.4 |
| RNA Concentration: | 157 ng/µl |
| rRNA Ratio [28s / 18s]: | 1.9 |
| RNA Integrity Number (RIN): | 9.9 (B.02.03) |

**Fragment table for sample 10 : Sample 10**

| Name | Start Time [s] | End Time [s] | Area | % of total Area |
|---|---|---|---|---|
| 18S | 39.66 | 40.96 | 90.9 | 27.1 |
| 28S | 44.65 | 47.74 | 173.9 | 51.8 |

Sample 11

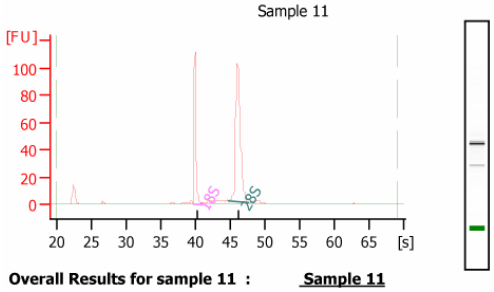


**Overall Results for sample 11 : Sample 11**

| | |
|---|---|
| RNA Area: | 311.0 |
| RNA Concentration: | 145 ng/µl |
| rRNA Ratio [28s / 18s]: | 1.9 |
| RNA Integrity Number (RIN): | 10.0 (B.02.03) |

**Fragment table for sample 11 : Sample 11**

| Name | Start Time [s] | End Time [s] | Area | % of total Area |
|---|---|---|---|---|
| 18S | 39.65 | 40.85 | 85.5 | 27.5 |
| 28S | 44.70 | 47.70 | 159.4 | 51.3 |

Sample 12

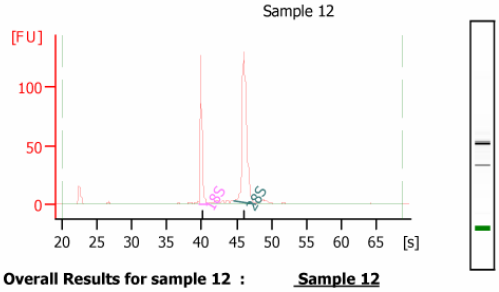


**Overall Results for sample 12 : Sample 12**

| | |
|---|---|
| RNA Area: | 355.5 |
| RNA Concentration: | 166 ng/µl |
| rRNA Ratio [28s / 18s]: | 2.0 |
| RNA Integrity Number (RIN): | 10.0 (B.02.03) |

**Fragment table for sample 12 : Sample 12**

| Name | Start Time [s] | End Time [s] | Area | % of total Area |
|---|---|---|---|---|
| 18S | 39.61 | 40.91 | 96.6 | 27.2 |
| 28S | 44.75 | 47.79 | 191.4 | 53.8 |

  

**2100 expert_EukaryoteTotal RNA Nano_DE34903905_2005-07-21_11-34-40.xad** Page 1 of 3

Assay Class: EukaryoteTotal RNA Nano
Data Path: C:\... EukaryoteTotal RNA Nano DE34903905 2005-07-21 11-34-40.xad

Created: 21/07/2005 11:34:40 AM
Modified: 21/07/2005 12:04:15 PM

**Electropherogram Summary**

Sample 1

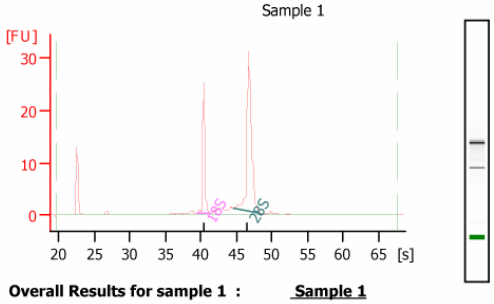


**Overall Results for sample 1 : Sample 1**

| | |
|---|---|
| RNA Area: | 93.7 |
| RNA Concentration: | 44 ng/µl |
| rRNA Ratio [28s / 18s]: | 2.2 |
| RNA Integrity Number (RIN): | 10.0 (B.02.03) |

**Fragment table for sample 1 : Sample 1**

| Name | Start Time [s] | End Time [s] | Area | % of total Area |
|---|---|---|---|---|
| 18S | 39.51 | 41.23 | 20.4 | 21.8 |
| 28S | 44.61 | 48.38 | 45.4 | 48.4 |

Sample 2

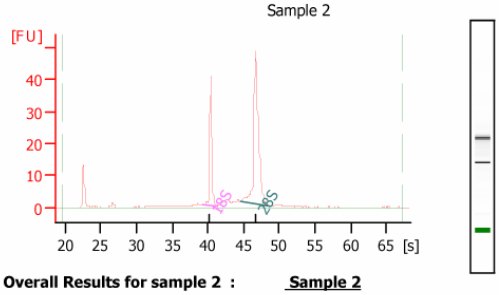


**Overall Results for sample 2 : Sample 2**

| | |
|---|---|
| RNA Area: | 153.3 |
| RNA Concentration: | 72 ng/µl |
| rRNA Ratio [28s / 18s]: | 2.1 |
| RNA Integrity Number (RIN): | 10.0 (B.02.03) |

**Fragment table for sample 2 : Sample 2**

| Name | Start Time [s] | End Time [s] | Area | % of total Area |
|---|---|---|---|---|
| 18S | 39.24 | 41.29 | 35.1 | 22.9 |
| 28S | 44.56 | 48.71 | 75.2 | 49.1 |

Sample 3

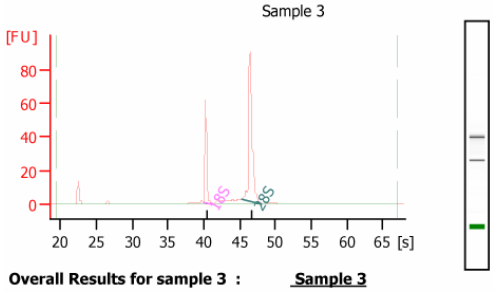


**Overall Results for sample 3 : Sample 3**

| | |
|---|---|
| RNA Area: | 201.6 |
| RNA Concentration: | 95 ng/µl |
| rRNA Ratio [28s / 18s]: | 2.0 |
| RNA Integrity Number (RIN): | 10.0 (B.02.03) |

**Fragment table for sample 3 : Sample 3**

| Name | Start Time [s] | End Time [s] | Area | % of total Area |
|---|---|---|---|---|
| 18S | 39.95 | 41.21 | 48.9 | 24.3 |
| 28S | 45.39 | 48.11 | 99.2 | 49.2 |

Sample 4

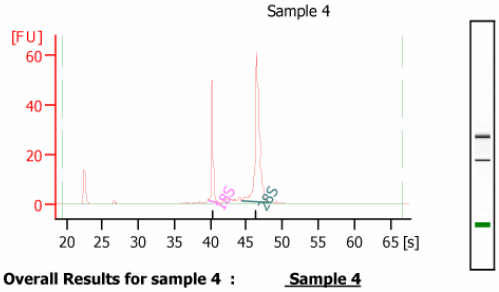


**Overall Results for sample 4 : Sample 4**

| | |
|---|---|
| RNA Area: | 165.7 |
| RNA Concentration: | 78 ng/µl |
| rRNA Ratio [28s / 18s]: | 2.3 |
| RNA Integrity Number (RIN): | 10.0 (B.02.03) |

**Fragment table for sample 4 : Sample 4**

| Name | Start Time [s] | End Time [s] | Area | % of total Area |
|---|---|---|---|---|
| 18S | 39.92 | 41.03 | 39.0 | 23.5 |
| 28S | 44.42 | 48.24 | 88.7 | 53.5 |

Assay Class: EukaryoteTotal RNA Nano
Data Path: C:\... EukaryoteTotal RNA Nano DE34903905 2005-07-21 11-34-40.xad

Created: 21/07/2005 11:34:40 AM
Modified: 21/07/2005 12:04:15 PM

**Electropherogram Summary Continued ...**

Sample 5

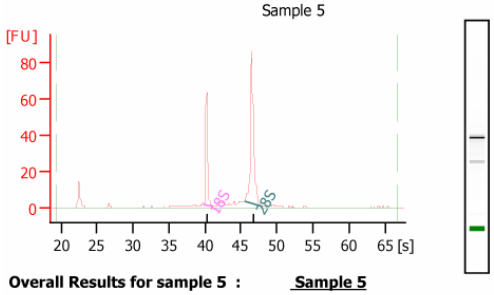


**Overall Results for sample 5 : Sample 5**

| | |
|---|---|
| RNA Area: | 204.0 |
| RNA Concentration: | 96 ng/µl |
| rRNA Ratio [28s / 18s]: | 2.0 |
| RNA Integrity Number (RIN): | 10.0 (B.02.03) |

**Fragment table for sample 5 : Sample 5**

| Name | Start Time [s] | End Time [s] | Area | % of total Area |
|---|---|---|---|---|
| 18S | 39.92 | 41.08 | 49.0 | 24.0 |
| 28S | 45.48 | 48.00 | 97.4 | 47.7 |

Sample 6

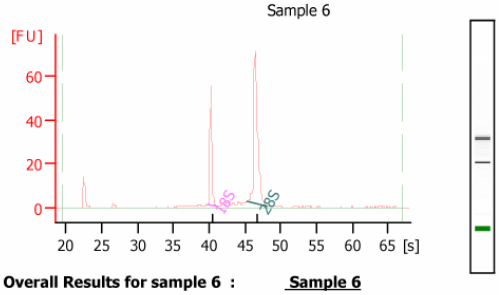


**Overall Results for sample 6 : Sample 6**

| | |
|---|---|
| RNA Area: | 180.1 |
| RNA Concentration: | 85 ng/µl |
| rRNA Ratio [28s / 18s]: | 2.1 |
| RNA Integrity Number (RIN): | 10.0 (B.02.03) |

**Fragment table for sample 6 : Sample 6**

| Name | Start Time [s] | End Time [s] | Area | % of total Area |
|---|---|---|---|---|
| 18S | 39.90 | 41.16 | 43.0 | 23.9 |
| 28S | 45.39 | 48.11 | 88.6 | 49.2 |

Sample 7

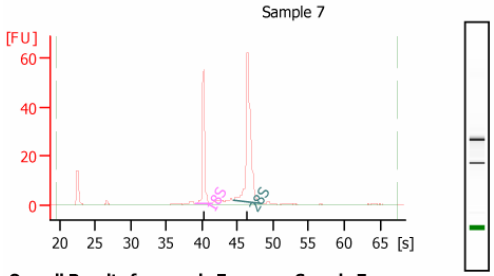


**Overall Results for sample 7 : Sample 7**

| | |
|---|---|
| RNA Area: | 184.6 |
| RNA Concentration: | 87 ng/µl |
| rRNA Ratio [28s / 18s]: | 2.0 |
| RNA Integrity Number (RIN): | 10.0 (B.02.03) |

**Fragment table for sample 7 : Sample 7**

| Name | Start Time [s] | End Time [s] | Area | % of total Area |
|---|---|---|---|---|
| 18S | 39.03 | 41.33 | 46.1 | 25.0 |
| 28S | 44.46 | 48.47 | 90.5 | 49.0 |

Sample 8

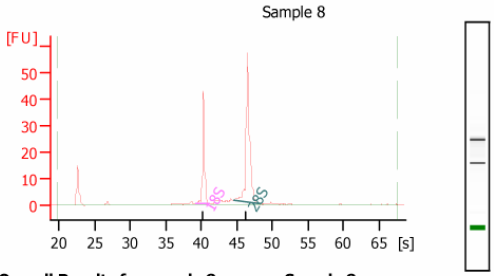


**Overall Results for sample 8 : Sample 8**

| | |
|---|---|
| RNA Area: | 140.8 |
| RNA Concentration: | 66 ng/µl |
| rRNA Ratio [28s / 18s]: | 2.1 |
| RNA Integrity Number (RIN): | 10.0 (B.02.03) |

**Fragment table for sample 8 : Sample 8**

| Name | Start Time [s] | End Time [s] | Area | % of total Area |
|---|---|---|---|---|
| 18S | 39.22 | 41.18 | 35.1 | 24.9 |
| 28S | 44.46 | 47.99 | 72.7 | 51.6 |

  

Assay Class: EukaryoteTotal RNA Nano
Data Path: C:\... EukaryoteTotal RNA Nano DE34903905 2005-07-21 11-34-40.xad

Created: 21/07/2005 11:34:40 AM
Modified: 21/07/2005 12:04:15 PM

**Electropherogram Summary Continued ...**

Sample 9

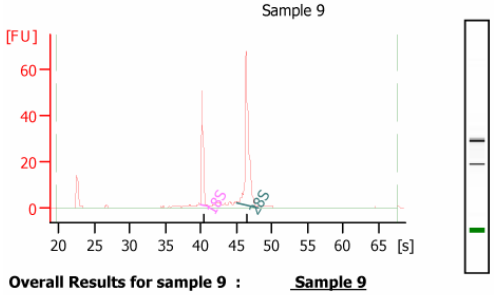


**Overall Results for sample 9 : Sample 9**

| | |
|---|---|
| RNA Area: | 158.2 |
| RNA Concentration: | 75 ng/µl |
| rRNA Ratio [28s / 18s]: | 2.2 |
| RNA Integrity Number (RIN): | 10.0 (B.02.03) |

**Fragment table for sample 9 : Sample 9**

| Name | Start Time [s] | End Time [s] | Area | % of total Area |
|---|---|---|---|---|
| 18S | 39.85 | 41.08 | 38.2 | 24.1 |
| 28S | 45.05 | 48.09 | 82.8 | 52.3 |

Sample 10

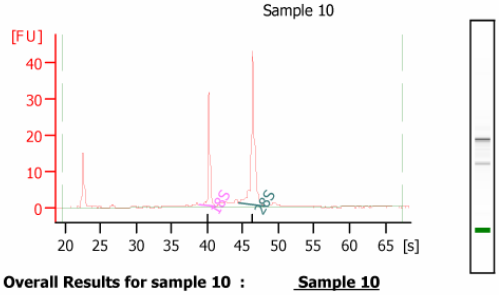


**Overall Results for sample 10 : Sample 10**

| | |
|---|---|
| RNA Area: | 112.3 |
| RNA Concentration: | 53 ng/µl |
| rRNA Ratio [28s / 18s]: | 2.0 |
| RNA Integrity Number (RIN): | 10.0 (B.02.03) |

**Fragment table for sample 10 : Sample 10**

| Name | Start Time [s] | End Time [s] | Area | % of total Area |
|---|---|---|---|---|
| 18S | 38.93 | 41.18 | 25.6 | 22.8 |
| 28S | 44.41 | 48.13 | 50.5 | 45.0 |

Sample 11

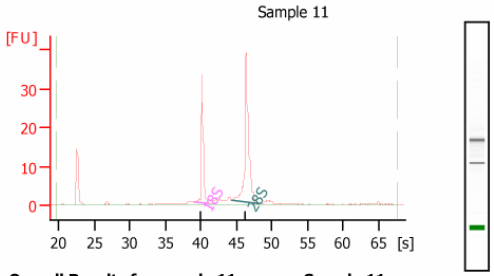


**Overall Results for sample 11 : Sample 11**

| | |
|---|---|
| RNA Area: | 116.2 |
| RNA Concentration: | 55 ng/µl |
| rRNA Ratio [28s / 18s]: | 1.8 |
| RNA Integrity Number (RIN): | 10.0 (B.02.03) |

**Fragment table for sample 11 : Sample 11**

| Name | Start Time [s] | End Time [s] | Area | % of total Area |
|---|---|---|---|---|
| 18S | 39.02 | 41.13 | 27.9 | 24.0 |
| 28S | 44.36 | 48.14 | 51.7 | 44.5 |

Sample 12

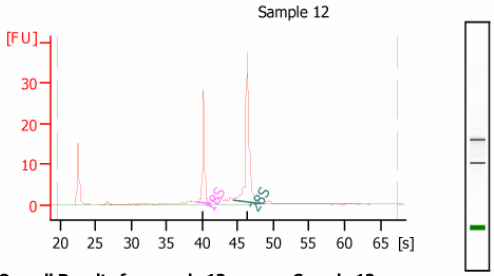


**Overall Results for sample 12 : Sample 12**

| | |
|---|---|
| RNA Area: | 102.8 |
| RNA Concentration: | 48 ng/µl |
| rRNA Ratio [28s / 18s]: | 2.0 |
| RNA Integrity Number (RIN): | 10.0 (B.02.03) |

**Fragment table for sample 12 : Sample 12**

| Name | Start Time [s] | End Time [s] | Area | % of total Area |
|---|---|---|---|---|
| 18S | 39.23 | 41.14 | 22.6 | 22.0 |
| 28S | 44.36 | 48.08 | 45.5 | 44.3 |

  

# References

**Aas, P. A., Otterlei, M., Falnes, P. O., Vagbo, C. B., Skorpen, F., Akbari, M., Sundheim, O., Bjoras, M., Slupphaug, G., Seeberg, E. et al.** (2003). Human and bacterial oxidative demethylases repair alkylation damage in both RNA and DNA. *Nature* **421**, 859-63.

**Abdollahi, A., Lord, K. A., Hoffman-Liebermann, B. and Liebermann, D. A.** (1991). Sequence and expression of a cDNA encoding MyD118: a novel myeloid differentiation primary response gene induced by multiple cytokines. *Oncogene* **6**, 165-7.

**Abraham, R. T.** (2001). Cell cycle checkpoint signaling through the ATM and ATR kinases. *Genes Dev* **15**, 2177-96.

**Ace, C. I. and Okulicz, W. C.** (2004). Microarray profiling of progesterone-regulated endometrial genes during the Rhesus monkey secretory phase. *Reprod Biol Endocrinol* **2**, 54.

**Afshari, C. A., Nuwaysir, E. F. and Barrett, J. C.** (1999). Application of complementary DNA microarray technology to carcinogen identification, toxicology, and drug safety evaluation. *Cancer Res* **59**, 4759-60.

**Agarwala, K. L., Kokame, K., Kato, H. and Miyata, T.** (2000). Phosphorylation of RTP, an ER stress-responsive cytoplasmic protein. *Biochem Biophys Res Commun* **272**, 641-7.

**Ahn, S., Olive, M., Aggarwal, S., Krylov, D., Ginty, D. D. and Vinson, C.** (1998). A Dominant-Negative Inhibitor of CREB Reveals that It Is a General Mediator of Stimulus-Dependent Transcription of c-fos. *Mol. Cell. Biol.* **18**, 967-977.

**Aktories, K. and Barbieri, J. T.** (2005). Bacterial Cytotoxins: Targeting Eukaryotic Switches. *Nature Reviews MicrobiologyNat Rev Micro* **3**, 397-410.

**Alarcon-Vargas, D. and Ronai, Z.** (2004). c-Jun-NH2 kinase (JNK) contributes to the regulation of c-Myc protein stability. *J Biol Chem* **279**, 5008-16.

**Alberts, B., Johnson, A., Lewis, J., Raff, M., Roberts, K. and Walter, P.** (2002). Molecular Biology of the Cell. NY, USA: Garland Science.

**Altschul, S. F., Gish, W., Miller, W., Myers, E. W. and Lipman, D. J.** (1990). Basic local alignment search tool. *J Mol Biol* **215**, 403-10.

**Ameis, D., Merkel, M., Eckerskorn, C. and Greten, H.** (1994). Purification, characterization and molecular cloning of human hepatic lysosomal acid lipase. *Eur J Biochem* **219**, 905-14.

**Amin, R. P., Vickers, A. E., Sistare, F., Thompson, K. L., Roman, R. J., Lawton, M., Kramer, J., Hamadeh, H. K., Collins, J., Grissom, S. et al.** (2004). Identification of putative gene based markers of renal toxicity. *Environ Health Perspect* **112**, 465-79.

**Amundson, S. A., Do, K. T., Shahab, S., Bittner, M., Meltzer, P., Trent, J. and Fornace, A. J., Jr.** (2000). Identification of Potential mRNA Biomarkers in Peripheral Blood Lymphocytes for Human Exposure to Ionizing Radiation. *Radiation Research* **154**, 342-346.

**Amundson, S. A., Patterson, A., Do, K. T. and Fornace, A. J., Jr.** (2002). A nucleotide excision repair master-switch: p53 regulated coordinate induction of global genomic repair genes. *Cancer Biol Ther* **1**, 145-9.

**Angel, P., Hattori, K., Smeal, T. and Karin, M.** (1988). The jun proto-oncogene is positively autoregulated by its product, Jun/AP-1. *Cell* **55**, 875-885.

**Arner, E. S. J. and Holmgren, A.** (2000). Physiological functions of thioredoxin and thioredoxin reductase. *European Journal of Biochemistry* **267**, 6102-6109.

**Ashburner, M., Ball, C. A., Blake, J. A., Botstein, D., Butler, H., Cherry, J. M., Davis, A. P., Dolinski, K., Dwight, S. S., Eppig, J. T. et al.** (2000). Gene ontology: tool for the unification of biology. The Gene Ontology Consortium. *Nat Genet* **25**, 25-9.

**Ausubel, F. M., Brent, R., Kingston, R. E. and Moore, D. D.** (1999). Short Protocols in Molecular Biology : A Compendium of Methods from Current Protocols in Molecular Biology.

**Baek, J. Y., Jun, D. Y., Taub, D. and Kim, Y. H.** (2003). Characterization of human phosphoserine aminotransferase involved in the phosphorylated pathway of L-serine biosynthesis. *Biochem J* **373**, 191-200.

**Baeuerle, P. A. and Baltimore, D.** (1988). I kappa B: a specific inhibitor of the NF-kappa B transcription factor. *Science* **242**, 540-6.

**Baker, J. B., Low, D. A., Simmer, R. L. and Cunningham, D. D.** (1980). Protease-nexin: a cellular component that links thrombin and plasminogen activator and mediates their binding to cells. *Cell* **21**, 37-45.

**Bakiri, L., Matsuo, K., Wisniewska, M., Wagner, E. F. and Yaniv, M.** (2002). Promoter specificity and biological activity of tethered AP-1 dimers. *Mol Cell Biol* **22**, 4952-64.

**Banin, S., Moyal, L., Shieh, S., Taya, Y., Anderson, C. W., Chessa, L., Smorodinsky, N. I., Prives, C., Reiss, Y., Shiloh, Y. et al.** (1998). Enhanced phosphorylation of p53 by ATM in response to DNA damage. *Science* **281**, 1674-7.

**Banker, R., Carmeli, S., Hadas, O., Teltsch, B., Porat, R. and Sukenik, A.** (1997). Identification of cylindrospermopsin in *Aphanizomenon ovalisporum* (cyanophyceae) isolated from Lake Kinneret, Israel. *Journal of Phycology* **33**, 613-616.

**Banker, R., Carmeli, S., Werman, M., Teltsch, B., Porat, R. and Sukenik, A.** (2001). Uracil moiety is required for toxicity of the cyanobacterial hepatotoxin cylindrospermopsin. *Journal of Toxicology and Environmental Health-Part A* **62**, 281-288.

**Barr, R. K. and Bogoyevitch, M. A.** (2001). The c-Jun N-terminal protein kinase family of mitogen-activated protein kinases (JNK MAPKs). *Int J Biochem Cell Biol* **33**, 1047-63.

**Barrie, A. P., Clohessy, A. M., Buensuceso, C. S., Rogers, M. V. and Allen, J. M.** (1997). Pituitary adenylyl cyclase-activating peptide stimulates extracellular signal-regulated kinase 1 or 2 (ERK1/2) activity in a Ras-independent, mitogen-activated protein Kinase/ERK kinase 1 or 2-dependent manner in PC12 cells. *J Biol Chem* **272**, 19666-71.

**Bartek, J. and Lukas, J.** (2006). The stress of finding NEMO. *Science* **311**, 1110-1.

**Begley, T. J. and Samson, L. D.** (2003). Molecular biology: A fix for RNA. **421**, 795-796.

**Bell, M., Schreiner, S., Damianov, A., Reddy, R. and Bindereif, A.** (2002). p110, a novel human U6 snRNP protein and U4/U6 snRNP recycling factor. *Embo J* **21**, 2724-35.

**Bellacosa, A. and Moss, E. G.** (2003). RNA Repair: Damage Control. *Current Biology* **13**, R482-R484.

**Ben-Yosef, T., Yanuka, O. and Benvenisty, N.** (1996). ECA39 is regulated by c-Myc in human and by a Jun/Fos homolog, Gcn4, in yeast. *Oncogene* **13**, 1859-66.

**Benassi, B., Fanciulli, M., Fiorentino, F., Porrello, A., Chiorino, G., Loda, M., Zupi, G. and Biroccio, A.** (2006). c-Myc phosphorylation is required for cellular response to oxidative stress. *Mol Cell* **21**, 509-19.

**Berger, J., Hauber, J., Hauber, R., Geiger, R. and Cullen, B. R.** (1988). Secreted placental alkaline phosphatase: a powerful new quantitative indicator of gene expression in eukaryotic cells. *Gene* **66**, 1-10.

**Bernard, C., Harvey, M., Briand, J. F., Bire, R., Krys, S. and Fontaine, J. J.** (2003). Toxicological comparison of diverse Cylindrospermopsis raciborskii strains: Evidence of liver damage caused by a French C-raciborskii strain. *Environmental Toxicology* **18**, 176-186.

**Berridge, M. V. and Tan, A. S.** (1993). Characterization of the cellular reduction of 3-(4,5-dimethylthiazol-2-yl)-2,5-diphenyltetrazolium bromide (MTT): subcellular

localization, substrate dependence, and involvement of mitochondrial electron transport in MTT reduction. *Arch Biochem Biophys* **303**, 474-82.

**Beyaert, R., Heyninck, K. and Van Huffel, S.** (2000). A20 and A20-binding proteins as cellular inhibitors of nuclear factor-kappa B-dependent gene expression and apoptosis. *Biochem Pharmacol* **60**, 1143-51.

**Bianchi, V. and Spychala, J.** (2003). Mammalian 5'-Nucleotidases. *J. Biol. Chem.* **278**, 46195-46198.

**Bischoff, J., Friedman, P., Marshak, D., Prives, C. and Beach, D.** (1990). Human p53 is Phosphorylated by p60-cdc2 and Cyclin B-cdc2. *PNAS* **87**, 4766-4770.

**Blanchet, S., Ramgolam, K., Baulig, A., Marano, F. and Baeza-Squiban, A.** (2004). Fine particulate matter induces amphiregulin secretion by bronchial epithelial cells. *Am J Respir Cell Mol Biol* **30**, 421-7.

**Blaydes, J. P., Luciani, M. G., Pospisilova, S., Ball, H. M.-L., Vojtesek, B. and Hupp, T. R.** (2001). Stoichiometric Phosphorylation of Human p53 at Ser315 Stimulates p53-dependent Transcription. *J. Biol. Chem.* **276**, 4699-4708.

**Bogoyevitch, M. A. and Kobe, B.** (2006). Uses for JNK: the Many and Varied Substrates of the c-Jun N-Terminal Kinases. *Microbiol. Mol. Biol. Rev.* **70**, 1061-1095.

**Bourke, A. T. and Hawes, R. B.** (1983). Freshwater cyanobacteria (blue-green algae) and human health. *Med J Aust* **1**, 491-2.

**Bouton, C. M. L. S., Hossain, M. A., Frelin, L. P., Laterra, J. and Pevsner, J.** (2001). Microarray Analysis of Differential Gene Expression in Lead-Exposed Astrocytes. *Toxicology and Applied Pharmacology* **176**, 34-53.

**Bregeon, D. and Sarasin, A.** (2005). Hypothetical role of RNA damage avoidance in preventing human disease. *Mutation Research/Fundamental and Molecular Mechanisms of Mutagenesis* **577**, 293-302.

**Bressac, B., Galvin, K. M., Liang, T. J., Isselbacher, K. J., Wands, J. R. and Ozturk, M.** (1990). Abnormal structure and expression of p53 gene in human hepatocellular carcinoma. *Proc Natl Acad Sci U S A* **87**, 1973-7.

**Brooks, C. L. and Gu, W.** (2003). Ubiquitination, phosphorylation and acetylation: the molecular basis for p53 regulation. *Current Opinion in Cell Biology* **15**, 164-171.

**Brostrom, M. A., Prostko, C. R., Gmitter, D. and Brostrom, C. O.** (1995). Independent Signaling of grp78 Gene Transcription and Phosphorylation of Eukaryotic Initiation Factor 2alpha by the Stressed Endoplasmic Reticulum. *J. Biol. Chem.* **270**, 4127-4132.

**Bulavin, D. V., Saito, S., Hollander, M. C., Sakaguchi, K., Anderson, C. W., Appella, E. and Fornace, A. J., Jr.** (1999). Phosphorylation of human p53 by p38 kinase coordinates N-terminal phosphorylation and apoptosis in response to UV radiation. *Embo J* **18**, 6845-54.

**Bulmer, J. T., Zacal, N. J. and Rainbow, A. J.** (2005). Human cells deficient in transcription-coupled repair show prolonged activation of the Jun N-terminal kinase and increased sensitivity following cisplatin treatment. *Cancer Chemotherapy and Pharmacology* **V56**, 189-198.

**Burns, J., Chapman, A., Williams, C., Flewelling, L., Carmichael, W. and Pawlowicz, M.** (2000). Cyanotoxic blooms in Florida's lakes, rivers and tidal river estuaries: the recent invasion of toxigenic Cylindrospermopsis raciborskii and consequences for Florida's drinking water supplies. In *Proceedings of the 9th International Conference on Harmful Algae*, (ed. G. M. Hallegraeff S. Blackburn C. Bolch and R. Lewis). Hobart, Australia.

**Buschmann, T., Potapova, O., Bar-Shira, A., Ivanov, V. N., Fuchs, S. Y., Henderson, S., Fried, V. A., Minamoto, T., Alarcon-Vargas, D., Pincus, M. R. et al.** (2001). Jun NH2-Terminal Kinase Phosphorylation of p53 on Thr-81 Is Important for p53 Stabilization and Transcriptional Activities in Response to Stress. *Mol. Cell. Biol.* **21**, 2743-2754.

**Bush, K. T., Hendrickson, B. A. and Nigam, S. K.** (1994). Induction of the FK506-binding protein, FKBP13, under conditions which misfold proteins in the endoplasmic reticulum. *Biochem J* **303 ( Pt 3)**, 705-8.

**Byth, S.** (1980). Palm Island mystery disease. *Med J Aust* **2**, 40, 42.

**Cadigan, K. M. and Liu, Y. I.** (2006). Wnt signaling: complexity at the surface. *J Cell Sci* **119**, 395-402.

**Cadigan, K. M. and Nusse, R.** (1997). Wnt signaling: a common theme in animal development. *Genes Dev.* **11**, 3286-3305.

**Campbell, K. J., Rocha, S. and Perkins, N. D.** (2004). Active Repression of Antiapoptotic Gene Expression by RelA(p65) NF-[kappa]B. *Molecular Cell* **13**, 853-865.

**Canman, C. E., Lim, D. S., Cimprich, K. A., Taya, Y., Tamai, K., Sakaguchi, K., Appella, E., Kastan, M. B. and Siliciano, J. D.** (1998). Activation of the ATM kinase by ionizing radiation and phosphorylation of p53. *Science* **281**, 1677-9.

**Castenholz, R. W. and Waterbury, J. B.** (1989). Bergey's Manual of Systematic Bacteriology, vol. 3 (ed. J. T. Staley, Bryant M.P., Pffennig, M., and Holt J.G.), pp. 1710-1727. Baltimore: Williams and Wilkins.

**Chen, J. and Patton, J. R.** (1999). Cloning and characterization of a mammalian pseudouridine synthase. *Rna* **5**, 409-19.

**Chen, S., Guttridge, D. C., You, Z., Zhang, Z., Fribley, A., Mayo, M. W., Kitajewski, J. and Wang, C.-Y.** (2001). Wnt-1 Signaling Inhibits Apoptosis by Activating {beta}-Catenin/T Cell Factor-mediated Transcription. *J. Cell Biol.* **152**, 87-96.

**Chen, X., Shen, J. and Prywes, R.** (2002). The Luminal Domain of ATF6 Senses Endoplasmic Reticulum (ER) Stress and Causes Translocation of ATF6 from the ER to the Golgi. *J. Biol. Chem.* **277**, 13045-13052.

**Chen, Z. J.** (2005). Ubiquitin signalling in the NF-[kappa]B pathway. *Nature Cell Biology* **7**, 758-765.

**Chicheportiche, Y., Bourdon, P. R., Xu, H., Hsu, Y.-M., Scott, H., Hession, C., Garcia, I. and Browning, J. L.** (1997). TWEAK, a New Secreted Ligand in the Tumor Necrosis Factor Family That Weakly Induces Apoptosis. *J. Biol. Chem.* **272**, 32401-32410.

**Chipuk, J. E., Kuwana, T., Bouchier-Hayes, L., Droin, N. M., Newmeyer, D. D., Schuler, M. and Green, D. R.** (2004). Direct Activation of Bax by p53 Mediates Mitochondrial Membrane Permeabilization and Apoptosis. *Science* **303**, 1010-1014.

**Chiswell, R. K., Shaw, G. R., Eaglesham, G., Smith, M. J., Norris, R. L., Seawright, A. A. and Moore, M. R.** (1999). Stability of cylindrospermopsin, the toxin from the cyanobacterium, Cylindrospermopsis raciborskii: Effect of pH, temperature, and sunlight on decomposition. *Environmental Toxicology* **14**, 155-161.

**Cho, H. M., Jun, D. Y., Bae, M. A., Ahn, J. D. and Kim, Y. H.** (2000). Nucleotide sequence and differential expression of the human 3-phosphoglycerate dehydrogenase gene. *Gene* **245**, 193-201.

**Chong, M. W., Wong, B. S., Lam, P. K., Shaw, G. R. and Seawright, A. A.** (2002). Toxicity and uptake mechanism of cylindrospermopsin and lophyrotomin in primary rat hepatocytes. *Toxicon* **40**, 205-11.

**Choudhuri, S.** (2004). Gene Regulation and Molecular Toxicology. *Toxicology Mechanisms and Methods* **15**, 1 - 23.

**CLONTECH.** (1998). NFkB transcription reporter vectors. *CLONTECHniques* **XIII**, 24-35.

**Cooper, J. A.** (1987). Effects of cytochalasin and phalloidin on actin. *J Cell Biol* **105**, 1473-8.

**Cory, A. H., Owen, T. C., Barltrop, J. A. and Cory, J. G.** (1991). Use of an aqueous soluble tetrazolium/formazan assay for cell growth assays in culture. *Cancer Commun* **3**, 207-12.

**Cullen, B. R. and Malim, M. H.** (1992). Secreted placental alkaline phosphatase as a eukaryotic reporter gene. In *Methods in Enzymology vol. 216 (Recombinant DNA Part G)*, (ed. R. Wu), pp. 362-368. San Diego, CA, USA: Academic Press.

**D'Orazi, G., Cecchinelli, B., Bruno, T., Manni, I., Higashimoto, Y., Saito, S., Gostissa, M., Coen, S., Marchetti, A., Del Sal, G. et al.** (2002). Homeodomain-interacting protein kinase-2 phosphorylates p53 at Ser 46 and mediates apoptosis. *Nat Cell Biol* **4**, 11-9.

**Dani, C., Blanchard, J. M., Piechaczyk, M., El Sabouty, S., Marty, L. and Jeanteur, P.** (1984). Extreme instability of myc mRNA in normal and transformed human cells. *Proc Natl Acad Sci U S A* **81**, 7046-50.

**Dani, C., Mechti, N., Piechaczyk, M., Lebleu, B., Jeanteur, P. and Blanchard, J. M.** (1985). Increased rate of degradation of c-myc mRNA in interferon-treated Daudi cells. *Proc Natl Acad Sci U S A* **82**, 4896-9.

**Davis, R. J.** (2000). Signal Transduction by the JNK Group of MAP Kinases. *Cell* **103**, 239-252.

**Davoodi, J., Drown, P. M., Bledsoe, R. K., Wallin, R., Reinhart, G. D. and Hutson, S. M.** (1998). Overexpression and characterization of the human mitochondrial and cytosolic branched-chain aminotransferases. *J Biol Chem* **273**, 4982-9.

**Dawson, R. M.** (1998). The toxicology of microcystins. *Toxicon* **36**, 953-62.

**de La Coste, A., Romagnolo, B., Billuart, P., Renard, C. A., Buendia, M. A., Soubrane, O., Fabre, M., Chelly, J., Beldjord, C., Kahn, A. et al.** (1998). Somatic mutations of the beta-catenin gene are frequent in mouse and human hepatocellular carcinomas. *Proc Natl Acad Sci U S A* **95**, 8847-51.

**Deak, M., Clifton, A. D., Lucocq, L. M. and Alessi, D. R.** (1998). Mitogen- and stress-activated protein kinase-1 (MSK1) is directly activated by MAPK and SAPK2/p38, and may mediate activation of CREB. *Embo J* **17**, 4426-41.

**Decker, T. and Lohmann-Matthes, M.-L.** (1988). A quick and simple method for the quantitation of lactate dehydrogenase release in measurements of cellular cytotoxicity and tumor necrosis factor (TNF) activity. *Journal of Immunological Methods* **115**, 61-69.

**Dennis, G., Sherman, B., Hosack, D., Yang, J., Gao, W., Lane, H. and Lempicki, R.** (2003). DAVID: Database for Annotation, Visualization, and Integrated Discovery. *Genome Biology* **4**, R60.

**Derijard, B., Hibi, M., Wu, I.-H., Barrett, T., Su, B., Deng, T., Karin, M. and Davis, R. J.** (1994). JNK1: A protein kinase stimulated by UV light and Ha-Ras that binds and phosphorylates the c-Jun activation domain. *Cell* **76**, 1025-1037.

**Deschamps, J., Meijlink, F. and Verma, I. M.** (1985). Identification of a transcriptional enhancer element upstream from the proto-oncogene fos. *Science* **230**, 1174-7.

**Dualan, R., Brody, T., Keeney, S., Nichols, A. F., Admon, A. and Linn, S.** (1995). Chromosomal localization and cDNA cloning of the genes (DDB1 and DDB2) for the p127 and p48 subunits of a human damage-specific DNA binding protein. *Genomics* **29**, 62-9.

**Durham, T. R. and Snow, E. T.** (2005). Metal ions and carcinogensis. In *Cancer: Cell structures, carcinogens and genomic instability*, (ed. L. P. Bignold), pp. 97-130: Birkhauser, Basel, Switzerland.

**Edinger, A. L. and Thompson, C. B.** (2004). Death by design: apoptosis, necrosis and autophagy. *Current Opinion in Cell Biology* **16**, 663-669.

**Edwards, D. R.** (1994). Cell signalling and the control of gene transcription. *Trends in Pharmacological Sciences* **15**, 239-244.

**Eisen, M. B., Spellman, P. T., Brown, P. O. and Botstein, D.** (1998). Cluster analysis and display of genome-wide expression patterns. *Proc Natl Acad Sci U S A* **95**, 14863-8.

**el-Deiry, W. S., Tokino, T., Velculescu, V. E., Levy, D. B., Parsons, R., Trent, J. M., Lin, D., Mercer, W. E., Kinzler, K. W. and Vogelstein, B.** (1993). WAF1, a potential mediator of p53 tumor suppression. *Cell* **75**, 817-25.

**Falconer, I. R.** (1999). Human Health Aspects. In *Toxic Cyanobacteria in Water: A guide to their public health consequences, monitoring and management*, pp. 113-141. London: E & FN Spon.

**Falconer, I. R.** (2005). Cyanobacterial Toxins of Drinking Water Supplies - Cylindrospermopsins and Microcystins. Boca Raton, FL: CRC Press.

**Fan, W., Jin, S., Tong, T., Zhao, H., Fan, F., Antinore, M. J., Rajasekaran, B., Wu, M. and Zhan, Q.** (2002). BRCA1 regulates GADD45 through its interactions with the OCT-1 and CAAT motifs. *J Biol Chem* **277**, 8061-7.

**Farrell, D. H. and Cunningham, D. D.** (1986). Human fibroblasts accelerate the inhibition of thrombin by protease nexin. *Proc Natl Acad Sci U S A* **83**, 6858-62.

**Fedi, P., Bafico, A., Nieto Soria, A., Burgess, W. H., Miki, T., Bottaro, D. P., Kraus, M. H. and Aaronson, S. A.** (1999). Isolation and biochemical characterization of the human Dkk-1 homologue, a novel inhibitor of mammalian Wnt signaling. *J Biol Chem* **274**, 19465-72.

**Fessard, V. and Bernard, C.** (2003). Cell alterations but no DNA strand breaks induced in vitro by cylindrospermopsin in CHO K1 cells. *Environ Toxicol* **18**, 353-359.

**Firestein, G. S. and Pisetsky, D. S.** (2002). DNA microarrays: Boundless technology or bound by technology? Guidelines for studies using microarray technology. *Arthritis & Rheumatism* **46**, 859-861.

**Fischer, G. and Bang, H.** (1985). The refolding of urea-denatured ribonuclease A is catalyzed by peptidyl-prolyl cis-trans isomerase. *Biochim Biophys Acta* **828**, 39-42.

**Fischer, U., Janicke, R. U. and Schulze-Osthoff, K.** (2003). Many cuts to ruin: a comprehensive update of caspase substrates. *Cell Death Differ* **10**, 76-100.

**Fitch, M. E., Nakajima, S., Yasui, A. and Ford, J. M.** (2003). In vivo recruitment of XPC to UV-induced cyclobutane pyrimidine dimers by the DDB2 gene product. *J Biol Chem* **278**, 46906-10.

**Fitzgerald, K. A. and O'Neill, L. A. J.** (2000). The role of the interleukin-1/Toll-like receptor superfamily in inflammation and host defence. *Microbes and Infection* **2**, 933-943.

**Fornace, A. J., Alamo, I. and Hollander, M. C.** (1988). DNA Damage-Inducible Transcripts in Mammalian Cells. *PNAS* **85**, 8800-8804.

**Fornace, A. J., Jr., Nebert, D. W., Hollander, M. C., Luethy, J. D., Papathanasiou, M., Fargnoli, J. and Holbrook, N. J.** (1989). Mammalian genes coordinately regulated by growth arrest signals and DNA-damaging agents. *Mol Cell Biol* **9**, 4196-203.

**Froscio, S. M., Humpage, A. R., Burcham, P. C. and Falconer, I. R.** (2001). Cell-free protein synthesis inhibition assay for the cyanobacterial toxin cylindrospermopsin. *Environmental Toxicology* **16**, 408-412.

**Froscio, S. M., Humpage, A. R., Burcham, P. C. and Falconer, I. R.** (2003). Cylindrospermopsin-induced protein synthesis inhibition and its dissociation from acute toxicity in mouse hepatocytes. *Environ Toxicol* **18**, 243-51.

**Gabai, V. L., Mabuchi, K., Mosser, D. D. and Sherman, M. Y.** (2002). Hsp72 and stress kinase c-jun N-terminal kinase regulate the bid-dependent pathway in tumor necrosis factor-induced apoptosis. *Mol Cell Biol* **22**, 3415-24.

**Gaccioli, F., Huang, C. C., Wang, C., Bevilacqua, E., Franchi-Gazzola, R., Gazzola, G. C., Bussolati, O., Snider, M. D. and Hatzoglou, M.** (2006). Amino acid starvation induces the SNAT2 neutral amino acid transporter by a mechanism that involves eukaryotic initiation factor 2alpha phosphorylation and cap-independent translation. *J Biol Chem* **281**, 17929-40.

**Garrido, C., Gurbuxani, S., Ravagnan, L. and Kroemer, G.** (2001). Heat shock proteins: endogenous modulators of apoptotic cell death. *Biochem Biophys Res Commun* **286**, 433-42.

**Gartel, A. L., Serfas, M. S., Gartel, M., Goufman, E., Wu, G. S., el-Deiry, W. S. and Tyner, A. L.** (1996). p21 (WAF1/CIP1) expression is induced in newly nondividing cells in diverse epithelia and during differentiation of the Caco-2 intestinal cell line. *Exp Cell Res* **227**, 171-81.

**Gautier, T., Berges, T., Tollervey, D. and Hurt, E.** (1997). Nucleolar KKE/D repeat proteins Nop56p and Nop58p interact with Nop1p and are required for ribosome biogenesis. *Mol Cell Biol* **17**, 7088-98.

**Gennari, A., Pazos, P., Boveri, M., Callaghan, R., Casado, J., Maurici, D., Corsini, E. and Prieto, P.** (2004). New insights into the mechanisms involved in renal proximal tubular damage induced in vitro by ochratoxin A. *Journal of Biochemical and Molecular Toxicology* **18**, 43-49.

**Ghosh, S., May, M. J. and Kopp, E. B.** (1998). NF-kappa B and Rel proteins: evolutionarily conserved mediators of immune responses. *Annu Rev Immunol* **16**, 225-60.

**Gilman, M. Z., Wilson, R. N. and Weinberg, R. A.** (1986). Multiple protein-binding sites in the 5'-flanking region regulate c-fos expression. *Mol Cell Biol* **6**, 4305-16.

**Goh, K. C., deVeer, M. J. and Williams, B. R.** (2000). The protein kinase PKR is required for p38 MAPK activation and the innate immune response to bacterial endotoxin. *Embo J* **19**, 4292-7.

**Goldwasser, F., Bae, I., Fornace, A. J., Jr. and Pommier, Y.** (1996). Differential GADD45, p21CIP1/WAF1, MCL-1 and topoisomerase II gene induction and secondary DNA fragmentation after camptothecin-induced DNA damage in two mutant p53 human colon cancer cell lines. *Oncol Res* **8**, 317-23.

**Gomez-Quiroz, L., Bucio, L., Souza, V., Escobar, C., Farfan, B., Hernandez, E., Konigsberg, M., Vargas-Vorackova, F., Kershenobich, D. and Gutierrez-Ruiz, M. C.** (2003). Interleukin 8 response and oxidative stress in HepG2 cells treated with ethanol, acetaldehyde or lipopolysaccharide. *Hepatol Res* **26**, 134-141.

**Green, D. R.** (2000). Apoptotic pathways: paper wraps stone blunts scissors. *Cell* **102**, 1-4.

**Gulledgea, B. M., Aggena, J. B., Huangb, H. B., Nairnc, A. C. and Chamberlin, A. R.** (2002). The microcystins and nodularins: cyclic polypeptide inhibitors of PP1 and PP2A. *Curr Med Chem* **9**, 1991-2003.

**Habraken, Y. and Piette, J.** (2006). NF-kappaB activation by double-strand breaks. *Biochem Pharmacol* **72**, 1132-41.

**Hagiwara, M., Brindle, P., Harootunian, A., Armstrong, R., Rivier, J., Vale, W., Tsien, R. and Montminy, M. R.** (1993). Coupling of hormonal stimulation and transcription via the cyclic AMP-responsive factor CREB is rate limited by nuclear entry of protein kinase A. *Mol Cell Biol* **13**, 4852-9.

**Haider, S., Naithani, V., Viswanathan, P. N. and Kakkar, P.** (2003). Cyanobacterial toxins: a growing environmental concern. *Chemosphere* **52**, 1-21.

**Hainaut, P. and Hollstein, M.** (2000). p53 and human cancer: the first ten thousand mutations. *Adv Cancer Res* **77**, 81-137.

**Hamadeh, H. K., Bushel, P. R., Jayadev, S., DiSorbo, O., Bennett, L., Li, L., Tennant, R., Stoll, R., Barrett, J. C., Paules, R. S. et al.** (2002a). Prediction of Compound Signature Using High Density Gene Expression Profiling. *Toxicological Sciences* **67**, 232-240.

**Hamadeh, H. K., Bushel, P. R., Jayadev, S., Martin, K., DiSorbo, O., Sieber, S., Bennett, L., Tennant, R., Stoll, R., Barrett, J. C. et al.** (2002b). Gene expression analysis reveals chemical-specific profiles. *Toxicol Sci* **67**, 219-31.

**Han, S., Yoon, K., Lee, K., Kim, K., Jang, H., Lee, N. K., Hwang, K. and Young Lee, S.** (2003). TNF-related weak inducer of apoptosis receptor, a TNF receptor superfamily member, activates NF-kappa B through TNF receptor-associated factors. *Biochem Biophys Res Commun* **305**, 789-96.

**Harada, K., Yamada, A., Yang, D., Itoh, K. and Shichijo, S.** (2001). Binding of a SART3 tumor-rejection antigen to a pre-mRNA splicing factor RNPS1: a possible regulation of splicing by a complex formation. *Int J Cancer* **93**, 623-8.

**Harada, K. I., Ohtani, I., Iwamoto, K., Suzuki, M., Watanabe, M. F., Watanabe, M. and Terao, K.** (1994). Isolation of cylindrospermopsin from a cyanobacterium Umezakia natans and its screening method. *Toxicon* **32**, 73-84.

**Harding, H. P., Novoa, I., Zhang, Y., Zeng, H., Wek, R., Schapira, M. and Ron, D.** (2000). Regulated translation initiation controls stress-induced gene expression in mammalian cells. *Mol Cell* **6**, 1099-108.

**Harris, A. J., Dial, S. L. and Casciano, D. A.** (2004). Comparison of basal gene expression profiles and effects of hepatocarcinogens on gene expression in cultured primary human hepatocytes and HepG2 cells. *Mutat Res* **549**, 79-99.

**Harris, M. H. and Thompson, C. B.** (2000). The role of the Bcl-2 family in the regulation of outer mitochondrial membrane permeability. *Cell Death Differ* **7**, 1182-91.

**Hawkins, P. R., Chandrasena, N. R., Jones, G. J., Humpage, A. R. and Falconer, I. R.** (1997). Isolation and toxicity of Cylindrospermopsis raciborskii from an ornamental lake. *Toxicon* **35**, 341-6.

**Hawkins, P. R., Runnegar, M. T., Jackson, A. R. and Falconer, I. R.** (1985). Severe hepatotoxicity caused by the tropical cyanobacterium (blue-green alga) Cylindrospermopsis raciborskii (Woloszynska) Seenaya and Subba Raju isolated from a domestic water supply reservoir. *Appl Environ Microbiol* **50**, 1292-5.

**Hay, R. T., Vuillard, L., Desterro, J. M. and Rodriguez, M. S.** (1999). Control of NF-kappa B transcriptional activation by signal induced proteolysis of I kappa B alpha. *Philos Trans R Soc Lond B Biol Sci* **354**, 1601-9.

**Hayakawa, M., Miyashita, H., Sakamoto, I., Kitagawa, M., Tanaka, H., Yasuda, H., Karin, M. and Kikugawa, K.** (2003). Evidence that reactive oxygen species do not mediate NF-kappaB activation. *Embo J* **22**, 3356-66.

**Hayano, T. and Kikuchi, M.** (1995). Molecular cloning of the cDNA encoding a novel protein disulfide isomerase-related protein (PDIR). *FEBS Letters* **372**, 210-214.

**Hayano, T., Yanagida, M., Yamauchi, Y., Shinkawa, T., Isobe, T. and Takahashi, N.** (2003). Proteomic analysis of human Nop56p-associated pre-ribosomal ribonucleoprotein complexes. Possible link between Nop56p and the nucleolar protein treacle responsible for Treacher Collins syndrome. *J Biol Chem* **278**, 34309-19.

**Hayman, J.** (1992). Beyond the Barcoo--probable human tropical cyanobacterial poisoning in outback Australia. *Med J Aust* **157**, 794-6.

**Haze, K., Yoshida, H., Yanagi, H., Yura, T. and Mori, K.** (1999). Mammalian transcription factor ATF6 is synthesized as a transmembrane protein and activated by proteolysis in response to endoplasmic reticulum stress. *Mol Biol Cell* **10**, 3787-99.

**Heinemeyer, T., Wingender, E., Reuter, I., Hermjakob, H., Kel, A. E., Kel, O. V., Ignatieva, E. V., Ananko, E. A., Podkolodnaya, O. A., Kolpakov, F. A. et al.** (1998). Databases on transcriptional regulation: TRANSFAC, TRRD and COMPEL. *Nucleic Acids Res* **26**, 362-7.

**Hernandez, M. C., Andres-Barquin, P. J., Holt, I. and Israel, M. A.** (1998). Cloning of human ENC-1 and evaluation of its expression and regulation in nervous system tumors. *Exp Cell Res* **242**, 470-7.

**Herschman, H. R.** (1991). Primary response genes induced by growth factors and tumor promoters. *Annu Rev Biochem* **60**, 281-319.

**Hess, J., Angel, P. and Schorpp-Kistner, M.** (2004). AP-1 subunits: quarrel and harmony among siblings. *J Cell Sci* **117**, 5965-73.

**Heyninck, K. and Beyaert, R.** (2005). A20 inhibits NF-kappaB activation by dual ubiquitin-editing functions. *Trends Biochem Sci* **30**, 1-4.

**Higashi, T., Isomoto, A., Tyuma, I., Kakishita, E., Uomoto, M. and Nagai, K.** (1985). Quantitative and continuous analysis of ATP release from blood platelets with firefly luciferase luminescence. *Thromb Haemost* **53**, 65-9.

**Hildesheim, J., Bulavin, D. V., Anver, M. R., Alvord, W. G., Hollander, M. C., Vardanian, L. and Fornace, A. J., Jr.** (2002). Gadd45a protects against UV irradiation-

induced skin tumors, and promotes apoptosis and stress signaling via MAPK and p53. *Cancer Res* **62**, 7305-15.

**Hockley, S. L., Arlt, V. M., Brewer, D., Giddings, I. and Phillips, D. H.** (2006). Time- and concentration-dependent changes in gene expression induced by benzo(a)pyrene in two human cell lines, MCF-7 and HepG2. *BMC Genomics* **7**, 260.

**Hoglund, L. and Reichard, P.** (1990). Cytoplasmic 5'(3')-nucleotidase from human placenta. *J Biol Chem* **265**, 6589-95.

**Holcik, M. and Sonenberg, N.** (2005). Translational control in stress and apoptosis. *Nat Rev Mol Cell Biol* **6**, 318-27.

**Holden, P. R., James, N. H., Brooks, A. N., Roberts, R. A., Kimber, I. and Pennie, W. D.** (2000). Identification of a possible association between carbon tetrachloride-induced hepatotoxicity and interleukin-8 expression. *J Biochem Mol Toxicol* **14**, 283-90.

**Hollander, M., Alamo, I., Jackman, J., Wang, M., McBride, O. and Fornace, A., Jr.** (1993). Analysis of the mammalian gadd45 gene and its response to DNA damage. *J. Biol. Chem.* **268**, 24385-24393.

**Honda, R., Tanaka, H. and Yasuda, H.** (1997). Oncoprotein MDM2 is a ubiquitin ligase E3 for tumor suppressor p53. *FEBS Lett* **420**, 25-7.

**Honda, R. and Yasuda, H.** (1999). Association of p19(ARF) with Mdm2 inhibits ubiquitin ligase activity of Mdm2 for tumor suppressor p53. *Embo J* **18**, 22-7.

**Hong, S. Y., Yoon, W. H., Park, J. H., Kang, S. G., Ahn, J. H. and Lee, T. H.** (2000). Involvement of two NF-kappa B binding elements in tumor necrosis factor alpha -, CD40-, and epstein-barr virus latent membrane protein 1-mediated induction of the cellular inhibitor of apoptosis protein 2 gene. *J Biol Chem* **275**, 18022-8.

**Hoppe-Seyler, F. and Butz, K.** (1993). Repression of endogenous p53 transactivation function in HeLa cervical carcinoma cells by human papillomavirus type 16 E6, human mdm-2, and mutant p53. *J Virol* **67**, 3111-7.

**Hopper, A. K. and Phizicky, E. M.** (2003). tRNA transfers to the limelight. *Genes Dev* **17**, 162-80.

**Horibe, T., Gomi, M., Iguchi, D., Ito, H., Kitamura, Y., Masuoka, T., Tsujimoto, I., Kimura, T. and Kikuchi, M.** (2004). Different contributions of the three CXXC motifs of human protein-disulfide isomerase-related protein to isomerase activity and oxidative refolding. *J Biol Chem* **279**, 4604-11.

**Horndasch, M., Lienkamp, S., Springer, E., Schmitt, A., Pavenstadt, H., Walz, G. and Gloy, J.** (2006). The C/EBP homologous protein CHOP (GADD153) is an inhibitor of Wnt/TCF signals. *Oncogene* **25**, 3397-407.

**Hossain, M. A., Bouton, C. M. L., Pevsner, J. and Laterra, J.** (2000). Induction of Vascular Endothelial Growth Factor in Human Astrocytes by Lead. *J. Biol. Chem.* **275**, 27874-27882.

**Houseley, J., LaCava, J. and Tollervey, D.** (2006). RNA-quality control by the exosome. *Nat Rev Mol Cell Biol* **7**, 529-39.

**Hrudey, S., Burch, M, Drikas M and Gregory, R.** (1999). Remedial measures. In *Toxic Cyanobacteria in Water: A guide to their public health consequences, monitoring and management*. London: E & FN Spon.

**Hsiao, E. C., Koniaris, L. G., Zimmers-Koniaris, T., Sebald, S. M., Huynh, T. V. and Lee, S. J.** (2000). Characterization of growth-differentiation factor 15, a transforming growth factor beta superfamily member induced following liver injury. *Mol Cell Biol* **20**, 3742-51.

**Huang, Q., Jin, X., Gaillard, E. T., Knight, B. L., Pack, F. D., Stoltz, J. H., Jayadev, S. and Blanchard, K. T.** (2004). Gene expression profiling reveals multiple toxicity endpoints induced by hepatotoxicants. *Mutation Research/Fundamental and Molecular Mechanisms of Mutagenesis* **549**, 147-167.

**Huang, Z.** (2004). Stress signaling and Myc downregulation: implications for cancer. *Cell Cycle* **3**, 593-6.

**Humpage, A., Fontaine, F., Froscio, S., Burcham, P. and Falconer, I.** (2005). Cylindrospermopsin Genotoxicity and Cytotoxicity: Role Of Cytochrome P-450 and Oxidative Stress. *Journal of Toxicology and Environmental Health Part A* **68**, 739-753.

**Humpage, A. R., Fenech, M., Thomas, P. and Falconer, I. R.** (2000). Micronucleus induction and chromosome loss in transformed human white cells indicate clastogenic and aneugenic action of the cyanobacterial toxin, cylindrospermopsin. *Mutation Research-Genetic Toxicology and Environmental Mutagenesis* **472**, 155-161.

**Ilyin, S. E., Belkowski, S. M. and Plata-Salaman, C. R.** (2004). Biomarker discovery and validation: technologies and integrative approaches. *Trends in Biotechnology* **22**, 411-416.

**Iordanov, M. S., Pribnow, D., Magun, J. L., Dinh, T. H., Pearson, J. A., Chen, S. L. and Magun, B. E.** (1997). Ribotoxic stress response: activation of the stress-activated protein kinase JNK1 by inhibitors of the peptidyl transferase reaction and by sequence-specific RNA damage to the alpha-sarcin/ricin loop in the 28S rRNA. *Mol Cell Biol* **17**, 3373-81.

**Jackson, R. J.** (2005). Alternative mechanisms of initiating translation of mammalian mRNAs. *Biochem Soc Trans* **33**, 1231-41.

**Janssens, S. and Tschopp, J.** (2006). Signals from within: the DNA-damage-induced NF-[kappa]B response. **13**, 773-784.

**Jarrous, N., Eder, P. S., Guerrier-Takada, C., Hoog, C. and Altman, S.** (1998). Autoantigenic properties of some protein subunits of catalytically active complexes of human ribonuclease P. *Rna* **4**, 407-17.

**Jarrous, N., Reiner, R., Wesolowski, D., Mann, H., Guerrier-Takada, C. and Altman, S.** (2001). Function and subnuclear distribution of Rpp21, a protein subunit of the human ribonucleoprotein ribonuclease P. *Rna* **7**, 1153-64.

**Jeong, J. K., Huang, Q., Lau, S. S. and Monks, T. J.** (1997). The response of renal tubular epithelial cells to physiologically and chemically induced growth arrest. *J Biol Chem* **272**, 7511-8.

**Jiang, T., Guerrier-Takada, C. and Altman, S.** (2001). Protein-RNA interactions in the subunits of human nuclear RNase P. *Rna* **7**, 937-41.

**Jin, H. S. and Lee, T. H.** (2006). Cell cycle-dependent expression of cIAP2 at G2/M phase contributes to survival during mitotic cell cycle arrest. *Biochem J* **399**, 335-42.

**Kamimura, D., Ishihara, K. and Hirano, T.** (2003). IL-6 signal transduction and its physiological roles: the signal orchestration model. *Rev Physiol Biochem Pharmacol* **149**, 1-38.

**Kanemoto, S., Kondo, S., Ogata, M., Murakami, T., Urano, F. and Imaizumi, K.** (2005). XBP1 activates the transcription of its target genes via an ACGT core sequence under ER stress. *Biochem Biophys Res Commun* **331**, 1146-53.

**Kapoor, M. and Lozano, G.** (1998). Functional activation of p53 via phosphorylation following DNA damage by UV but not gamma radiation. *PNAS* **95**, 2834-2837.

**Karin, M.** (1995). The Regulation of AP-1 Activity by Mitogen-activated Protein Kinases. *J. Biol. Chem.* **270**, 16483-16486.

**Kastan, M. B.** (1993). P53: a determinant of the cell cycle response to DNA damage. *Adv Exp Med Biol* **339**, 291-3; discussion 295-6.

**Kaufman, R. J.** (1999). Stress signaling from the lumen of the endoplasmic reticulum: coordination of gene transcriptional and translational controls

10.1101/gad.13.10.1211. *Genes Dev.* **13**, 1211-1233.

**Kauzmann, W. J., Chase, A. M. and Brigham, E. H.** (1949). Studies on cell enzyme systems; effect of temperature on the constants in the Michaelis-Menten relation for the luciferin-luciferase system. *Arch Biochem* **24**, 281-8.

**Kearns, J. D., Basak, S., Werner, S. L., Huang, C. S. and Hoffmann, A.** (2006). IkappaBepsilon provides negative feedback to control NF-kappaB oscillations, signaling dynamics, and inflammatory gene expression. *J Cell Biol* **173**, 659-64.

**Keller, D. M., Zeng, X., Wang, Y., Zhang, Q. H., Kapoor, M., Shu, H., Goodman, R., Lozano, G., Zhao, Y. and Lu, H.** (2001). A DNA Damage-Induced p53 Serine 392 Kinase Complex Contains CK2, hSpt16, and SSRP1. *Molecular Cell* **7**, 283-292.

**Khanna, K. K., Lavin, M. F., Jackson, S. P. and Mulhern, T. D.** (2001). ATM, a central controller of cellular responses to DNA damage. *Cell Death Differ* **8**, 1052-65.

**Kim, J. S., Lee, C., Bonifant, C. L., Ressom, H. and Waldman, T.** (2007). Activation of p53-Dependent Growth Suppression in Human Cells by Mutations in PTEN or PIK3CA. *Mol Cell Biol* **27**, 662-677.

**Kim, W. K., In, Y. J., Kim, J. H., Cho, H. J., Kang, S., Lee, C. Y. and Lee, S. C.** (2006). Quantitative relationship of dioxin-responsive gene expression to dioxin response element in Hep3B and HepG2 human hepatocarcinoma cell lines. *Toxicol Lett* **165**, 174-81.

**Kis, E., Szatmari, T., Keszei, M., Farkas, R., Esik, O., Lumniczky, K., Falus, A. and Safrany, G.** (2006). Microarray analysis of radiation response genes in primary human fibroblasts. *Int J Radiat Oncol Biol Phys*.

**Koivu, J., Myllyla, R., Helaakoski, T., Pihlajaniemi, T., Tasanen, K. and Kivirikko, K. I.** (1987). A single polypeptide acts both as the beta subunit of prolyl 4-hydroxylase and as a protein disulfide-isomerase. *J Biol Chem* **262**, 6447-9.

**Kokame, K., Agarwala, K. L., Kato, H. and Miyata, T.** (2000). Herp, a new ubiquitin-like membrane protein induced by endoplasmic reticulum stress. *J Biol Chem* **275**, 32846-53.

**Kokame, K., Kato, H. and Miyata, T.** (1996). Homocysteine-respondent Genes in Vascular Endothelial Cells Identified by Differential Display Analysis. GRP78/BiP AND NOVEL GENES

10.1074/jbc.271.47.29659. *J. Biol. Chem.* **271**, 29659-29665.

**Kokame, K., Kato, H. and Miyata, T.** (2001). Identification of ERSE-II, a new cis-acting element responsible for the ATF6-dependent mammalian unfolded protein response. *J Biol Chem* **276**, 9199-205.

**Korzeniewski, C. and Callewaert, D. M.** (1983). An enzyme-release assay for natural cytotoxicity. *Journal of Immunological Methods* **64**, 313-320.

**Kristensen, M. S., Paludan, K., Larsen, C. G., Zachariae, C. O., Deleuran, B. W., Jensen, P. K., Jorgensen, P. and Thestrup-Pedersen, K.** (1991). Quantitative determination of IL-1 alpha-induced IL-8 mRNA levels in cultured human keratinocytes, dermal fibroblasts, endothelial cells, and monocytes. *J Invest Dermatol* **97**, 506-10.

**Kucharczak, J., Simmons, M. J., Fan, Y. and Gelinas, C.** (2003). To be, or not to be: NF-kappaB is the answer--role of Rel/NF-kappaB in the regulation of apoptosis. *Oncogene* **22**, 8961-82.

**Kunsch, C. and Rosen, C. A.** (1993). NF-kappa B subunit-specific regulation of the interleukin-8 promoter. *Mol Cell Biol* **13**, 6137-46.

**Kwon, Y. W., Masutani, H., Nakamura, H., Ishii, Y. and Yodoi, J.** (2003). Redox regulation of cell growth and cell death. *Biol Chem* **384**, 991-6.

**Lagos, N., Onodera, H., Zagatto, P. A., Andrinolo, D., Azevedo, S. M. and Oshima, Y.** (1999). The first evidence of paralytic shellfish toxins in the fresh water cyanobacterium Cylindrospermopsis raciborskii, isolated from Brazil. *Toxicon* **37**, 1359-73.

**Laitusis, A. L., Brostrom, M. A. and Brostrom, C. O.** (1999). The Dynamic Role of GRP78/BiP in the Coordination of mRNA Translation with Protein Processing. *J. Biol. Chem.* **274**, 486-493.

**Lakin, N. D. and Jackson, S. P.** (1999). Regulation of p53 in response to DNA damage. *Oncogene* **18**, 7644-55.

**Le Jan, S., Le Meur, N., Cazes, A., Philippe, J., Le Cunff, M., Leger, J., Corvol, P. and Germain, S.** (2006). Characterization of the expression of the hypoxia-induced genes neuritin, TXNIP and IGFBP3 in cancer. *FEBS Letters* **580**, 3395-3400.

**Lee, A. H., Iwakoshi, N. N. and Glimcher, L. H.** (2003). XBP-1 regulates a subset of endoplasmic reticulum resident chaperone genes in the unfolded protein response. *Mol Cell Biol* **23**, 7448-59.

**Lee, P. D., Sladek, R., Greenwood, C. M. and Hudson, T. J.** (2002). Control genes and variability: absence of ubiquitous reference transcripts in diverse mammalian expression studies. *Genome Res* **12**, 292-7.

**Levine, A. J.** (1989). The p53 tumor suppressor gene and gene product. *Princess Takamatsu Symp* **20**, 221-30.

**Levine, A. J., Hu, W. and Feng, Z.** (2006). The P53 pathway: what questions remain to be explored? **13**, 1027-1036.

**Lewis, M. J. and Pelham, H. R.** (1990). A human homologue of the yeast HDEL receptor. *Nature* **348**, 162-3.

**Lewis, M. J. and Pelham, H. R.** (1992). Ligand-induced redistribution of a human KDEL receptor from the Golgi complex to the endoplasmic reticulum. *Cell* **68**, 353-64.

**Li, N. and Karin, M.** (1999). Is NF-{kappa}B the sensor of oxidative stress? *FASEB J.* **13**, 1137-1143.

**Li, P. X., Wong, J., Ayed, A., Ngo, D., Brade, A. M., Arrowsmith, C., Austin, R. C. and Klamut, H. J.** (2000). Placental transforming growth factor-beta is a downstream mediator of the growth arrest and apoptotic response of tumor cells to DNA damage and p53 overexpression. *J Biol Chem* **275**, 20127-35.

**Li, Q. and Engelhardt, J. F.** (2006). Interleukin-1beta induction of NFkappaB is partially regulated by H2O2-mediated activation of NFkappaB-inducing kinase. *J Biol Chem* **281**, 1495-505.

**Li, Q., Sanlioglu, S., Li, S., Ritchie, T., Oberley, L. and Engelhardt, J. F.** (2001a). GPx-1 Gene Delivery Modulates NF-kappaB Activation Following Diverse Environmental Injuries Through a Specific Subunit of the IKK Complex. *Antioxidants & Redox Signaling* **3**, 415-432.

**Li, R., Carmichael, W. W., Brittain, S., Eaglesham, G. K., Shaw, G. R., Mahakhant, A., Noparatnaraporn, N., Yongmanitchai, W., Kaya, K. and Watanabe, M. M.** (2001b). Isolation and identification of the cyanotoxin cylindrospermopsin and deoxy-cylindrospermopsin from a Thailand strain of Cylindrospermopsis raciborskii (Cyanobacteria). *Toxicon* **39**, 973-980.

**Li, R. H., Carmichael, W. W., Brittain, S., Eaglesham, G. K., Shaw, G. R., Liu, Y. D. and Watanabe, M. M.** (2001c). First report of the cyanotoxins cylindrospermopsin and deoxycylindrospermopsin from Raphidiopsis curvata (Cyanobacteria). *Journal of Phycology* **37**, 1121-1126.

**Li, W. W., Alexandre, S., Cao, X. and Lee, A. S.** (1993). Transactivation of the grp78 promoter by Ca2+ depletion. A comparative analysis with A23187 and the endoplasmic reticulum Ca(2+)-ATPase inhibitor thapsigargin. *J Biol Chem* **268**, 12003-9.

**Liang, X. H., Volkmann, M., Klein, R., Herman, B. and Lockett, S. J.** (1993). Co-localization of the tumor-suppressor protein p53 and human papillomavirus E6 protein in human cervical carcinoma cell lines. *Oncogene* **8**, 2645-52.

**Liao, J., Piwien-Pilipuk, G., Ross, S. E., Hodge, C. L., Sealy, L., MacDougald, O. A. and Schwartz, J.** (1999). CCAAT/enhancer-binding protein beta (C/EBPbeta) and C/EBPdelta contribute to growth hormone-regulated transcription of c-fos. *J Biol Chem* **274**, 31597-604.

**Libermann, T. A. and Baltimore, D.** (1990). Activation of interleukin-6 gene expression through the NF-kappa B transcription factor. *Mol Cell Biol* **10**, 2327-34.

**Linder, P.** (2006). Dead-box proteins: a family affair--active and passive players in RNP-remodeling. *Nucl. Acids Res.* **34**, 4168-4180.

**Liu, E. S. and Lee, A. S.** (1991). Common sets of nuclear factors binding to the conserved promoter sequence motif of two coordinately regulated ER protein genes, GRP78 and GRP94. *Nucleic Acids Res* **19**, 5425-31.

**Liu, J. and Levens, D.** (2006). Making myc. *Curr Top Microbiol Immunol* **302**, 1-32.

**Livak, K. J. and Schmittgen, T. D.** (2001). Analysis of relative gene expression data using real-time quantitative PCR and the 2(-Delta Delta C(T)) Method. *Methods* **25**, 402-8.

**Lu, T., Liu, J., LeCluyse, E. L., Zhou, Y. S., Cheng, M. L. and Waalkes, M. P.** (2001). Application of cDNA microarray to the study of arsenic-induced liver diseases in the population of Guizhou, China. *Toxicol Sci* **59**, 185-92.

**Luethy, J. D. and Holbrook, N. J.** (1992). Activation of the gadd153 promoter by genotoxic agents: a rapid and specific response to DNA damage. *Cancer Res* **52**, 5-10.

**Ma, T., Van Tine, B. A., Wei, Y., Garrett, M. D., Nelson, D., Adams, P. D., Wang, J., Qin, J., Chow, L. T. and Harper, J. W.** (2000). Cell cycle-regulated phosphorylation of p220NPAT by cyclin E/Cdk2 in Cajal bodies promotes histone gene transcription

10.1101/gad.829500. *Genes Dev.* **14**, 2298-2313.

**Mackenzie, B. and Erickson, J. D.** (2004). Sodium-coupled neutral amino acid (System N/A) transporters of the SLC38 gene family. *Pflugers Arch* **447**, 784-95.

**Maglott, D., Ostell, J., Pruitt, K. D. and Tatusova, T.** (2005). Entrez Gene: gene-centered information at NCBI. *Nucleic Acids Res* **33**, D54-8.

**Maity, S. N. and de Crombrugghe, B.** (1998). Role of the CCAAT-binding protein CBF/NF-Y in transcription. *Trends Biochem Sci* **23**, 174-8.

**Malek, S., Huxford, T. and Ghosh, G.** (1998). Ikappa Balpha functions through direct contacts with the nuclear localization signals and the DNA binding sequences of NF-kappaB. *J Biol Chem* **273**, 25427-35.

**Malinin, N. L., Boldin, M. P., Kovalenko, A. V. and Wallach, D.** (1997). MAP3K-related kinase involved in NF-kappaB induction by TNF, CD95 and IL-1. *Nature* **385**, 540-4.

**Marionnet, A. V., Lizard, G., Chardonnet, Y. and Schmitt, D.** (1997). Comparative evaluation of the antiproliferative effect of cyclosporin A and gamma-interferon on normal and HPV-transformed keratinocytes by cell counting, MTT assay and tritiated thymidine incorporation. *Cell Biology and Toxicology* **13**, 115-123.

**Martin, M. U. and Wesche, H.** (2002). Summary and comparison of the signaling mechanisms of the Toll/interleukin-1 receptor family. *Biochim Biophys Acta* **1592**, 265-80.

**Masutani, C., Kusumoto, R., Yamada, A., Dohmae, N., Yokoi, M., Yuasa, M., Araki, M., Iwai, S., Takio, K. and Hanaoka, F.** (1999). The XPV (xeroderma pigmentosum variant) gene encodes human DNA polymerase eta. *Nature* **399**, 700-4.

**Masutani, C., Sugasawa, K., Yanagisawa, J., Sonoyama, T., Ui, M., Enomoto, T., Takio, K., Tanaka, K., van der Spek, P. J., Bootsma, D. et al.** (1994). Purification and cloning of a nucleotide excision repair complex involving the xeroderma pigmentosum group C protein and a human homologue of yeast RAD23. *Embo J* **13**, 1831-43.

**Matsumoto, S., Tsuji-Takayama, K., Aizawa, Y., Koide, K., Takeuchi, M., Ohta, T. and Kurimoto, M.** (1997). Interleukin-18 activates NF-kappaB in murine T helper type 1 cells. *Biochem Biophys Res Commun* **234**, 454-7.

**Matsuoka, S., Huang, M. and Elledge, S. J.** (1998). Linkage of ATM to Cell Cycle Regulation by the Chk2 Protein Kinase. *Science* **282**, 1893-1897.

**Mattick, J. S. and Makunin, I. V.** (2006). Non-coding RNA. *Hum Mol Genet* **15 Spec No 1**, R17-29.

**Mayer, M. P. and Bukau, B.** (2005). Hsp70 chaperones: cellular functions and molecular mechanism. *Cell Mol Life Sci* **62**, 670-84.

**McCoy, C. E., Campbell, D. G., Deak, M., Bloomberg, G. B. and Arthur, J. S.** (2005). MSK1 activity is controlled by multiple phosphorylation sites. *Biochem J* **387**, 507-17.

**McGregor, G. B. and Fabbro, L. D.** (2000). Dominance of *Cylindrospermopsis raciborskii* (Nostocales, Cyanoprokaryota) in Queensland tropical and subtropical reservoirs: Implications for monitoring and management. *Lakes Reserv Res Manage* **5**, 195-205.

**McGuire, M., Lipsky, P. and Thiele, D.** (1993). Generation of active myeloid and lymphoid granule serine proteases requires processing by the granule thiol protease dipeptidyl peptidase I. *J. Biol. Chem.* **268**, 2458-2467.

**Meek, D. W.** (1998). Multisite phosphorylation and the integration of stress signals at p53. *Cell Signal* **10**, 159-66.

**Meek, D. W.** (2004). The p53 response to DNA damage. *DNA Repair* **3**, 1049-1056.

**Meighan-Mantha, R. L., Hsu, D. K. W., Guo, Y., Brown, S. A. N., Feng, S.-L. Y., Peifley, K. A., Alberts, G. F., Copeland, N. G., Gilbert, D. J., Jenkins, N. A. et al.** (1999). The Mitogen-inducible Fn14 Gene Encodes a Type I Transmembrane Protein that Modulates Fibroblast Adhesion and Migration

10.1074/jbc.274.46.33166. *J. Biol. Chem.* **274**, 33166-33176.

**Mercurio, F. and Manning, A. M.** (1999). NF-kappaB as a primary regulator of the stress response. *Oncogene* **18**, 6163-71.

**Metcalf, J. S., Barakate, A. and Codd, G. A.** (2004). Inhibition of plant protein synthesis by the cyanobacterial hepatotoxin, cylindrospermopsin. *FEMS Microbiol Lett* **235**, 125-9.

**Metcalf, J. S., Lindsay, J., Beattie, K. A., Birmingham, S., Saker, M. L., Torokne, A. K. and Codd, G. A.** (2002). Toxicity of cylindrospermopsin to the brine shrimp Artemia salina: comparisons with protein synthesis inhibitors and microcystins. *Toxicon* **40**, 1115-120.

**Meyer, N., Kim, S. S. and Penn, L. Z.** (2006). The Oscar-worthy role of Myc in apoptosis. *Semin Cancer Biol* **16**, 275-87.

**Mikule, K., Delaval, B., Kaldis, P., Jurcyzk, A., Hergert, P. and Doxsey, S.** (2007). Loss of centrosome integrity induces p38-p53-p21-dependent G1-S arrest. **9**, 160-170.

**Milne, D. M., Campbell, L. E., Campbell, D. G. and Meek, D. W.** (1995). p53 Is Phosphorylated in Vitro and in Vivo by an Ultraviolet Radiation-induced Protein Kinase Characteristic of the c-Jun Kinase, JNK1

10.1074/jbc.270.10.5511. *J. Biol. Chem.* **270**, 5511-5518.

**Mitchel, R. E. J., Azzam, E. I. and de Toledo, S. M.** (1997). Adaptation to Ionizing Radiation in Eukaryotic Cells. In *Stress-Inducible Processes in Higher Eukaryotic Cells*, (ed. T. M. Koval): Plenum Press, New York, U.S.A.

**Mitchison, T.** (1995). Evolution of a Dynamic Cytoskeleton. *Philosophical Transactions of the Royal Society B: Biological Sciences* **349**, 299-304.

**Miyazaki, Y., Shinomura, Y., Tsutsui, S., Yasunaga, Y., Zushi, S., Higashiyama, S., Taniguchi, N. and Matsuzawa, Y.** (1996). Oxidative stress increases gene expression of heparin-binding EGF-like growth factor and amphiregulin in cultured rat gastric epithelial cells. *Biochem Biophys Res Commun* **226**, 542-6.

**Moon, Y. and Pestka, J. J.** (2003). Cyclooxygenase-2 mediates interleukin-6 upregulation by vomitoxin (deoxynivalenol) in vitro and in vivo. *Toxicol Appl Pharmacol* **187**, 80-8.

**Moravec, R. A.** (1994). Total cell quantitation using the CytoTox 96® Non-Radioactive Cytotoxicity Assay. *Promega Notes* **45**, 11-12.

**Morgan, I. M. and Birnie, G. D.** (1992). The serum response element and an AP-1/ATF sequence immediately downstream co-operate in the regulation of c-fos transcription. *Cell Prolif* **25**, 205-15.

**Mori, N. and Prager, D.** (1996). Transactivation of the interleukin-1alpha promoter by human T-cell leukemia virus type I and type II Tax proteins. *Blood* **87**, 3410-7.

**Mosmann, T.** (1983). Rapid colorimetric assay for cellular growth and survival: application to proliferation and cytotoxicity assays. *J Immunol Methods* **65**, 55-63.

**Munishkin, A. and Wool, I. G.** (1995). Systematic deletion analysis of ricin A-chain function. Single amino acid deletions. *J Biol Chem* **270**, 30581-7.

**Munro, S. and Pelham, H. R.** (1986). An Hsp70-like protein in the ER: identity with the 78 kd glucose-regulated protein and immunoglobulin heavy chain binding protein. *Cell* **46**, 291-300.

**Munro, S. and Pelham, H. R. B.** (1987). A C-terminal signal prevents secretion of luminal ER proteins. *Cell* **48**, 899-907.

**Mur, L. R., Skulberg, O. M. and Utkilen, H.** (1999). Cyanobacteria in the Environment. In *Toxic Cyanobacteria in Water: A guide to their public health consequences, monitoring and management*, pp. 14-39. London: E & FN Spon.

**Nakamura, H.** (2005). Thioredoxin and its related molecules: update 2005. *Antioxid Redox Signal* **7**, 823-8.

**Nakano, H., Nakajima, A., Sakon-Komazawa, S., Piao, J. H., Xue, X. and Okumura, K.** (2006). Reactive oxygen species mediate crosstalk between NF-kappaB and JNK. *Cell Death Differ* **13**, 730-7.

**Nakayama, M., Ishidoh, K., Kayagaki, N., Kojima, Y., Yamaguchi, N., Nakano, H., Kominami, E., Okumura, K. and Yagita, H.** (2002). Multiple Pathways of TWEAK-Induced Cell Death. *J Immunol* **168**, 734-743.

**Neilan, B. A., Saker, M. L., Fastner, J., Torokne, A. and Burns, B. P.** (2003). Phylogeography of the invasive cyanobacterium Cylindrospermopsis raciborskii. *Molecular Ecology* **12**, 133-140.

**Nelson, D. E., Ihekwaba, A. E., Elliott, M., Johnson, J. R., Gibney, C. A., Foreman, B. E., Nelson, G., See, V., Horton, C. A., Spiller, D. G. et al.** (2004). Oscillations in NF-kappaB signaling control the dynamics of gene expression. *Science* **306**, 704-8.

**Nelson, D. M., Ye, X., Hall, C., Santos, H., Ma, T., Kao, G. D., Yen, T. J., Harper, J. W. and Adams, P. D.** (2002). Coupling of DNA Synthesis and Histone Synthesis in S Phase Independent of Cyclin/cdk2 Activity. *Mol. Cell. Biol.* **22**, 7459-7472.

**Nigam, S. K., Goldberg, A. L., Ho, S., Rohde, M. F., Bush, K. T. and Sherman, M.** (1994). A set of endoplasmic reticulum proteins possessing properties of molecular chaperones includes Ca(2+)-binding proteins and members of the thioredoxin superfamily. *J Biol Chem* **269**, 1744-9.

**Niida, A., Hiroko, T., Kasai, M., Furukawa, Y., Nakamura, Y., Suzuki, Y., Sugano, S. and Akiyama, T.** (2004). DKK1, a negative regulator of Wnt signaling, is a target of the beta-catenin/TCF pathway. *Oncogene* **23**, 8520-6.

**Nishiyama, A., Matsui, M., Iwata, S., Hirota, K., Masutani, H., Nakamura, H., Takagi, Y., Sono, H., Gon, Y. and Yodoi, J.** (1999). Identification of thioredoxin-binding protein-2/vitamin D(3) up-regulated protein 1 as a negative regulator of thioredoxin function and expression. *J Biol Chem* **274**, 21645-50.

**Norris, R. L., Eaglesham, G. K., Shaw, G. R., Senogles, P., Chiswell, R. K., Smith, M. J., Davis, B. C., Seawright, A. A. and Moore, M. R.** (2001). Extraction and purification of the zwitterions cylindrospermopsin and deoxycylindrospermopsin from Cylindrospermopsis raciborskii. *Environ Toxicol* **16**, 391-6.

**Nottrott, S., Urlaub, H. and Luhrmann, R.** (2002). Hierarchical, clustered protein interactions with U4/U6 snRNA: a biochemical role for U4/U6 proteins. *Embo J* **21**, 5527-38.

**Novina, C. D. and Roy, A. L.** (1996). Core promoters and transcriptional control. *Trends Genet* **12**, 351-5.

**O'Day, C., Chavanikamannil, F. and Abelson, J.** (1996). 18S rRNA processing requires the RNA helicase-like protein Rrp3. *Nucl. Acids Res.* **24**, 3201-3207.

**Oda, K., Arakawa, H., Tanaka, T., Matsuda, K., Tanikawa, C., Mori, T., Nishimori, H., Tamai, K., Tokino, T., Nakamura, Y. et al.** (2000). p53AIP1, a Potential Mediator of p53-Dependent Apoptosis, and Its Regulation by Ser-46-Phosphorylated p53. *Cell* **102**, 849-862.

**Offer, H., Erez, N., Zurer, I., Tang, X., Milyavsky, M., Goldfinger, N. and Rotter, V.** (2002). The onset of p53-dependent DNA repair or apoptosis is determined by the level of accumulated damaged DNA. *Carcinogenesis* **23**, 1025-32.

**Ogata, H., Goto, S., Sato, K., Fujibuchi, W., Bono, H. and Kanehisa, M.** (1999). KEGG: Kyoto Encyclopedia of Genes and Genomes. *Nucleic Acids Res* **27**, 29-34.

**Ohtani, I., Moore, R. E. and Runnegar, M. T. C.** (1992). Cylindrospermopsin: A potent hepatotoxin from blue-green algae Cylindrospermopsis raciborskii. *J. Amer. Chem. Soc.* **114**, 7941-7942.

**Okano, J.-i. and Rustgi, A. K.** (2001). Paclitaxel Induces Prolonged Activation of the Ras/MEK/ERK Pathway Independently of Activating the Programmed Cell Death Machinery

10.1074/jbc.M011164200. *J. Biol. Chem.* **276**, 19555-19564.

**Owellen, R. J., Owens, A. H., Jr. and Donigian, D. W.** (1972). The binding of vincristine, vinblastine and colchicine to tubulin. *Biochem Biophys Res Commun* **47**, 685-91.

**Oyadomari, S. and Mori, M.** (2004). Roles of CHOP/GADD153 in endoplasmic reticulum stress. *Cell Death Differ* **11**, 381-9.

**Padisak, J.** (1997). Cylindrospermopsis raciborskii (Woloszynska) Seenayya et Subba Raju, an expanding, highly adaptive cyanobacterium: worldwide distribution and review of its ecology. *Archiv Hydrobiologie* **107**, 563-593.

**Pahl, H. L.** (1999). Activators and target genes of Rel/NF-kappaB transcription factors. *Oncogene* **18**, 6853-66.

**Palii, S. S., Chen, H. and Kilberg, M. S.** (2004). Transcriptional control of the human sodium-coupled neutral amino acid transporter system A gene by amino acid availability is mediated by an intronic element. *J Biol Chem* **279**, 3463-71.

**Papa, S., Zazzeroni, F., Bubici, C., Jayawardena, S., Alvarez, K., Matsuda, S., Nguyen, D. U., Pham, C. G., Nelsbach, A. H., Melis, T. et al.** (2004). Gadd45 beta mediates the NF-kappa B suppression of JNK signalling by targeting MKK7/JNKK2. *Nat Cell Biol* **6**, 146-53.

**Paralkar, V. M., Vail, A. L., Grasser, W. A., Brown, T. A., Xu, H., Vukicevic, S., Ke, H. Z., Qi, H., Owen, T. A. and Thompson, D. D.** (1998). Cloning and characterization of a novel member of the transforming growth factor-beta/bone morphogenetic protein family. *J Biol Chem* **273**, 13760-7.

**Patterson, C. E., Gao, J., Rooney, A. P. and Davis, E. C.** (2002). Genomic organization of mouse and human 65 kDa FK506-binding protein genes and evolution of the FKBP multigene family. *Genomics* **79**, 881-9.

**Patton, J. R., Bykhovskaya, Y., Mengesha, E., Bertolotto, C. and Fischel-Ghodsian, N.** (2005). Mitochondrial myopathy and sideroblastic anemia (MLASA): missense mutation in the pseudouridine synthase 1 (PUS1) gene is associated with the loss of tRNA pseudouridylation. *J Biol Chem* **280**, 19823-8.

**Pelengaris, S. and Khan, M.** (2003). The many faces of c-MYC. *Arch Biochem Biophys* **416**, 129-36.

**Pelham, H. R.** (1988). Evidence that luminal ER proteins are sorted from secreted proteins in a post-ER compartment. *Embo J* **7**, 913-8.

**Pennie, W., Pettit, S. D. and Lord, P. G.** (2004). Toxicogenomics in risk assessment: an overview of an HESI collaborative research program. *Environ Health Perspect* **112**, 417-9.

**Pestka, S.** (1976). Insights into protein biosynthesis and ribosome function through inhibitors. *Prog Nucleic Acid Res Mol Biol* **17**, 217-45.

**Pfaffl, M. W., Horgan, G. W. and Dempfle, L.** (2002). Relative expression software tool (REST) for group-wise comparison and statistical analysis of relative expression results in real-time PCR. *Nucleic Acids Res* **30**, e36.

**Pihlajaniemi, T., Helaakoski, T., Tasanen, K., Myllyla, R., Huhtala, M. L., Koivu, J. and Kivirikko, K. I.** (1987). Molecular cloning of the beta-subunit of human prolyl 4-hydroxylase. This subunit and protein disulphide isomerase are products of the same gene. *Embo J* **6**, 643-9.

**Piquemal, D., Joulia, D., Balaguer, P., Basset, A., Marti, J. and Commes, T.** (1999). Differential expression of the RTP/Drg1/Ndr1 gene product in proliferating and growth arrested cells. *Biochim Biophys Acta* **1450**, 364-73.

**Pisano, C., Battistoni, A., Antoccia, A., Degrassi, F. and Tanzarella, C.** (2000). Changes in microtubule organization after exposure to a benzimidazole derivative in Chinese hamster cells. *Mutagenesis* **15**, 507-15.

**Promega.** (2003a). CellTiter-Glo® Luminescent Cell Viability Assay Technical Bulletin #TB288, Promega Corporation.

**Promega.** (2003b). CellTiter 96 ® AQueous One Solution Cell Proliferation Assay Technical Bulletin #TB112, Promega Corporation.

**Promega.** (2003c). CytoTox ONE™ Homogenous Membrane Integrity Assay, Technical Bulletin #TB306, (ed.

**Pulverer, B. J., Kyriakis, J. M., Avruch, J., Nikolakaki, E. and Woodgett, J. R.** (1991). Phosphorylation of c-jun mediated by MAP kinases. **353**, 670-674.

**Rabbitts, P. H., Watson, J. V., Lamond, A., Forster, A., Stinson, M. A., Evan, G., Fischer, W., Atherton, E., Sheppard, R. and Rabbitts, T. H.** (1985). Metabolism of c-myc gene products: c-myc mRNA and protein expression in the cell cycle. *Embo J* **4**, 2009-15.

**Rajeevan, M. S., Vernon, S. D., Taysavang, N. and Unger, E. R.** (2001). Validation of array-based gene expression profiles by real-time (kinetic) RT-PCR. *J Mol Diagn* **3**, 26-31.

**Ramirez, S., Ait-Si-Ali, S., Robin, P., Trouche, D. and Harel-Bellan, A.** (1997). The CREB-binding protein (CBP) cooperates with the serum response factor for transactivation of the c-fos serum response element. *J Biol Chem* **272**, 31016-21.

**Rampazzo, C., Johansson, M., Gallinaro, L., Ferraro, P., Hellman, U., Karlsson, A., Reichard, P. and Bianchi, V.** (2000). Mammalian 5'(3')-deoxyribonucleotidase, cDNA cloning, and overexpression of the enzyme in Escherichia coli and mammalian cells. *J Biol Chem* **275**, 5409-15.

**Rangatia, J., Vangala, R. K., Singh, S. M., Peer Zada, A. A., Elsasser, A., Kohlmann, A., Haferlach, T., Tenen, D. G., Hiddemann, W. and Behre, G.** (2003). Elevated c-Jun expression in acute myeloid leukemias inhibits C/EBPalpha DNA binding via leucine zipper domain interaction. *Oncogene* **22**, 4760-4.

**Ravagnan, L., Gurbuxani, S., Susin, S. A., Maisse, C., Daugas, E., Zamzami, N., Mak, T., Jaattela, M., Penninger, J. M., Garrido, C. et al.** (2001). Heat-shock protein 70 antagonizes apoptosis-inducing factor. *Nat Cell Biol* **3**, 839-43.

**Reddy, P.** (2004). Interleukin-18: recent advances. *Curr Opin Hematol* **11**, 405-10.

**Ricicki, E. M., Luo, W., Fan, W., Zhao, L. P., Zarbl, H. and Vouros, P.** (2006). Quantification of N-(deoxyguanosin-8-yl)-4-aminobiphenyl adducts in human lymphoblastoid TK6 cells dosed with N-hydroxy-4-acetylaminobiphenyl and their relationship to mutation, toxicity, and gene expression profiling. *Anal Chem* **78**, 6422-32.

**Rinaldo, C., Prodosmo, A., Mancini, F., Iacovelli, S., Sacchi, A., Moretti, F. and Soddu, S.** (2007). MDM2-Regulated Degradation of HIPK2 Prevents p53Ser46 Phosphorylation and DNA Damage-Induced Apoptosis. *Mol Cell* **25**, 739-50.

**Ririe, K. M., Rasmussen, R. P. and Wittwer, C. T.** (1997). Product differentiation by analysis of DNA melting curves during the polymerase chain reaction. *Anal Biochem* **245**, 154-60.

**Rodriguez-Antona, C., Donato, M. T., Boobis, A., Edwards, R. J., Watts, P. S., Castell, J. V. and Gomez-Lechon, M.-J.** (2002). Cytochrome P450 expression in human hepatocytes and hepatoma cell lines: molecular mechanisms that determine lower expression in cultured cells. *Xenobiotica* **32**, 505-520.

**Roebuck, K. A.** (1999). Regulation of interleukin-8 gene expression. *J Interferon Cytokine Res* **19**, 429-38.

**Rosenberg, H. F. and Dyer, K. D.** (1995). Human ribonuclease 4 (RNase 4): coding sequence, chromosomal localization and identification of two distinct transcripts in human somatic tissues. *Nucleic Acids Res* **23**, 4290-5.

**Rouault, J. P., Falette, N., Guehenneux, F., Guillot, C., Rimokh, R., Wang, Q., Berthet, C., Moyret-Lalle, C., Savatier, P., Pain, B. et al.** (1996). Identification of BTG2, an antiproliferative p53-dependent component of the DNA damage cellular response pathway. *Nat Genet* **14**, 482-6.

**Roy, B. and Lee, A.** (1999). The mammalian endoplasmic reticulum stress response element consists of an evolutionarily conserved tripartite structure and interacts with a novel stress-inducible complex

10.1093/nar/27.6.1437. *Nucl. Acids Res.* **27**, 1437-1443.

**Rozen, S. and Skaletsky, H.** (2000). Primer3 on the WWW for general users and for biologist programmers. *Methods Mol Biol* **132**, 365-86.

**Ruegsegger, U., Beyer, K. and Keller, W.** (1996). Purification and characterization of human cleavage factor Im involved in the 3' end processing of messenger RNA precursors. *J Biol Chem* **271**, 6107-13.

**Rundlof, A.-K., Carlsten, M. and Arner, E. S. J.** (2001). The Core Promoter of Human Thioredoxin Reductase 1. *J. Biol. Chem.* **276**, 30542-30551.

**Rundlof, A. K., Janard, M., Miranda-Vizuete, A. and Arner, E. S.** (2004). Evidence for intriguingly complex transcription of human thioredoxin reductase 1. *Free Radic Biol Med* **36**, 641-56.

**Runnegar, M., Berndt, N., Kong, S. M., Lee, E. Y. and Zhang, L.** (1995a). In vivo and in vitro binding of microcystin to protein phosphatases 1 and 2A. *Biochem Biophys Res Commun* **216**, 162-9.

**Runnegar, M. T., Kong, S. M., Zhong, Y. Z., Ge, J. L. and Lu, S. C.** (1994). The role of glutathione in the toxicity of a novel cyanobacterial alkaloid cylindrospermopsin in cultured rat hepatocytes. *Biochem Biophys Res Commun* **201**, 235-41.

**Runnegar, M. T., Kong, S. M., Zhong, Y. Z. and Lu, S. C.** (1995b). Inhibition of reduced glutathione synthesis by cyanobacterial alkaloid cylindrospermopsin in cultured rat hepatocytes. *Biochem Pharmacol* **49**, 219-25.

**Runnegar, M. T., Xie, C. Y., Snider, B. B., Wallace, G. A., Weinreb, S. M. and Kuhlenkamp, J.** (2002). In vitro hepatotoxicity of the cyanobacterial alkaloid cylindrospermopsin and related synthetic analogues. *Toxicological Sciences* **67**, 81-87.

**Saker, M. L., Nogueira, I. C. G., Vasconcelos, V. M., Neilan, B. A., Eaglesham, G. K. and Pereira, P.** (2003). First report and toxicological assessment of the cyanobacterium Cylindrospermopsis raciborskii from Portuguese freshwaters. *Ecotoxicology and Environmental Safety* **55**, 243-250.

**Sakurai, A., Nishimoto, M., Himeno, S., Imura, N., Tsujimoto, M., Kunimoto, M. and Hara, S.** (2005). Transcriptional regulation of thioredoxin reductase 1 expression by cadmium in vascular endothelial cells: role of NF-E2-related factor-2. *J Cell Physiol* **203**, 529-37.

**Sambrook, J. and Russell, D. W.** (2003). Molecular cloning : a laboratory manual. Cold Spring Harbour, N.Y.: Cold Spring Harbor Laboratory Press.

**Sambuy, Y., Angelis, I. D., Ranaldi, G., Scarino, M. L., Stammati, A. and Zucco, F.** (2005). The Caco-2 cell line as a model of the intestinal barrier: influence of cell and culture-related factors on Caco-2 cell functional characteristics. *Cell Biology and Toxicology* **V21**, 1-26.

**Samuel, C.** (1993). The eIF-2 alpha protein kinases, regulators of translation in eukaryotes from yeasts to humans. *J. Biol. Chem.* **268**, 7603-7606.

**Sanchez-Prieto, R., Rojas, J. M., Taya, Y. and Gutkind, J. S.** (2000). A role for the p38 mitogen-acitvated protein kinase pathway in the transcriptional activation of p53 on genotoxic stress by chemotherapeutic agents. *Cancer Res* **60**, 2464-72.

**Sassa, S., Sugita, O., Galbraith, R. A. and Kappas, A.** (1987). Drug metabolism by the human hepatoma cell, Hep G2. *Biochemical and Biophysical Research Communications* **143**, 52-57.

**Savitz, A. J. and Meyer, D. I.** (1990). Identification of a ribosome receptor in the rough endoplasmic reticulum. *Nature* **346**, 540-4.

**Schiff, P. B., Fant, J. and Horwitz, S. B.** (1979). Promotion of microtubule assembly in vitro by taxol. *Nature* **277**, 665-7.

**Schiff, P. B. and Horwitz, S. B.** (1980). Taxol stabilizes microtubules in mouse fibroblast cells. *Proc Natl Acad Sci U S A* **77**, 1561-5.

**Schneeberger, C., Speiser, P., Kury, F. and Zeillinger, R.** (1995). Quantitative detection of reverse transcriptase-PCR products by means of a novel and sensitive DNA stain. *PCR Methods Appl* **4**, 234-8.

**Schneider, P., Schwenzer, R., Haas, E., Mühlenbeck, F., Schubert, G., Scheurich, P., Tschopp, J. and Wajant, H.** (1999). TWEAK can induce cell death via endogenous TNF and TNF receptor 1. *European Journal of Immunology* **29**, 1785-1792.

**Schug, J. and Overton, G. C.** (1997). TESS: Transcription Element Search Software on the WWW. In *Technical Report CBIL-TR-1997-1001-v0.0*, (ed.: School of Medicine, University of Pennsylvania.

**Schuler, M. and Green, D. R.** (2001). Mechanisms of p53-dependent apoptosis. *Biochem Soc Trans* **29**, 684-8.

**Schulze, P. C., Yoshioka, J., Takahashi, T., He, Z., King, G. L. and Lee, R. T.** (2004). Hyperglycemia Promotes Oxidative Stress through Inhibition of Thioredoxin Function by Thioredoxin-interacting Protein

10.1074/jbc.M400549200. *J. Biol. Chem.* **279**, 30369-30374.

**Scott, R., Bergman, B., Bajpai, A., Hersh, R., Rodriguez, H., Jones, B., Barreda, C., Watts, S. and Baker, J.** (1985). Protease nexin. Properties and a modified purification procedure. *J. Biol. Chem.* **260**, 7029-7034.

**Seawright, A. A., Nolan, C. C., Shaw, G. R., Chiswell, R. K., Norris, R. L., Moore, M. R. and Smith, M. J.** (1999). The oral toxicity for mice of the tropical cyanobacterium Cylindrospermopsis raciborskii (Woloszynska). *Environmental Toxicology* **14**, 135-142.

**Secchiero, P., Barbarotto, E., Tiribelli, M., Zerbinati, C., di Iasio, M. G., Gonelli, A., Cavazzini, F., Campioni, D., Fanin, R., Cuneo, A. et al.** (2006). Functional integrity of the p53-mediated apoptotic pathway induced by the nongenotoxic agent nutlin-3 in B-cell chronic lymphocytic leukemia (B-CLL). *Blood* **107**, 4122-9.

**Seibenhener, M. L., Babu, J. R., Geetha, T., Wong, H. C., Krishna, N. R. and Wooten, M. W.** (2004). Sequestosome 1/p62 is a polyubiquitin chain binding protein involved in ubiquitin proteasome degradation. *Mol Cell Biol* **24**, 8055-68.

**Sekiguchi, T., Hayano, T., Yanagida, M., Takahashi, N. and Nishimoto, T.** (2006). NOP132 is required for proper nucleolus localization of DEAD-box RNA helicase DDX47. *Nucleic Acids Res* **34**, 4593-608.

**Sen, R. and Baltimore, D.** (1986). Inducibility of [kappa] immunoglobulin enhancer-binding protein NF-[kappa]B by a posttranslational mechanism. *Cell* **47**, 921-928.

**Sengupta, S. and Harris, C. C.** (2005). p53: traffic cop at the crossroads of DNA repair and recombination. *Nat Rev Mol Cell Biol* **6**, 44-55.

**Senogles-Derham, P.-J., Seawright, A., Shaw, G., Wickramisingh, W. and Shahin, M.** (2003). Toxicological aspects of treatment to remove cyanobacterial toxins from drinking water determined using the heterozygous P53 transgenic mouse model. *Toxicon* **41**, 979-988.

**Shaulian, E. and Karin, M.** (2002). AP-1 as a regulator of cell life and death. *Nat Cell Biol* **4**, E131-6.

**Shaw, G. R., Seawright, A. A., Moore, M. R. and Lam, P. K. S.** (2000). Cylindrospermopsin, a cyanobacterial alkaloid: Evaluation of its toxicologic activity. *Therapeutic Drug Monitoring* **22**, 89-92.

**Shaw, G. R., Sukenik, A., Livne, A., Chiswell, R. K., Smith, M. J., Seawright, A. A., Norris, R. L., Eaglesham, G. K. and Moore, M. R.** (1999). Blooms of the cylindrospermopsin containing cyanobacterium, Aphanizomenon ovalisporum (Forti), in newly constructed lakes, Queensland, Australia. *Environmental Toxicology* **14**, 167-177.

**Shen, J., Chen, X., Hendershot, L. and Prywes, R.** (2002a). ER Stress Regulation of ATF6 Localization by Dissociation of BiP/GRP78 Binding and Unmasking of Golgi Localization Signals. *Developmental Cell* **3**, 99-111.

**Shen, X. Y., Lam, P. K. S., Shaw, G. R. and Wickramasinghe, W.** (2002b). Genotoxicity investigation of a cyanobacterial toxin, cylindrospermopsin. *Toxicon* **40**, 1499-1501.

**Shena, M., Shalon, D., Davis, R.W. and Brown, P.O.** (1995). Quantitative Monitoring of Gene Expression Patterns with a Complementary DNA Microarray. *Science*, 467-470.

**Sheng, M., Thompson, M. A. and Greenberg, M. E.** (1991). CREB: a Ca2+-regulated transcription factor phosphorylated by calmodulin-dependent kinases. *Science* **252**, 1427-431.

**Shieh, S.-Y., Ahn, J., Tamai, K., Taya, Y. and Prives, C.** (2000). The human homologs of checkpoint kinases Chk1 and Cds1 (Chk2) phosphorylate p53 at multiple DNA damage-inducible sites

10.1101/gad.14.3.289. *Genes Dev.* **14**, 289-300.

**Shieh, S. Y., Ikeda, M., Taya, Y. and Prives, C.** (1997). DNA damage-induced phosphorylation of p53 alleviates inhibition by MDM2. *Cell* **91**, 325-34.

**Shifrin, V. I. and Anderson, P.** (1999). Trichothecene mycotoxins trigger a ribotoxic stress response that activates c-Jun N-terminal kinase and p38 mitogen-activated protein kinase and induces apoptosis. *J Biol Chem* **274**, 13985-92.

**Shimono, A., Okuda, T. and Kondoh, H.** (1999). N-myc-dependent repression of Ndr1, a gene identified by direct subtraction of whole mouse embryo cDNAs between wild type and N-myc mutant. *Mechanisms of Development* **83**, 39-52.

**Shou, J., Ali-Osman, F., Multani, A. S., Pathak, S., Fedi, P. and Srivenugopal, K. S.** (2002). Human Dkk-1, a gene encoding a Wnt antagonist, responds to DNA damage and its overexpression sensitizes brain tumor cells to apoptosis following alkylation damage of DNA. *Oncogene* **21**, 878-89.

**Siu, F., Bain, P. J., LeBlanc-Chaffin, R., Chen, H. and Kilberg, M. S.** (2002). ATF4 is a mediator of the nutrient-sensing response pathway that activates the human asparagine synthetase gene. *J Biol Chem* **277**, 24120-7.

**Slater, T. F., Sawyer, B. and Strauli, U.** (1963). Studies on succinate-tetrazolium reductase systems : III. Points of coupling of four different tetrazolium salts III. Points of coupling of four different tetrazolium salts. *Biochimica et Biophysica Acta* **77**, 383-393.

**Smith, M. L., Ford, J. M., Hollander, M. C., Bortnick, R. A., Amundson, S. A., Seo, Y. R., Deng, C. X., Hanawalt, P. C. and Fornace, A. J., Jr.** (2000). p53-mediated DNA repair responses to UV radiation: studies of mouse cells lacking p53, p21, and/or gadd45 genes. *Mol Cell Biol* **20**, 3705-14.

**Smith, M. L. and Seo, Y. R.** (2002). p53 regulation of DNA excision repair pathways. *Mutagenesis* **17**, 149-56.

**Smith, W. E., Kane, A. V., Campbell, S. T., Acheson, D. W., Cochran, B. H. and Thorpe, C. M.** (2003). Shiga toxin 1 triggers a ribotoxic stress response leading to p38 and JNK activation and induction of apoptosis in intestinal epithelial cells. *Infect Immun* **71**, 1497-504.

**Snow, E. T.** (1992). Metal carcinogenesis: mechanistic implications. *Pharmacol Ther* **53**, 31-65.

**Sorensen, B. S., Torring, N., Bor, M. V. and Nexo, E.** (2004). The DNA damaging agent VP16 induces the expression of a subset of ligands from the EGF system in bladder

cancer cells, whereas none of the four EGF receptors are induced. *Mol Cell Biochem* **260**, 129-35.

**Stanchi, F., Bertocco, E., Toppo, S., Dioguardi, R., Simionati, B., Cannata, N., Zimbello, R., Lanfranchi, G. and Valle, G.** (2001). Characterization of 16 novel human genes showing high similarity to yeast sequences. *Yeast* **18**, 69-80.

**Stanley, P. E.** (1986). Extraction of adenosine triphosphate from microbial and somatic cells. *Methods Enzymol* **133**, 14-22.

**Stewart, I., Schluter, P. J. and Shaw, G. R.** (2006). Cyanobacterial lipopolysaccharides and human health - a review. *Environ Health* **5**, 7.

**Stommel, J. M. and Wahl, G. M.** (2004). Accelerated MDM2 auto-degradation induced by DNA-damage kinases is required for p53 activation. *Embo J* **23**, 1547-56.

**Strieter, R., Standiford, T., Huffnagle, G., Colletti, L., Lukacs, N. and Kunkel, S.** (1996). Commentary: "The good, the bad, and the ugly." The role of chemokines in models of human disease. *J Immunol* **156**, 3583-3586.

**Su, P. F., Hu, Y. J., Ho, I. C., Cheng, Y. M. and Lee, T. C.** (2006). Distinct gene expression profiles in immortalized human urothelial cells exposed to inorganic arsenite and its methylated trivalent metabolites. *Environ Health Perspect* **114**, 394-403.

**Sun, S., Han, J., Ralph, W. M., Jr., Chandrasekaran, A., Liu, K., Auborn, K. J. and Carter, T. H.** (2004). Endoplasmic reticulum stress as a correlate of cytotoxicity in human tumor cells exposed to diindolylmethane in vitro. *Cell Stress Chaperones* **9**, 76-87.

**Suter, L., Babiss, L. E. and Wheeldon, E. B.** (2004). Toxicogenomics in predictive toxicology in drug development. *Chem Biol* **11**, 161-71.

**Takagaki, Y., MacDonald, C. C., Shenk, T. and Manley, J. L.** (1992). The human 64-kDa polyadenylylation factor contains a ribonucleoprotein-type RNA binding domain and unusual auxiliary motifs. *Proc Natl Acad Sci U S A* **89**, 1403-7.

**Takagaki, Y. and Manley, J. L.** (2000). Complex protein interactions within the human polyadenylation machinery identify a novel component. *Mol Cell Biol* **20**, 1515-25.

**Tan, T. and Chu, G.** (2002). p53 Binds and activates the xeroderma pigmentosum DDB2 gene in humans but not mice. *Mol Cell Biol* **22**, 3247-54.

**Tanaka, H., Arakawa, H., Yamaguchi, T., Shiraishi, K., Fukuda, S., Matsui, K., Takei, Y. and Nakamura, Y.** (2000). A ribonucleotide reductase gene involved in a p53-dependent cell-cycle checkpoint for DNA damage. *Nature* **404**, 42-9.

**Tasanen, K., Oikarinen, J., Kivirikko, K. I. and Pihlajaniemi, T.** (1992). Promoter of the gene for the multifunctional protein disulfide isomerase polypeptide. Functional

significance of the six CCAAT boxes and other promoter elements. *J Biol Chem* **267**, 11513-9.

**Terao, K., Ohmori, S., Igarashi, K., Ohtani, I., Watanabe, M. F., Harada, K. I., Ito, E. and Watanabe, M.** (1994). Electron microscopic studies on experimental poisoning in mice induced by cylindrospermopsin isolated from blue-green alga Umezakia natans. *Toxicon* **32**, 833-43.

**Thomas, A. D., Saker, M. L., Norton, J. H. and Olsen, R. D.** (1998). Cyanobacterium Cylindrospermopsis raciborskii as a probable cause of death in cattle in northern Queensland. *Aust Vet J* **76**, 592-4.

**Townsley, F. M., Wilson, D. W. and Pelham, H. R.** (1993). Mutational analysis of the human KDEL receptor: distinct structural requirements for Golgi retention, ligand binding and retrograde transport. *Embo J* **12**, 2821-9.

**Treisman, R.** (1992). The serum response element. *Trends in Biochemical Sciences* **17**, 423-426.

**Tsuji-Takayama, K., Aizawa, Y., Okamoto, I., Kojima, H., Koide, K., Takeuchi, M., Ikegami, H., Ohta, T. and Kurimoto, M.** (1999). Interleukin-18 induces interferon-gamma production through NF-kappaB and NFAT activation in murine T helper type 1 cells. *Cell Immunol* **196**, 41-50.

**Tu, B. P. and Weissman, J. S.** (2004). Oxidative protein folding in eukaryotes: mechanisms and consequences. *J Cell Biol* **164**, 341-6.

**Ulrich, R. G., Rockett, J. C., Gibson, G. G. and Pettit, S. D.** (2004). Overview of an interlaboratory collaboration on evaluating the effects of model hepatotoxicants on hepatic gene expression. *Environ Health Perspect* **112**, 423-7.

**Vadlamudi, R. K. and Shin, J.** (1998). Genomic structure and promoter analysis of the p62 gene encoding a non-proteasomal multiubiquitin chain binding protein. *FEBS Lett* **435**, 138-42.

**Vairapandi, M., Balliet, A. G., Hoffman, B. and Liebermann, D. A.** (2002). GADD45b and GADD45g are cdc2/cyclinB1 kinase inhibitors with a role in S and G2/M cell cycle checkpoints induced by genotoxic stress. *J Cell Physiol* **192**, 327-38.

**van Belzen, N., Dinjens, W. N., Diesveld, M. P., Groen, N. A., van der Made, A. C., Nozawa, Y., Vlietstra, R., Trapman, J. and Bosman, F. T.** (1997). A novel gene which is up-regulated during colon epithelial cell differentiation and down-regulated in colorectal neoplasms. *Lab Invest* **77**, 85-92.

**van Dam, H., Duyndam, M., Rottier, R., Bosch, A., de Vries-Smits, L., Herrlich, P., Zantema, A., Angel, P. and van der Eb, A. J.** (1993). Heterodimer formation of cJun and ATF-2 is responsible for induction of c-jun by the 243 amino acid adenovirus E1A protein. *Embo J* **12**, 479-87.

**van Delft, S., Coffer, P., Kruijer, W. and van Wijk, R.** (1993). c-fos induction by stress can be mediated by the SRE. *Biochem Biophys Res Commun* **197**, 542-8.

**Vayssier, M. and Polla, B. S.** (1998). Heat shock proteins chaperoning life and death. *Cell Stress Chaperones* **3**, 221-7.

**Vrana, K. E., Freeman, W. M. and Aschner, M.** (2003). Use of microarray technologies in toxicology research. *Neurotoxicology* **24**, 321-32.

**Wain, H. M., Bruford, E. A., Lovering, R. C., Lush, M. J., Wright, M. W. and Povey, S.** (2002). Guidelines for Human Gene Nomenclature. *Genomics* **79**, 464-470.

**Waisberg, M., Joseph, P., Hale, B. and Beyersmann, D.** (2003). Molecular and cellular mechanisms of cadmium carcinogenesis. *Toxicology* **192**, 95-117.

**Wang, Q., Wang, X. and Evers, B. M.** (2003). Induction of cIAP-2 in human colon cancer cells through PKC delta/NF-kappa B. *J Biol Chem* **278**, 51091-9.

**Wang, X., Lawson, B., Brewer, J., Zinszner, H., Sanjay, A., Mi, L., Boorstein, R., Kreibich, G., Hendershot, L. and Ron, D.** (1996). Signals from the stressed endoplasmic reticulum induce C/EBP-homologous protein (CHOP/GADD153). *Mol. Cell. Biol.* **16**, 4273-4280.

**Wang, X. W., Zhan, Q., Coursen, J. D., Khan, M. A., Kontny, H. U., Yu, L., Hollander, M. C., O'Connor, P. M., Fornace, A. J., Jr. and Harris, C. C.** (1999). GADD45 induction of a G2/M cell cycle checkpoint. *Proc Natl Acad Sci U S A* **96**, 3706-11.

**Wang, Z., Rong, Y. P., Malone, M. H., Davis, M. C., Zhong, F. and Distelhorst, C. W.** (2006). Thioredoxin-interacting protein (txnip) is a glucocorticoid-regulated primary response gene involved in mediating glucocorticoid-induced apoptosis. *Oncogene* **25**, 1903-13.

**Waring, J. F., Ciurlionis, R., Jolly, R. A., Heindel, M. and Ulrich, R. G.** (2001). Microarray analysis of hepatotoxins in vitro reveals a correlation between gene expression profiles and mechanisms of toxicity. *Toxicol Lett* **120**, 359-68.

**Waterman, M. J., Stavridi, E. S., Waterman, J. L. and Halazonetis, T. D.** (1998). ATM-dependent activation of p53 involves dephosphorylation and association with 14-3-3 proteins. *Nat Genet* **19**, 175-8.

**Watson, W. H., Yang, X., Choi, Y. E., Jones, D. P. and Kehrer, J. P.** (2004). Thioredoxin and its role in toxicology. *Toxicol Sci* **78**, 3-14.

**Webster, G. A. and Perkins, N. D.** (1999). Transcriptional Cross Talk between NF-kappa B and p53. *Mol. Cell. Biol.* **19**, 3485-3495.

**Wei, Y. F., Carter, K. C., Wang, R. P. and Shell, B. K.** (1996). Molecular cloning and functional analysis of a human cDNA encoding an Escherichia coli AlkB homolog, a protein involved in DNA alkylation damage repair. *Nucleic Acids Res* **24**, 931-37.

**Weinstock, J. V., Blum, A., Metwali, A., Elliott, D. and Arsenescu, R.** (2003). IL-18 and IL-12 signal through the NF-kappa B pathway to induce NK-1R expression on T cells. *J Immunol* **170**, 5003-7.

**Welch, J. N. and Chrylogelos, S. A.** (2002). Positive mediators of cell proliferation in neoplastic transformation. In *The Molecular Basis of Human Cancer*, (ed. W. B. Coleman and G. J. Tsongalis), pp. 65-79: Humana Press, New Jersey, U.S.A.

**Werlen, G., Jacinto, E., Xia, Y. and Karin, M.** (1998). Calcineurin preferentially synergizes with PKC-theta to activate JNK and IL-2 promoter in T lymphocytes. *Embo J* **17**, 3101-11.

**Weyermann, J., Lochmann, D. and Zimmer, A.** (2005). A practical note on the use of cytotoxicity assays. *Int J Pharm* **288**, 369-76.

**White, R. J.** (2005). RNA polymerases I and III, growth control and cancer. *Nat Rev Mol Cell Biol* **6**, 69-78.

**Whiteside, S. T., Epinat, J. C., Rice, N. R. and Israel, A.** (1997). I kappa B epsilon, a novel member of the I kappa B family, controls RelA and cRel NF-kappa B activity. *Embo J* **16**, 1413-26.

**Wiggin, G. R., Soloaga, A., Foster, J. M., Murray-Tait, V., Cohen, P. and Arthur, J. S.** (2002). MSK1 and MSK2 are required for the mitogen- and stress-induced phosphorylation of CREB and ATF1 in fibroblasts. *Mol Cell Biol* **22**, 2871-81.

**Williams, B. R.** (1999). PKR; a sentinel kinase for cellular stress. *Oncogene* **18**, 6112-20.

**Williams, B. R. G.** (2001). Signal Integration via PKR. *Sci. STKE* **2001**, re2-.

**Wolters, P. J., Pham, C. T., Muilenburg, D. J., Ley, T. J. and Caughey, G. H.** (2001). Dipeptidyl peptidase I is essential for activation of mast cell chymases, but not tryptases, in mice. *J Biol Chem* **276**, 18551-6.

**Wong, S.-S., Zhou, H.-R. and Pestka, J. J.** (2002). Effects of vomitoxin (deoxynivalenol) on the binding of transcription factors AP-1, NF-kB, and NF-IL6 in RAW 264.7 macrophage cells. *Journal of Toxicology and Environmental Health, Part A: Current Issues* **65**, 1161 - 1180.

**Wooten, M. W., Geetha, T., Seibenhener, M. L., Babu, J. R., Diaz-Meco, M. T. and Moscat, J.** (2005). The p62 scaffold regulates nerve growth factor-induced NF-kappaB activation by influencing TRAF6 polyubiquitination. *J Biol Chem* **280**, 35625-9.

**Wu, B., Hunt, C. and Morimoto, R.** (1985). Structure and expression of the human gene encoding major heat shock protein HSP70. *Mol Cell Biol* **5**, 330-41.

**Wu, M., Xu, L. G., Zhai, Z. and Shu, H. B.** (2003). SINK is a p65-interacting negative regulator of NF-kappaB-dependent transcription. *J Biol Chem* **278**, 27072-9.

**Wu, S., Kumar, K. U. and Kaufman, R. J.** (1998). Identification and Requirement of Three Ribosome Binding Domains in dsRNA-Dependent Protein Kinase (PKR). *Biochemistry* **37**, 13816-13826.

**Wu, Z. H., Shi, Y., Tibbetts, R. S. and Miyamoto, S.** (2006). Molecular linkage between the kinase ATM and NF-kappaB signaling in response to genotoxic stimuli. *Science* **311**, 1141-6.

**Xu, Y.** (2003). Regulation of p53 responses by post-translational modifications. *Cell Death Differ* **10**, 400-3.

**Yang, G., Zhang, G., Pittelkow, M. R., Ramoni, M. and Tsao, H.** (2006). Expression Profiling of UVB Response in Melanocytes Identifies a Set of p53-Target Genes. *J Invest Dermatol* **126**, 2490-506.

**Yang, G. H., Li, S. and Pestka, J. J.** (2000). Down-regulation of the endoplasmic reticulum chaperone GRP78/BiP by vomitoxin (Deoxynivalenol). *Toxicol Appl Pharmacol* **162**, 207-17.

**Yang, J., Yu, Y., Hamrick, H. E. and Duerksen-Hughes, P. J.** (2003). ATM, ATR and DNA-PK: initiators of the cellular genotoxic stress responses. *Carcinogenesis* **24**, 1571-80.

**Ye, J., Rawson, R. B., Komuro, R., Chen, X., Dave, U. P., Prywes, R., Brown, M. S. and Goldstein, J. L.** (2000). ER Stress Induces Cleavage of Membrane-Bound ATF6 by the Same Proteases that Process SREBPs. *Molecular Cell* **6**, 1355-1364.

**Yin, M. B., Voigt, W., Panadero, A., Vanhoefer, U., Frank, C., Pajovic, S., Azizkhan, J. and Rustum, Y. M.** (1997). p53 and WAF1 are induced and Rb protein is hypophosphorylated during cell growth inhibition by the thymidylate synthase inhibitor ZD1694 (Tomudex). *Mol Pharmacol* **51**, 630-6.

**Yoshida, H., Haze, K., Yanagi, H., Yura, T. and Mori, K.** (1998). Identification of the cis-Acting Endoplasmic Reticulum Stress Response Element Responsible for Transcriptional Induction of Mammalian Glucose-regulated Proteins. *J. Biol. Chem.* **273**, 33741-33749.

**Yoshida, H., Matsui, T., Yamamoto, A., Okada, T. and Mori, K.** (2001). XBP1 mRNA is induced by ATF6 and spliced by IRE1 in response to ER stress to produce a highly active transcription factor. *Cell* **107**, 881-91.

**Yoshida, H., Okada, T., Haze, K., Yanagi, H., Yura, T., Negishi, M. and Mori, K.** (2000). ATF6 activated by proteolysis binds in the presence of NF-Y (CBF) directly to the cis-acting element responsible for the mammalian unfolded protein response. *Mol Cell Biol* **20**, 6755-67.

**Zamanian-Daryoush, M., Mogensen, T. H., DiDonato, J. A. and Williams, B. R. G.** (2000). NF-kappa B Activation by Double-Stranded-RNA-Activated Protein Kinase (PKR) Is Mediated through NF-kappa B-Inducing Kinase and Ikappa B Kinase. *Mol. Cell. Biol.* **20**, 1278-1290.

**Zhan, Q.** (2005). Gadd45a, a p53- and BRCA1-regulated stress protein, in cellular response to DNA damage. *Mutat Res* **569**, 133-43.

**Zhang, C., Gao, C., Kawauchi, J., Hashimoto, Y., Tsuchida, N. and Kitajima, S.** (2002). Transcriptional activation of the human stress-inducible transcriptional repressor ATF3 gene promoter by p53. *Biochem Biophys Res Commun* **297**, 1302-10.

**Zhang, J. P., Ying, K., Xiao, Z. Y., Zhou, B., Huang, Q. S., Wu, H. M., Yin, M., Xie, Y., Mao, Y. M. and Rui, Y. C.** (2004). Analysis of gene expression profiles in human HL-60 cell exposed to cantharidin using cDNA microarray. *Int J Cancer* **108**, 212-8.

**Zhang, Q. Y., Hammerberg, C., Baldassare, J. J., Henderson, P. A., Burns, D., Ceska, M., Voorhees, J. J. and Fisher, G. J.** (1992). Retinoic acid and phorbol ester synergistically up-regulate IL-8 expression and specifically modulate protein kinase C-epsilon in human skin fibroblasts. *J Immunol* **149**, 1402-8.

**Zhao, B., Natarajan, R. and Ghosh, S.** (2005). Human liver cholesteryl ester hydrolase: cloning, molecular characterization, and role in cellular cholesterol homeostasis. *Physiol Genomics* **23**, 304-10.

**Zhou, D., Salnikow, K. and Costa, M.** (1998). Cap43, a novel gene specifically induced by Ni2+ compounds. *Cancer Res* **58**, 2182-9.

**Zhou, H. M. and Strydom, D. J.** (1993). The amino acid sequence of human ribonuclease 4, a highly conserved ribonuclease that cleaves specifically on the 3' side of uridine. *Eur J Biochem* **217**, 401-10.

**Zhou, H. R., Islam, Z. and Pestka, J. J.** (2005a). Induction of competing apoptotic and survival signaling pathways in the macrophage by the ribotoxic trichothecene deoxynivalenol. *Toxicol Sci* **87**, 113-22.

**Zhou, H. R., Jia, Q. and Pestka, J. J.** (2005b). Ribotoxic stress response to the trichothecene deoxynivalenol in the macrophage involves the SRC family kinase Hck. *Toxicol Sci* **85**, 916-26.

**Zhou, H. R., Lau, A. S. and Pestka, J. J.** (2003). Role of double-stranded RNA-activated protein kinase R (PKR) in deoxynivalenol-induced ribotoxic stress response. *Toxicol Sci* **74**, 335-44.

**Zhou, Z., Tan, H. L., Xu, B. X., Ma, Z. C., Gao, Y. and Wang, S. Q.** (2005c). Microarray analysis of altered gene expression in diallyl trisulfide-treated HepG2 cells. *Pharmacol Rep* **57**, 818-23.

**Zhu, C., Johansen, F. E. and Prywes, R.** (1997a). Interaction of ATF6 and serum response factor. *Mol Cell Biol* **17**, 4957-66.

**Zhu, S., Romano, P. R. and Wek, R. C.** (1997b). Ribosome Targeting of PKR Is Mediated by Two Double-stranded RNA-binding Domains and Facilitates in Vivo Phosphorylation of Eukaryotic Initiation Factor-2. *J. Biol. Chem.* **272**, 14434-14441.

**Zimmers, T. A., Jin, X., Hsiao, E. C., McGrath, S. A., Esquela, A. F. and Koniaris, L. G.** (2005). Growth differentiation factor-15/macrophage inhibitory cytokine-1 induction after kidney and lung injury. *Shock* **23**, 543-8.

**Zinck, R., Cahill, M. A., Kracht, M., Sachsenmaier, C., Hipskind, R. A. and Nordheim, A.** (1995). Protein synthesis inhibitors reveal differential regulation of mitogen-activated protein kinase and stress-activated protein kinase pathways that converge on Elk-1. *Mol Cell Biol* **15**, 4930-8.

**Zindy, F., Eischen, C. M., Randle, D. H., Kamijo, T., Cleveland, J. L., Sherr, C. J. and Roussel, M. F.** (1998). Myc signaling via the ARF tumor suppressor regulates p53-dependent apoptosis and immortalization. *Genes Dev.* **12**, 2424-2433.

**Zinszner, H., Kuroda, M., Wang, X., Batchvarova, N., Lightfoot, R. T., Remotti, H., Stevens, J. L. and Ron, D.** (1998). CHOP is implicated in programmed cell death in response to impaired function of the endoplasmic reticulum. *Genes Dev.* **12**, 982-995.

**Zucco, F., De Angelis, I., Testai, E. and Stammati, A.** (2004). Toxicology investigations with cell culture systems: 20 years after. *Toxicol In Vitro* **18**, 153-63.

**Zuker, M.** (2003). Mfold web server for nucleic acid folding and hybridization prediction. *Nucl. Acids Res.* **31**, 3406-3415.